Terms and Conditions of Use of Digitised Theses from Trinity College Library Dublin

Copyright statement

All material supplied by Trinity College Library is protected by copyright (under the Copyright and Related Rights Act, 2000 as amended) and other relevant Intellectual Property Rights. By accessing and using a Digitised Thesis from Trinity College Library you acknowledge that all Intellectual Property Rights in any Works supplied are the sole and exclusive property of the copyright and/or other IPR holder. Specific copyright holders may not be explicitly identified. Use of materials from other sources within a thesis should not be construed as a claim over them.

A non-exclusive, non-transferable licence is hereby granted to those using or reproducing, in whole or in part, the material for valid purposes, providing the copyright owners are acknowledged using the normal conventions. Where specific permission to use material is required, this is identified and such permission must be sought from the copyright holder or agency cited.

Liability statement

By using a Digitised Thesis, I accept that Trinity College Dublin bears no legal responsibility for the accuracy, legality or comprehensiveness of materials contained within the thesis, and that Trinity College Dublin accepts no liability for indirect, consequential, or incidental, damages or losses arising from use of the thesis for whatever reason. Information located in a thesis may be subject to specific use constraints, details of which may not be explicitly described. It is the responsibility of potential and actual users to be aware of such constraints and to abide by them. By making use of material from a digitised thesis, you accept these copyright and disclaimer provisions. Where it is brought to the attention of Trinity College Library that there may be a breach of copyright or other restraint, it is the policy to withdraw or take down access to a thesis while the issue is being resolved.

Access Agreement

By using a Digitised Thesis from Trinity College Library you are bound by the following Terms & Conditions. Please read them carefully.

I have read and I understand the following statement: All material supplied via a Digitised Thesis from Trinity College Library is protected by copyright and other intellectual property rights, and duplication or sale of all or part of any of a thesis is not permitted, except that material may be duplicated by you for your research use or for educational purposes in electronic or print form providing the copyright owners are acknowledged using the normal conventions. You must obtain permission for any other use. Electronic or print copies may not be offered, whether for sale or otherwise to anyone. This copy has been supplied on the understanding that it is copyright material and that no quotation from the thesis may be published without proper acknowledgement.

Studies into the Phosphorylation of MyD88 adapter-like (Mal)

Thesis submitted to the

University of Dublin

For the

Degree of Doctor of Philosophy

By

Pearl Gray

Department of Biochemistry

Trinity College

Dublin

Ireland

October 2005

Declaration

This thesis is submitted by the undersigned to the University of Dublin for the examination of Doctorate in Philosophy. The work herein is entirely my own and has not been submitted as an exercise for a degree to any other university. The library at Trinity College, Dublin, has my full permission to lend or copy this thesis upon request.

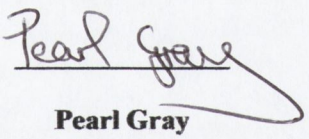

Pearl Gray

Acknowledgements

Firstly, I would sincerely like to thank Professor Luke O'Neill for his continued support, enthusiasm and invaluable advice throughout the project. I would also like to thank everyone in the lab for making my time here so enjoyable and for their assistance and advice. A special thanks to Aisling, and thanks to Anne, Beth, Cait, Caroline J., Caroline M., Claudia, Cos, Emma, Eva, Gareth, Kathy, Kiva, Sarah, Sinead and Susan. To everyone in the department, thanks for always being so helpful throughout the years. An extra special mention is needed for Claudia, Cos and Orla - thanks for keeping me sane!

I would especially like to thank my family, Billy, Phil, Alice, Hazel and Bill for always being so supportive and encouraging. Thanks also to all my friends and relatives for being continually interested in how things were going.

Finally, I would like to dedicate this work to my granddad Larry Curran.

Table of Contents

Abstract

Members of the Toll-like receptor (TLR) family are essential players in activating the host innate immune response against infectious microorganisms. All TLRs signal through Toll/IL-1 receptor (TIR) domain-containing adapter proteins. MyD88 adapter-like (Mal) is one such adapter, which is specifically involved in TLR-2 and TLR-4 signalling. The aim of this study was to further characterise signalling via Mal. In particular, this study focussed on the mechanisms of Mal phosphorylation.

Initial studies determined that overexpressed Mal undergoes phosphorylation. *In vitro* it was determined that Mal is a substrate for Interleukin-1 receptor-associated kinase-1 (IRAK1), IRAK4 and Bruton's tyrosine kinase (Btk). Furthermore Btk immunoprecipitated from THP-1 cells activated by LPS could phosphorylate Mal. Activation of THP-1 monocytic cells with the TLR4 agonist lipopolysaccharide (LPS) and the TLR2 agonist, macrophage activating lipopeptide-2 (MALP-2), induced phosphorylation of Mal on tyrosine residues. Pre-treatment of THP-1 monocytic cells with the Btk inhibitor LFM-A13 could block the endogenous phosphorylation of Mal on tyrosine in cells treated with MALP-2 or LPS. Three possible phospho-accepting tyrosines were identified at positions 86, 106 and 187, and two mutant forms of Mal in which tyrosines 86 and 187 were mutated to phenylalanine acted as dominant negative inhibitors of NF-κB activation by LPS.

In addition, association studies revealed that Mal interacts with SOCS-1. Co-expression of Mal with SOCS-1 resulted in Mal degradation. Degradation of Mal was abolished in mice containing a null mutant of Btk, suggesting that phosphorylation of

Mal by Btk is likely to be required to recruit SOCS-1, thereby resulting in Mal degradation.

Our study therefore provides the first demonstration of the key role of Mal phosphorylation on tyrosine during signalling by TLR2 and TLR4 and identifies a novel function for Btk as the kinase involved in regulating Mal signalling.

Abbreviations

AcP	Accessory Protein
AP-1	Activator protein 1
BSA	Bovine Serum Albumin
cAMP	Cyclic AMP
DD	Death Domain
DTT	Dithiothreitol
EDTA	Ethylenediaminetetracetic acid
ERK	Extracellular signal-regulated kinase
EST	Expressed sequence tag
FCS	Fetal Calf Serum
GST	Glutathione S transferase
HKSA	Heat killed *Staphylococcus aureus*
IFN	Interferon
Ig	Immunoglobulin
IKK	IκB kinase
IL	Interleukin
IL1RAcP	IL-1 receptor accessory protein
IL-1RI	IL-1 receptor type I
IPTG	Isopropyl-β-D-thiogalactopyranoside
IRAK	Interleukin 1 receptor associated kinase
IRF-3	Interferon Response Factor-3
ISRE	Interferon Stimulated Response Element
JNK	Jun-N-terminal kinase
kDa	Kilodalton

KO	Knock-out
LB broth	Luria-Bertani broth
LPS	Lipopolysaccharide
LRR	Leucine rich repeat
LTA	Lipoteichoic acid
MALP-2	Macrophage-activating lipoprotein-2kDa
MAPK	Mitogen activated protein kinase
Mal	MyD88 adaptor like
MyD88	Myeloid differentiation factor 88
NEMO	NF-κB essential modifier
NFAT	Nuclear factor of activated T cells
NF-κB	Nuclear factor kappa B
NIK	Nuclear localisation sequence
PAGE	Polyacrylamide gel electrophoresis
PAMPS	Pathogen associated molecular patterns
PBS	Phosphate buffered saline
PCR	Polymerase chain reaction
PGN	Peptidoglycan
PI3K	Phosphatidylinositol 3-kinase
PKR	Protein kinase R
PKC	Protein kinase C
PMSF	Phenylmethylsuphonylflouride
PVDF	Polyvinylidene diflouride
RHD	Rel homology domain
SARM	Sterile alpha and HEAT/Armadillo motif protein

SDS	Sodium dodecyl sulphate
SIGIRR	Single immunoglobulin IL-1R related protein
SOCS	Suppressor of cytokine signalling
STAT	Signal transducer and activator of transcription
TAB	TAK1 binding protein
TAK	TGFβ-activated kinase
TBE	Tris borate EDTA
TBK1	Tank binding kinase -1
TEMED	N, N, N', N',-Tetramethylethylenediamine
TICAM-1	TIR domain containing adaptor-1
TIR	Toll-IL-1R receptor
TIRAP	TIR accessory protein
TIRP	TIR-containing protein
TLR	Toll like receptor
TNF	Tumour necrosis factor
Tollip	Toll/IL1R interacting protein
TRIF	TIR domain-containing adapter inducing IFN-beta
TRAF	TNF-receptor associated factor

Chapter 1

Introduction

1.1 General Introduction

The immune system is often segregated into two main components, namely innate and adaptive immunity. The major difference between these two arms of the immune system is that the innate immune response uses a subset of germline encoded receptors termed pattern recognition receptors (PRRs), whereas the adaptive immune response uses somatic gene rearrangement to produce specific antigen receptors.

In recent years the mechanism by which the innate immune system recognises invading microorganisms, has been further elucidated with the discovery of PRRs termed Toll-like receptors (TLRs). The term Toll was originally coined for a cell surface receptor governing dorsal/ventral polarity in the early *Drosophila* embryo (Hashimoto, Hudson et al. 1988; Stein and Stevens 1991). Toll was later found to play a crucial role in anti-fungal defence in the adult fly (Lemaitre, Nicolas et al. 1996). A year subsequent to this discovery, a mammalian homologue of *Drosophila* Toll was described (Mitcham, Parnet et al. 1996; Medzhitov, Preston-Hurlburt et al. 1997; Rock, Hardiman et al. 1998). To date 13 Toll homologues have been identified in mice and 10 in humans, all of which have been assigned to a new superfamily, known as the TLR/Interleukin-1 receptor (IL-1R) superfamily (Medzhitov, Preston-Hurlburt et al. 1997; Rock, Hardiman et al. 1998; Chuang and Ulevitch 2000; Hemmi, Takeuchi et al. 2000; Zhang, Zhang et al. 2004).

In addition to their vital role in controlling the innate immune response, it has transpired that TLRs are required to enhance the adaptive immune response. Dendritic cells (DCs) are the key components in linking both the innate and the adaptive immune response. TLR signalling in DCs leads to their activation and maturation and controls secretion of cytokines such as IL-12 which generally results in the induction of T helper

type 1 (Th1) responses (Trinchieri 2003). In addition, TLR signal transduction in DCs induces the up-regulation of co-stimulatory molecules required to translate the nonclonal pattern recognition signal into clonal antigen-specific immune responses (Steinman 2003). The sequential activation of innate and subsequent adaptive immunity mediated by TLRs is now known to be crucial step in sensing and eradicating invading pathogens.

1.2 The TLR/ IL-1R superfamily

All members of the TLR/IL-1R superfamily are defined by the presence of an evolutionary conserved intracellular TIR domain, which is characterised by three conserved sequence boxes, termed Box 1, 2 and 3. Members of the TLR/IL-1R superfamily can be further classified into three distinct subgroups: the IL-1R subgroup, whose members contain immunoglobulin (Ig)-like domains extracellularly; the TLR subgroup, whose members contain a tandem array of leucine-rich repeats (LRRs) in their extracellular region and lastly the third subgroup, which comprises of cytosolic adapter molecules (Figure 1.1).

1.2.1 The IL-1R subgroup

In brief, the IL-1R subgroup includes the founder member of the family, type I IL-1 receptor (IL-1RI) (Sims, March et al. 1988), which directly binds the pro-inflammatory cytokine IL-1; the IL-1 receptor accessory protein (IL1RAcP) (Greenfeder, Nunes et al. 1995); the IL-18 receptor (Parnet, Garka et al. 1996; Torigoe, Ushio et al. 1997) and its accessory protein (IL1-18RAcP) (Born, Thomassen et al. 1998). Other members include T1/ST2 (Klemenz, Hoffmann et al. 1989; Tominaga 1989;

Figure 1.1 Schematic representation depicting members of the TLR/IL-1R superfamily. The TLR/IL-1R superfamily share a region of homology in their intracellular domain termed the TIR domain. The IL-1R subgroup is typified by having multiple Ig-like domains in their extracellular domain whereas the TLR subgroup has a leucine-rich repeat domain in its place. TLR3, TLR7, TLR8, and TLR9 are located in intracellular compartments. The third subgroup consists of cytosolic adapters.

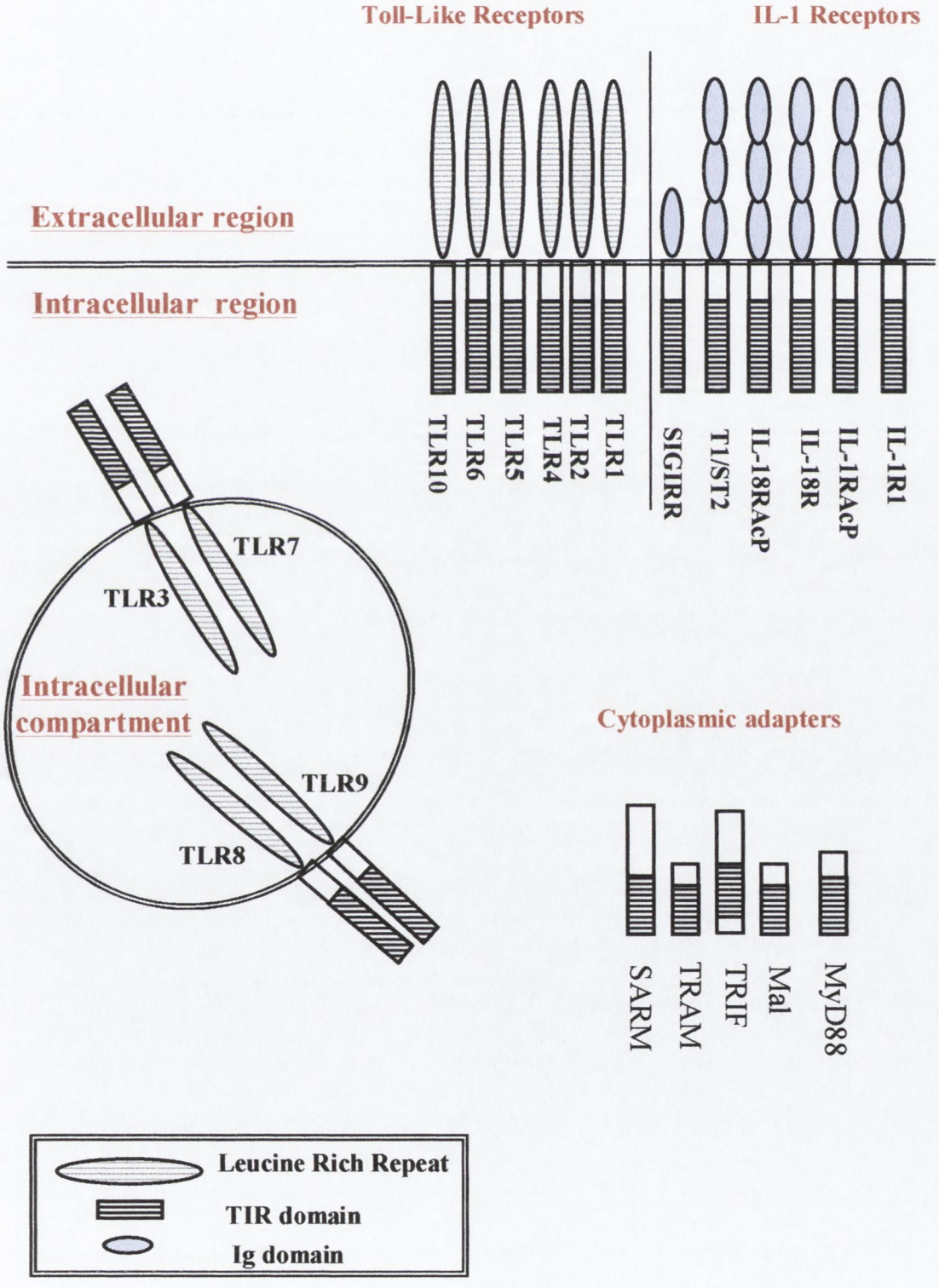
Toll-Like Receptors
IL-1 Receptors
Extracellular region
Intracellular region
TLR10
TLR6
TLR5
TLR4
TLR2
TLR1
SIGIRR
T1/ST2
IL-18RAcP
IL-18R
IL-1RAcP
IL-1R1
TLR7
TLR3
Intracellular compartment
TLR9
TLR8
Cytoplasmic adapters
SARM
TRAM
TRIF
Mal
MyD88
Leucine Rich Repeat
TIR domain
Ig domain

Werenskiold, Hoffmann et al. 1989) and single Ig-domain containing IL-1 receptor related molecule (SIGIRR) (Thomassen, Renshaw et al. 1999).

1.2.2 The TLR subgroup

TLRs have been referred to as PRRs as they recognise conserved molecular patterns that are essential for the survival of microorganisms. These invariant structures, among microorganisms of a particular class, are called pathogen-associated molecular patterns (PAMPs). The beauty of PAMPS is that they are not expressed on host cells, thereby making them an excellent target for the immune response. It has emerged that TLR1, TLR2, TLR4, TLR5 and TLR6 are all localised to the plasma membrane whereas TLR3, TLR7, TLR8 and TLR9 are preferentially expressed in intracellular compartments such as endosomal vesicles (Figure 1.1) (Takeda and Akira 2005).

1.2.2.1 Ligands for the TLRs

TLRs are expressed differentially among immune cells (Muzio, Polntarutti et al. 2000)and it has emerged that, despite their similarities, TLRs respond to different invading microorganisms. Combinations of overexpression studies, ex vivo studies and knock-out (KO) mice have been used to identify specific ligands for each of the TLRs (Figure 1.2).

TLR4 is the prototypical receptor of this subgroup and has been identified as the long sought after receptor for lipopolysaccharide (LPS), a gram-negative bacterial cell wall component (Poltorak, He et al. 1998; Qureshi, Lariviere et al. 1999). Recognition of LPS at the receptor level is instigated through a series of events. In brief, LPS is initially

Figure 1.2 Schematic diagram depicting the natural ligands recognised by members of the TLR family. Recent studies have revealed that each member of the TLR family can selectively mediate responses to invariant structures on invading microorganims. Bacterial LPS responds to TLR4, whereas TLR2 dimerises with either TLR1 or TLR6 to elicit an immune response against triacylated and diacylated bacterial lipoproteins respectively. TLR2 also recognises peptidoglycan (PGN); it has yet to be determined if additional TLRs are required (TLRX). CpG DNA produced by both bacteria and viruses, activates TLR9, the ligand for TLR3 is double-stranded RNA, and flagellin is recognized by TLR5. In mice, TLR11 responds to uropathogenic bacteria. TLR4 also recognises the Respiratory Syncytial Virus (RSV) fusion (F) protein. Double stranded RNA (dsRNA) signals through TLR3, whereas TLR7 and TLR8 respond to single stranded RNA (ssRNA). TLR3, TLR7, TLR8 and TLR9 reside within the endosomal membrane. LRR: Leucine rich repeat.

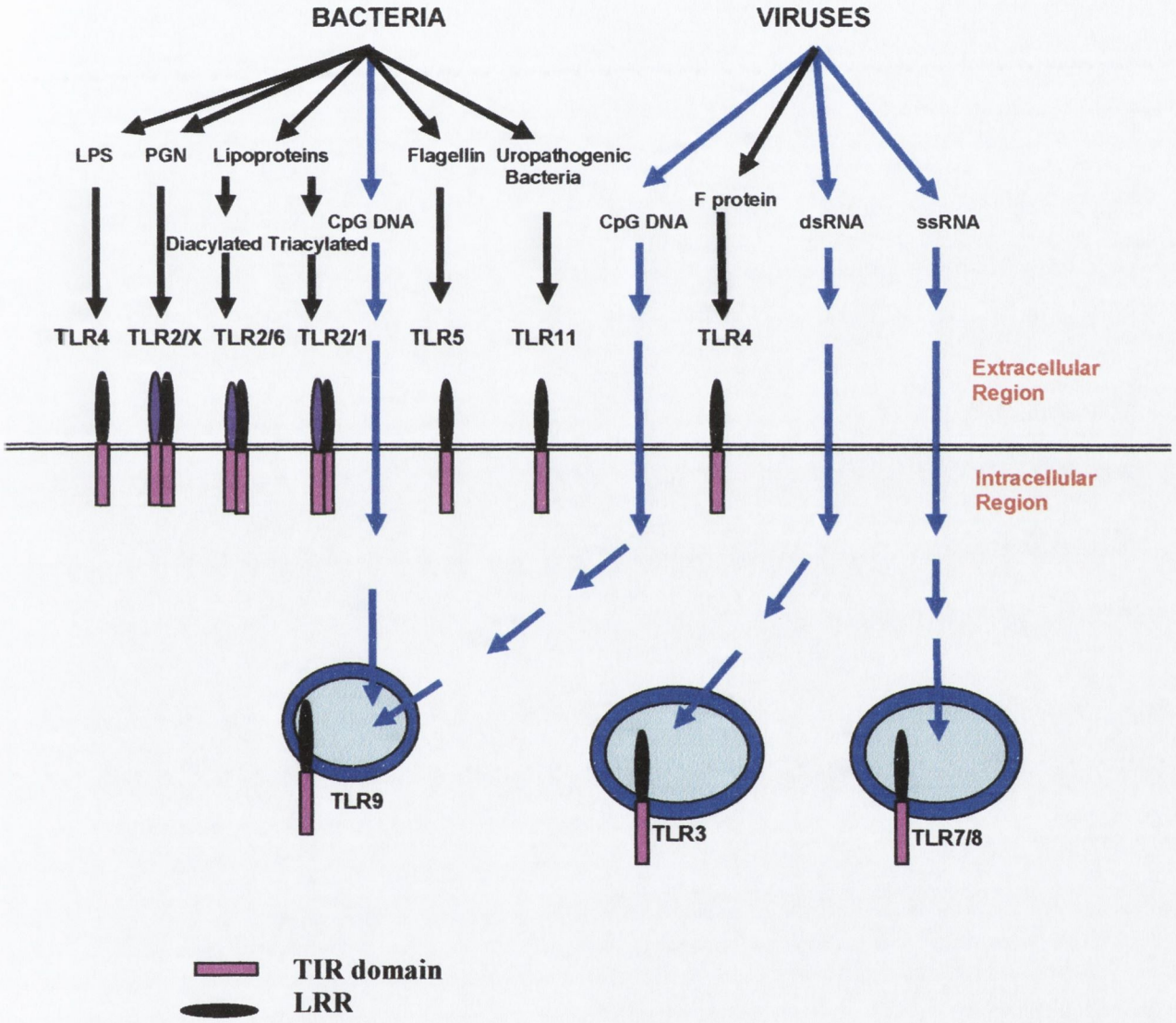
BACTERIA
VIRUSES
LPS
PGN
Lipoproteins
Flagellin
Uropathogenic Bacteria
CpG DNA
F protein
dsRNA
ssRNA
Diacylated
Triacylated
TLR4
TLR2/X
TLR2/6
TLR2/1
TLR5
TLR11
TLR4
Extracellular Region
Intracellular Region
TLR9
TLR3
TLR7/8
TIR domain
LRR

recognised *via* its lipid A moiety by the LPS-binding protein (LBP) (Schumann, Leong et al. 1990). It has been reported that the function of LBP is to directly enhance LPS activity by transferring LPS to CD14 (Jack, Fan et al. 1997; Wurfel and Wright 1997). LPS is subsequently presented by CD14 to the extracellular adapter protein, MD-2 and TLR-4, which results in TLR4 activation (Yu and Wright 1996).

TLR2 appears to be unique in its requirement for cooperation with other TLRs, namely TLR1 and TLR6 to mediate cell signalling. Triacylated lipoprotein has been identified as the natural ligand for TLR2 in cooperation with TLR1 (Takeda, Takeuchi et al. 2002). Furthermore, the TLR2/6 heterodimer is required for the recognition of diacylated lipoproteins. Macrophage activating lipopeptide-2 (MALP-2), a proinflammatory lipopeptide from *Mycoplasma fermentans*, is one such diacylated molecule (Takeuchi, Kawai et al. 2001). It has also been reported that TLR2 elicits an immune response against peptidoglycan, a component of the bacterial cell wall (Takeuchi, Hoshino et al. 1999). However, recent evidence has emerged indicating that TLR2 does not in fact recognize peptidoglycan, but rather that the TLR2 response was due to minor contaminants present in the peptidoglycan preparation, such as lipoproteins (Travassos, Girardin et al. 2004).. Moreover it has been determined that rather than initiating a TLR response, peptidoglycan degradation products in the form of muropeptides may be recognized by other PRRs, namely nucleotide-binding oligomerization domains (NODs) and NACHT-, LRR- and pyrin domain (PYD)-containing proteins (NALPs) (Travassos, Girardin et al. 2004). It remains to be determined however, if NODs and NALPs recognize the peptidoglycan degradation

products directly or whether recognition occurs through the use of a linker protein (Travassos, Girardin et al. 2004).

The ligand for TLR3 is double-stranded RNA, which is a frequent byproduct of viral infection (Alexopoulou, Holt et al. 2001). Flagellin, a protein monomer obtained from bacterial flagella, is recognised by TLR5 (Hayashi, Smith et al. 2001) and unmethylated bacterial CpG DNA is the ligand for TLR9 (Hemmi, Takeuchi et al. 2000). The antiviral synthetic compound R-848 is recognized by TLR7 and TLR8 and recently single-stranded RNA has been identified as their natural ligand (Hemmi, Kaisho et al. 2002; Diebold, Kaisho et al. 2004; Heil, Hemmi et al. 2004). TLR11 is essential in mediating an immune response to bacterial infections of the urinary tract but only in mice (Zhang, Zhang et al. 2004). No ligand has been identified for TLR10, which was identified in humans, but not mice. In addition, natural ligands for TLR12 and TLR13 have yet to be identified.

1.2.3 TIR domain-containing adapter subgroup

Once the TLRs are activated by their respective agonists, receptor dimerisation *via* the TIR domain is thought to occur. This leads to recruitment of cytosolic TIR domain-containing adapter proteins (Vogel, Fitzgerald et al. 2003; Dunne and O'Neill 2005). Five such adapters have been discovered to date, including (in order of their discovery) myeloid differentiation factor 88 (MyD88) (Lord, Hoffman-Liebermann et al. 1990); MyD88 adapter-like (Mal) (Fitzgerald, Palsson-McDermott et al. 2001), also called TIR domain-containing adapter protein (TIRAP)(Horng, Barton et al. 2001); Toll/IL-1 receptor domain-containing adapter inducing IFN-β (TRIF) also referred to as

TIR-containing adapter molecule-1 (TICAM-1) (Yamamoto, Sato et al. 2002; Oshiumi, Matsumoto et al. 2003); TRIF-related adapter protein (TRAM) (Fitzgerald, Rowe et al. 2003)also known as TIR-containing protein (TIRP) (Bin, Xu et al. 2003) and TIR-containing adapter molecule-2 (TICAM-2) (Oshiumi, Sasai et al. 2003) and Sterile alpha and HEAT/Armadillo motif protein (SARM) (Mink, Fogelgren et al. 2001) (Figure 1.3).

It has emerged that specificity with respect to adapter usage exists among the TLRs (Vogel, Fitzgerald et al. 2003). The prototype TIR-containing adapter protein, MyD88, has been being implicated in signalling from all the tested TLRs with the probable exception of TLR3. Conversely Mal participates solely in TLR2 and TLR4 signal transduction where it may act as a bridging adapter for MyD88 recruitment (Fitzgerald, Palsson-McDermott et al. 2001; Horng, Barton et al. 2001; Horng, Barton et al. 2002; Yamamoto, Sato et al. 2002). The third adapter to be identified, TRIF, is an essential adapter in TLR3 signalling and is required for initiation of the MyD88-independent activation of the transcription factor interferon-regulated factor-3 (IRF-3), induced by both TLR3 and TLR4 ligands (Yamamoto, Sato et al. 2002; Oshiumi, Matsumoto et al. 2003). TRAM on the other hand is believed to act as a linker adapter in the MyD88-independent signalling pathway, as it has emerged that it is required to bring TLR4 and TRIF into close proximity (Oshiumi, Sasai et al. 2003). A role for SARM in TLR signalling has yet to be determined, as recent studies suggest that it is unable to activate either the NF-κB or the IRF-3 pathways (Liberati, Fitzgerald et al. 2004).

Figure 1.3 Schematic representation of known mammalian TLR adapter molecules. **A.** MyD88, TIRAP/Mal, TRIF/TICAM-1, and TIRP/TRAM/TICAM-2 are all known TLR adapter proteins, while the function of SARM is not yet known. **B.** CLUSTAL W alignment of the TIR domains of human and mouse MyD88, TIRAP/Mal, TRIF/TICAM-1, and TIRP/TRAM/TICAM-2. The amino acid colours are based on their physicochemical properties where yellow = small, green = hydrophobic, turquoise = aromatic, blue = positively charged and red = negatively charged. The three important regions, Box 1, 2, and 3 are labelled. Adapted from Vogel, Fitzgerald et al. 2003.

(a)

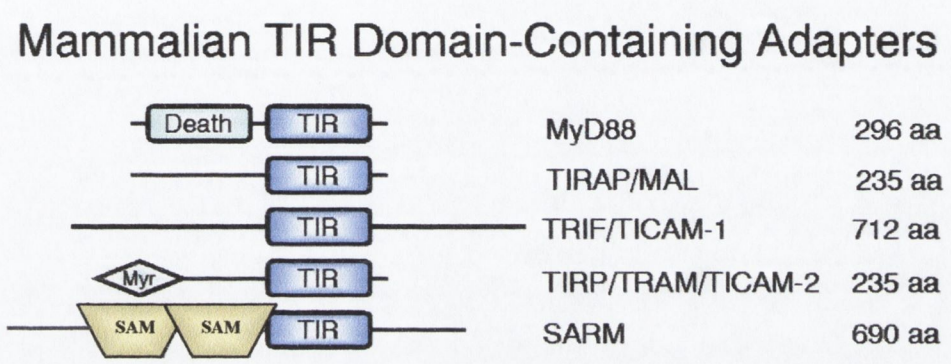
Mammalian TIR Domain-Containing Adapters
Death
TIR
MyD88
296 aa
TIR
TIRAP/MAL
235 aa
TIR
TRIF/TICAM-1
712 aa
Myr
TIR
TIRP/TRAM/TICAM-2
235 aa
SAM
SAM
TIR
SARM
690 aa

(b)

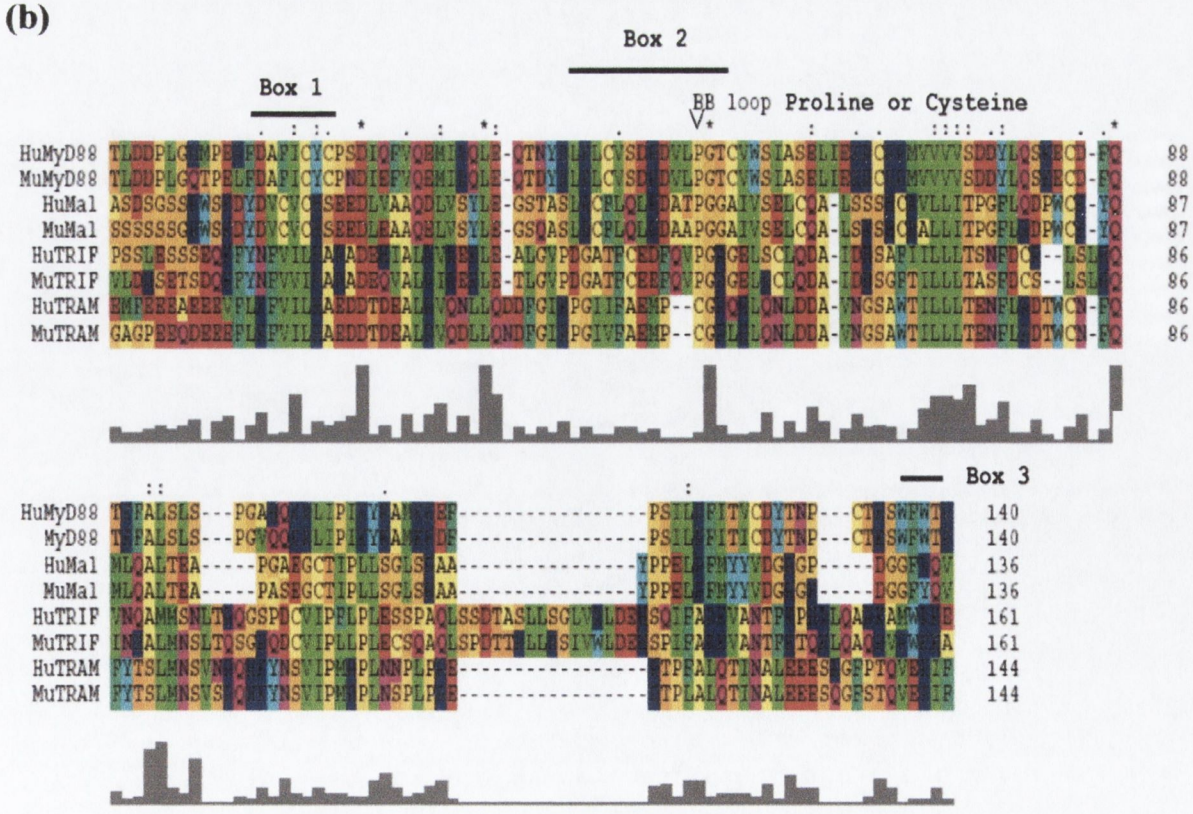
Box 2
Box 1
BB loop
Proline or Cysteine
Box 3
HuMyD88
MuMyD88
HuMal
MuMal
HuTRIF
MuTRIF
HuTRAM
MuTRAM

1.3 Mal

Mal was initially identified during high-throughput sequencing of a human dendritic cell expressed sequence tag (EST), complementary DNA library and found to have sequence similarity to MyD88 and other TIR-domain-containing genes (Fitzgerald, Palsson-McDermott et al. 2001). In particular, the TIR domain of Mal was found to contain the signature sequence (F/Y) D of Box 1, and the consensus sequence RD and PG of Box 2, while Box 3 is absent (Figure 1.3a).

Initial research into the function of Mal, determined that it is required for NF-κB, Jun amino-terminal kinase (JNK) and extracellular signal-regulated kinase (ERK)-1 and ERK-2 activation (Fitzgerald, Palsson-McDermott et al. 2001; Horng, Barton et al. 2001). Mal also promotes phosphorylation of the p65 subunit of the NF-κB complex, which is required for transactivation of gene expression (Mansell, Brint et al. 2004). It was established that Mal interacted with TLR4, but not with TLR9, and that overexpression of the isolated TIR domain of Mal and a cell-permeable Mal blocking peptide both inhibited LPS signalling, clearly demonstrating that TLR4-signalling is Mal-dependent (Horng, Barton et al. 2001). The generation of Mal-deficient mice has since confirmed that Mal is required for LPS signalling, as Mal knock-out (KO) macrophages showed delayed NF-κB translocation and MAPK phosphorylation following stimulation with LPS (Horng, Barton et al. 2002; Yamamoto, Sato et al. 2002). Interestingly, it was noted that NF-κB translocation was essentially eliminated in Mal KO macrophages following MALP-2 stimulation, establishing an additional role for Mal in TLR2 signalling. A direct interaction between Mal and TLR2 has been observed (Gray, P., unpublished), furthermore Mal has also been reported to interact with TLR1 (Fitzgerald, K.,

unpublished). Mal-deficient macrophages responded normally to poly(I:C) (TLR3), flagellin (TLR5), R-848 (TLR7), CpG DNA (TLR9), IL-1 (IL-1R) and IL-18 (IL-18R), indicating that Mal is not required to mediate responses *via* these receptors.

Yeast-two hybrid analysis has shown that Mal can also form homodimers, and that it heterodimerises with MyD88 (Fitzgerald, Palsson-McDermott et al. 2001). Although both adapters bind to TLR2 and TLR4, molecular modelling based on electrostatic surface representations suggest that Mal and MyD88 do not compete for the same binding site, and that both adapters are believed to bind to each other at a non-overlapping site (Dunne, Ejdeback et al. 2003). It has also been determined that Mal associates with the adapters TRIF and TRAM (Bin, Xu et al. 2003; Fitzgerald, Rowe et al. 2003)

Recent work has determined that Mal interacts with tumour-necrosis factor-receptor (TNFR)-associated factor (TRAF6) and contains a TRAF6 binding motif (Pro-Pro-Glu-Leu-Arg-Phe) (Mansell, Brint et al. 2004). TRAF6 is an ubiquitin ligase that recruits the ubiquitin-UBC13 (ubiquitin-conjugating enzyme 13)-UEV1 (ubiquitin-conjugating enzyme E2 variant 1) complex which promotes its auto-ubiquitination (Deng, Wang et al. 2000). Mutation of the critical glycine residue within the TRAF6 binding site located within Mal, to an alanine (Mal-E190A), did not effect the Mal-TRAF6 interaction, suggesting that other regions of Mal, yet to be identified, may be required to mediate this association. Nevertheless although the TRAF6 binding site was not required for TRAF6 association, it was determined that it was essential for Mal signalling. In particular, it was required for Mal to mediate NF-κB, JNK and p42/p44 MAPK activation. Furthermore, Mal-E190A failed to activate p65-mediated transactivation of

gene expression, and inhibited TLR2- and TLR4-mediated NF-κB activation. It has already been established that the MyD88/IRAK complex recruits TRAF6, therefore it has been suggested that the ability of Mal to interact with TRAF6 may be an essential mechanism required to recruit additional TRAF6 molecules to the TLR signalling pathway.

Regarding interactions with protein kinases that have been implicated in TLR signalling, it has been reported that Mal interacts with IRAK2 but not with overexpressed IRAK1 (Fitzgerald, Palsson-McDermott et al. 2001). However although Mal does not bind to overexpressed IRAK1, studies with Mal-deficient cells revealed that similar to MyD88, Mal is required for IRAK1 kinase activity in response to stimuli activating the TLR2 and TLR4 pathways (Yamamoto, Sato et al. 2002). Mal has also been shown to interact with a non-receptor protein-tyrosine kinase, termed Bruton's tyrosine kinase (Btk) (Jefferies, Doyle et al. 2003) (see Section 1.5.2 for further discussion). In addition, Mal associates with the interferon (IFN)-regulated, double-stranded RNA (dsRNA)-activated protein kinase R (PKR), a kinase that has been recently implicated in LPS signalling (Horng, Barton et al. 2001). Mal was also observed to bind to the negative regulator of PKR activity termed p58, and a dsRNA-binding domain-containing protein that activates PKR, known as protein activator of PKR (PACT). These interactions were specific for Mal as association of MyD88 with PKR was not observed. Furthermore, a peptide designed to encompass the box 2 region in Mal inhibited PKR phosphorylation induced by LPS but not CpG (Horng, Barton et al. 2001). These observations support the theory that PKR functions downstream of Mal, although the exact mechanism has yet to be deciphered.

1.4 TLR signalling: an overview

1.4.1 The MyD88-dependent Pathway

Although MyD88- and Mal-deficient mice were resistant to the lethal effects of LPS, NF-κB activation and IRF-3 activation still occurred, albeit delayed (Horng, Barton et al. 2002; Yamamoto, Sato et al. 2002). This pointed to a role for MyD88 and Mal in the early response to LPS, known as the MyD88-dependent pathway (Figure 1.4). Much of what is known concerning the downsteam events mediated by the TLRs has been initially provided from studying the signalling mechanisms of IL1-RI. In brief, following association of the TIR domain-containing adapter proteins, IRAK1, IRAK2 and IRAK4 are recruited to the receptor complex along with the adapter TRAF-6 (Fig. 1.4) (Cao, Henzel et al. 1996; Cao, Xiong et al. 1996; Li, Commane et al. 1999; Li, Strelow et al. 2002; Suzuki, Suzuki et al. 2002). IRAK1 is then hyperphosphorylated, both by itself and by IRAK4. Hyperphosphorylation of IRAK1 decreases its affinity for the receptor complex while increasing its affinity for TRAF6 (Cao, Xiong et al. 1996). IRAK1 and TRAF6 interact with a membrane bound pre-associated complex of TGF-β activated kinase 1 (TAK1), and two TAK1-binding proteins (TAB), termed TAB1 and TAB2 (Jiang, Ninomiya-Tsuji et al. 2002). Phosphorylation of TAK1 and TAB2 occurs in this membrane bound complex, initiating the dissociation of TRAF6/TAK1/TAB1/TAB2 from the membrane to the cytosol, and IRAK1 degradation (Jiang, Ninomiya-Tsuji et al. 2002). TAK1 is subsequently activated which in turn activates the IκB kinase (IKK) complex consisting of IKKα, IKKβ and NEMO/IKKγ (Karin and Ben-Neriah 2000). The IKK complex consequently phosphorylates a set of inhibitory-binding proteins κB (IκBs), which triggers their ubiquitination and degradation. NF-κB is then released and

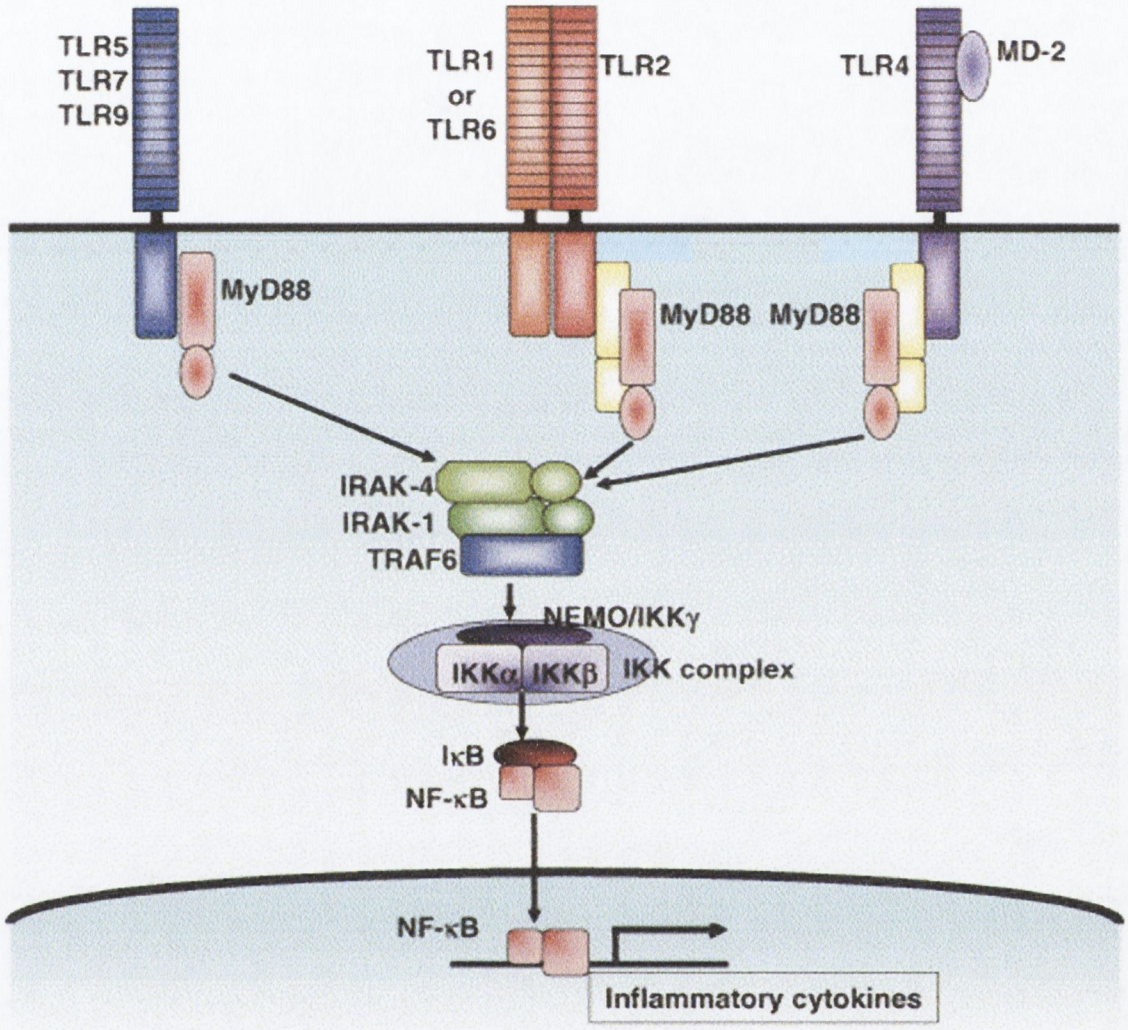

Figure 1.4 MyD88-dependent signaling pathway. MyD88, associates with the cytoplasmic TIR domain of TLRs, and recruits IRAK to the receptor upon ligand binding. IRAK then activates TRAF6, leading to the activation of the IκB kinase (IKK) complex consisting of IKKα, IKKβ and NEMO/IKKγ. The IKK complex phosphorylates IκB, resulting in nuclear translocation of NF-κB that induces expression of inflammatory cytokines. Mal is involved in the MyD88-dependent signaling pathway via TLR2 and TLR4.Taken from Takeda and Akira 2004.

translocated into the nucleus, which results in the induction of pro-inflammatory gene expression (Mercurio, Zhu et al. 1997; Regnier, Song et al. 1997; Woronicz, Gao et al. 1997; Zandi, Rothwarf et al. 1997).

1.4.2 The MyD88-independent/TRIF-dependent pathway

Thus far, TLR3 and TLR4 appear to be the only receptors that can signal in the absence of MyD88. Moreover, TLR3 seems to be unique in that it signals exclusively through the adapter protein TRIF, whereas TLR4 signalling in the absence of MyD88, requires both TRIF and TRAM (Yamamoto, Sato et al. 2003; Yamamoto, Sato et al. 2003). *In vitro* studies suggest that TRAM functions as a bridging adapter to recruit TRIF to the receptor complex as it has emerged that TRIF does not directly bind to the TIR domain of TLR4 (Oshiumi, Sasai et al. 2003). The MyD88-independent/TRIF-dependent pathway is required to initiate the delayed activation of NF-κB and IRF-3 (Figure 1.5). Following recruitment of TRAM and TRIF in the case of TLR4, or TRIF alone in response to TLR3 activation, the model for NF-κB activation is presumed to involve a similar series of events as noted above, with TLR3 signalling being shown to require the receptor-interacting protein-1 (RIP-1) for sufficient NF-κB activation (Sun, Yin et al. 2002). The activation of IRF-3 however involves the noncanonical IKKs, IKKε, (also called IKK-i), and TANK-binding kinase-1 (TBK1), (also known as tumour necrosis factor (TNF) receptor-associated factor 2 (TRAF-2)-associated kinase (T2K)). In brief, IKKε and TBK-1 mediate phosphorylation and activation of IRF-3 through interaction with TRIF and TRAM. Full activation of IRF-3 is reported to require further phosphorylation which is dependent on recruitment of the lipid kinase, phosphoinositol 3-

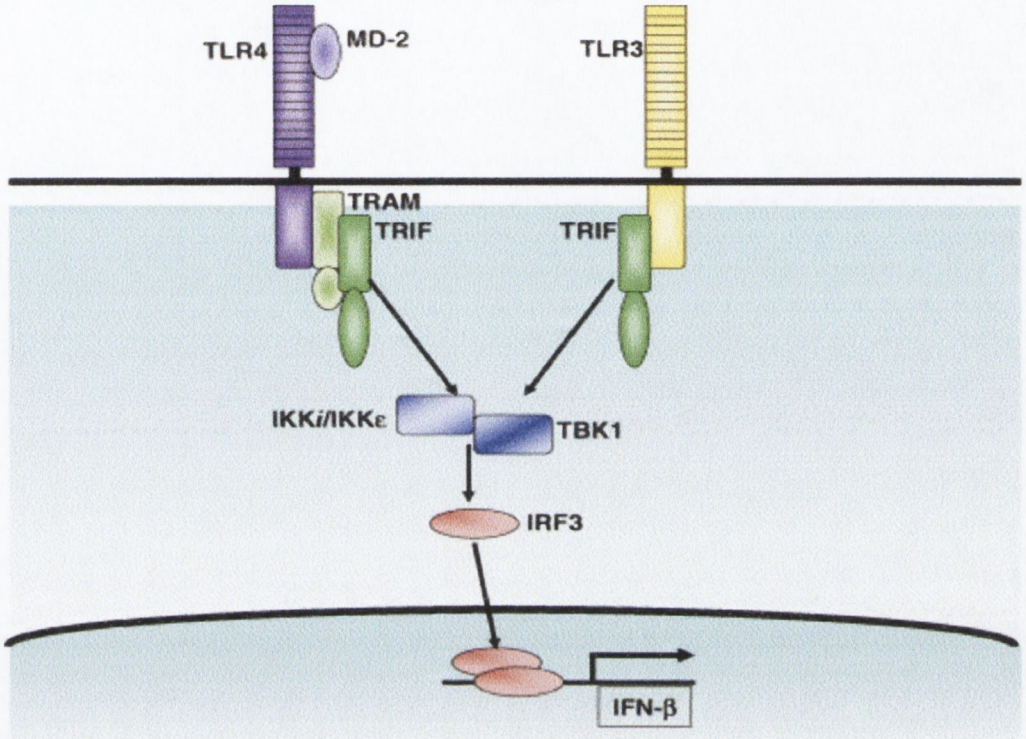

Figure 1.5 MyD88-independent signaling pathway. In TLR3- and TLR4-mediated signaling pathways, activation of IRF-3 and induction of IFN-β are observed in a MyD88-independent manner. A third TIR domain-containing adaptor, TRIF, is essential for the MyD88-independent pathway. Non-typical IKKs, IKK*i*/IKKε and TBK1, mediate activation of IRF-3 downstream of TRIF. A fourth TIR domain-containing adaptor, TRAM, is specific to the TLR4-mediated MyD88-independent (TRIF-dependent) pathway. Taken from Takeda and Akira 2004.

kinase (PI3K) to tyrosine phosphorylated TLR3 (see section 1.4.3, for further discussion) (Sarkar, Smith et al. 2003). IRF-3 dimerisation and nuclear translocation subsequently occurs, allowing IRF-3 to bind to the interferon-sensitive response element (ISRE), thereby inducing the IFN-β promoter which leads to the induced expression of IFN-inducible genes (Arbibe, Mira et al. 2000; Fitzgerald, Rowe et al. 2003; Sharma, tenOever et al. 2003)

1.5 Phosphorylated proteins in the TLR and adapter molecule subgroups

1.5.1 TLR4

It has long been thought that tyrosine kinases were intrinsically involved in the signalling pathway mediated by LPS (Ziegler, Wilson et al. 1988). Recently, it has been determined that TLR4 itself, undergoes time dependent tyrosine phosphorylation upon LPS stimulation (Chen, Zuraw et al. 2003). To date, the tyrosine residue or residues that are phosphorylated remain undetermined, as does the LPS activated protein tyrosine kinase.

1.5.2 TLR2

Studies have also indicated that TLR2 is tyrosine phosphorylated following stimulation with heat killed *Staphylococcus aureus* (HKSA) (Arbibe, Mira et al. 2000). It is believed that the small GTPase Rac1 mediates this phosphorylation event. Results demonstrated that a signalling complex is formed upon stimulation with HKSA consisting of Rac1, the cytoplasmic domain of TLR2 and the p85 subunit of the lipid kinase, phosphoinositol 3-kinase (PI3K). PI3K consists of a catalytic subunit (p110)

associated with a regulatory subunit (p50α, p55α and p85α) (Leevers, Vanhaesebroeck et al. 1999). The regulatory subunit of PI3K consists of tandem SH2 domains, which interact with phosphotyrosine YXXM motifs (Fry 1994). It has been hypothesized that this signalling complex activates NF-κB by phosphorylation of the p65 subunit of NF-κB.

Simultaneous mutation of two tyrosine residues located in two putative PI3K binding sites in the cytosolic region of TLR2, at positions 616 and 761, abolished NF-κB activity and p85 association (Arbibe, Mira et al. 2000). As TLR2 was found not to exhibit intrinsic tyrosine kinase activity, autophosphorylation can be ruled out. Therefore it is assumed that TLR2 tyrosine phosphorylation is regulated by a yet to be identified tyrosine kinase, that is activated upon HKSA stimulation through a Rac1-dependent pathway.

1.5.3 TLR3

In addition to TLR2 and TLR4, TLR3 has been reported to contain phosphotyrosine residues (Sarkar, Smith et al. 2003). It was determined that phosphorylation of TLR3 on tyrosine in response to dsRNA, was essential for TLR3 signalling. Further investigation revealed that tyrosine phosphorylation of TLR3 is required to recruit PI3K to its cytoplasmic domain. This event most likely initiates a kinase cascade, which leads to full activation of IRF-3 as a result of further phosphorylation events on yet to be identified residues in IRF-3 (Sarkar, Smith et al. 2003).

1.5.4 MyD88

In addition to TLR2 it has determined that both TLR4 and MyD88 associate with PI3K, upon LPS stimulation. MyD88 interaction with PI3K was observed even when cells were untreated, however upon LPS stimulation, formation of this complex increased rapidly and transiently (Ojaniemi, Glumoff et al. 2003). Further investigations revealed that MyD88 is tyrosine phosphorylated, and that tyrosine phosphorylation was enhanced upon stimulation with LPS. Additional work is required to identify the tyrosine kinase responsible for phosphorylating MyD88.

1.5.5 TRIF

Reminiscent of TLR4 and MyD88, TRIF was also found to be phosphorylated upon LPS stimulation, and once phosphorylated TRIF was observed to bind to TRAF6 (Sato, Sugiyama et al. 2003). In addition, co-expression of either IKKε or TBK1, with the N terminal and TIR domain of TRIF resulted in TRIF phosphorylation (Shimada, Kawai et al. 1999; Bonnard, Mirtsos et al. 2000; Peters and Maniatis 2001), suggesting that these kinases might mediate this phosphorylation event. Although TRIF phosphorylation appears to be regulated by LPS, the real significance of this phosphorylation event has yet to be determined.

1.5.6 TRAM

It has also been reported that TRAM is phosphorylated following TLR4-mediated NF-κB activation (Bin, Xu et al. 2003). However, the mechanisms of TRAM

phosphorylation have yet to be deciphered, as neither the region that is phosphorylated, nor the kinase responsible for mediating phosphorylation of TRAM, have been identified.

1.6 Protein Kinases implicated in TLR Signalling

1.6.1 Serine/Threonine Kinases

As previously mentioned, following recruitment of the TIR domain-containing proteins, a cascade of kinase activity is initiated involving the IRAKs. To date there are four members in this family, IRAK1, and IRAK4, both of which possess kinase activity and the kinase inactive proteins, IRAK2 and IRAKM. All four members contain a death domain at the N-terminus followed by a regulatory domain, a kinase domain, and a C-terminal undefined region (Figure 1.6).

1.6.1.1 IRAK1

Initial studies into the function of IRAK1, established that IRAK1 activates NF-κB and is required for IL-1-mediated NF-κB activation (Wesche, Henzel et al. 1997). Analysis of IRAK1-deficent mice demonstrated that in addition to IL-1 signalling, IRAK1 is also required to mediate responses to LPS (Thomas, Allen et al. 1999; Swantek, Tsen et al. 2000) Studies have revealed that IRAK1 associates with MyD88 upon activation of the TLR signalling pathway, and that this association is mediated through the death domains present in both proteins (Wesche, Henzel et al. 1997). Once IRAK1 is associated with the receptor complex it is phosphorylated both by IRAK4 and by autophosphorylation on multiple residues (Li, Strelow et al. 2002).

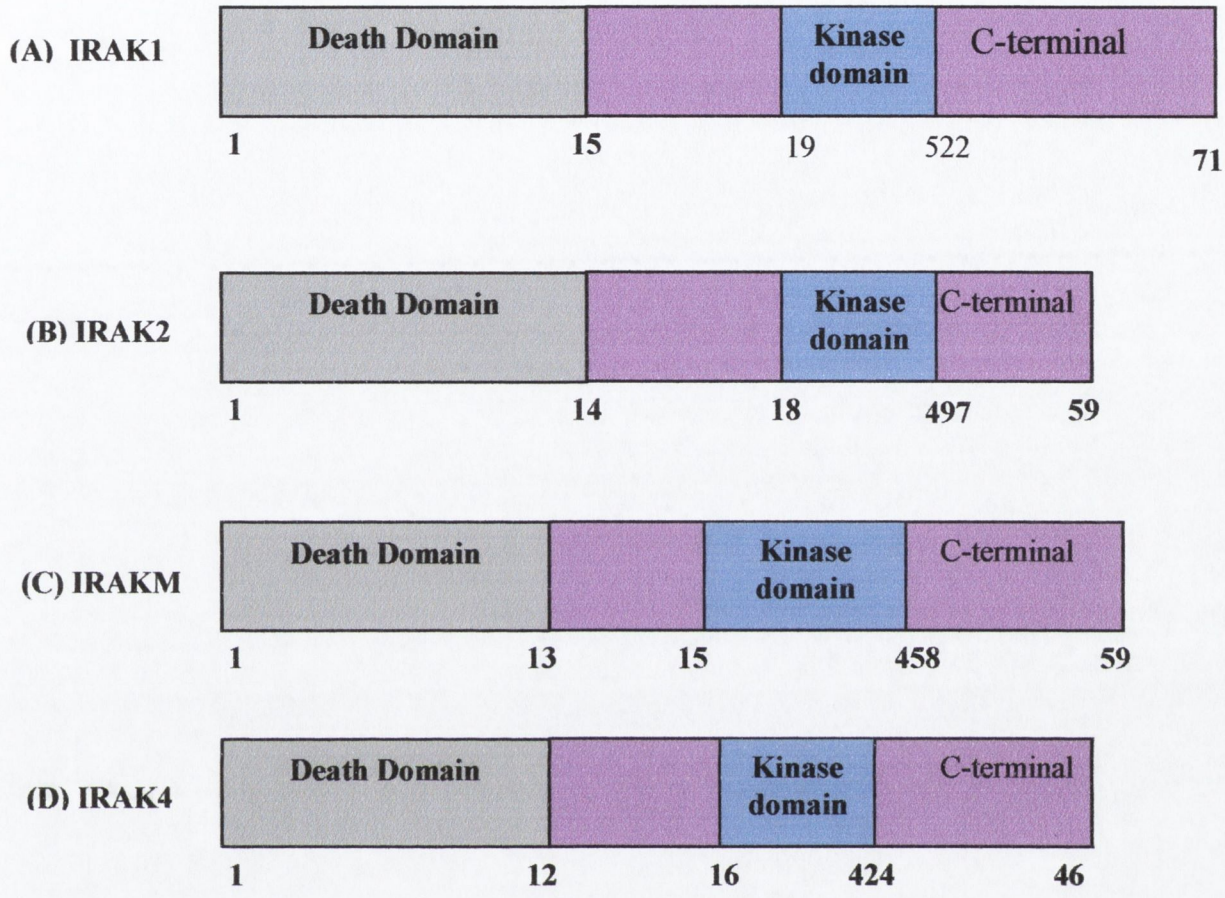

Figure 1.6 Schematic representation of IRAK family members (IRAK1, 2, M and 4). All four members contain a death domain at the N-terminus followed by a regulatory domain, a kinase domain, and a C-terminal undefined region.

Recent investigations have clarified the complex series of events resulting in IRAK1 activation. In brief, three sequential autophosphorylation steps are required for phosphorylation of IRAK1, the sites of which have been mapped to Thr-209 and Thr-387, culminating in the hyperphosphorylation of several residues in the ProST region located between the death domain and kinase domain. Although Thr-209 and Thr-387 were found to be phosphorylated by IRAK1 itself, peptide analysis has shown that these residues are also potential targets for phosphorylation by IRAK4. It is believed that phosphorylation of IRAK1 by IRAK4 triggers IRAK1 autophosphorylation (Kollewe, Mackensen et al. 2004). Results have shown that hyperphosphorylation of IRAK1 releases IRAK1 from the adapter molecule Tollip and the receptor-MyD88 complex (Burns, Clatworthy et al. 2000). This leads to the formation of a new protein complex comprising of hyperphosphorylated IRAK1 and TRAF6. Hyperphosphorylation of IRAK1 leads to its ubiquitin-mediated proteolysis, thus depleting the intracellular pool of IRAK1 available for signal transduction. To date the only substrates known for IRAK1 are IRAK1 itself, Tollip, Pellino2 and IRF-7, but their phosphorylation sites for Tollip, Pellino2 and IRF-7 have yet to be determined (Burns, Clatworthy et al. 2000; Strelow, Kollewe et al. 2003; Uematsu, Sato et al. 2005).

1.6.1.2 IRAK4

Preliminary studies investigating the role of IRAK4 in TLR signalling determined that IRAK4 activates the ERK, JNK and NF-κB pathways (Li, Strelow et al. 2002). In addition, it has been ascertained that upon overexpression IRAK4 undergoes auto- and/or cross-phosphorylation (Li, Strelow et al. 2002). Interestingly, it was noted that in contrast

to the other members of the IRAK family, IRAK4 requires its kinase activity to activate NF-κB (Li, Strelow et al. 2002). Reconstitution of IRAK4 in cells deficient in IRAK1 cannot activate NF-κB in response to IL-1 (Li, Strelow et al. 2002). Further investigation revealed that IRAK1 autophosphorylation is partially inhibited in cells overexpressing a kinase-inactive form of IRAK4 (Li, Strelow et al. 2002). It has also emerged that only the kinase-inactive form of IRAK4 can interact with IRAK1, MyD88 and TRAF6 (Li, Strelow et al. 2002). Taken together these results suggest that the kinase activity of IRAK4 important for mediating TIR-domain signalling.

Studies with IRAK4-deficient mice confirmed an essential role for IRAK4 in TLR signalling (Suzuki, Suzuki et al. 2003). In brief, mice lacking IRAK4 were completely resistant to LPS-induced septic shock and showed virtually no cytokine response. Following LPS stimulation, IRAK4-deficient macrophages exhibited delayed and decreased activation of NF-κB. Similar to LPS treatment, IRAK4-deficient macrophages stimulated with ligands for TLR2, TLR3 and TLR9 failed to produce inflammatory mediators. The position of IRAK4 in the TLR signalling pathway was also investigated and it was determined using IRAK4-deficient cells that both MyD88 and Mal require IRAK-4 for signal transduction, whereas TRAF6 does not (Suzuki, Suzuki et al. 2003). As mentioned above, IRAK4 signalling is dependent on its kinase activity, suggesting that it may be required to mediate a series of phosphorylation events for efficient TLR signalling. Thus far the only known substrates for IRAK4 are IRAK4 itself, IRAK1 and Pellino2 (Li, Strelow et al. 2002; Strelow, Kollewe et al. 2003; Kollewe, Mackensen et al. 2004). However, the exact phosphorylated residues of IRAK4 or Pellino2 that are phosphorylated by IRAK4 have yet to be elucidated.

1.6.1.3 The IκB kinase (IKK) complex

In addition to the IRAKs, it has also emerged that serine-specific kinases termed the IκB kinases (IKKs), are essential components of TLR-mediated NF-κB activation. The IKK complex contains two closely related kinases, IKKα (also known as IKK1) and IKKβ (also known as IKK2), and a structural subunit termed IKKγ (Karin and Ben-Neriah 2000). TAK1 phosphorylates and activates IKKβ on serine 177 and 181 (Malinin, Boldin et al. 1997). The activated IKK complex then phosphorylates the NF-κB inhibitor protein, IκBα, on serine residues 32 and 36 (Karin and Ben-Neriah 2000). This leads to the polyubiquitination and degradation of IκBα, thereby allowing NF-κB to translocate into the nucleus. To date it is believed that the kinase activity of both IKKε and TBK1 are essential components of the IRF-3 signalling pathway mediated by the adapter protein TRIF, however it has yet to be determined if these kinases phosphorylate IRF-3 directly (Fitzgerald, Rowe et al. 2003).

In addition, IKKβ, IKKε and TBK1 have been shown to phosphorylate the p65 subunit of NF-κB, on Ser-536 resulting in its enhanced transactivating activity (Weinstein, Gold et al. 1991; Fitzgerald, McWhirter et al. 2003).

1.6.1.4 The mitogen activated protein kinases (MAPKs)

A large family of serine/threonine kinases termed the mitogen activated protein kinases (MAPKs) have also been implicated in TLR signal transduction. Three major groups of the MAPKs regulate TLR signalling in humans, namely the extracellular signal regulated kinases (ERKs), c-Jun N-terminal kinase (JNK) and p38 MAPK.

Activation of MAPKs themselves require initial phosphorylation on both threonine and tyrosine residues by the MAP kinase kinases (MAPKK), which are in turn activated by serine/threonine phosphorylation by MAPKK kinases (MAPKKKs). TAK1 is a member of the MAPKKK family, which is required for the phosphorylation and activation of IKKβ (Malinin, Boldin et al. 1997). TLR mediated activation of the MAPKs leads to the phosphorylation of many proteins, the best studied of which is the activating protein-1 (AP-1) family of transcription factors which cooperate with NF-κB in mediating an immune response against the invading pathogen.

1.6.1.5 Receptor-interacting protein (RIP) family kinases

The RIP family of serine/threonine kinases consists of seven members (RIP1-7), all of which are closely related to the IRAK family (Meylan and Tschopp 2005). Previous studies have shown that RIP1 mediates NF-κB activation independent of its kinase activity (Hsu, Huang et al. 1996; Ting, Pimentel-Muinos et al. 1996). However, the ability of RIP3 to induce NF-κB activation remains controversial, as conflicting reports show that RIP3 can both activate and inhibit NF-κB (Pazdernik, Donner et al. 1999; Sun, Lee et al. 1999; Yu, Huang et al. 1999; Kasof, Prosser et al. 2000). A short region of approximately 35 amino acids, termed the RIP homotypic interaction motif (RHIM), was identified in the intermediary domains of RIP1 and RIP3. Association studies have revealed that RIP3 and RIP1 interact *via* their RHIMs, which subsequently results in RIP1 phosphorylation by RIP3 (Sun, Yin et al. 2002). It has since emerged that TRIF also possesses a RHIM, which mediates recruitment of RIP1 and RIP3 to the TLR3 signalling pathway (Meylan, Burns et al. 2004). TLR3- but not TLR4-mediated NF-κB activation

was abolished in the absence of RIP1, indicating that RIP1 plays a crucial role on the signalling pathway emanating from TLR3 (Meylan, Burns et al. 2004). In contrast to RIP1, RIP3 negatively regulated the capacity of TRIF to activate NF-κB by competing with the interaction between RIP1 and TRIF (Meylan, Burns et al. 2004). Similar to RIP1 and RIP3, RIP2 overexpression results in activation of NF-κB. RIP2 KO studies have revealed a role for RIP2 in mediating signals emanating from TLR2, TLR4, and TLR3 (Chin, Dempsey et al. 2002).

1.6.1.6 PKR

PKR is an additional serine/threonine kinase involved in TLR signalling. Studies have revealed that mice deficient in PKR were unable to activate p38 and JNK MAPKs following LPS treatment (Goh, deVeer et al. 2000). It has also been determined that following LPS signalling, PKR is a critical component in mediating apoptosis (Hsu, Park et al. 2004). As has been discussed in Section 1.2.2, PKR has been shown to interact with Mal, further implicating PKR in the TLR signalling pathway (Horng, Barton et al. 2001)

1.6.2 Tyrosine Kinases

1.6.2.1 Src-family

In addition to serine/threonine kinases, it has long been thought that tyrosine kinases were intrinsically involved in the signalling pathway mediated by LPS (Weinstein, Gold et al. 1991). In particular, it has been reported that inhibition of the non-receptor Src-family tyrosine kinase Lyn, following LPS treatment, impaired production of the cytokine TNF-α in monocytes (Stefanova, Corcoran et al. 1993). Further studies

have shown that upon LPS stimulation, the kinase activity of both Src and Lyn is increased in human dendritic cells (Napolitani, Bortoletto et al. 2003).In addition, increased synthesis of the Src kinases, Hck and Lyn following chronic exposure of macrophages to LPS has been reported.

Taken together these results suggested a role for the Src kinases in mediating the signalling pathway initiated by LPS. However, the generation of triple knockout mice deficient in the Src-family kinases, Hck, Fgr and Lyn demonstrated that these kinases are not essential for mediating the signalling pathway induced by LPS (Meng and Lowell 1997). Nonetheless, the investigators could not rule out the possibility that other members of the Src-family kinases could compensate for the lack of expression of Hck, Fgr and Lyn. Further work is therefore required to ascertain the exact role of the Src-family in TLR signalling.

1.6.2.2 Syk

Recent evidence has also ascribed a role for the tyrosine kinase Syk, in the LPS induced activation of JNK. Studies have determined that Syk is activated following LPS treatment. In addition, Syk was found to associate with TLR4, and this association increased upon LPS stimulation (Arndt, Suzuki et al. 2004). Further studies are required to elucidate the exact mechanisms of Syk-mediated JNK activation.

1.6.2.3 Btk

Btk was first identified as the gene responsible for X-linked agammaglobulinemia (XLA), an immune disorder in humans characterised by abnormal B cell development

(Bradley, Sweatman et al. 1994). A naturally occurring mutation in Btk leads to the less severe X-linked immune deficiency (Xid) in mice (Rawlings 1999). Btk is a non-receptor protein-tyrosine kinase, belonging to the Tec family. Its structure is divided into 4 main domains; a Src homology (SH) 2 domain; a SH3 domain; a pleckstrin homology (PH) domain responsible for membrane localisation due to its high affinity for phosphatidylinositol lipids; and a Tec homology (TH) domain which contains a proline-rich region (Figure 1.7a).

Btk was initially implicated as a participant in LPS signalling, following the discovery that B cells derived from Xid mice exhibited impaired responses following LPS treatment. (Mukhopadhyay, Mohanty et al. 2002; Jefferies, Doyle et al. 2003). Further investigation revealed that monocytes from patients with XLA were also unresponsive to LPS (Horwood, Mahon et al. 2003). A role for Btk in LPS signalling was further established following the observation that LPS treatment induced tyrosine phosphorylation of Btk and activated its kinase activity *in vitro* (Horwood, Mahon et al. 2003). Moreover the Btk inhibitor, LFM-A13, inhibited NF-κB activation mediated by LPS. Association studies have revealed that Btk interacts with key components of the TLR signalling pathway. At the receptor level, Btk associates with the TIR domains of TLR4, TLR6, TLR8 and TLR9 (Jefferies, Doyle et al. 2003). In addition, Btk interacts with the adapter molecules MyD88 and Mal, and with IRAK1.

Studies have shown that Btk is not required for IκB-α degradation in response to LPS. Rather, evidence has emerged indicating that Btk is involved in the LPS-induced pathway leading to phosphorylation of the p65 subunit of NF-κB on Ser-536, promoting transactivation of gene expression (Doyle, Jefferies et al. 2005).

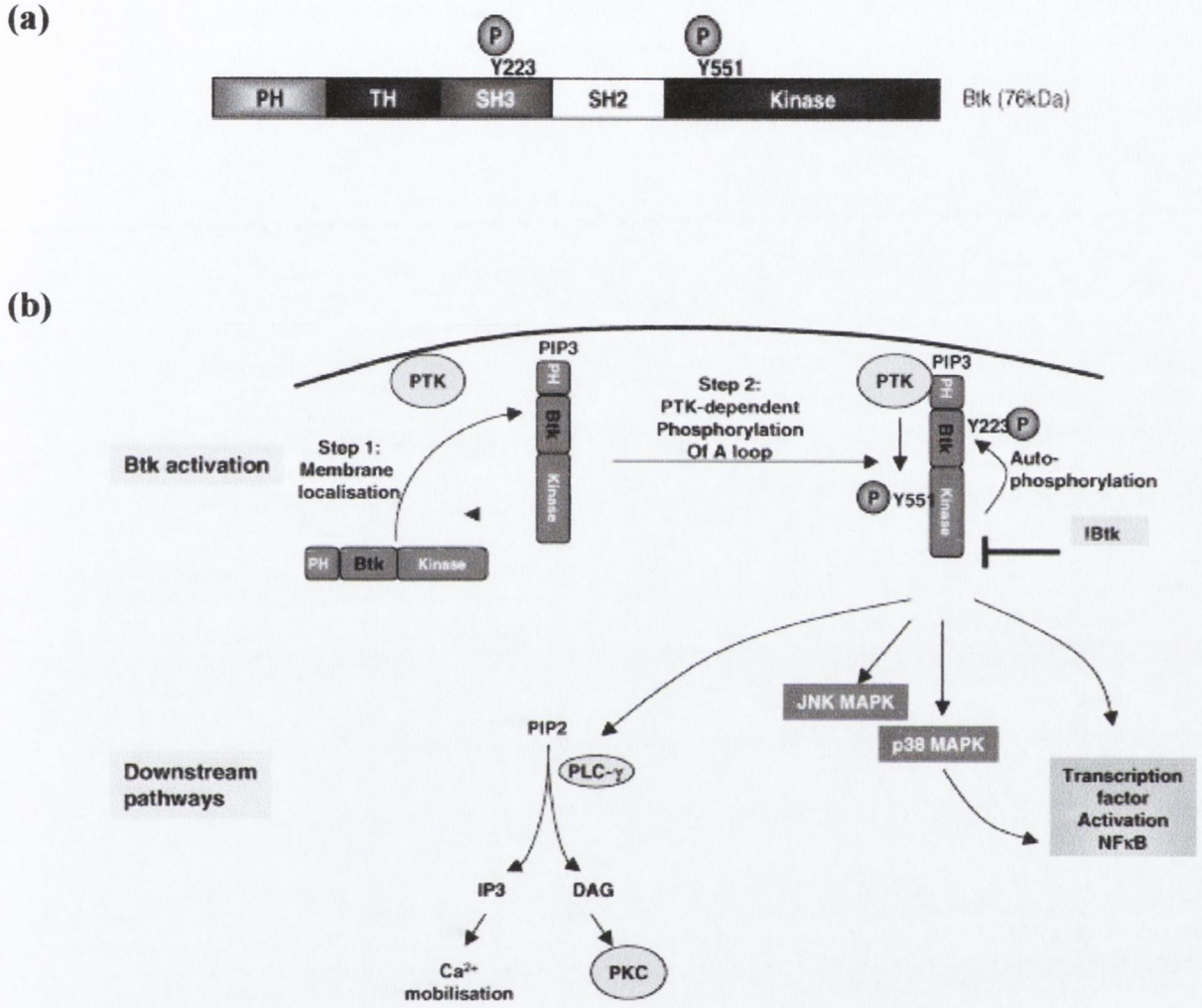

Figure 1.7 Schematic representation of the structure of Btk and the its activation pathway. (a) Domain structure of Btk. The tyrosine phosphorylation sites located in Btk are as indicated. PH, pleckstrin homology domain; TH, Tec homology region; SH3, Src-homology 3 domain; SH2, Src-homology 2 domain; Kinase, kinase domain. (b) The two step process of Btk activation. See text for details. PTK, protein tyrosine kinase; A loop, activation loop. Taken from Jefferies, Doyle et al. 2003.

The exact mechanisms leading to Btk activation following LPS stimulation have yet to be elucidated. However, normally Btk activation is a two step process, with membrane targeting of Btk being required initially (Figure 1.7b). The PH domain of Btk binds selectively to phosphatidylinositol(3,4,5) triphosphate (PIP3), a product of PI3-Kinase, which results in recruitment of Btk to the plasma membrane of the cell, an event that is essential for Btk activation as this relieves intramolecular inhibition of its kinase domain (Suzuki, Terauchi et al. 1999). Incidentally, PI3K is activated by TLR2, TLR4 and TLR9 signalling. Given that Btk interacts directly with multiple TLRs, it remains to be elucidated if these interactions are sufficient to promote translocation of Btk to the membrane. Btk can also become membrane bound *via* its interaction with the G protein βγ subunit and F-actin, again through its PH domain. Membrane targeting of Btk is a prerequisite for its phosphorylation, as it is here that Btk comes in close proximity with an array of protein kinases.

The second step in Btk activation involves phosphorylation of Btk by members of the Src family, such as Lyn. This phosphorylation event has been mapped to Tyr-551 which is located on the activating loop of Btk. Src kinases are known to be activated following LPS treatment, suggesting that Src kinases may phosphorylate Btk in response to LPS stimulation. Transphosphorylation of Btk, results in the autophosphorylation of Tyr-223 in the SH3 domain of Btk, thereby activating downstream signalling pathways. (Kurosaki and Kurosaki 1997).

The crystal structure of Btk has been resolved, revealing that Btk displays an extended conformation with no, or little, inter-domain interactions (Marquez 2003). This implies that unlike Src kinases, Btk does not require an assembled conformation for the

regulation of its kinase activity. As Btk lacks a negative regulatory domain which is present in the Src kinases, it has led to speculation that Btk may rely on cytoplasmic proteins to regulate its kinase activity. Indeed, recent evidence has reported the identification of a new Btk-interacting protein, termed IBtk which inhibited Btk kinase activity and NF-κB activation mediated by Btk upon anti-IgM stimulation (Liu, Quinto et al. 2001). In addition Sab and c-Cbl are known negative regulators of Btk kinase activity (Marquez, Smith et al. 2003).

Recent evidence has revealed that Btk directly phosphorylates the transcription factor, cAMP response element-binding (CREB) on Ser-133, during neuronal differentiation (Yang, Yoon et al. 2004). This observation revealed that Btk can act as a dual specific protein kinase, as it can phosphorylate both tyrosine and serine/threonine residues of exogenous substrates. To date, the only other identified substrate for Btk is the B cell antigen receptor (BCR)-associated protein (BCAP), which is transiently phosphorylated on tyrosine in response to BCR engagement (Yang and Desiderio 1997).

1.6.3 P13K

Studies have also implicated PI3K, a kinase that catalyses the phosphorylation of phosphoinositides, in TLR signal transduction (Leevers, Vanhaesebroeck et al. 1999). In particular it has been determined that LPS-induced IκB-α degradation is dependent on PI3K activity in primary B cells and that mice deficient in p85, p55 and p50 subunits of PI3K, failed to respond normally to LPS treatment (Fruman, Snapper et al. 1999). Furthermore, inhibition of P13K has been reported to impair TLR3-mediated signalling (Sarkar, Smith et al. 2003). As has been previously discussed, PI3K has been shown to

interact with members of the TLR signalling pathway, namely TLR2, TLR3, TLR4 and MyD88 (Arbibe, Mira et al. 2000; Ojaniemi, Glumoff et al. 2003; Sarkar, Smith et al. 2003)

In addition, recent reports have suggested a negative regulatory role for PI3K, as IL-12 synthesis by dendritic cells from PI3K-deficient mice was enhanced following activation of the TLR2, TLR4, and TLR9 pathways (Fukao, Tanabe et al. 2002). To date, evidence has emerged implying that PI3K is both a positive and negative regulator of TLR signalling. Further work is therefore required to elucidate the exact role of PI3K in the TLR signalling pathway.

1.7 Negative regulation of TLR-mediated immune responses

1.7.1 Soluble decoy TLRs

Activation of the TLR signalling pathway, if left unrestrained, can contribute to severe immunopathologies including Crohn's disease and septic shock. It is for this reason that it is essential that TLR signal transduction is tightly regulated in order to prevent tissue damage that arises from sustained inflammation. Multiple checkpoints are in place in order to control TLR signalling. Beginning at the receptor level, the first-line of negative regulation is performed by naturally produced soluble TLRs. These proteins are believed to behave as decoy receptors by preventing a direct interaction between TLRs and their bacterial ligands. To date only soluble forms of TLR2 and TLR4 have been described (Iwami, Matsuguchi et al. 2000; LeBouder, Rey-Nores et al. 2003).

1.7.2 Intracellular and transmembrane negative regulators

1.7.2.1 MyD88s, ST2

Upon activation, the TLRs can be further controlled by intracellular negative regulators which are present either constitutively or are upregulated. These proteins can interfere with the formation of signalling competent TLR complexes thus limiting TLR signalling. An example of a TIR domain-containing negative regulator is MyD88s, an alternatively spliced form of MyD88 which lacks the short intermediate domain (ID) that separates the death domain and the TIR domain in the full-length form of MyD88 (Janssens, Burns et al. 2002). MyD88s limits the TLR response by preventing recruitment of IRAK4 to the receptor signalling complex, thereby inhibiting the ability of IRAK4 to phosphorylate IRAK1. In addition to MyD88s, the orphan transmembrane receptor, ST2, is an important TIR-domain containing negative regulator. ST2 is present in two forms, the full length version (ST2L) and a soluble form (sST2). The mode of action for sST2 has yet to be deciphered, whereas ST2L is known to sequester MyD88 and Mal through its TIR domain (Brint, Xu et al. 2004). Other proteins that negatively regulate TLR activation but do not contain TIR domains include IRAKM, splice variants of IRAK1 and IRAK2, Tollip, PI3K, and suppressor of cytokine signalling (SOCS-1) (Liew, Xu et al. 2005).

1.7.2.2 SOCS-1

SOCS-1 is a member of the SOCS family of proteins, and comprises of an N-terminal kinase inhibitory region (KIR) thought to function as a pseudosubstrate, a central SH2 domain which binds phosphorylated tyrosine residues, and a C-terminal SOCS box,

which has been reported to mediate interactions with elongins B and C, both of which are members of the E3 ubiquitin ligase complex (Figure 1.8) (Larsen and Ropke 2002). It is well established that most cytokine receptors activate intracellular non-receptor protein tyrosine kinases of the Janus family (JAK1, JAK2, JAK3 and Tyk2). Cytokine binding induces oligomerization of receptor subunits leading in turn to trans-phosphorylation and activation of JAKs. Activated JAKs subsequently phosphorylate the cytoplasmic domain of the receptor, thereby creating a docking site for SH2 domains of signal transducer and activation of transcription (STAT) molecules. STATs are then phosphorylated on specific tyrosine residues by JAKs, resulting in their dimerisation and translocation into the nucleus to induce transcription of cytokine responsive genes (Larsen and Ropke 2002).

SOCS-1 was initially identified as an intracellular negative-feedback molecule that inhibits overactivation of the JAK-STAT-mediated signal cascade initiated by various stimuli, such as IFN-γ, IL-4 and IL-6 (Starr, Willson et al. 1997). A role for SOCS-1 in TLR signalling has also been established from studies using SOCS-1-deficient mice. In particular, it was noted that SOCS-1-deficient macrophages produced heightened levels of nitric oxide and pro-inflammatory cytokines in response to stimulation with the TLR4 and TLR9 ligands, LPS and CpG DNA respectively (Kinjyo, Hanada et al. 2002; Nakagawa, Naka et al. 2002). Mice lacking SOCS-1 have also been shown to be hypersensitive to LPS-induced endotoxic shock compared to wild-type mice (Kinjyo, Hanada et al. 2002; Nakagawa, Naka et al. 2002). Furthermore, SOCS-1 expression was induced in macrophages following stimulation with LPS, MALP-2 and CpG DNA (Kinjyo, Hanada et al. 2002). In response to LPS stimulation, macrophages from SOCS-1-deficient mice exhibited enhanced phosphorylation of STAT-1, IκB-α, p38 and JNK.

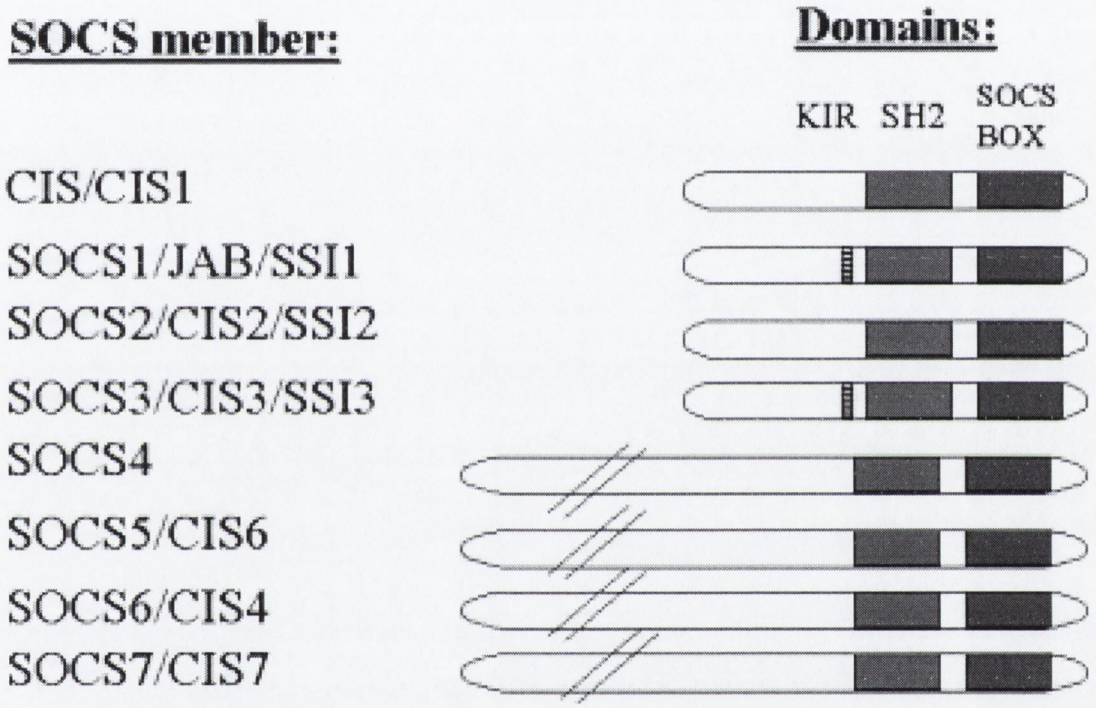

Figure 1.8 Schematic drawimg depicting the domain structures of the SOCS family members. The kinase inhibitory region of SOCS-1 and SOCS-3 is dashed. KIR, kinase inhibitory region. Taken fron Larsen and Ropke 2002.

Furthermore, overexpression of SOCS-1 abolished LPS-induced NF-κB activation. It has been reported that SOCS-1 interacts with IRAK-1 through its SH2 domain, indicating that IRAK-1 may be its target for regulating TLR4 and TLR9 signalling (Nakagawa, Naka et al. 2002). Taken together these results suggest a negative-feedback regulatory mechanism for TLR4 and TLR9 signalling.

1.7.3 Degradation of TLRs and TIR domain adapters

TLR activation can be further controlled by downregulation of essential components in the signalling pathway, resulting in a reduced inflammatory response. Regarding members of the TLR family, evidence has emerged indicating that Triad3A, an E3 ubiquitin-protein ligase, downregulates TLR4 and TLR9 expression through ubiquitination and degradation (Chuang and Ulevitch 2004). Moreover, TLR2 has been shown to be basally ubiquitinated although the exact mechanisms leading to this have yet to be determined.

In addition, it has been reported that the anti-inflammatory cytokine, transforming growth factor-β1 (TGF-β1) downregulates TLR4 expression and induces degradation of MyD88, thereby limiting TLR signalling (Naiki, Michelsen et al. 2004).

1.8 Aims and Objectives

Preliminary evidence suggested that Mal may be post-translationally modified upon overexpression. This study sought to further define this event. The specific aims were as follows:

- To investigate if Mal was post-translationally modified by phosphorylation.
- To identify the kinase or kinases involved, having determined that Mal was phosphorylated.
- To identify the phospho-accepting Mal residues.
- To determine the functional relevance of Mal phosphorylation for signal transduction

.

The overall aim of the project was to provide novel insights into TLR signalling by focusing on Mal phosphorylation.

Chapter 2

Materials and Methods

2.1 Materials

Lipopolysaccharide from *Escherichia coli* serotype O26:B6 (Cat. No. L8274) was purchased from Sigma (Poole, Dorset, UK). γ-^{32}P-ATP, 9.25 Ci/mmol was obtained from Amersham Life Sciences (Uppsala, Sweden). The FLAG M2 antibody was obtained from Sigma (Poole, Dorset, UK). Maxi prep and endotoxin free plasmid purification kits were obtained from Promega (Madison, Wisconsin, USA). The human macrophage THP-1 cell line was obtained from the European Collection of Animal Cell Cultures (Salisbury, U.K.) The human embryonic kidney cell line 293 (HEK293) was a gift from Tularik Inc, San Francisco, CA 94080. All cell culture materials, RPMI 1640, DMEM, penicillin, streptomycin, gentamycin, trypsin, L-glutamine and foetal calf serum were obtained from Sigma (Poole Dorset, UK). Genejuice was purchased from Novagen. General laboratory chemicals were purchased from Sigma (Poole, Dorset, UK), with the exception of Glutathione-Sepharose 4B (Amersham), coelentrazine (Argus Fine Chemicals), Passive Lysis Buffer (Promega), Broad band pre-stained protein marker (New England Biolabs Ltd.), and ECL reagent (Amersham). The Btk specific inhibitor, LFM-A13, was obtained from Calbiochem (Nottingham, United Kingdom).

N-terminal His-tagged, recombinant, full-length, human BTK, expressed by baculovirus in Sf21 insect cells, was purchased from Upstate (Catalogue number: 14-552). Recombinant His-tagged IRAK1 and recombinant His-tagged IRAK4 were expressed from a baculovirus in insect cells and were gifts from Holger Wesche, Tularik, Inc.

2.2 Expression vectors

The empty vector pCDNA3.1 was purchased from Invitrogen. The expression vector pCDNA3-Mal and pCDNA3-Mal-(P125H) was a kind gift from Dr. Mikael Edjeback. pGex4T2-Mal was a kind gift from Dr. Aisling Dunne. The pGL3-5κB-luc plasmid was a kind gift from Dr. R Hofmeister (Universitat Regensburg, Germany). The plasmid encoding MyD88 was a gift from M. Muzio (Mario Negri Institute, Milan, Italy). IRAK1 (wild type and dominant negative versions) were kind gifts from Emma-Louise Cooke (Glaxo-Welcome, Stevenage UK). The plasmid encoding CD4-TLR4 was a kind gift from Dr. R. Medzhitov (Yale, New Haven, CT, USA).

2.3 Cell culture

The HEK293 cell line was cultured in DMEM medium while the THP-1 cell line was cultured in RPMI 1640 medium. All medium contained 10% (v/v) foetal calf serum, 100 U/ml gentamycin and 2 mM L-glutamine. Cells were maintained at 37°C in a humidified atmosphere of 5% CO_2. For use in transfection assays, HEK293 were typically seeded at $1x10^5$ ml^{-1} in 96 well plates or 10 cm dishes, 24 hrs prior to transfection. For continuing cell culture cells were seeded at 1×10^5 ml^{-1} and sub-cultured every 3-4 days. In all cases cell viability was determined using the dye Trypan blue, which is excluded from healthy cells but taken up by non-viable cells. Cells were counted using a haemocytometer and a bright light microscope.

2.4 DNA plasmid mutagenesis

2.4.1 *In vitro* site-directed mutagenesis

The parental DNA used in all reactions was either pCDNA3-Mal or pGEX4T2-Mal in the case of GST fusion proteins. DNA had been purified using Wizard® PureFection Plasmid DNA Purification System from Promega, isolated from the dam^+ DH5α *Escherichia coli* strain. The mutant oligonucleotide primers are depicted below.

Y86F Forward: 5' GCT GGA GCA AAG ACT TCG ACG TCT GCG TGT GC 3'

Y86F Reverse: 5' GCA CAC GCA GAC GTC GAA GTC TTT GCT CCA GC 3'

S105A Forward: 5' CAG GAC CTG GTC GCC TAC TTG GAA GGC 3'

S105A Reverse: 5' GCC TTC CAA GTA GTA GGC GAC CAGGTC CTG 3'

Y106E Forward: 5' GAC CTG GTC TCC GAA TTG GAA GGC AGC 3'

Y106E Reverse: 5' GCT GCC TTC CAA TTC GGA GAC CAG GTC 3'

Y106F Forward: 5' GAC CTG GTC TCC TCC TTG GAA GGC AGC 3'

Y106F Reverse: 5' GCT GCC TTC CAA GAA GGA GAC CAG GTC 3'

Y159F Forward: 5' CCC CTG GTG CAA GTT CCA GAT GCT GCA GG 3'

Y159F Reverse: 5' CCT GCA GCA TCT GGA ACT TGC ACC AGG GG 3'

Y187F Forward: 5' CAG CAG AGC TGC CTT CCC ACC TGA GCT CC 3'

Y187F Reverse: 5' GGA GCT CAG GTG GGA AGG CAG CTC TGC TG 3'

Y195F Forward: 5' GAG CTC CGA TTC TAC GTC GAT GGC AGG 3'

Y195F Reverse: 5' CCT GCC ATC GAC GTA GAA CAT GAA TCG GAG CTC 3'

Y196F Forward: 5' CTCCGA TTC ATG TAC TTC GTC GAT GGC AGG GGC 3'

Y196F Reverse: 5' GCC CCT GCC ATC GAC GAA GTA CAT GAA TCG 3'

Mutant strand synthesis reaction was conducted using the Quick-Change® Site-Directed Mutagenesis Kit supplied by Stratagene. Sample reactions were prepared as indicated below:

5µl of 10x reaction buffer

10ng of parental DNA

125ng of Forward Primer

125ng of Reverse Primer

1µl of dNTP mix

Sterile distilled H_2O to a final volume of 50µl

Finally 1µl of *PfuTurbo* DNA polymerase (2.5 U/µl) was added. The cycling parameters for the Site-Directed Mutagenesis were as follows:

95°C for 30 seconds

16 cycles of 95°C for 30 seconds

55°C for 60 seconds

68°C for 6 minutes

Following temperature cycling, the reaction was placed on ice for 2 minutes to cool the reaction to approximately 37°C. 1µl of the *Dpn I* restriction enzyme (10 U/µl) was added directly to each amplification reaction and mixed thoroughly. The reaction mixture was spun down in a microcentrifuge for 1 minute and incubated immediately at 37°C for 1 hour to digest the parental supercoiled dsDNA.

2.4.2 DNA plasmid transformation

Samples were then transformed into XL1-Blue supercompetent cells (Stratagene). Cells were gently thawed on ice and once thawed, 50µl of the supercompetent cells were aliquoted into pre-chilled Falcon® 2059 polypropylene tubes. 1µl of the *Dpn I*-treated DNA from the sample reaction was transferred to separate aliquots of the supercompetent cells. The transformation reaction was swirled gently to mix and incubated on ice for 30 minutes. Following this incubation period the transformation reaction was heat pulsed for 45 seconds at 42°C and then placed on ice for 2 minutes. 500 µl of Luria Broth pre-heated to 42°C was added to each sample and the transformation reaction was incubated for 1 hour at 37°C with shaking at 250 rpm. 250 µl of the transformation reaction was plated on agar plates containing the antibiotic ampicillin. The transformation plates were incubated at 37°C for 18 hours.

2.4.3 Restriction digestion of DNA plasmids

Approximately 1 µg DNA to be digested was incubated with 1 unit of the appropriate restriction enzyme and 1X buffer as recommended by the manufacturers in a final volume of 20 µl. BSA was also added to the mixture if required, to a final concentration of 100 µg/ml. The reaction mix was then incubated at 37°C for 1 hour.

2.4.4 Mini-preparation of plasmid DNA

DNA from bacterial colonies was isolated using Wizard® *Plus* SV Minipreps DNA Purification System (Promega, Madison WI, USA). Briefly, bacterial cultures were grown in 5 ml LB medium. Bacteria cultures were then centrifuged and resuspended in

250 µl Cell Resuspension Solution. Cells were incubated for 5 minutes with the addition of 250 µl Cell Lysis Solution before addition of 350 µl neutralization solution. The mixture was centrifuged at 13,000 x g for 10 minutes at room temperature. The cleared lysate was transferred to a spin column inserted into a 2 ml collection tube. The supernatant was centrifuged for 1 minute at room temperature and then washed with 750 µl and then 250 µl Column wash solution. The DNA was eluted by addition of 100 µl Nuclease Free H_20. The insert was then sequenced to verify that selected clones contained the desired mutation.

2.5 DNA plasmid purification for transient transfection

2.5.1 Preparation of competent DH5α cells

One colony of the bacterial strain DH5α grown from a glycerol stock was picked and transferred to 10 ml of L-broth and cultured overnight shaking at 37°C overnight. 150 µl of this culture was transferred to 10 ml of fresh L-broth and cultured for 2 hours or until it reached an absorbance of 0.6 at 600nm. The cells were centrifuged at 10,000 rpm for 10 min at 4°C and resuspended in 5 ml of autoclaved ice cold 50 mM $CaCl_2$. The cells were incubated on ice for 30 minutes before repeating the centrifugation and finally resuspended in 1 ml of $CaCl_2$. The cells were then incubated on ice for 1-1.5 hours, aliquoted and frozen in liquid N_2 and stored at -70°C.

2.5.2 DNA plasmid transformation

DH5α competent cells were prepared as described in section 2.5.1 and 1 µg of plasmid DNA was transformed into these competent cells as in section 2.4.2.

2.5.3 DNA plasmid purification procedure

Plasmids were purified using Wizard® PureFection Plasmid DNA Purification System from Promega. Bacterial cultures were pelleted by centrifugation at 10,000 x g for 10 minutes at 4°C. Cells were resuspended in 6.25 ml resuspension buffer (50 mM Tris-HCL pH 7.5, 10 mM EDTA, 100 mg/ml RNAse A). 8.25 ml cell lysis buffer (0.2M NaOH, 1% (w/v) SDS) was then added and allowed to incubate for 5 minutes at room temperature. The reaction was then stopped by the addition of 8.75 ml Neutralisation Buffer (1.32 M potassium acetate, pH 4.8) and mixed thoroughly. Cellular debris was removed by centrifugation at 10,000 x g for 40 minutes. Supernatant was retained and endotoxin removed by addition of 2.5 ml Endotoxin Removal Resin. Plasmid DNA was then mixed with 5 ml of 5 M guanidine thiocyanate and purified using MagneSil™ paramagnetic particles. In order to purify the DNA further it was washed with 5 ml 4/40 Wash Solution (4.2 M guanidine-HCL/40% (v/v) isoproponal) and multiple times with 80% (v/v) ethanol. Plasmid DNA was then dissolved in 6 ml water and precipitated using 3 ml 7.5M sodium acetate and 22.5 ml 95% ethanol. DNA was pelleted by centrifugation at 14,000 x g for 15 minutes, washed in 70% ethanol and pelleted again by centrifugation at 14,000 x g for 5 minutes before dissolving in 500 ml TE buffer pH 7.4. Plasmid DNA quality and concentration was determined on a 0.8% (w/v) agarose gel stained with ethidium bromide and by obtaining the A_{260} of the DNA.

2.6 Transient transfection

GeneJuice Transfection Reagent from Novagen was used for transfection of HEK293 cells. For a 96 well plate transfection, cells were seeded at $1x10^5$ ml^{-1} and

grown overnight. Cells were transfected in triplicate with 220 ng DNA per transfection. In all cases the amount of DNA used per transfection was normalised using the appropriate amount of relevant empty vector control. 0.8 µl Gene Juice was mixed with 9.2 µl serum free DMEM per transfection and incubated at room temperature for 5 minutes. 30 µl of this mixture was added to triplicate amounts of DNA and incubated for 15 minutes at room temperature. 10 µl per well was then added to the cells, which were allowed to recover for 16 hours at 37°C prior to stimulation. For 6 well plate transfection the total DNA used was 1-2 µg, 8 µl Gene Juice and 92 µl DNA. For transfection of 100 mm plates, 4-8 µg DNA was used in combination with 15 µl Gene Juice and 235 µl serum free DMEM.

2.7 Luciferase gene reporter assay

2.7.1 Preparation of cellular lysates

HEK293 cells were transfected in 96 well plates as described in section 2.6. Cells were washed with 1x PBS, they were then lysed for 15 minutes at room temperature with 50 µl 1x Passive Lysis Buffer (Promega, Madison, Wisconsin, USA). Following centrifugation of plates for 10 minutes (2000 x g) at room temperature, 50% of the supernatant was used to determine Firefly luciferase activity and an equivalent amount used for *Renilla* luciferase activity.

2.7.2 Measurement of luciferase activity

Firefly luciferase activity was assayed by the addition of 40 µl of luciferase assay mix (20 mM tricine, 1.07 mM $(MgCO_3)_4Mg(OH)_2.5H_2O$, 2.67 mM MgSO4, 0.1 M

EDTA, 33.3 mM DTT, 270 mM coenzyme A, 470 mM luciferin, 530 mM ATP) to the sample and *Renilla* luciferase was read by the addition of 40 ng Coelentrazine (Innovation Centre, University of Sussex, Falmer, Brighton, UK) in PBS. Luminescence was read using Mediators PHL luminometer. Firefly luminescence readings were corrected for *Renilla* activity and expressed as fold stimulation over unstimulated empty vector (EV) control.

2.8 Western blot analysis

2.8.1 Preparation of cell extracts

Cells were seeded as in 2.4. Reactions were terminated with the addition of ice-cold PBS to the cells followed by centrifugation at 1500 x g for 5 minutes. Pellets were resuspended in 1 ml PBS and transferred to eppendorfs. The samples were centrifuged at 12000 x g (5 minutes, 4°C) and the pellets resuspended in 150-300 µl of RIPA buffer (PBS buffer containing 1% Nonidet P40, 0.5% (w/v) sodium deoxycholate and 0.1% SDS containing 10 µg/ml PMSF, 30 µl/ml aprotinin and 1 µl/ml sodium orthovanadate). The cells were then incubated on ice for 30 minutes with the addition of a further 3 µl 10 µg/ml PMSF. Following this incubation period, samples were centrifuged at 13000 x g for 20 minutes at 4°C. The supernatants (total cell lysate) were assayed for protein (see section 2.9) and aliquots containing equal amounts of protein were mixed with 5 µl SDS sample buffer (5 ml glycerol, 10 ml 10% SDS, 10 mg bromophenol blue, 6.25 ml 1M Tris pH 6.25, 28.75 ml H_2O). 250 µl β-mercaptoethanol was added per ml of sample buffer immediately prior to use. Samples were then boiled for 5 minutes.

2.8.2 SDS Polyacrylamide Gel Electrophoresis (SDS-PAGE)

Samples were resolved on Sodium Dodecylsulphate (SDS) polyacrylamide gel using a constant current of 25 mA per gel. Samples were first run through a stacking gel (1 ml 30% bisacrylamide mix, 0.75 ml 1 M Tris pH 6.8, 60 µl 10% ammonium persulphate and 6 µl TEMED made up to 6ml with H_2O) to condense protein and then resolved according to size using 10-15% polyacrylamide gels (required volume of 30% bisacrylamide mix, 3.75 ml 1.5 M Tris pH 8.8, 150 µl 10% (w/v) ammonium persulphate, 6 µl TEMED made up to 15 ml with H2O) Samples were then run with pre-stained protein markers (New England Biolabs) as molecular weight standards.

2.8.3 Transfer of proteins to membrane

The resolved proteins were transferred to either nitrocellulose or polyvinylidene diflouride (PVDF) using a wet transfer system with all components soaked beforehand in transfer buffer (25 mM Tris-HCl pH 8.0, 0.2 M glycine, 20% methanol). Briefly, the gel was placed on a sponge followed by a layer of filter paper and overlaid with nitrocellulose paper. A second piece of filter paper was placed on top followed by a second sponge. The entire assembly was placed in a cassette and an electric current of 150 mA was applied for 2 hours.

2.8.4 Immunodetection

Membranes were blocked to prevent non-specific binding by incubation in blocking buffer (5% (w/v) non-fat dried milk in 1% (v/v) Tris Buffered Saline (TBS)-Tween at 4°C overnight. The membrane was washed for 5 minutes in 1% (v/v) TBS-

Tween three times. The membrane was then incubated for 1 hour at room temperature with the antibody of interest at 1:100 to 1:1000 dilutions depending on antibody. Next the membrane was washed three times and incubated with the appropriate secondary horseradish peroxidase linked antibody. Blots were developed by enhanced chemiluminescence (ECL) according to manufacturers instructions (Amersham).

2.8.5 Coomassie staining

Resolved gels were soaked in Coomassie Brilliant blue G stain (50% (v/v) methanol, 10% (v/v) glacial acetic acid, 2.5 g/L Coomassie blue dye) for at least 1 hour and then washed several times with destain Solution (50% (v/v) methanol, 10% (v/v) glacial acetic acid) until clear bands appeared.

2.9 Protein concentration determination

Protein determination was carried out by the method of Bradford. Samples were diluted 1:10 with Tris-HCl to give a final volume of 20 µl and 200 µl Bradford Reagent (0.01% (w/v) Coomassie Brilliant Blue G-250, 4.7% (v/v) ethanol, 8.5% (v/v) orthophosphoric acid) was added to each. The reaction was allowed to develop for 5 minutes after which time the plates were read at OD_{570} using a Dynatech MR5000 plate reader. Protein concentrations were determined using a standard curve constructed using BSA concentrations in the range 0-20 µg/20 µl. A typical standard curve is shown in figure 2.1.

2.10 Immunoprecipitation

The relevant antibodies were pre-coupled to either protein A (polyclonal antibodies) or protein G Sepharose (monoclonal antibodies), by incubating 30 µl of a 50% protein A/G slurry per immunoprecipitation sample with gentle rotation overnight at 4°C.

HEK293 cells were seeded into 10 cm dishes (1 x 10^5 cells/ml) 24 hours prior to transfection. Transfections were carried out using Genejuice™ Transfection Reagent as described in Section 2.6. For co-immunoprecipitations, 4 µg of each construct was transfected, where only one construct was expressed the total amount of DNA (8µg) was kept constant by supplementation with empty vector (pCDNA3.1). The cells were harvested 24 hours post-transfection by scraping in 1ml of ice-cold PBS. The samples were centrifuged at 13,200 rpm for 5 minutes and the supernatant discarded. The pellets were resuspended in 1ml of ice-cold PBS and centrifuged again at 13,200 rpm for 5 minutes. The supernatant was discarded and the cells were lysed in 800µl of lysis buffer (50mM HEPES, pH 7.5, 100mM NaCl, 1mM EDTA, 10% glycerol, 0.5% NP-40, containing 1mM Aprotinin, 1mM sodium orthovanadate (Na_3VO_4) and 1mM PMSF) for 20 minutes. Samples were then centrifuged for 10 minutes at 13,200 rpm. Protein concentration of the supernatant was determined by the method of Bradford (Section 2.9) and lysates containing equal protein were added to the relevant pre-coupled antibody. Samples were incubated for 2 hours at 4°C with gentle rotation. For immunoprecipitation of phospho-Mal, cell lysates were incubated with anti-phosphotyrosine-agarose; clone PT-66, overnight at 4°C. A portion of the lysate was retained to confirm that the protein of interest was expressed, which was added to sample buffer and boiled for 4 minutes.

Following the incubation of samples at 4°C, the immune complexes were washed twice with 1ml of lysis buffer; the final wash contained 1ml of ice-cold PBS. The beads were then resuspended in 40µl of sample buffer, samples were boiled for 4 minutes and SDS-PAGE analysis was performed on the precipitated complexes.

2.11 GST-fusion proteins

2.11.1 Purification of GST-fusion proteins

10 ml of an overnight culture of BL21 transformed with the pGEX vector containing the relevant insert specified in the result section, was diluted into 500 ml LB and incubated at 37°C until the OD_{600} reached approximately 0.6. Cultures were pelleted by centrifugation at 10,000 x g for 20 minutes and the supernatant removed. Cells were then lysed in 30 ml of ice-cold NETN lysis buffer (100 mM NaCl, 1 mM EDTA, 20 mM Tris-HCL pH 8.0, 0.5% (v/v) NP-40). 20 µg/ml lysozyme was added and the lysate incubated on ice for 30 minutes. This was followed by sonication on ice with 5 second pulses followed by 5 second pauses to prevent over heating of the preparation. The suspension was cleared of insoluble material by centrifugation at 15,000 x g for 30 minutes. The lysate was then incubated with 0.5 ml of a 50% solution glutathione-agarose beads/PBS for 2 hours at 4°C. The beads were pelleted by centrifugation at 2000 x g for 5 minutes and washed 5 times with 25 ml washes of NETN. Finally the beads were resuspended in an equal volume of PBS and a 10 µl aliquot removed, added to 20 µl 5X SDS sample buffer (125 mM Tris-HCL pH 6.8, 10% glycerol, 2% (w/v) SDS, 0.0002% (w/v) bromophenol blue, 1% (v/v) β-mercaptoethanol) and boiled for 5

minutes. The protein-containing supernatant was then analysed by SDS-PAGE and Coomassie staining for the expression of the fusion proteins.

2.11.2 Affinity purification of complexes using GST-fusion proteins

Cells were transiently transfected with the indicated plasmids as described in section 2.6. After 24 hours cells were washed with ice-cold PBS and lysed on ice for 30 minutes in 1 ml lysis buffer (10 mM CHAPS, 150 mM NaCl, 2 mM EDTA, 10 mM Na_3VO_4, 2 mg/ml aprotinin,1 mM phenylmethylsulphonylflouride). Lysates were cleared by centrifugation at 13,200 x g for 5 minutes at 4°C and the protein concentration of the supernatant determined by the method of Bradford. Lysates containing equal protein were incubated for 1 hour at 4°C with approximately 10 μg of each GST-fusion protein or 10 μg of GST alone pre-coupled to glutathione agarose beads. The bead pellet was washed three times in lysis buffer and finally resuspended in 25 μl SDS sample buffer. Proteins were separated by SDS-PAGE and following transfer of proteins to nitrocellulose membranes, the precipitated complexes were analysed by western blotting.

2.12 Phosphatase treatment

2.12.1 Digestion of phosphoproteins with Calf intestine alkaline phosphatase (CIP)

Phosphoproteins were immunoprecipitated as described in Section 2.10, except that when cells were lysed 10 mM Na_3VO_4 was omitted in the preparation of the lysis buffer. The immunocomplexes were washed once more with the phosphatase digestion buffer (50 mM Tris-HCl, pH 7.5, 1 mM $MgCl_2$). 30 μl of the phosphatase buffer was

added per sample and where indicated, 100U of Calf intestine alkaline phosphatase (CIP) was added. Samples were incubated at 37°C for 3 hours. The reaction was terminated with the addition of SDS-PAGE sample buffer.

2.12.2 Digestion of phosphoproteins with protein tyrosine phosphatase (PTP-1B)

Phosphoproteins were immunoprecipitated as described in Section 2.10, except that when cells were lysed 10 mM Na_3VO_4 was omitted in the preparation of the lysis buffer. The immunocomplexes were washed once more with the phosphatase digestion buffer (50 mM imidazole, pH 7.5) for 10 minutes at 37°C. 10 U of protein tyrosine phosphatase-1B (PTP-1B) was added to each sample, were indicated, for 30 minutes at 37°C. The dephosphorylation reaction was terminated with the addition of SDS-PAGE sample buffer.

2.13 *In vitro* kinase assay

Immunoprecipitations and affinity purification of complexes using GST-fusion proteins were performed as described in sections 2.10 and 2.11 respectively. After immunocomplexes were washed twice with 1 ml of lysis buffer, they were washed an additional three times with kinase buffer (20 mM Hepes, pH 7.5, 2 mM DTT, 10 mM $MgCl_2$, 50 mM NaCl, 100 μM Na_3VO_4 and 20 mM β-glycerol phosphate, plus protease inhibitors namely 1mM Aprotinin, 1mM sodium orthovanadate and 1mM PMSF). On the final wash the remainder of the kinase buffer was removed. The indicated concentration of the substrate was then added to the immune complexes.

For direct *in vitro* kinase assays 100ng of the recombinant kinase, plus the indicated concentration of the recombinant substrate were used.

30μl of kinase buffer plus 2 μCi [γ^{32}P] ATP, 0.6 μM of cold ATP was then added to each sample. Samples were subsequently incubated at 37°C for 30 minutes. 20 μl of sample buffer was added to each sample and samples were analysed by SDS-PAGE. Gels were transferred onto polyvinylidene diflouride membrane and visualised by autoradiography

2.14 Two-dimensional SDS-PAGE

2.14.1 Sample preparation

HEK293 cells were seeded into 15 cm dishes (1 x 10^5 cells/ml) 24 hours prior to transfection. Transfections were carried out using Genejuice™ Transfection Reagent as described in Section 2.6.1 using 10 μg of DNA. Immunoprecipitations were carried out as described in Section 2.10.2 using the anti-HA antibody. After the immune complexes were washed, samples were resuspended in 400 μl of Sample solubilisation solution (8M Urea, 50mM DTT, 4% (w/v) CHAPS, 0.2% (w/v) carrier ampholytes, 0.0002% (w/v) bromophenol blue).

2.14.2 Isoelectric focusing

Sample was transferred to the rehydration tray. The 17 cm IPG strip (pH 4-7) obtained from Amersham was placed over the sample, and allowed to rehydrate over night at room temperature. Rehydrated strips were then moved to the focusing tray and were overlaid with mineral oil. The focusing conditions were as follows:

Step 1: Linear Slope to 500V for 1 hour

Step 2: Constant 500V for 5hours

Step 3: Linear slope to 3 500V for 5 hours

Step 4: Constant 3 500 for 12 hours

Step 5: Hold at 50V

2.14.3 Rehydration of IPG strips

IPG strips were incubated in DTT equilibration buffer (6M Urea, 375 mM Tris, pH8.8, 2% SDS, 20% glycerol and 2% DTT) for 10 minutes, followed by iodoacetamide equilibration buffer (6M Urea, 375 mM Tris, pH8.8, 2% SDS, 20% glycerol and 2.5% iodoacetamide) for 10 minutes.

2.14.4 Second dimension

IPG strips were positioned on top of the second dimension gel (12%) (16ml 30% bisacrylamide, 10ml 1.5M Tris, pH 8.8, 400 µl 10% SDS, 400 µl 10% APS, 16µl TEMED). The IPG strip was secured in place by overlaying it with 0.5% molten agarose prepared in SDS-PAGE running buffer with a small amount of bromophenol blue, used to track the ion front during electrophoresis. Samples were resolved on a SDS polyacrylamide gel using a constant current of 25 mA per gel. Samples were transferred and immunoblotted as described in Sections 2.8.3 and 2.8.4

2.15 Isolation and generation of murine splenocytes

Mice were euthanised in a CO_2 chamber. Using sterile instruments, the skin was cut away from the abdomen to expose the peritoneal membrane and sprayed with 70% alcohol. The spleen should be visible as a dark red brown organ at the mid-body region on the dorsal side. The peritoneal membrane was cut and the spleen was removed with a sterile forceps and placed in a petri dish. A sterile syringe and 26 gauge needle containing 10ml of DMEM supplemented medium (DMEM, 25 mM HEPES pH 7.3, 2 mM L-glutamine, 5% FCS, 100 U/ml gentamycin) was inserted into the spleen. Cells were flushed out by pressing the syringe plunger gently. The cell suspension was collected and centrifuged at 1000 rpm for 10 minutes. Cells were washed once in 10 ml of supplemented DMEM. Any red blood cells were removed at this stage using Red Blood Cell Lysis Buffer (Sigma). The supernatant was discarded and the pellet resuspended in 10 ml of medium. Cells were counted, and an appropriate quantity of medium was added to result in a seeding density of 1×10^6 ml^{-1}. Cells were maintained at 37° in a humidified atmosphere of 5% CO_2

3.1 Introduction

Intense investigations over the past 5 years have greatly improved our understanding of the complexity of the TLR signalling pathway. It is now well recognised that upon ligand binding activated TLRs initiate a kinase cascade which culminates in the activation of transcription factors, including NF-κB, AP1 and IRF-3. Several serine/threonine protein kinases are known to be activated during TLR signal transduction. In particular, the most receptor proximal serine/threonine protein kinases, which are recruited by TIR domain-containing adapters, are IRAK4 and IRAK1, RIP-1 and RIP-3, TBK-1 and PKR (Horng, Barton et al. 2001; Suzuki, Suzuki et al. 2002; Li, Strelow et al. 2002; Li, Commane et al. 1999; Cao, Henzel et al. 1996; Cao, Xiong et al. 1996). Regarding tyrosine kinase activation, the tyrosine kinases Src, Fgr, Hck, Lyn and Btk have all been shown to be activated upon TLR signal transduction (Stefanova, Corcoran et al. 1993; Jefferies, Doyle et al. 2003; Napolitani, Bortoletto et al. 2003).

Studies investigating the functional role of Mal have revealed that its electrophoretic mobility is reduced following SDS-PAGE analysis, which is often an indication that the protein may be post-translationally modified. Given that kinases play a crucial role in the activation and regulation of TLR signaling pathways, it was of interest to investigate if Mal was phosphorylated upon activation. Therefore, this investigation focused on the phosphorylation status of Mal and as a comparison MyD88. Having determined that Mal was covalently modified, the identity of the kinases involved was next assessed.

It has been reported that Mal interacts directly with the tyrosine kinase Btk. Immunoprecipitation studies in this chapter, determined that Mal also interacted with the

serine/threonine kinase IRAK1. Given that endogenous IRAK4 interacts with IRAK1 (Li, Strelow et al. 2002), investigations were carried out to determine if Btk, IRAK1, or IRAK4 were required for Mal phosphorylation. It was revealed that Mal is indeed a substrate for Btk, IRAK1 and IRAK4 *in vitro*.

Chapter 3

Analysis of Mal phosphorylation and identification of kinases involved

3.2 Results

3.2.1 Overexpressed Mal migrates as multiple species on SDS-PAGE

Previous data originally describing Mal revealed that in addition to the predominant 32 kDa form, slower migrating forms of Mal could be detected following SDS-PAGE analysis, suggesting that Mal may be covalently modified (Fitzgerald, Palsson-McDermott et al. 2001) To examine this, a plasmid encoding wild-type Mal tagged at its N-terminus with HA, was transiently transfected into the HEK293 cell line, samples were analysed by SDS-PAGE and immunoblotted with an anti-HA antibody. The observation that the mobility of Mal is retarded following SDS-PAGE analysis was verified and it was determined that Mal exists as four distinct forms, ranging in molecular size from approximately 29 to 36 kDa, with the predominant form corresponding to a 32 kDa protein (Figure 3.2.1a). Recent evidence has determined that the fastest migrating form of Mal detected in immunoprecipitates is a by-product of Mal cleavage by caspase-1. As a comparison, the mobility pattern of the adapter MyD88 was analysed. HEK293 cells were transiently transfected with a plasmid encoding AU1-MyD88, samples were analysed by SDS-PAGE and immunoblotted with an anti-AU1 antibody. In contrast to Mal, MyD88 was detected as a single band (Figure 3.2.1b).

Given that the mobility of Mal was retarded on SDS-PAGE, it was of interest to analyse the mobility pattern of the N-terminus of Mal and its TIR domain. Similar to wild-type Mal, the truncated versions of Mal contained slower migrating species. In particular, it was observed that two species could be detected for the N-terminus of Mal (Figure 3.2.2a), whereas the TIR domain of Mal existed as three distinct forms (Figure 3.2.2b).

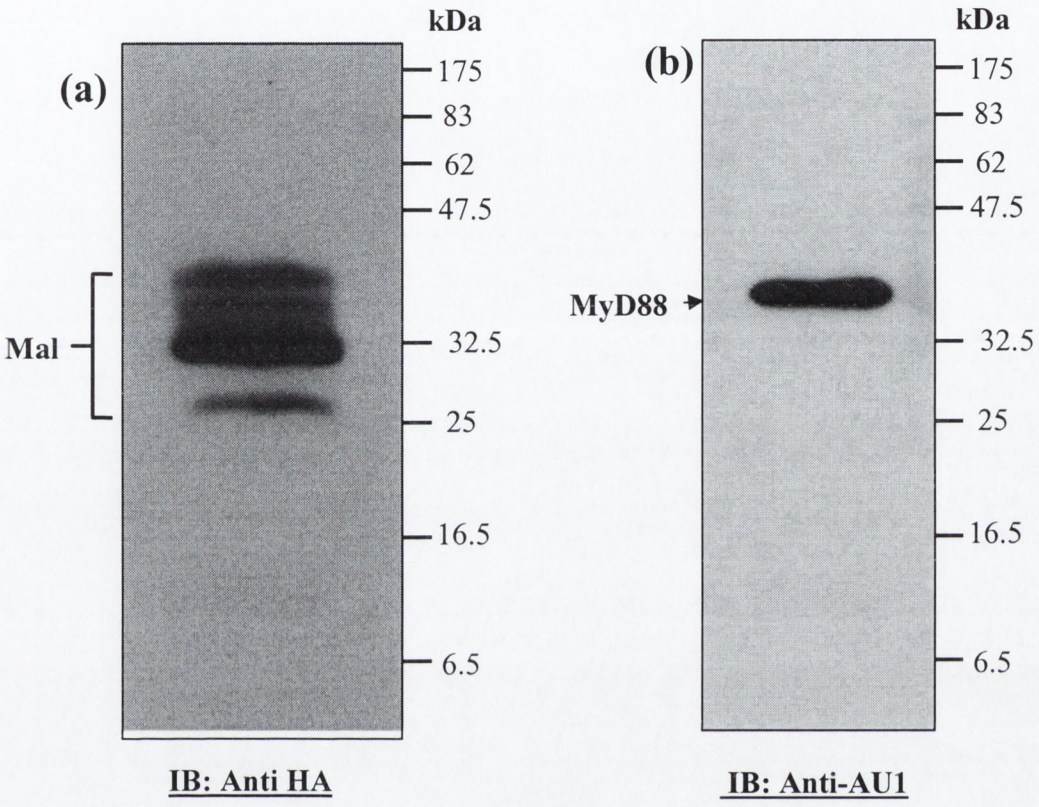

Figure 3.2.1 Slower migrating forms of overexpressed Mal were detected upon immunoblotting, whereas MyD88 migrates as a single form. HEK293 cells (1x 10^6) were transiently transfected with 4μg of plasmid encoding (a) HA-Mal or (b) AU1-MyD88 for 24 hours. Cells were lysed in high stringency lysis buffer and centrifuged to remove cell debris. 25 μl of the cell lysate was added to SDS-PAGE sample buffer and analysed by SDS-PAGE, which was followed by immunoblotting with the indicated antibody. Data shown is a representative experiment from four separate experiments.

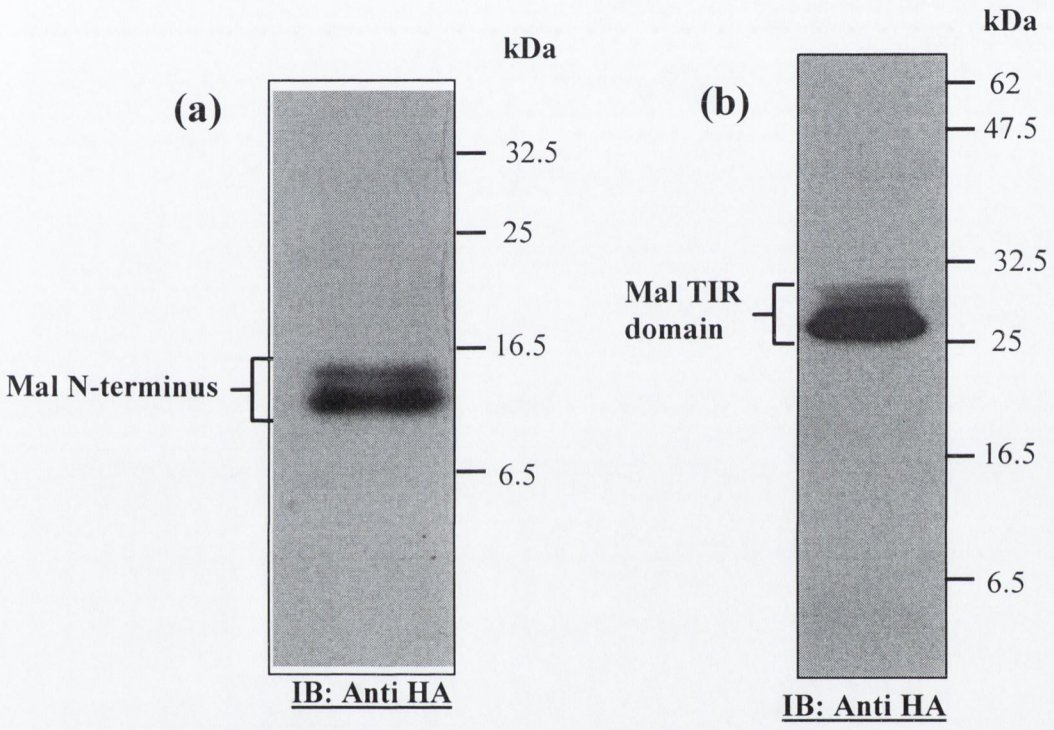

Figure 3.2.2 Similar to full length Mal, both the N-terminal and the TIR domain of Mal, contain slower migrating forms when analysed by SDS-PAGE. HEK293 cells ($1x10^6$) were transiently transfected with 4 μg of plasmid encoding (a) the N-terminal of Mal or (b) the TIR domain of Mal. Cells were lysed in high stringency lysis buffer and centrifuged to remove cell debris. 25 μl of the cell lysate was added to SDS sample buffer and analysed by SDS PAGE, followed by immunoblotting with the anti-HA antibody. Data shown is a representative experiment from four separate experiments.

3.2.2 Two-dimensional analysis of Mal

As the isoelectric point of a protein is always altered once phosphorylation occurs, the electrophoretic mobility of Mal by two-dimensional (2-D) gel analysis was examined. Using the computer programme, Compute pI/Mw, located on the ExPASy Proteomics Server, it was determined that the theoretical isoelectric point of Mal was 5.95. In order to determine if the isoelectric point of Mal was altered, HEK 293 cells were transiently transfected with a plasmid encoding HA-Mal or untransfected. Cell lysates were prepared and proteins were immunoprecipitated with an anti-HA antibody. Proteins were eluted with 2-D sample solution and separated in the first dimension by isoelectric focusing on Immobiline dry strips, with a linear pH 4-7. Focused proteins were then separated in the second dimension by SDS-PAGE. In contrast to one dimensional SDS-PAGE analysis only two forms of Mal were detected on a 2-D SDS-PAGE (Figure 3.2.3a). It was observed that the slower migrating form of Mal had a lower isoelectric point than the predominant 32 kDa form, which is most likely an unresolved mixture of the two slower migrating forms detected following one dimensional SDS-PAGE analysis, whilst the form with the higher isoelectric point corresponding to the theoretical isoelectric point of 5.95, is probably an unresolved mixture of the two faster migrating forms. It was confirmed that the two forms that were detected were specific for Mal as they were not present in the immunoprecipitates that contained no HA-Mal (Figure 3.2.3b).

3.2.3 Calf intestinal phosphatase (CIP) treatment of Mal

It has been reported that upon overexpression, IRAK1 spontaneously autophosphorylates, resulting in the reduction of its electrophoretic mobility on SDS-

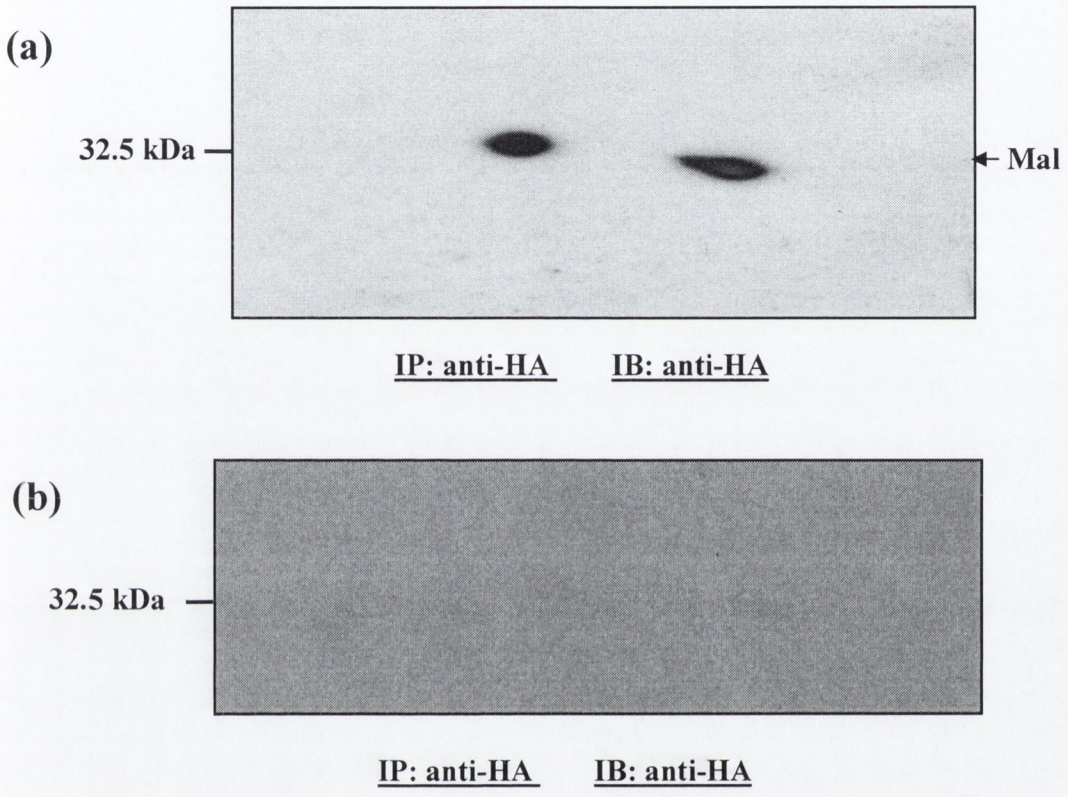

Figure 3.2.3 Two-dimensional gel analysis of the phosphorylation status of Mal. HEK293 cells were transiently transfected with a plasmid encoding (a) HA-Mal or (b) empty vector (EV). Cell lysates were prepared and HA-Mal was immunoprecipitated with an anti-HA antibody. Samples were then isoelectrophoretically focused under a pH gradient of 4 to 7. Focused proteins were then separated in the second dimension by SDS-PAGE, followed by immunoblotting with anti-HA antibody. Data shown is a representative experiment from three separate experiments.

PAGE (Cao, Henzel et al. 1996). Studies have shown that following incubation with calf intestinal phosphatase (CIP), which can remove phosphates from serine, threonine and tyrosine residues, the 100 kDa phosphorylated form of IRAK1, is converted into an 80 kDa protein which corresponds to dephosphorylated IRAK1. The *in vitro* CIP assay was therefore employed as a means to investigate the phosphorylation status of overexpressed Mal, using overexpressed IRAK1 acting as a positive control. HEK293 cells were transiently transfected with plasmids encoding IRAK1 (Figure 3.2.4), HA-Mal (Figure 3.2.5) or AU1-MyD88 (Figure 3.2.6). Proteins were immunoprecipitated from cell lysates with the relevant antibodies and treated with 100 U of CIP for three hours at 37°C.

In agreement with previous reports, it was observed that CIP treatment converted phosphorylated IRAK1 into a dephosphorylated 80 kDa protein (Figure 3.2.4, lane 2), whilst the addition of phosphatase inhibitors retained IRAK1 in its phosphorylated state (Figure 3.2.4, lane 1) (Huang, Gao et al. 1997; Greene and O'Neill 1999). Treatment of Mal with CIP also converted its slower migrating forms into a dephosphorylated 32 kDa protein (Figure 3.2.5, lane 2), an effect that was blocked by the addition of phosphatase inhibitors (Figure 3.2.5, lane 1). This indicates that the slower migrating forms of Mal represent phosphorylated Mal. Similar treatment had no effect on the molecular size of MyD88 (Figure 3.2.6, compare lane 1 to lane 2).

3.2.4 GST-Mal is phosphorylated by cellular kinases *in vitro*.

To confirm that Mal could incorporate phosphate, an *in vitro* kinase assay was carried out, using GST-Mal conjugated to glutathione Sepharose. The GST and GST-Mal fusion proteins were expressed in the BL21 strain of *Escherichia coli* as described in the

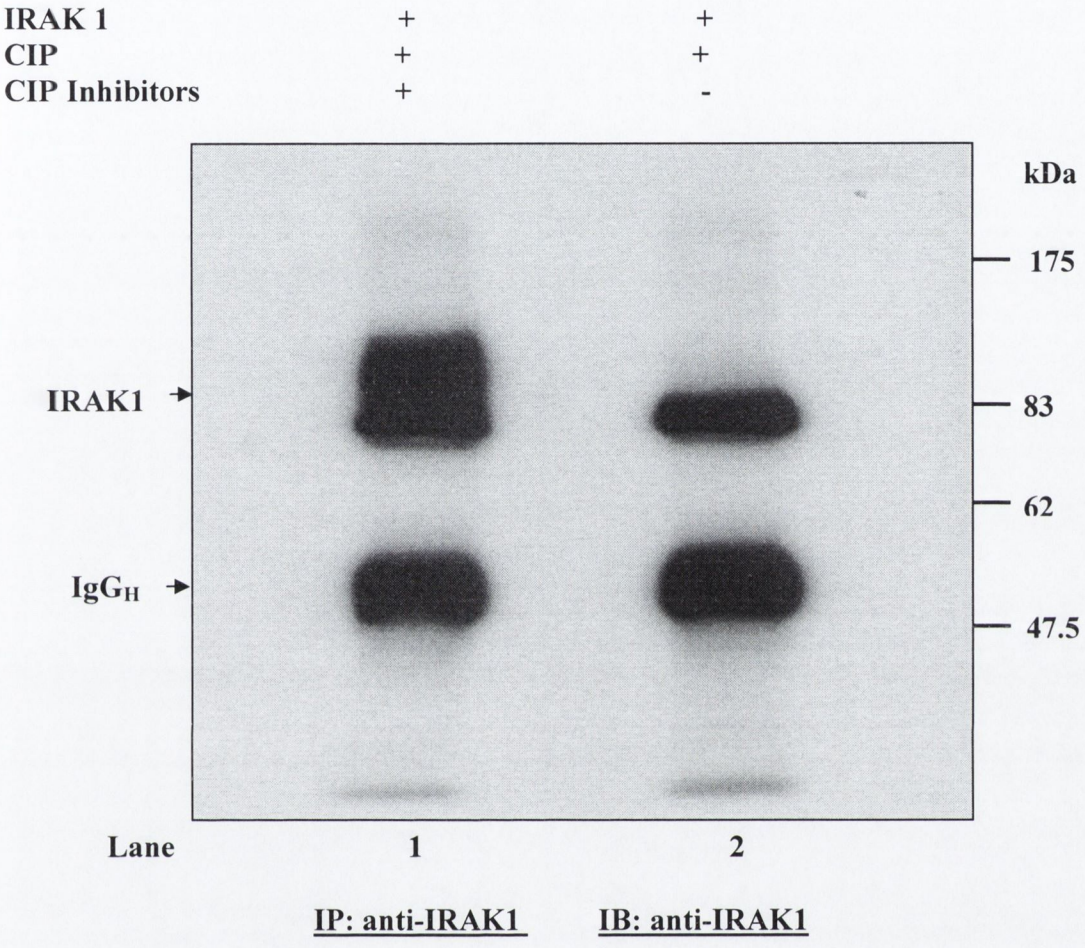

Figure 3.2.4 Phosphatase treatment results in the disappearance of the slower migrating forms of overexpressed IRAK1. HEK293 cells were transiently transfected with 4 μg of a plasmid encoding IRAK1, as a positive control. Cell lysates were prepared and IRAK1 was immunoprecipitated with an anti-IRAK1 antibody. Immunoprecipitates were incubated at 37°C for 3 hrs in phosphatase buffer with 100 U of Calf Intestinal Phosphatase (CIP), in the presence (lane 1) or absence of CIP inhibitors (lane 2). Samples were separated by 8% SDS-PAGE, transferred to PVDF and immunoblotted with anti-IRAK1 antibody. Data shown is a representative experiment from three separate experiments.

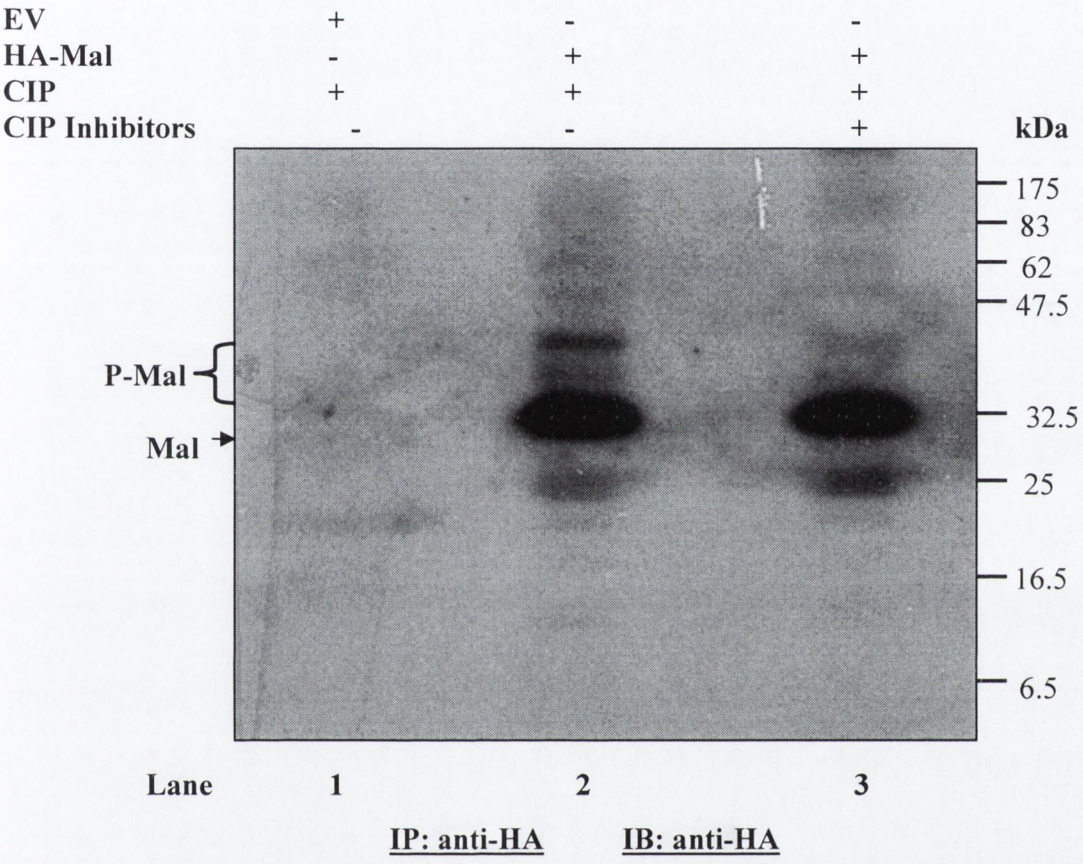

Figure 3.2.5 Phosphatase treatment results in the disappearance of the slower migrating forms of overexpressed Mal. HEK293 cells were mock transfected with empty vector (EV) (lane 1) or transiently transfected with 4μg of a plasmid encoding HA-Mal (lanes 2 and 3). Cell lysates were prepared and HA-Mal was immunoprecipitated with an anti-HA antibody. Immunoprecipitates were incubated at 37°C for 3 hrs with 50 U of CIP, in the presence (lane 1 and 2) or absence of CIP inhibitors (lane 3). Samples were analysed by SDS-PAGE and immunoblotted with an anti-HA antibody. Data shown is a representative experiment from three separate experiments.

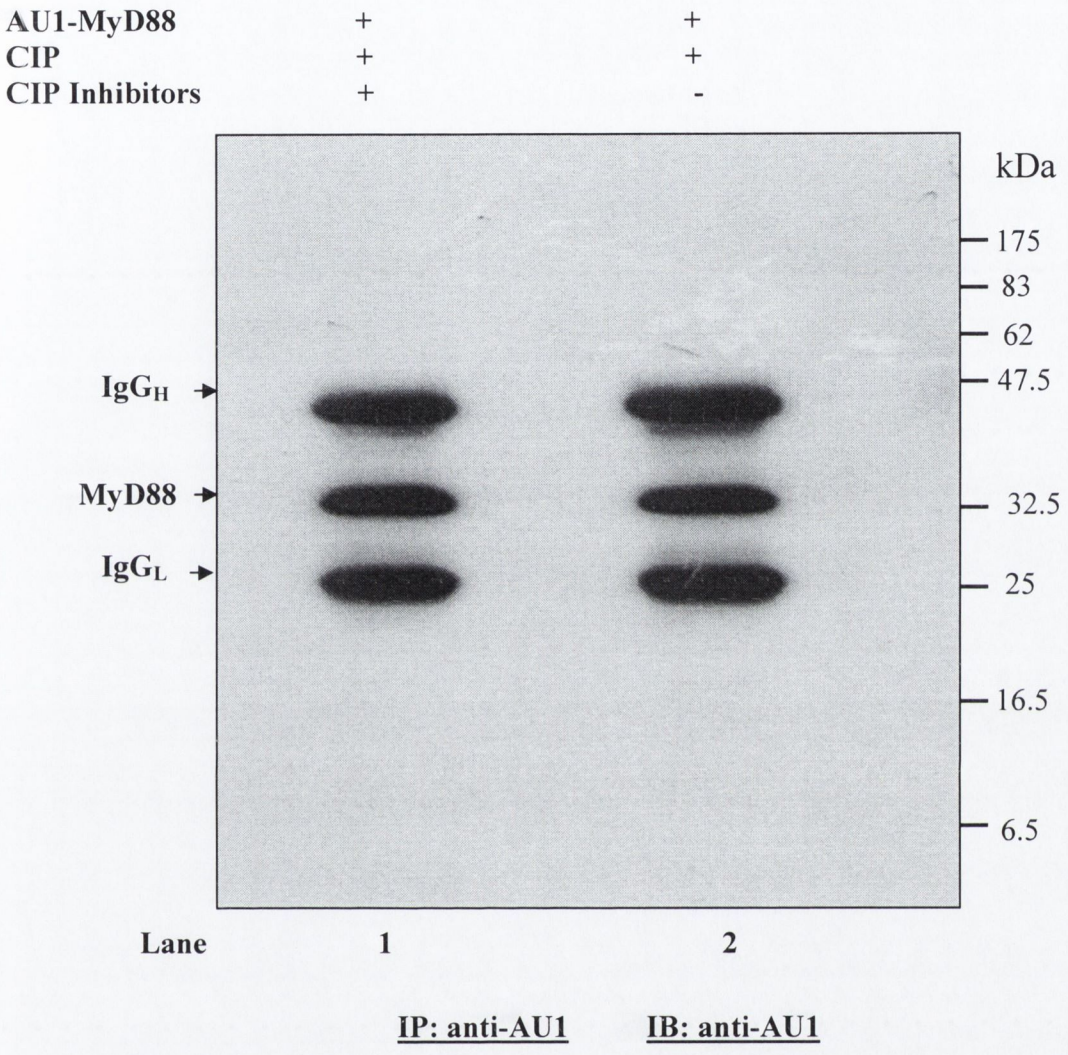

Figure 3.2.6 Phosphatase treatment had no affect on the expression profile of overexpressed MyD88. HEK293 cells were transiently transfected with 4 μg of a plasmid encoding AU1 tagged MyD88. Cell lysates were prepared and Au1-MyD88 was immunoprecipitated with an anti-AU1 antibody. Immunoprecipitates were incubated at 37°C, in phosphatase buffer, for 3 hours with 100 U of Calf Intestinal Phosphatase (CIP), in the presence (lane 1) or absence of CIP inhibitors (lane 2). Samples were separated by 12% SDS-PAGE, transferred to PVDF and immunoblotted with anti-AU1 antibody. Data shown is a representative experiment from three separate experiments.

Materials and Methods section. As indicated in Figure 3.2.7, a protein of the expected molecular weight of GST-Mal (50 kDa) was expressed following induction of the cells with IPTG compared with uninduced cells, and following purification of GST-Mal from the bacterial cell lysates a single band corresponding to GST-Mal was observed. Firstly, a GST-pulldown assay was performed using the purified glutathione-coupled GST-tagged Mal or GST and HEK 293 cell lysates, which served as the kinase source. It was reasoned that GST-Mal would interact with the protein kinase or kinases that were responsible for mediating Mal phosphorylation, and thereby phosphorylate Mal. In addition, GST-Mal and GST were incubated with lysis buffer alone to determine if Mal can undergo autophosphorylation. The samples were then subjected to *in vitro* kinase assays and analysed by SDS-PAGE, followed by autoradiography. As can be seen in Figure 3.2.8a, lane 1, GST-Mal becomes phosphorylated by cellular kinases. GST alone is not phosphorylated (Figure 3.2.8a, lane 2 and 4) and Mal does not undergo autophosphorylation (Figure 3.2.8a, lane 3). To ensure that the amount of GST-Mal and GST was equivalent in all samples the gel was stained with Coomassie Brillant Blue (G250) stain (Figure 3.2.8b).

3.2.5 GST-MyD88 is phosphorylated by cellular kinases *in vitro*.

As Mal was phosphorylated in an *in vitro* kinase assay, it was of interest to investigate if the adaptor protein MyD88 was phosphorylated under the same conditions. The GST and GST-MyD88 fusion proteins were expressed in the BL21 strain of *Escherichia coli* as described in the Materials and Methods section and the resulting purified fusion proteins were analysed by SDS-PAGE. As indicated in figure 3.2.9, a

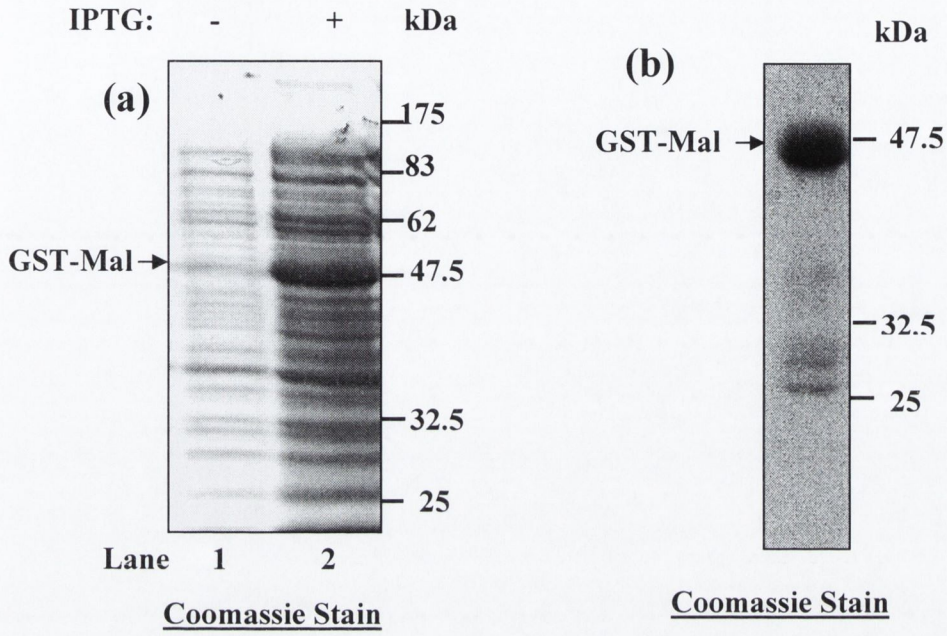

Figure 3.2.7 Production of recombinant GST-Mal. GST-Mal fusion protein was purified from the BL21 strain of *Escherichia coli,* grown to an OD_{600} of 0.6 and induced with 100 μM IPTG for 3 hours. (a) 1ml of cells was removed pre-induction with IPTG (lane 1), and post-induction (lane 2). Cells were centrifuged, supernatants were removed and pellets were lysed in 25 μl of SDS-PAGE sample buffer. **(b)** 0.5 L of BL21 cells transformed with GST-Mal, were grown as above and centrifuged at 16 000 x g for 30 minutes. The supernatant was incubated with 600 μl of glutathione-agarose beads at 4° C for 2 hours. The beads were washed five times with NETN buffer; a 20 μl sample was then removed and added to 20 μl of SDS-PAGE sample buffer. For (a) and (b), samples were boiled and analysed for protein content on a 12 % SDS-PAGE gel. Gels were subsequently stained with Coomassie Brilliant Blue stain. Data shown is a representative experiment from three separate experiments.

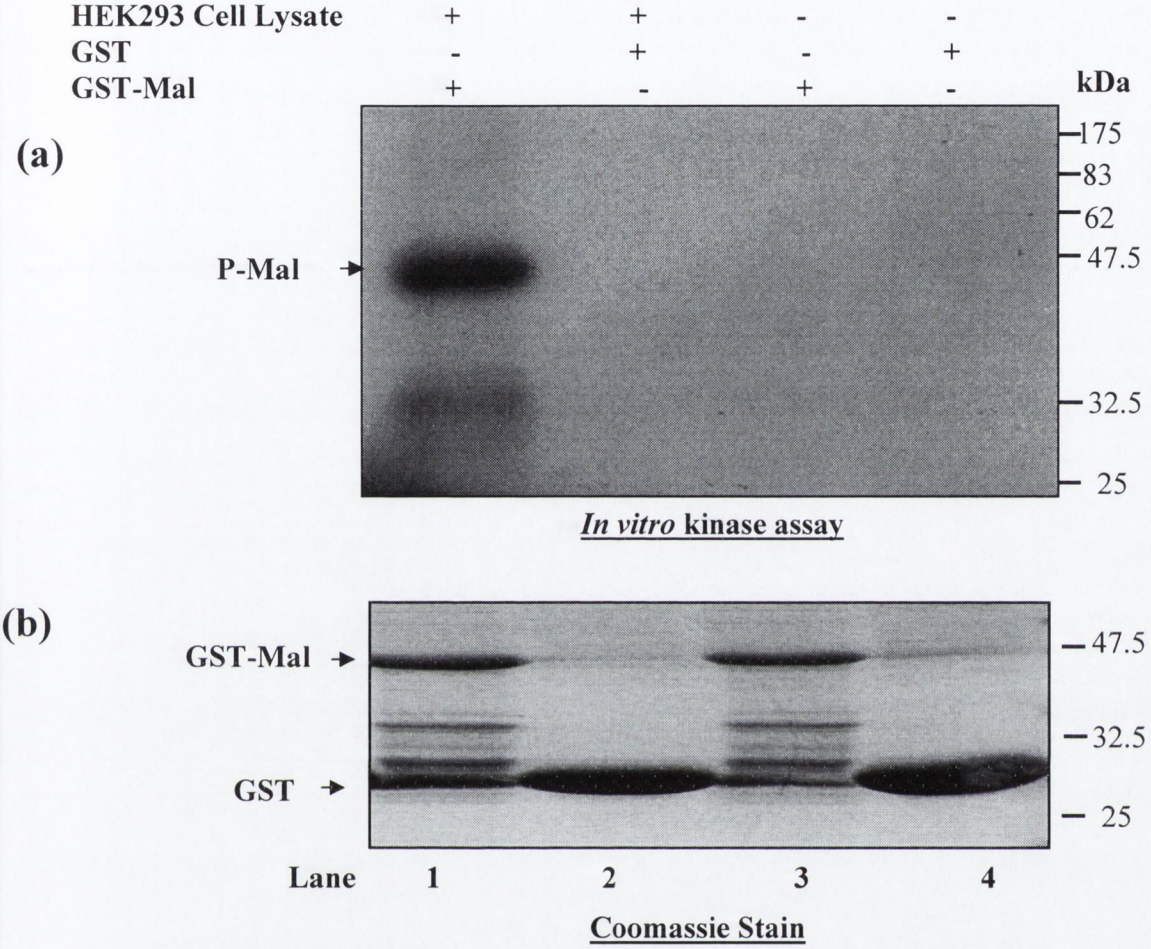

Figure 3.2.8 GST-Mal is phosphorylated by cellular kinases *in vitro*. GST-Mal is phosphorylated, but does not undergo autophosphorylation when subjected to an *in vitro* kinase assay. GST-Mal (lane 1) and GST (lane 2) were incubated with cell lysates from the HEK293 cell line, or with lysis buffer alone (lanes 3 and 4) for 2 hours at 4°C. **(a)** Samples were subjected to an *in vitro* kinase assay, separated by SDS-PAGE, and visualised by autoradiography. **(b)** Samples were also stained with Coomassie Stain (lower panel). Data shown is a representative experiment from six separate experiments.

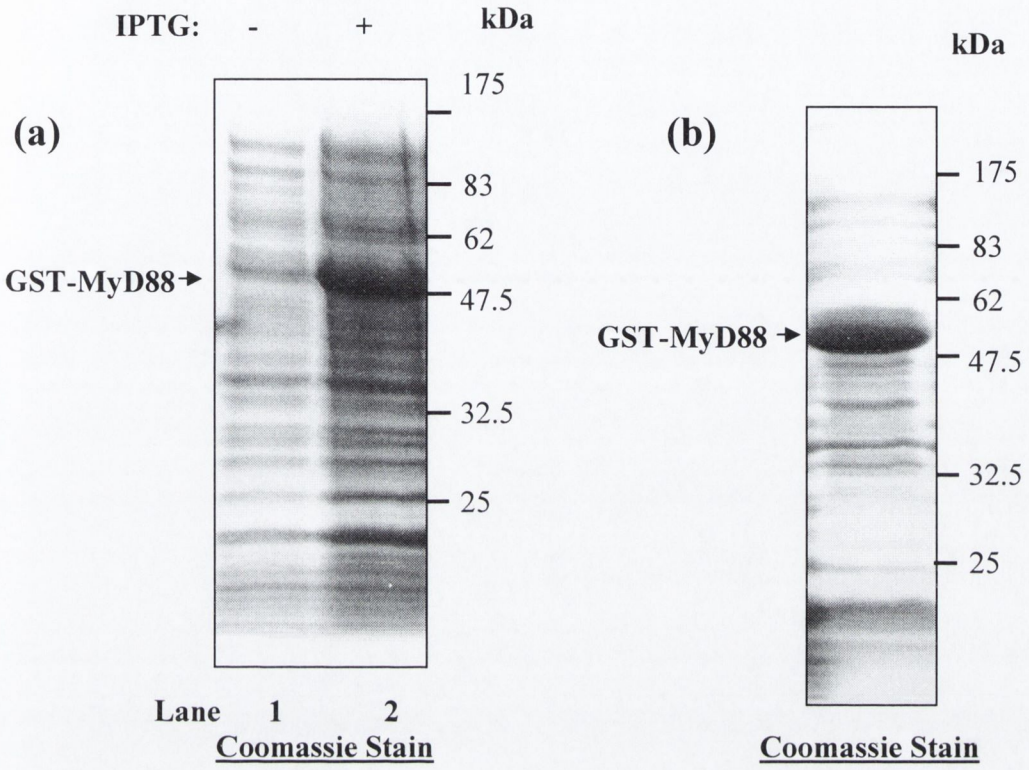

Figure 3.2.9 (a) **Production of GST-MyD88**. GST-MyD88 fusion protein was purified from the BL21 strain of *Escherichia coli,* grown to an OD_{600} of 0.6 and induced with 100 μM IPTG for 3 hours. 1ml of cells was removed pre-induction with IPTG (lane 1), and post-induction (lane 2). Cells were centrifuged, supernatants were removed and pellets were lysed in 25 μl of SDS-PAGE sample buffer. (b) 0.5 L of BL21 cells transformed with GST-MyD88 were grown as above and centrifuged at 16 000 x g for 30 minutes. The supernatant was incubated with 600 μl of glutathione-agarose beads at 4° C for 2 hours. The beads were washed five times with NETN buffer; a 20 μl sample was then removed and added to 20 μl of SDS PAGE sample buffer. For (a) and (b), samples were boiled and analysed for protein content on a 12 % SDS-PAGE gel. Gels were subsequently stained with Coomassie Blue stain. Data shown is a representative experiment from three separate experiments.

protein of the expected molecular weight of GST-MyD88 was expressed following induction of the cells compared with uninduced cells and following purification of GST-MyD88 from the bacterial cell lysates a single band corresponding to GST-MyD88 was observed. Cell lysates from the HEK293 cell line were subsequently prepared and a GST-pulldown assay was carried out with GST-MyD88 or GST. In addition, GST-MyD88 and GST were incubated with lysis buffer alone to determine if MyD88 can autophosphorylate. *In vitro* kinase assays were performed and samples were analysed by SDS-PAGE analysis followed by autoradiography. A ^{32}P-labelled band was observed at the molecular mass corresponding to GST-MyD88, following incubation with cell lysates (Figure 3.2.10a, lane 1). This band was only detected if GST-MyD88 was pre-incubated with cell lysates (Figure 3.2.10a, lane 2). This suggests that similar to Mal, MyD88 can be phosphorylated, although phospho-MyD88 does not display altered mobility following SDS-PAGE analysis. In addition it was determined that MyD88 is unlikely to undergo auto-phosphorylation. To ensure that the amount of GST-MyD88 was equivalent in both samples the gel was stained with Coomassie stain (Figure 3.2.10b).

3.2.6 Mal interacts with unphosphorylated IRAK1

Previous investigations have determined that MyD88 interacts with the faster migrating unphosphorylated form of IRAK1 and does not associate with the phosphorylated form of IRAK1(Wesche, Henzel et al. 1997). Coimmunoprecipitation studies in this laboratory have determined that similar to MyD88, Mal does not interact with overexpressed IRAK1. As has been stated, overexpression of IRAK1 in HEK293 cells results in its autophosphorylation, it was of interest therefore to determine if like

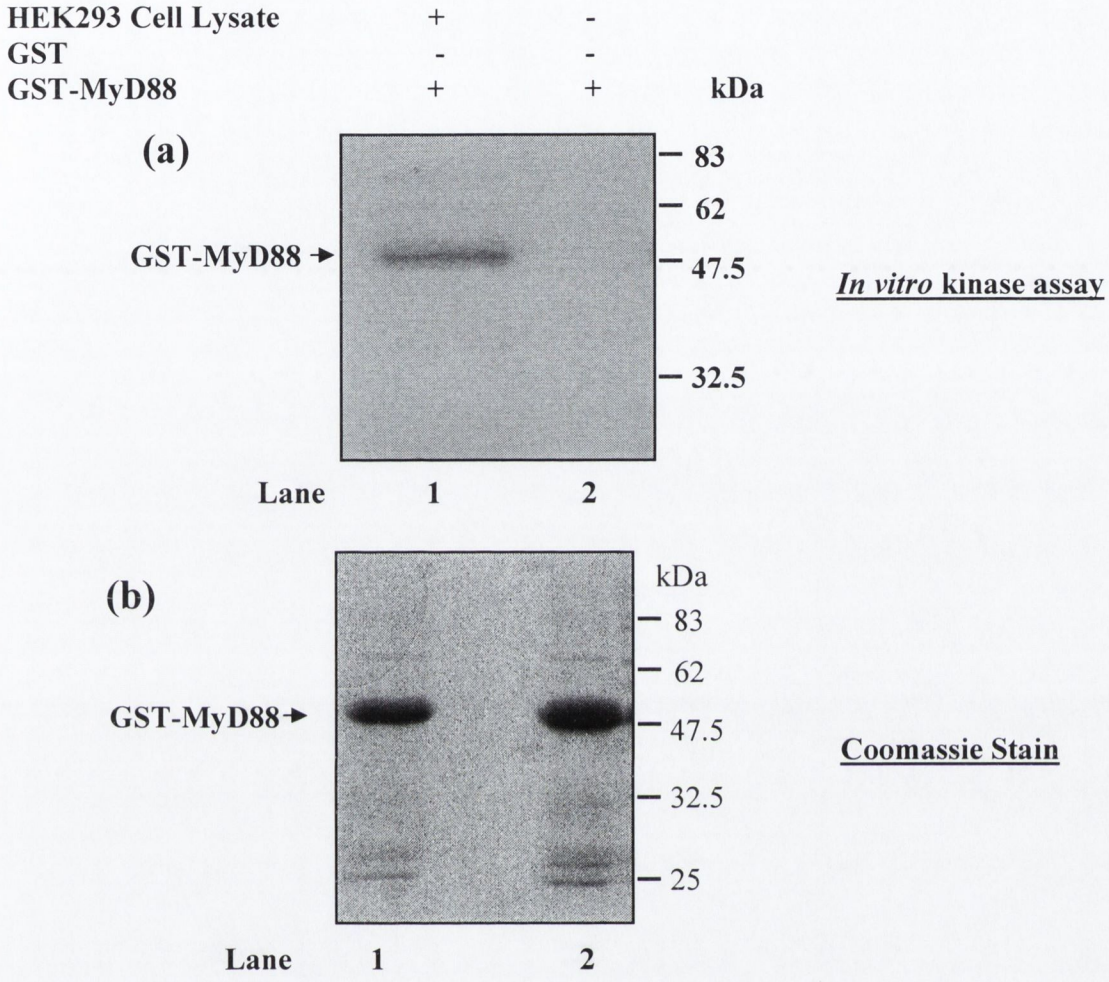

Figure 3.2.10 GST-MyD88 is phosphorylated, but similar to Mal does not undergo autophosphorylation, when subjected to an in vitro kinase assay. HEK293 cells ($1x10^6$) were lysed in lysis buffer and centrifuged to remove cell debris. (a) 10 μg of GST-MyD88 (lane 1) was incubated with proteins prepared from HEK293 cell lysates, or with high stringency lysis buffer alone (lane 2), for 2 hours at 4°C. Samples were washed and incubated with [γ^{32}P]ATP for 30 min, at 37°C . Following incubation in an *in vitro* kinase assay, samples were analysed by SDS-PAGE, and subjected to autoradiography. (b) Coomassie stained gel depicting expression of GST-MyD88. Data shown is a representative experiment from three separate experiments.

MyD88, Mal only interacted with the unphosphorylated form of IRAK1. In order to assess this possibility, HEK293 cells were transiently transfected with plasmids encoding HA-Mal alone (Figure 3.2.11a, lane 2) or left un-transfected (Figure 3.2.11a, lane 1). Cell lysates were prepared, and proteins were immunoprecipitated with an anti-IRAK1 antibody. Samples were analysed by SDS-PAGE and immunoblotted with an anti-HA antibody. As can be seen in Figure 3.2.11a, lane 1, Mal associated with endogenous IRAK1, which corresponds to the unphosphosphorylated form of IRAK1. Cell lysates were immunoblotted with an anti-IRAK1 antibody to confirm expression of endogenous IRAK1 (Figure 3.2.11b, lanes 1 and 2). Cell lysates were also immunoblotted with an anti-HA antibody to confirm expression of HA-Mal (Figure 3.2.11c, lane 1).

3.2.7 Mal is phosphorylated by IRAK-1

Having determined that recombinant Mal could be phosphorylated following incubation with (γ-^{32}P) ATP, the identity of the kinase or kinases involved, was next explored. The most immediate candidates that are known to belong to the MyD88-dependent pathway are the active kinases, IRAK1 and IRAK4. As shown above, Mal interacted with unphosphorylated IRAK1, suggesting that IRAK1 could be required for Mal phosphorylation. In order to assess if Mal was a substrate for IRAK1, HEK293 cells were mock-transfected or transiently transfected with plasmids encoding IRAK1 or a kinase-inactive form of IRAK1. Cell lysates were prepared and Flag-tagged proteins were immunoprecipitated with an anti-Flag antibody cross-linked to Sepharose beads. 100 ng of recombinant Mal was added to each sample, after which samples were then subjected to *in vitro* kinase assays and separated by SDS-PAGE. Gels were dried and analysed

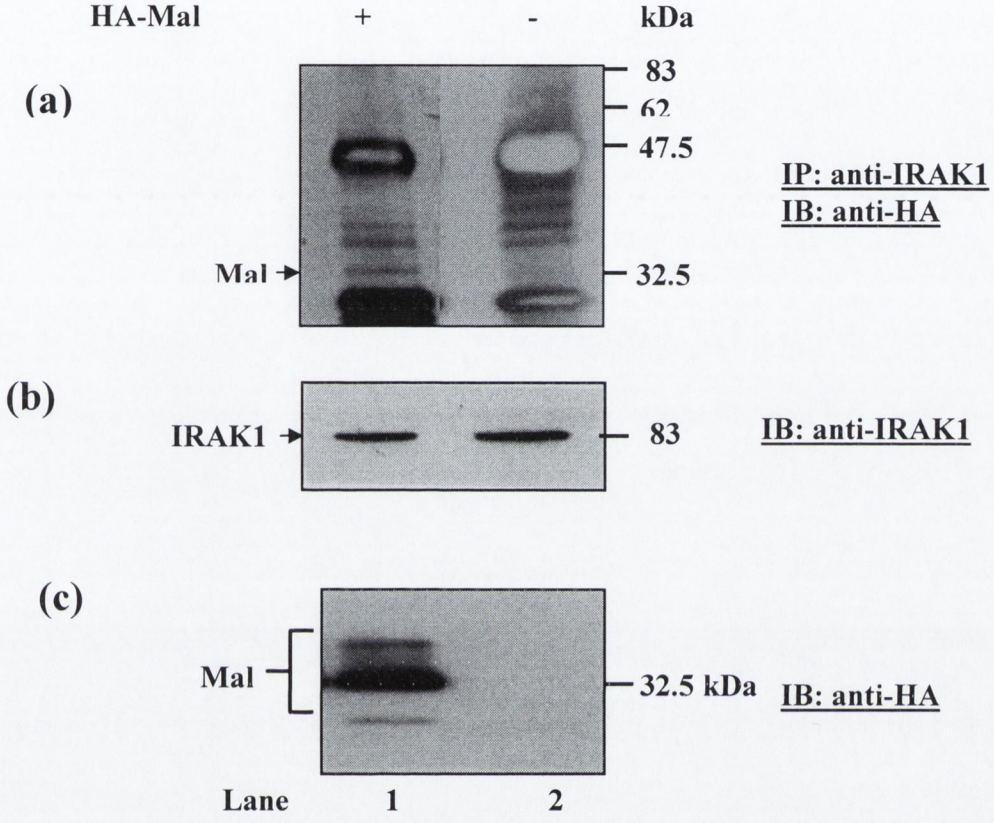

Figure 3.2.11 Mal interacts with unphosphorylated endogenous IRAK1. (a) HEK293 cells were transiently transfected with a plasmid encoding HA-Mal (lane 1-2) or with a plasmid encoding IRAK1. Cell lysates were prepared and proteins were immunoprecipitated with an anti-IRAK1 antibody. Samples were analysed by SDS-PAGE and immunoblotted with an anti-HA antibody. (b) Samples were also immunoblotted with an anti-IRAK1 antibody. (c) Cell lysates were likewise analysed to confirm expression of HA-Mal in the appropriate sample by immunoblotting with an anti-HA antibody.

autoradiography. As figure 3.2.12 illustrates, IRAK1 autophosphorylation was evident in the broad band detected at 100 kDa following incubation with radiolabelled ATP (Figure 3.2.12a, lane 1). A faint band at approximately 100 kDa in the kinase-inactive IRAK1 sample was also detected, which most likely corresponds to endogenous autophosphorylated IRAK1 (Figure 3.2.12a, lane 2). The identity of the faint band corresponding to the molecular mass of 83 kDa in mock transfected cells is unknown (Figure 3.2.12a, lane 3). It was noted that Mal phosphorylation was not detected following incubation with either kinase-inactive IRAK1 or with immunoprecipitates that did not contain IRAK1 protein (Figure 3.2.12a, lane 2 and 3 respectively). However, when *in vitro* kinase assays were performed with samples containing both IRAK1 and Mal, Mal phosphorylation by kinase active IRAK1 occurred (Figure 3.2.12a, lane 1). Similar to the expression profile of overexpressed Mal, distinct forms of recombinant Mal were detected, indicating that phosphorylation of Mal by IRAK-1 results in the production of three phosphoproteins.

3.2.8 Recombinant Mal is phosphorylated by recombinant IRAK1

Having established that recombinant Mal was phosphorylated in vitro by overexpressed IRAK1, it was necessary to confirm that it was IRAK1 that was directly phosphorylating Mal and not an unidentified kinase that was interacting with phosphorylated IRAK1. In order to address this, a direct *in vitro* kinase assay with recombinant Mal and recombinant IRAK1 was performed in a cell-free system. As figure 3.2.13 illustrates, incubating IRAK1 with radiolabelled ATP results in its autophosphorylation (lane 1 and lane 2). When recombinant Mal was combined with

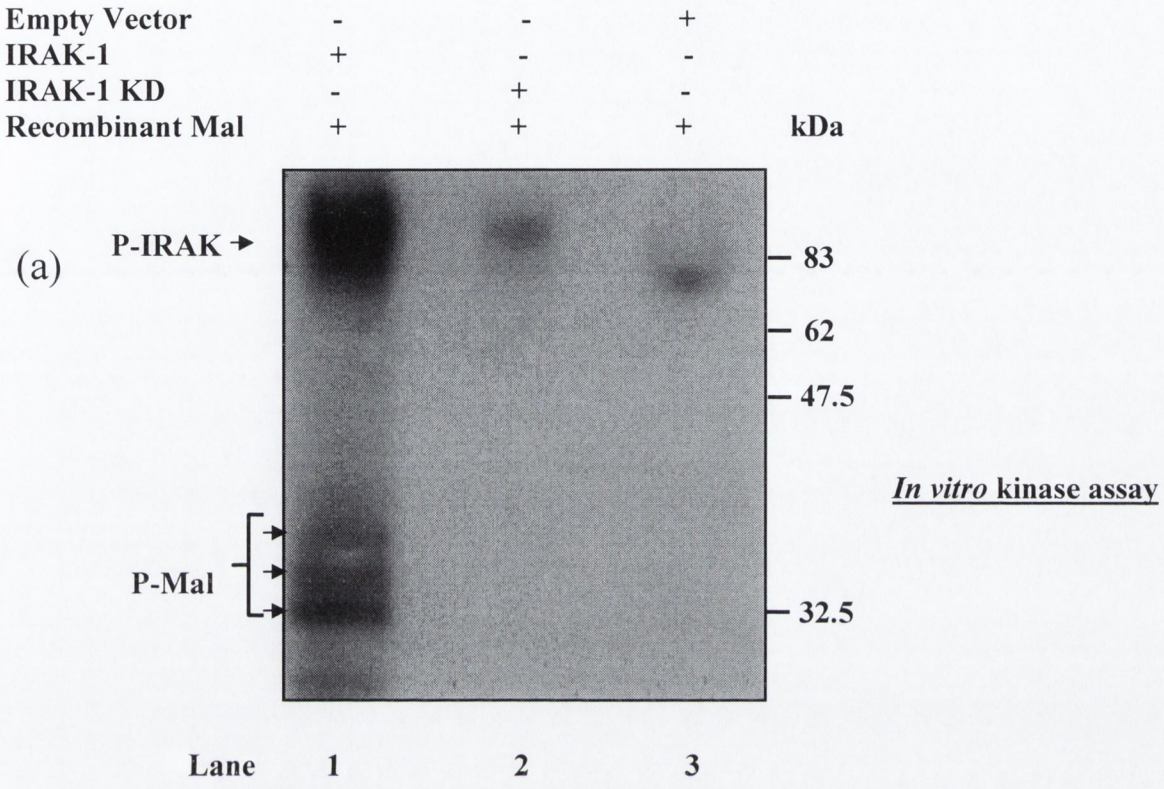

Figure 3.2.12 Overexpressed IRAK1 phosphorylates recombinant Mal. (a) HEK293 cells ($1x10^6$) were transfected with 8 μg of plasmid encoding Flag-IRAK1 or Flag-IRAK1 KD, for 24 hours. Proteins were immunoprecipitated from cell lysates with an anti-Flag antibody. The immunoprecipitates were washed and recombinant Mal was then added to each sample and incubated with [γ^{32}P] ATP for 30 min, at 37°C. Following incubation in an *in vitro* kinase assay, samples were analysed by SDS-PAGE, the gel was dried and subjected to autoradiography. Data shown is a representative experiment from three separate experiments. KD, kinase dead.

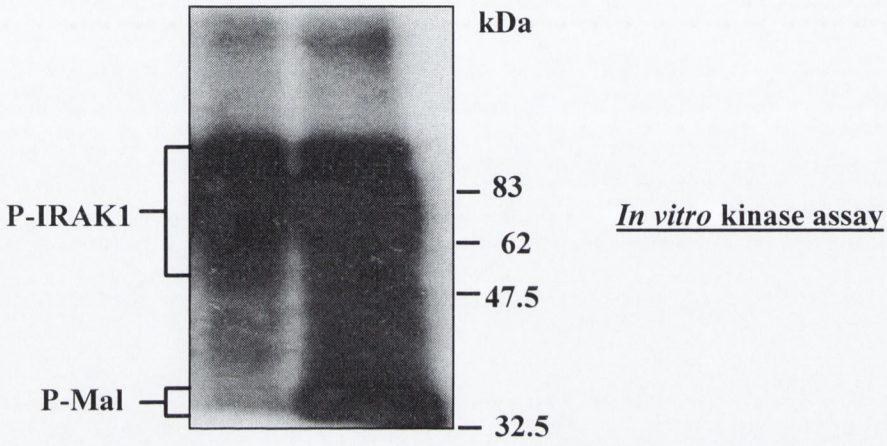

Figure 3.2.13 Recombinant Mal is phosphorylated *in vitro* by recombinant IRAK1.

Recombinant IRAK1 (100 ng) was incubated alone (lane 1), or with 250 ng of recombinant Mal (lane 2). Samples were subjected to an *in vitro* kinase assay, analysed by SDS-PAGE, and visualised by autoradiography.

recombinant IRAK1, phosphorylation of Mal occurred, demonstrating that Mal is a substrate for IRAK1 (Figure 3.2.13, lane 2).

3.2.9 Recombinant Mal is phosphorylated by overexpressed IRAK4

Based on the observation that Mal is phosphorylated by IRAK1, the possibility that Mal is also a substrate for IRAK4 was subsequently investigated. HEK293 cells were mock-transfected or transiently transfected with plasmids encoding IRAK4, or a kinase-inactive form of IRAK4. Cell lysates were prepared and subjected to immunoprecipitation with an anti-Flag antibody cross-linked to Sepharose. 100 ng of recombinant Mal was added to each sample. Samples were then subjected to *in vitro* kinase assays, separated by SDS-PAGE and visualised by autoradiography. As has been previously reported, incubation of IRAK4 with radiolabelled ATP resulted in IRAK4 autophosphorylation (Fig. 3.2.14a, lane 1). As expected no kinase activity was detectable in the samples containing kinase-inactive IRAK-4 or cells that were mock-transfected (Fig. 3.2.14a, lane 2 and 3 respectively). Phosphorylated Mal was observed only when it was incubated with kinase active IRAK-4 (Figure 3.2.14a, lane 1). While IRAK1 phosphorylation resulted in the formation of three Mal phosphoproteins, Mal phosphorylation by IRAK-4 produced two phosphoproteins.

3.2.10 Recombinant Mal is phosphorylated by recombinant IRAK4

As has been discussed above for IRAK1, it was necessary to confirm that IRAK4 was directly phosphorylating Mal, and not another kinase that was interacting with IRAK4 with the same molecular weight. Therefore *in vitro* kinase assays were performed

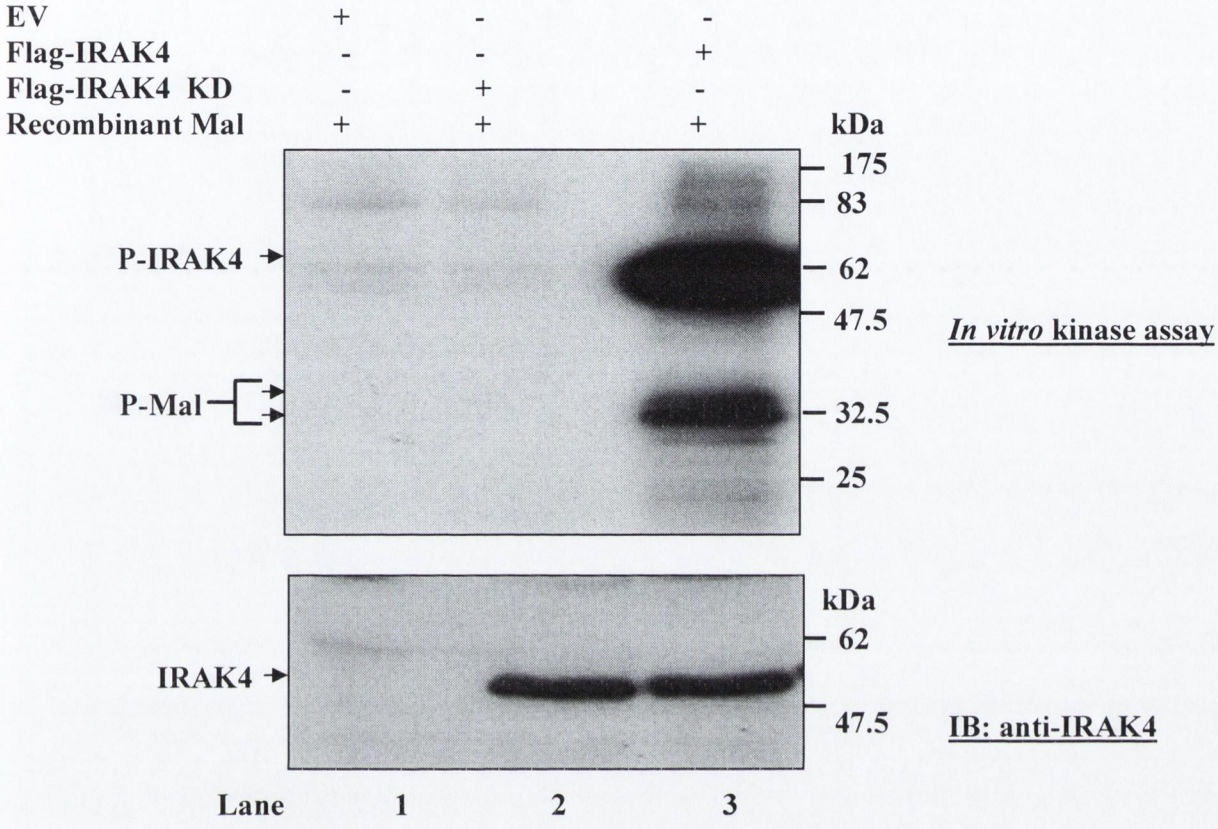

Figure 3.2.14 Overexpressed IRAK-4 phosphorylates recombinant Mal in an *in vitro* kinase assay. HEK293 cells ($1x10^6$) were transiently transfected with plasmids encoding Flag-IRAK4 (lane 1), Flag-IRAK4 KD (lane 2) and mock-transfected (EV, lane 3, negative control) for 24 hours. Proteins from cell lysates were immunoprecipitated with an anti-Flag antibody cross-linked to Sepharose, samples were washed three times with lysis buffer and twice with kinase buffer. 250 ng of recombinant Mal was added to each sample, which was then incubated for 30 min. at 37°C with [γ32P] PO4. Following incubation in an *in vitro* kinase assay, samples were analysed by SDS-PAGE, the gel was dried and subjected to autoradiography. (b) Cell lysates were subsequently immunoblotted with an anti-IRAK4 antibody in order to confirm expression of IRAK4 and IRAK4KD in the relevant samples. Data shown is a representative experiment from three separate experiments. EV, empty vector. KD, kinase dead.

in a cell-free system that contained only recombinant IRAK4 and recombinant Mal. Samples were analysed by SDS-PAGE and visualised by autoradiography. In agreement with the literature, IRAK4 autophosphorylation was detected upon incubation with radiolabelled ATP (Figure 3.2.15 lanes 1 and 2) (Li, Strelow et al. 2002). When recombinant Mal was added to recombinant IRAK4, it was observed that IRAK4 was able to efficiently phosphorylate Mal (Figure 3.2.15 lane 2).

3.2.11 The TIR domain of Mal is not phosphorylated by recombinant IRAK4

Given that Mal was phosphorylated by IRAK4, it was of interest to determine whether the phosphorylated residues were located within the TIR domain of Mal. The GST and GST-Mal-TIR fusion proteins were expressed in the BL21 strain of *Escherichia coli* as described in the Materials and Methods section and the resulting purified fusion proteins were analysed by SDS-PAGE. As indicated in figure 3.2.16a, a protein of the expected molecular weight of GST-Mal-TIR was expressed following induction of the cells compared with uninduced cells. Following purification of GST-Mal-TIR from the bacterial cell lysates a single band corresponding to GST-Mal-TIR was observed (Figure 3.2.16b). HEK293 cells were subsequently transiently transfected with a plasmid encoding Flag-IRAK4; cell lysates were prepared and subjected to immunoprecipitation using an anti-Flag antibody cross-linked to Sepharose. 100 ng of recombinant Mal, GST-Mal-TIR or GST protein was then added to the indicated sample (Figure 3.2.17a). *In vitro* kinase assays were performed and samples were separated by SDS-PAGE. Gels were then dried and visualised by autoradiography. Similar to previous results, incubation of IRAK4 with radiolabelled ATP resulted in IRAK4 autophosphorylation (Figure 3.2.17a,

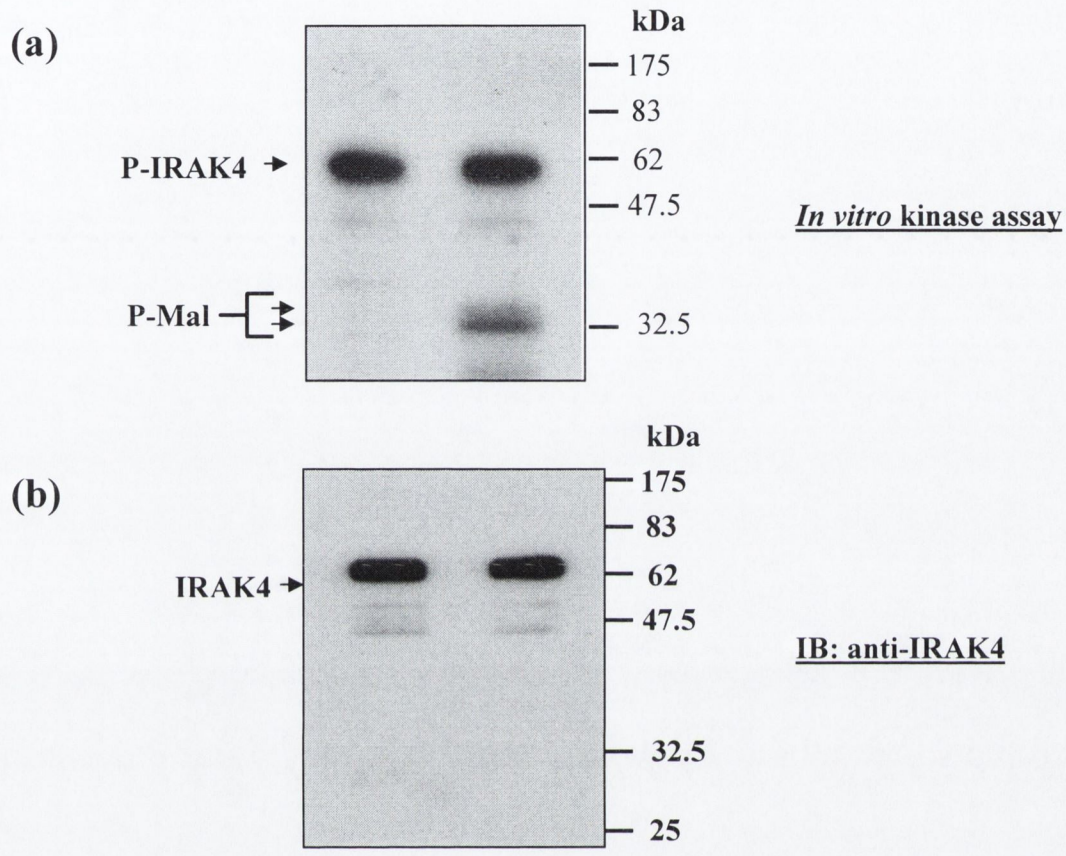

Figure 3.2.15 Recombinant Mal is phosphorylated *in vitro* by recombinant IRAK4.

Recombinant IRAK4 (100 ng) was incubated alone (lane 1), or with 250 ng of recombinant Mal (lane 2). Samples were subjected to an *in vitro* kinase assay, analysed on SDS-PAGE, and visualised by autoradiography. Samples were subsequently immunoblotted with (b) an anti-IRAK4 antibody. Data shown is a representative experiment from two separate experiments.

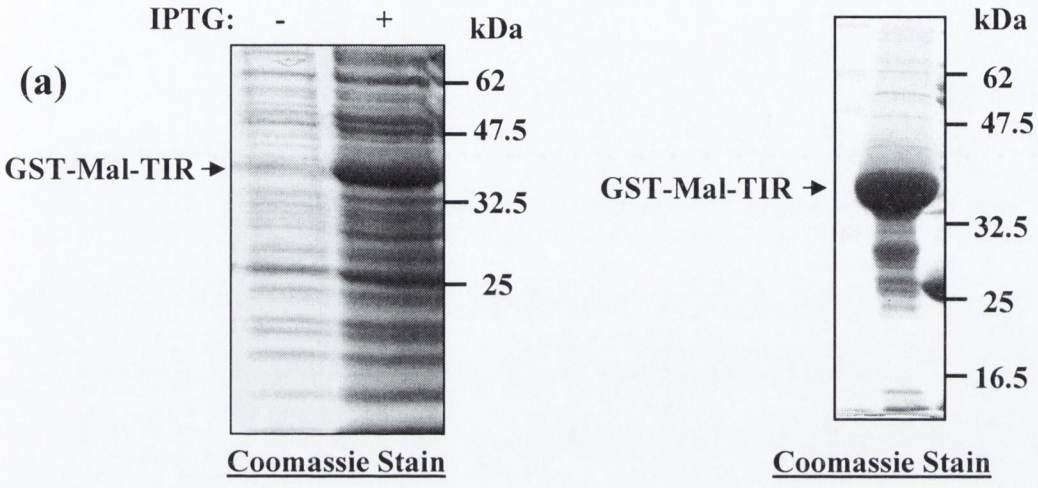

Figure 3.2.16 (a) GST-Mal-TIR fusion protein was purified from the BL21 strain of *Escherichia coli,* grown to an OD_{600} of 0.6 and induced with 100 μM IPTG for 3 hours. 1ml of cells was removed before induction with IPTG (lane 1), and post-induction (lane 2). Cells were centrifuged, supernatants were removed and pellets were lysed in 25 μl of SDS-PAGE sample buffer. (b) 0.5 L of BL21 cells transformed with GST-Mal-TIR were grown as above and centrifuged at 16 000 x g for 30 minutes. The supernatant was incubated with 600 μl of glutathione-agarose beads at 4° C for 2 hours. The beads were washed five times with NETN buffer; a 20 μl sample was then removed and added to 20 μl of SDS PAGE sample buffer. For (a) and (b), samples were boiled and analysed for protein content on a 12 % SDS-PAGE gel. Gels were subsequently stained with Coomassie Blue stain.

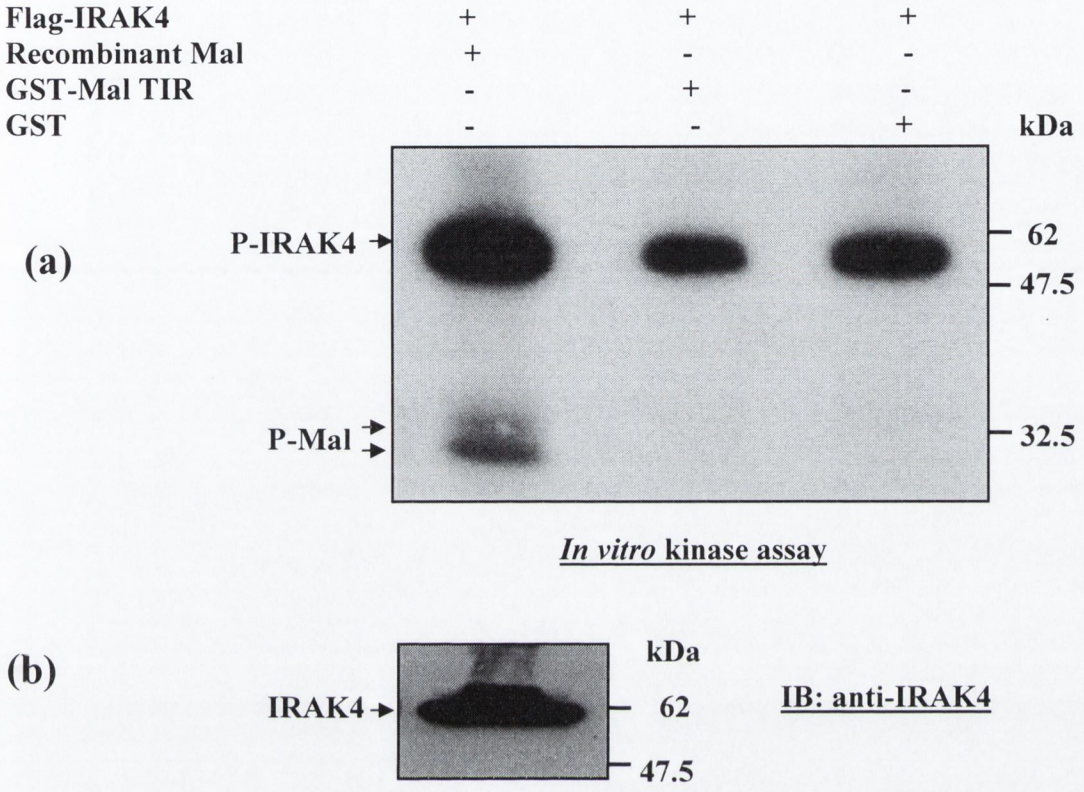

Figure 3.2.17 The TIR domain of Mal is not phosphosylated by IRAK4. HEK293 cells ($1x10^6$) were transiently transfected with plasmids encoding Flag-IRAK4 for 24 hours. Cell lysates were prepared and combined to a total volume of 1.6 ml. 750 µl of cell lysate was then aliquoted into three separate eppendorfs and proteins were immunoprecipitated from the cell lysate with an anti-Flag antibody. Recombinant Mal (lane 2), and the recombinant TIR domain of Mal (lane 3) were added as indicated. The samples were then incubated for 30 min. at 37°C with [γ32P] PO4. Following incubation in an *in vitro* kinase assay, samples were analysed by SDS-PAGE and subjected to autoradiography. (b) Cell lysates were subsequently immunoblotted with an anti-IRAK4 antibody in order to verify the expression of IRAK4. Data shown is a representative experiment from two separate experiments.

lanes 1-3). As a positive control, recombinant Mal was shown to be phosphorylated by IRAK4, (Figure 3.2.17a, lane 2). However, it was observed that IRAK4 did not phosphorylate the TIR domain of Mal (Figure 3.2.17a, lane 3), suggesting that either Mal must be intact for phosphorylation by IRAK4 to occur or the residues that are phosphorylated are located in the N-terminal region of Mal.

3.2.12 MyD88 is not phosphorylated by recombinant IRAK1 or recombinant IRAK4

Given that MyD88 is phosphorylated by intracellular kinases in an *in vitro* kinase assay, it was of interest to determine if MyD88 was phosphorylated by either IRAK1 or IRAK4. Interaction studies have shown that MyD88 associates with unphosphorylated IRAK1 and kinase-inactive IRAK4. *In vitro* kinase assays were performed in a cell-free system that contained only recombinant proteins. Samples were analysed by SDS-PAGE and visualised by autoradiography. In agreement with the literature, IRAK1 autophosphorylation was detected upon incubation with radiolabelled ATP (Figure 3.2.18, lanes 1-2)(Cao, Henzel et al. 1996). When recombinant MyD88 was added to recombinant IRAK1, it was observed that IRAK1 did not phosphorylate MyD88 (Figure 3.2.18, lane 2).

It was next tested if IRAK4 could selectively phosphorylate MyD88 by performing *in vitro* kinase assays. As has been previously noted incubation of IRAK4 with radiolabelled ATP resulted in its autophosphorylation (Figure 3.2.19a, lanes 1-2). However similar to IRAK1, IRAK4 was unable to phosphorylate MyD88 (Figure 3.2.19a, lane 2). Samples were subsequently immunoblotted with an anti-IRAK4 antibody (Figure

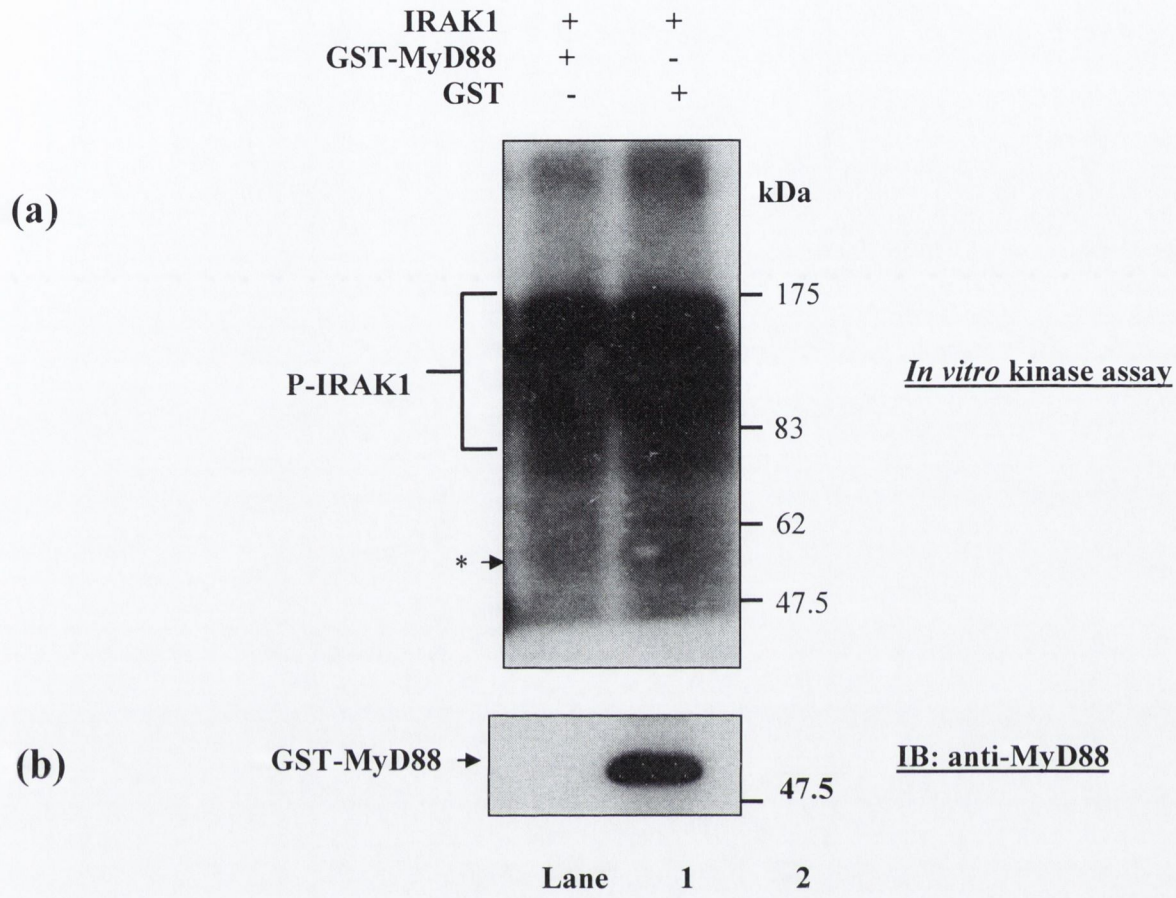

Figure 3.2.18 Recombinant MyD88 is not phosphorylated by recombinant IRAK1. Recombinant IRAK1 was incubated with GST-MyD88 (lane 1), or with GST alone (lane 2). The samples were incubated for 30 min. at 37°C with 2μCi [γ32P] PO4. Following incubation in an *in vitro* kinase assay, samples were analysed by SDS-PAGE, transferred to PVDF membrane and subjected to autoradiography. * Indicates the molecular weight of GST-MyD88. (b) Samples were also immunoblotted with an anti-MyD88 antibody to confirm the presence of GST-MyD88 in the relevant sample. Data shown is a representative experiment from two separate experiments.

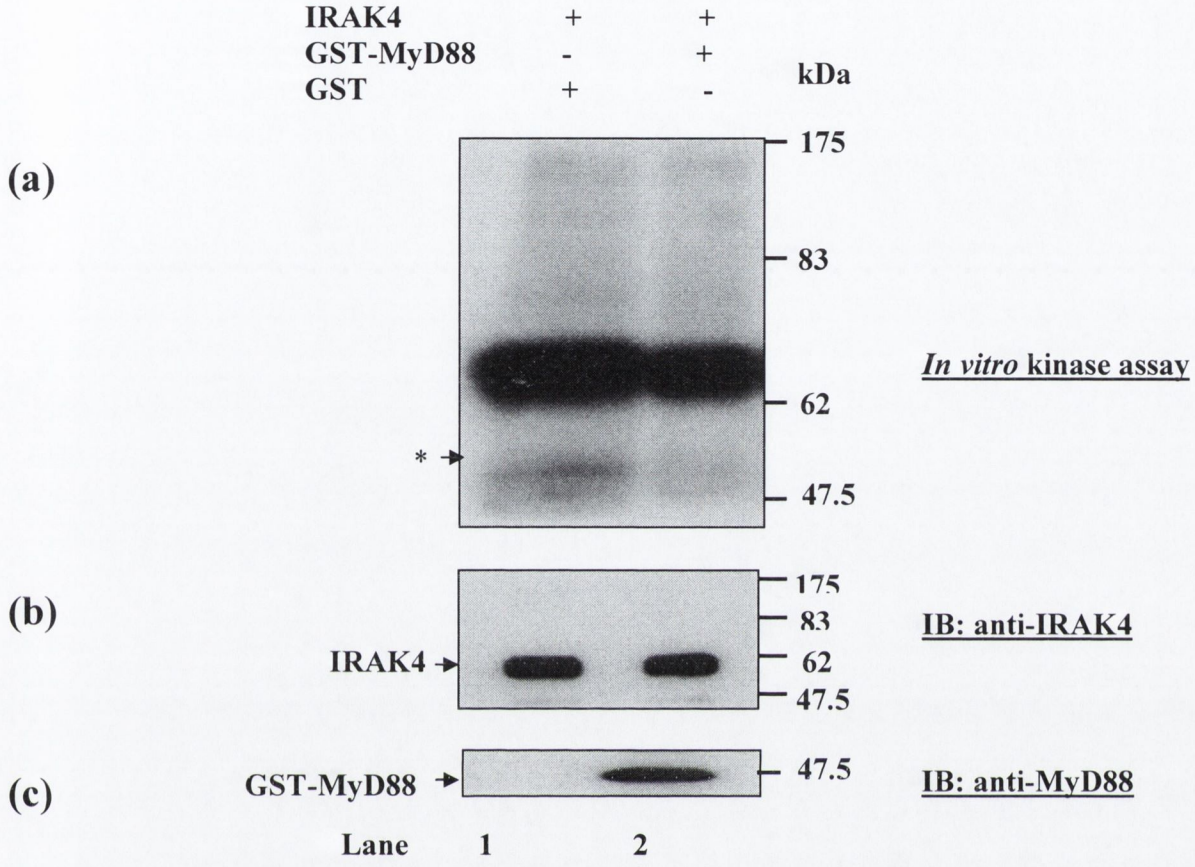

Figure 3.2.19 Recombinant MyD88 is not phosphorylated by recombinant IRAK4. (a) Recombinant IRAK4 was incubated with GST-MyD88 (lane 1), or with GST alone (lane 2). The samples were incubated for 30 min. at 37°C with 2μCi [γ32P] PO4. Following incubation in an *in vitro* kinase assay, samples were analysed by SDS-PAGE, transferred to PVDF membrane and subjected to autoradiography. * Indicates the molecular weight of GST-MyD88. Samples were immunoblottted with (b) an anti-IRAK4 antibody (c) an anti-MyD88 antibody. Data shown is a representative experiment from two separate experiments.

3.2.19b) or an anti-MyD88 antibody (Figure 3.2.19c) in order to verify the presence of the relevant proteins. Phosphorylation of Mal by IRAK1 and IRAK4 therefore indicates a distinct difference in the signalling mechanisms utilised by MyD88 and Mal.

3.2.13 Recombinant Mal is phosphorylated by recombinant Btk.

Given that Mal interacts directly with Btk, investigations were therefore carried out to determine if Btk could directly phosphorylate Mal (Jefferies, Doyle et al. 2003). In order to assess this possibility *in vitro* kinase assays were performed with recombinant active Btk and recombinant Mal. The GST-Mal fusion protein was expressed in the BL21 strain of *Escherichia coli* as previously described. *In vitro* kinase assays were then performed and in agreement with previous reports (Park, Wahl et al. 1996), incubation of Btk with radiolabelled ATP resulted in Btk autophosphorylation (Figure 4.2.20a, lane 1). To determine if Mal was indeed a substrate for Btk, recombinant Mal was then incubated with recombinant Btk. It was observed that Btk efficiently phosphorylated Mal, with two distinct phospho-forms appearing (Figure 4.2.20a, lane 2). Samples were also immunoblotted with an anti-Btk antibody (Figure 4.2.20b). Therefore Mal is also a substrate for Btk.

3.2.14 MyD88 is not a substrate for Btk

Although it has been reported in the literature that MyD88 is tyrosine phosphorylated, the identity of the kinase has yet to be resolved (Park, Wahl et al. 1996). Like Mal, MyD88 has been shown to associate with Btk in immunoprecipitation studies (Jefferies, Doyle et al. 2003). It was therefore of interest to determine if Btk could also

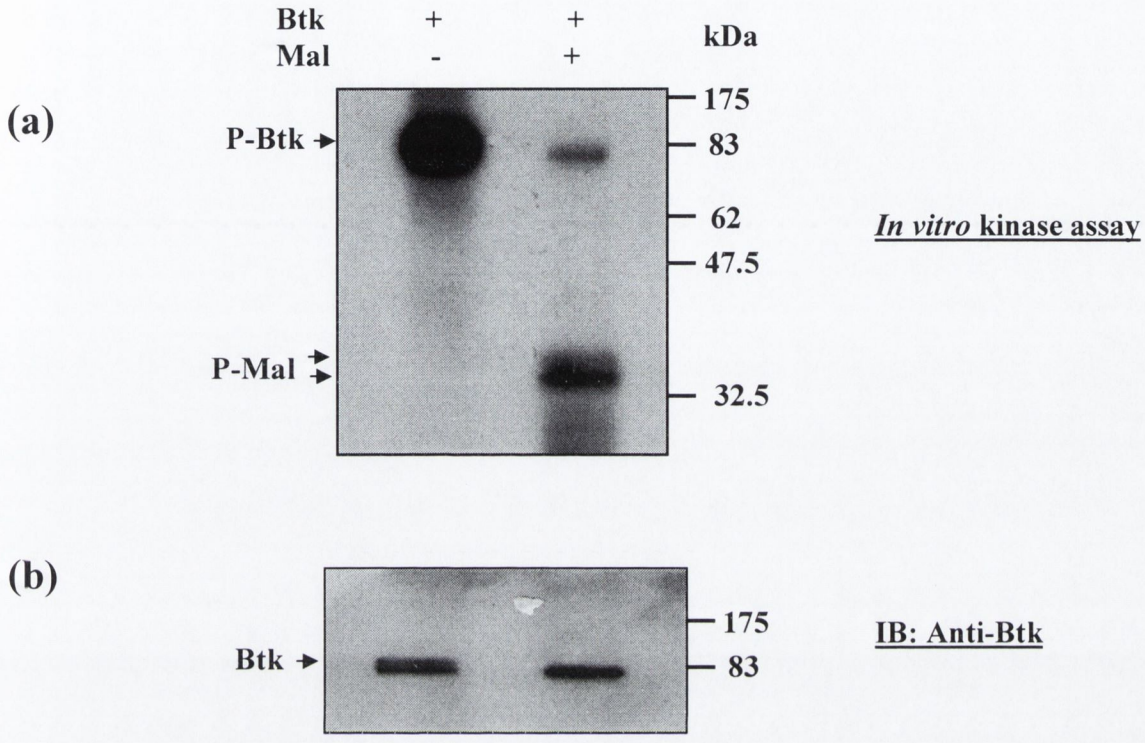

Figure 4.2.20 Recombinant Btk phosphorylates recombinant Mal. (a) Recombinant Btk was incubated alone (lane 1), or with recombinant Mal (lane 2). The samples were incubated for 30 min. at 37°C with 2μCi [γ32P] PO4. Following incubation in an *in vitro* kinase assay, samples were analysed by SDS-PAGE, transferred to PVDF membrane and subjected to autoradiography. (b) Samples were subsequently immunoblotted with an anti-Btk antibody. Data shown is a representative experiment from five separate experiments.

phosphorylate MyD88. *In vitro* kinase assays were therefore performed using GST-MyD88 and active recombinant Btk. As had been previously noted autophosphorylation of Btk occurred following incubation with radiolabelled ATP (Figure 4.2.21a, lane 1). However, unlike Mal, GST-MyD88 was not a substrate for Btk (Figure 4.2.21a, lane 2). Samples were immunoblotted with an anti-Btk antibody to verify that equal concentrations of Btk were present (Figure 4.2.21b). In addition, samples were immunoblotted with an anti-MyD88 antibody to confirm that GST-MyD88 had been added (Figure 4.2.21c).

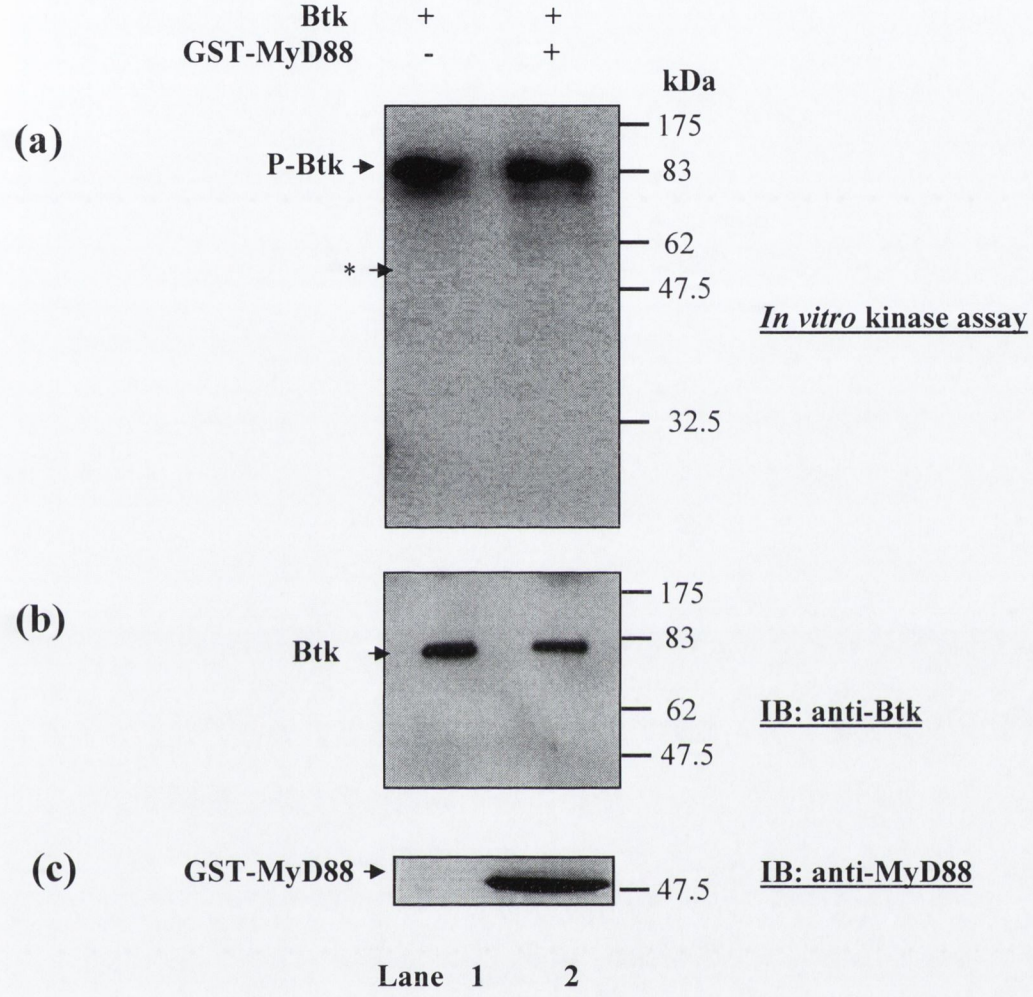

Figure 4.2.21 Recombinant MyD88 is not phosphorylated by Btk. Recombinant Btk was incubated alone (lane 1), or with recombinant GST-MyD88 (lane 2). The samples were incubated for 30 min. at 37°C with 2μCi [γ32P] PO4. Following incubation in an *in vitro* kinase assay, samples were analysed by SDS-PAGE, transferred to PVDF membrane and subjected to autoradiography. * Indicates the molecular weight of GST-MyD88. Samples were also immunblotted with (b) an anti-Btk antibody or (c) an anti-Mal antibody to confirm expression of Btk and MyD88 in the appropriate samples. Data shown is a representative experiment from three separate experiments.

3.3 Discussion

The past five years have witnessed an outburst of intense research activity in the pursuit to further decipher the components of the TLR signalling pathway. To date ten TLRs have been discovered in humans, all of which have a conserved cytosolic domain termed the TIR domain, which mediates signalling by TLRs. In addition to the TLR transmembrane proteins, it has emerged that cytoplasmic TIR-domain containing adapter proteins exist. Currently, there are five cytosolic TIR-containing TLR adapters, the first of which to be identified being the generically recruited MyD88 (O'Neill, Fitzgerald et al. 2003). Work in this laboratory identified the second adapter, known as Mal (Fitzgerald, Palsson-McDermott et al. 2001). In addition, the adapters TRIF, TRAM and SARM have recently been described.

During the initial investigations into the function of Mal, it was observed that the mobility of overexpressed Mal was retarded following SDS-PAGE analysis. Altered mobility of a protein on a SDS polyacrylamide gel is often indicative of phosphorylation or a post-translational modification. Therefore the phosphorylation status of Mal was investigated. Two dimensional SDS-PAGE analysis revealed that the slower migrating forms of Mal displayed a lower isoelectric point than the faster migrating forms. As the isoeletric point of a protein is almost always altered once phosphorylation occurs, this result further implied that Mal undergoes phosphorylation. Phosphatase treatment confirmed that the slower migrating forms of Mal represent phosphorylated Mal.

Biochemical evidence has shown that MyD88 associates with the unphosphorylated form of IRAK1 via DD-DD interactions (Burns, Martinon et al. 1998). In addition, MyD88 has been placed upstream of IRAK1 on the TLR signalling pathway,

as expression of IRAK1 (1-211), which encompasses the DD and ProST region, inhibited MyD88 mediated NF-κB activation. Data presented in this chapter, established that Mal also only interacts with the unphosphorylated form of IRAK1. The particular interaction sites between Mal and IRAK1 have yet to be mapped, however as Mal lacks a DD, the interaction sites between IRAK1 and Mal will be different to that observed between IRAK1 and MyD88. Indeed, Mal has been shown to interact with IRAK2 via its TIR domain {Fitzgerald, 2001 #8}. In contrast to MyD88, studies have shown that IRAK1(1-211) had no effect on NF-κB activation induced by Mal, leading investigators to rule out the possibility that IRAK1 is required for Mal to function(Fitzgerald, Palsson-McDermott et al. 2001). However IRAK1 (1-211) most likely inhibits MyD88-mediated NF-κB activation by disrupting the DD-DD interaction sites between MyD88 and IRAK1. As Mal may not interact with the DD of IRAK1, this may explain why IRAK1 (1-211) does not inhibit NF-κB activation mediated by Mal.

Given that Mal interacted with unphosphorylated IRAK1, the ability of IRAK1 to phosphorylate Mal was investigated. In addition, we examined the only other active kinase of the IRAK family, IRAK4, to determine if it could phosphorylate Mal. Results in this chapter, clearly demonstrate that Mal is a substrate for both IRAK1 and IRAK4 *in vitro*. Moreover, phosphorylation by IRAK1 resulted in the formation of three Mal phosphoproteins, whereas two phospho-forms of Mal were detected following phosphorylation of Mal by IRAK4, indicating that Mal is phosphorylated differentially by both IRAKs.

Recent investigations have clarified the complex series of events resulting in IRAK1 activation. Three sequential autophosphorylation steps are required for

phosphorylation of IRAK1, the sites of which have been mapped to Thr-209 and Thr-387, culminating in the hyperphosphorylation of several residues in the ProST region located between the death domain and kinase domain (Kollewe, Mackensen et al. 2004). Although Thr-209 and Thr-387 were found to be phosphorylated by IRAK1 itself, peptide analysis has shown that these residues are also potential targets for phosphorylation by IRAK4. It is believed that phosphorylation of IRAK1 by IRAK4 triggers IRAK1 autophosphorylation. Results have shown that hyperphosphorylation of IRAK1 releases IRAK1 from the adapter molecule Tollip and the receptor-MyD88 complex. This leads to the formation of a new protein complex comprising of hyperphosphorylated IRAK1 and TRAF6. IRAK1 is subsequently degraded, thus depleting the intracellular pool of IRAK1 available for signal transduction. To date the only substrates known for IRAK1 are IRAK1 itself, Tollip, Pellino2 and IRF-7, however the phosphorylation sites for Tollip, Pellino2 and IRF-7 have yet to be determined (Burns, Clatworthy et al. 2000; Strelow, Kollewe et al. 2003; Uematsu, Sato et al. 2005).

Studies into IRAK4 activation have revealed that like IRAK1, IRAK4 undergoes autophosphorylation. Moreover, it has emerged that only the kinase-inactive IRAK4 mutant protein can interact with IRAK1, MyD88 and TRAF6 (Li, Strelow et al. 2002). As of now, the known substrates for IRAK4 are IRAK1 and Pellino2(Li, Strelow et al. 2002; Strelow, Kollewe et al. 2003; Kollewe, Mackensen et al. 2004). Like IRAK1, the residues phosphorylated on Pellino2 by IRAK4 have yet to be determined. Therefore Mal joins IRAK1 and Pellino2 as a group of substrates phosphorylated *in vitro* by the serine/threonine kinases, IRAK1 and IRAK4. Further work will however be required to confirm that Mal is a substrate for IRAK1 and IRAK4 *in vivo*.

Interestingly, overexpression of Mal in cells lacking either IRAK1 or IRAK4 could not activate NF-κB, further indicating a critical role for both kinases in Mal signalling(Suzuki, Suzuki et al. 2003). In addition, following stimulation with TLR2 and TLR4 ligands, the kinase activity of IRAK1 was abolished in macrophages that were deficient for Mal(Yamamoto, Sato et al. 2002). This observation suggests that Mal may be required for IRAK1 activation. Indeed Mal may act as a bridging partner, facilitating IRAK1 recruitment to the TLR receptor complex, which may in turn reposition IRAK1 closer to IRAK4. This may then lead to phosphorylation of IRAK1 by IRAK4, thereby triggering IRAK1 autophosphorylation. Once activated, IRAK1 may then phosphorylate Mal. However, further work is required to determine if such a positive feedback mechanism is required to facilitate phosphorylation of IRAK1 and Mal during TLR signal transduction.

Recent evidence in our laboratory has emerged suggesting that phosphorylation of Mal by IRAK1 and IRAK4 may result in Mal degradation (Dunne, A., unpublished results). It has been reported that upon overexpression IRAK1 and IRAK4 spontaneously phosphorylate. Co-expression studies revealed that increasing concentrations of either IRAK1 or IRAK4 in HEK293 cells resulted in the depletion of Mal from the cell lysates. However, as IRAK1 is known to be activated upon overexpression of IRAK4, Mal degradation by IRAK4 may also be mediated by IRAK1. Given that overexpression of IRAK1 and IRAK4 activates their kinase activity, it is tempting to hypothesise that phosphorylation of Mal by IRAK1 and IRAK4 may result in the depletion of the intracellular pool of Mal. Degradation of a protein eliminates its availability for signal

transduction; Mal degradation may therefore be used as a further mechanism to ensure tight regulation of the TLR2 and TLR4 signaling pathways.

Although characterization of the TLR signaling pathway has mainly focused on the role of serine or threonine kinases, in recent years the importance of tyrosine phosphorylation following TLR activation has come to the forefront. In particular, it has been noted that stimulation with the TLR ligands, MALP-2 and LPS resulted in an increase in tyrosine phosphorylated proteins. Although tyrosine phosphorylation is known to occur following stimulation with MALP-2, to date the identity of the tyrosine kinases involved have yet to be ascertained. Regarding tyrosine kinase activation by LPS, the Src-family tyrosine kinases Src, Fgr, Hck, Lyn and the Tec family kinase, Btk have all been shown to be activated(Horwood, Mahon et al. 2003; Jefferies, Doyle et al. 2003; Napolitani, Bortoletto et al. 2003). The Src kinases have been implicated in TLR4 signaling mainly due to their enhanced expression and activation following LPS stimulation. However, the relative importance of the Src-family kinases in LPS signaling remains a controversial one, as the generation of triple knockout mice deficient in Hck, Fgr and Lyn demonstrated that these kinases are not essential for mediating the signaling pathway induced by LPS (Meng and Lowell 1997).

In contrast to the Src kinases, a role for Btk in LPS signal transduction is now widely accepted. Evidence establishing that Btk was involved in the LPS signaling pathway was initially observed in mice expressing an inactive form of Btk (Xid mice); as it was observed that B cells generated from these mutant mice showed impaired responses to LPS (Mukhopadhyay, Mohanty et al. 2002).. It has since emerged that LPS induces tyrosine phosphorylation of Btk and activates its kinase activity (Horwood,

Mahon et al. 2003; Jefferies, Doyle et al. 2003). In addition a Btk-specific inhibitor LFM-A13 blocked LPS induced NF-κB activation (Jefferies, Doyle et al. 2003). Furthermore, association studies also placed Btk on the TLR signaling pathway, as it has been revealed that Btk interacts with key proteins involved in TLR signal transduction, namely, TLR4, MyD88, Mal and IRAK1. Recent evidence has also determined that Btk is involved in p65-mediated transactivation and phosphorylation of p65 on Ser-536 during NF-κB activation by LPS (Doyle, Jefferies et al. 2005). Our findings here clearly demonstrated that Btk phosphorylates Mal *in vitro*. This observation therefore identifies Mal as the only known substrate for Btk on the TLR signaling pathway.

Previous studies have determined that MyD88 is tyrosine phosphorylated and that following LPS stimulation, tyrosine phosphorylation of MyD88 is enhanced (Ojaniemi, Glumoff et al. 2003). Results in this chapter revealed that similar to Mal, MyD88 is phosphorylated by cellular kinases. However, it was noted that MyD88 was not phosphorylated by IRAK1, IRAK4 or Btk. Moreover, overexpression of either IRAK1 or IRAK4 had no effect on the expression profile of MyD88, suggesting that Mal undergoes an alternative method of regulation compared to MyD88 (Dunne, A., unpublished results).

Numerous studies have shown that members of the TLR family are modified by phosphorylation. In particular MyD88, TLR2, TLR3 and TLR4 have all been shown to be tyrosine phosphorylated following activation. To date with the exception of the most recently identified TIR-domain containing adapter SARM, all other TIR adapters are phosphorylated, indicating that phosphorylation serves as an important mechanistic tool in mediating TLR signal transduction. Although members of the TLR family have been

shown to undergo phosphorylation, the kinases required have only been speculated upon. Therefore this chapter identifies for the first time, kinases that phosphorylate a TIR-domain containing protein.

Taken together data presented in this chapter clearly demonstrates that Mal is a phosphoprotein and an *in vitro* substrate for IRAK1, IRAK4 and Btk. In addition, phosphorylation of Mal by IRAK1, IRAK4 and Btk provides a distinguishing feature between Mal and MyD88 in mediating TLR signal transduction.

Chapter 4

Identification of phospho-accepting residues in Mal and their role in signaling

4.1 Introduction

In the previous chapter, it was shown that Mal was phosphorylated by IRAK1, IRAK4 and Btk *in vitro*. Having identified the kinases involved in Mal phosphorylation, it was of interest to establish the residues that were phosphorylated. Therefore, in this chapter mutational analysis of Mal was undertaken in order to identify potential phosphorylation sites.

It was observed that replacement of specific serine or threonine residues had no effect on Mal function. However, certain tyrosine residues of Mal, namely Tyr-86, Tyr-106 and Tyr-187 were identified as possible phospho-accepting residues. This chapter subsequently focused on examining the tyrosine phosphorylation status of Mal both endogenously and in overexpression studies. Furthermore, the effect of mutating Tyr-86, Tyr-106 and Tyr-187 on Mal signal transduction was assessed. In addition, the role of Btk with respect to tyrosine phosphorylation of Mal was further examined.

4.2 Results

4.2.1 Mutational Analysis of specific serine and threonine residues located within the sequence of Mal

As the previous chapter revealed that Mal was phosphorylated by IRAK1 and IRAK4, both of which are serine/threonine kinases, the sequence of Mal was next studied to determine possible serine/threonine phospho-accepting residues. Mal consists of 235 residues, out of which 31 are serines and 12 are threonine residues, of which 25 serines and 6 threonines are conserved in the mouse sequence. In order to predict possible phosphorylated residues, the sequence of Mal was analysed in the computer programme, NetPhos (www.cbs.dtu.dk). In total 15 serine residues and 3 threonine residues were selected as potential phospho-accepting residues. As illustrated in figure 4.2.1 the serines that displayed the highest score for potential phosphorylation sites, were located at positions 39, 52, 66, 83, 93, and 105. In order to assess if these serine residues were required for Mal phosphorylation, each residue was mutated conservatively to alanine by *in vitro* site directed mutagenesis. In addition Ser-3, Ser-4, Ser-5, Thr-6 and Ser-183, all of which are conserved in the murine sequence, were randomly chosen as possible phospho-accepting residues. Using the plasmid pCDNA3-HA-Mal as the parental DNA, *in vitro* site directed mutagenesis was performed. The mutagenic oligonucleotide primers for use were designed individually according to the desired mutation. The sequence of each construct was subsequently confirmed by DNA sequencing.

As CIP treatment of Mal in the previous chapter, had abolished the slower migrating phosphorylated forms of Mal, it was hypothesised that mutating a phospho-accepting residue to alanine should alter the electrophoretic mobility pattern of Mal.

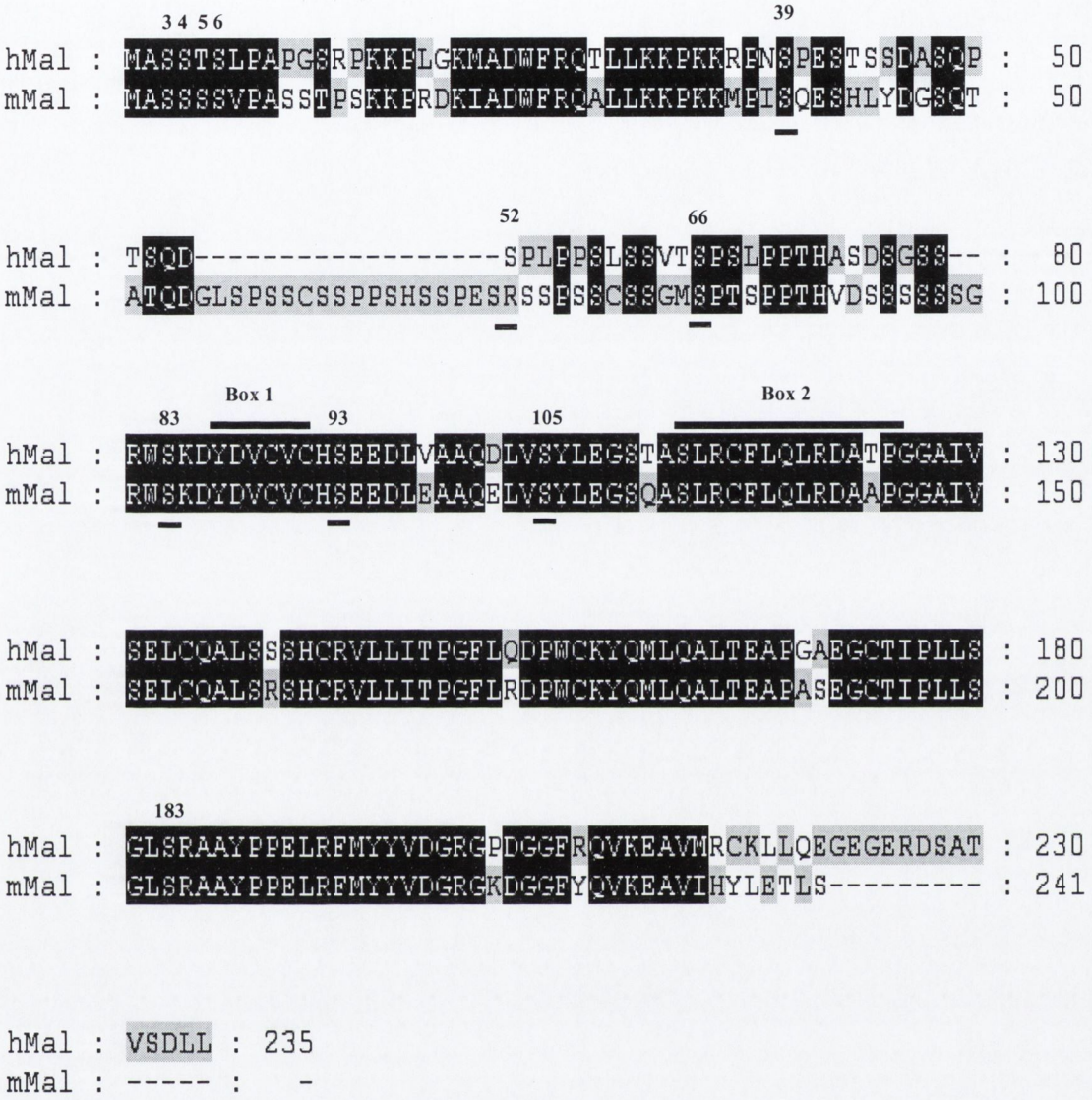

Figure 4.2.1 Alignment of human Mal (hMal) and murine Mal (mMal). Two regions, Box 1 and Box 2 that are conserved among all TIR domain containing proteins are over lined. The serine residues that displayed the highest score as possible phospho-accepting residues are underlined and numbered according to their location in human Mal. Other serine residues that were also mutated conservatively to alanine are also numbered according to their location in human Mal.

Therefore, HEK293 cells were transiently transfected with plasmids encoding HA-Mal and the serine Mal mutant proteins HA-Mal-S39A, HA-Mal-S52A, HA-Mal-S66A, HA-Mal-S83A, HA-Mal-S93A, HA-Mal-S39AS52A, HA-Mal-S3A, HA-Mal-S4A, HA-Mal-T5A, HA-Mal-S5A and HA-Mal-S183A, in order to investigate their expression profile. Cell lysates were prepared, samples were then analysed by SDS-PAGE and subsequently immunoblotted with an anti-HA antibody to detect expression. As shown in Fig. 4.2.2a and 4.2.2b, mutation of these specific serine residues displayed the same mobility pattern as wild-type Mal. A double mutant, Mal-S39AS52A, that was generated to determine if mutating both of these serine residues together would reduce or abolish the slower migrating forms of Mal, again displayed the same electrophoretic mobility pattern as wild-type Mal (Figure 4.2.2b, lane 7). As mutation of these specific serine residues had no effect on the electrophoretic mobility pattern of wild-type Mal, it suggests that they are not individually required to induce the mobility shift that occurs upon Mal overexpression.

Having established that the serine Mal mutant proteins did not affect the expression profile of Mal, their effect on NF-κB activation was next investigated. HEK293 cells were therefore transiently transfected with the Mal mutant proteins in conjunction with an NF-κB-dependent luciferase reporter gene. As figure 4.2.3 illustrates, the tested Mal mutant proteins activated NF-κB to the same extent as wild-type Mal.

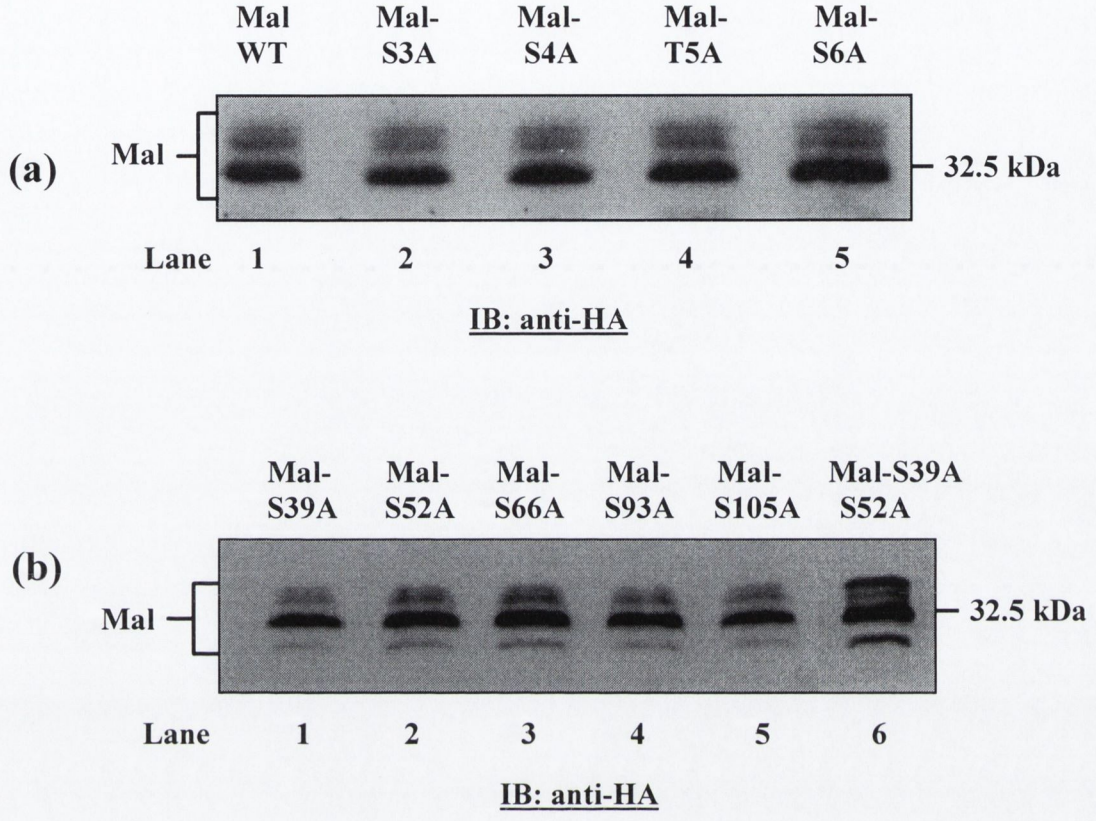

Figure 4.2.2 Serine Mal mutants still retain the slower migrating forms of wild-type Mal. (a) HEK293 cells ($1x10^6$) were transiently transfected with 2 μg of plasmids encoding the following proteins HA-Mal (lane 1), HA-Mal-S3A (lane 2), HA-Mal-S4A (lane 3), HA-Mal-T5A (lane 4), or HA-Mal-S6A (lane 5). Cell lysates were prepared and samples were analysed by SDS-PAGE, followed by immunoblotting with an anti-HA antibody. Data shown is a representative experiment from three separate experiments. (b) HEK293 cells ($1x10^6$) were transiently transfected with 2 μg of plasmids encoding the following proteins HA-Mal-S39A (lane 1), HA-Mal-S52A (lane 2), HA-Mal-S66A (lane 3), HA-Mal-S83A (lane 4), and HA-Mal-S93A (lane 5) or HA-MalS39AS52A (lane 6), for 24 hours. Cell lysates were prepared and samples were analysed by SDS-PAGE, followed by immunoblotting with an anti-HA antibody. Data shown is a representative experiment from three separate experiments.

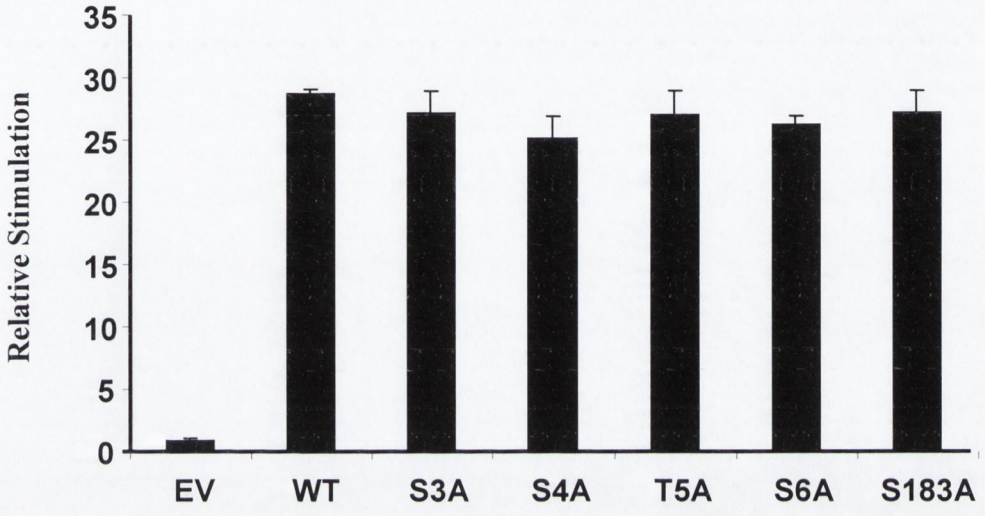

Figure 4.2.3 Mal serine mutant proteins activate NF-κB to the same extent as wild-type Mal. HEK293 cells were transiently transfected with plasmids encoding the following proteins empty vector (EV), HA-Mal, HA-Mal-S3A, HA-Mal-S4A, HA-Mal-T5A, HA-Mal-S6A and HA-Mal-S183A. Extracts were prepared and measured for luciferase activity. Results are normalized for *Renilla* luciferase activity and represented as fold induction relative to empty vector (EV) control. Results are expressed as mean ± standard deviation for a representative experiment from three separate experiments, each performed in triplicate.

4.2.2 Mutational analysis of the tyrosine residues located within the sequence of Mal

Having ascertained that Mal was also a substrate for the tyrosine kinase Btk, the sequence of Mal was next analysed to determine the number of potential phospho-accepting tyrosine residues. Mal contains six tyrosine residues, all of which are located at the carboxyl terminus within its TIR domain. As shown in figure 4.2.4, these six tyrosines are conserved in the mouse sequence, attesting to their possible importance in the functioning of Mal. One tyrosine, tyrosine 86 is a conserved residue among all TIR domain containing proteins, and is located within Box 1, the signature sequence of the TIR domain. Tyrosine 106 is situated between Box 1 and Box 2, whereas the remaining four other tyrosine residues at positions 159, 187, 195 and 196 are located distally to Box 2. In order to examine the role of these tyrosine residues in Mal phosphorylation the six tyrosine residues were mutated conservatively to phenylalanine. Using the plasmid pCDNA3-HA-Mal as the parental DNA, *in vitro* site directed mutagenesis was performed as described in the Materials and Methods section. The mutagenic oligonucleotide primers for use were designed individually according to the desired mutation. The sequence of each construct was subsequently confirmed by DNA sequence analysis.

As the electrophoretic mobility of Mal is retarded on SDS-PAGE, the mobility pattern of the Mal tyrosine mutants was analysed. HEK293 cells were transiently transfected with increasing concentrations of plasmids encoding the mutant proteins HA-Mal-Y86F, HA-Mal-Y106F, HA-Mal-Y159F, HA-Mal-Y187F, HA-Mal-Y195F or HA-Mal-Y196F. Cell lysates were prepared and samples were analysed by SDS-PAGE and immunoblotted with the anti-HA antibody. Interestingly, it was observed that the slowest

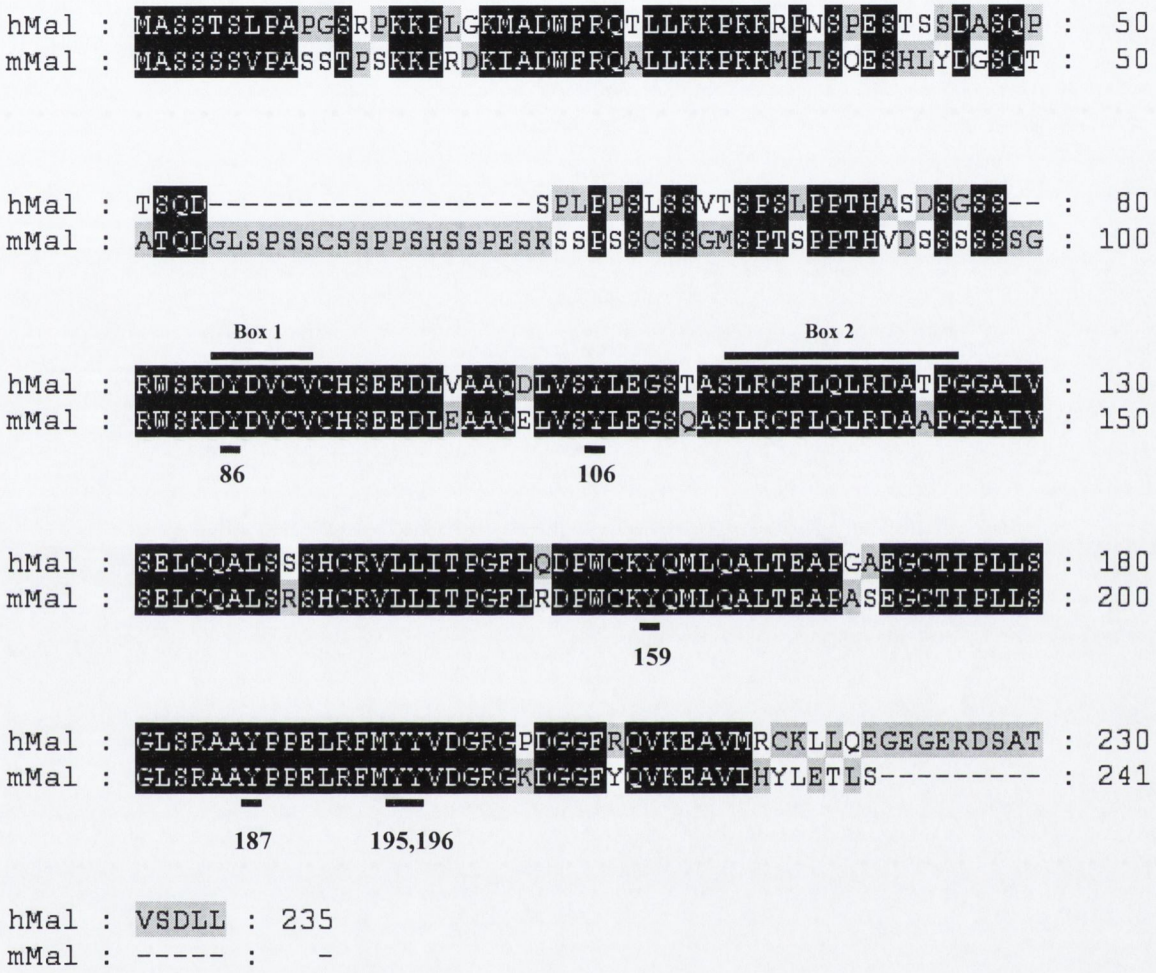

Figure 4.2.4 Alignment of human Mal (hMal) and murine Mal (mMal). Two regions, Box 1 and Box 2, which are conserved among all TIR domain containing proteins are over lined. The tyrosine residues conserved in both human and murine Mal are underlined and numbered according to their location in human Mal.

migrating form of wild-type Mal was no longer evident in Mal-Y86F (Figure 4.2.5, lanes 4-6), Mal-Y106F (Figure 4.2.5, lanes 7-9) or Mal-Y187F (Figure 4.2.6, lanes 4-6). In contrast the mutant proteins Mal-Y159F (Figure 4.2.6, lanes 1-3), Mal-Y195F (Figure 4.2.6, lanes 7-9), or Mal-Y196F (Figure 4.2.6, lanes 10-12), retained the same electrophoretic mobility pattern as wild-type Mal (Figure 4.2.5, lanes 1-3).

The effect of mutating the three tyrosine residues at position 86, 106 or 187 in different combinations was next examined. HEK 293 cells were transiently transfected with plasmids encoding HA-Mal-Y86F Y106F, HA-Mal-Y86F Y187F, HA-Mal-Y106F Y187F, and HA-Mal-Y86F Y106F Y187F, cell lysates were prepared and samples were separated by SDS-PAGE and immunoblotted with the anti-HA antibody to detect expression. Double and triple mutant forms of Tyr-86, Tyr-106 and Tyr-187 gave the same profile as a single mutant of each of these amino acids (Figure 4.2.7). These results suggested that the tyrosine residues located at positions 86, 106 and 187 were potential phosphorylation sites with all three tyrosine residues requiring phosphorylation for the altered mobility of Mal on SDS-PAGE.

4.2.3 Two-dimensional SDS-PAGE analysis of the Mal tyrosine mutants

Having established in the previous chapter that the isoelectric point of Mal is altered, the phosphorylation status of the tyrosine mutant proteins following 2-D gel analysis was next examined. HEK 293 cells were transiently transfected with plasmids encoding wild-type Mal and the mutant proteins HA-Mal-Y86F, HA-Mal-Y106F, HA-Mal-Y159F, HA-Mal-Y187F, HA-Mal-Y195F, HA-Mal-Y196F or HA-Mal-Y86F Y106F Y187F. Cell lysates were prepared and the Mal mutant proteins were

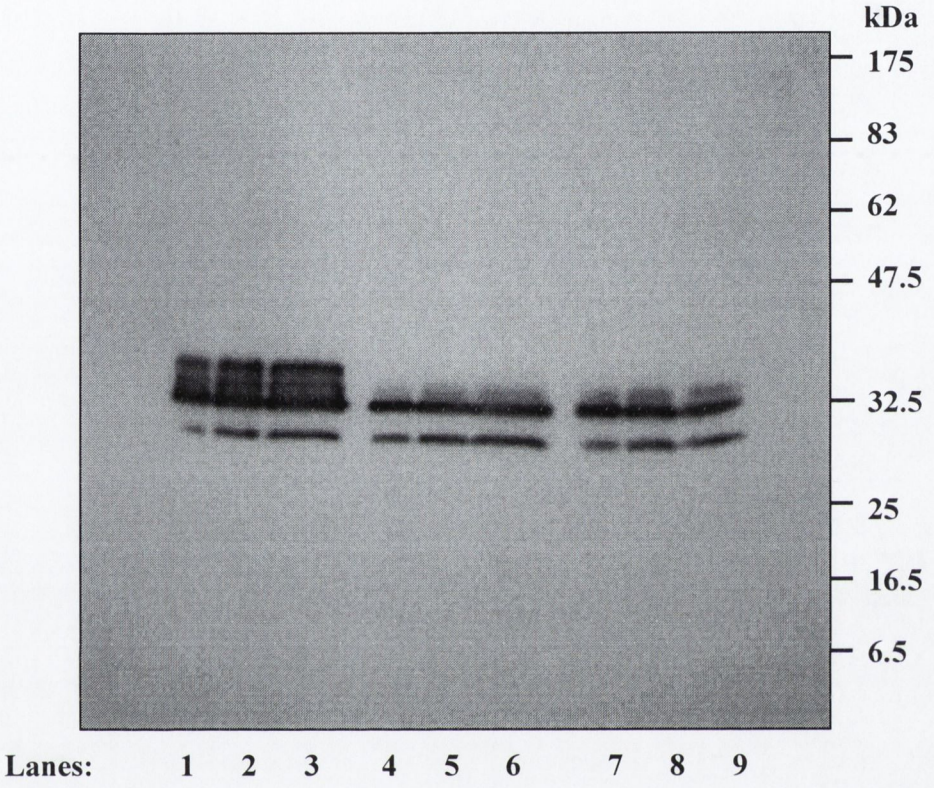

Figure 4.2.5 Analysis of the expression profile of the Mal tyrosine mutants. HEK 293 cells were transfected with 0.15 μg, 0.3 μg, and 0.6 μg, of a plasmid encoding HA-Mal (lanes 1-3), or 0.25 μg, 0.5 μg, and 1 μg of expression plasmids encoding HA-Mal-Y86F (lanes 4-6) and HA-Mal-Y106F (lanes 7-9). Cell lysates were prepared, samples were subsequently analysed by SDS-PAGE and proteins were detected using an anti-HA antibody.

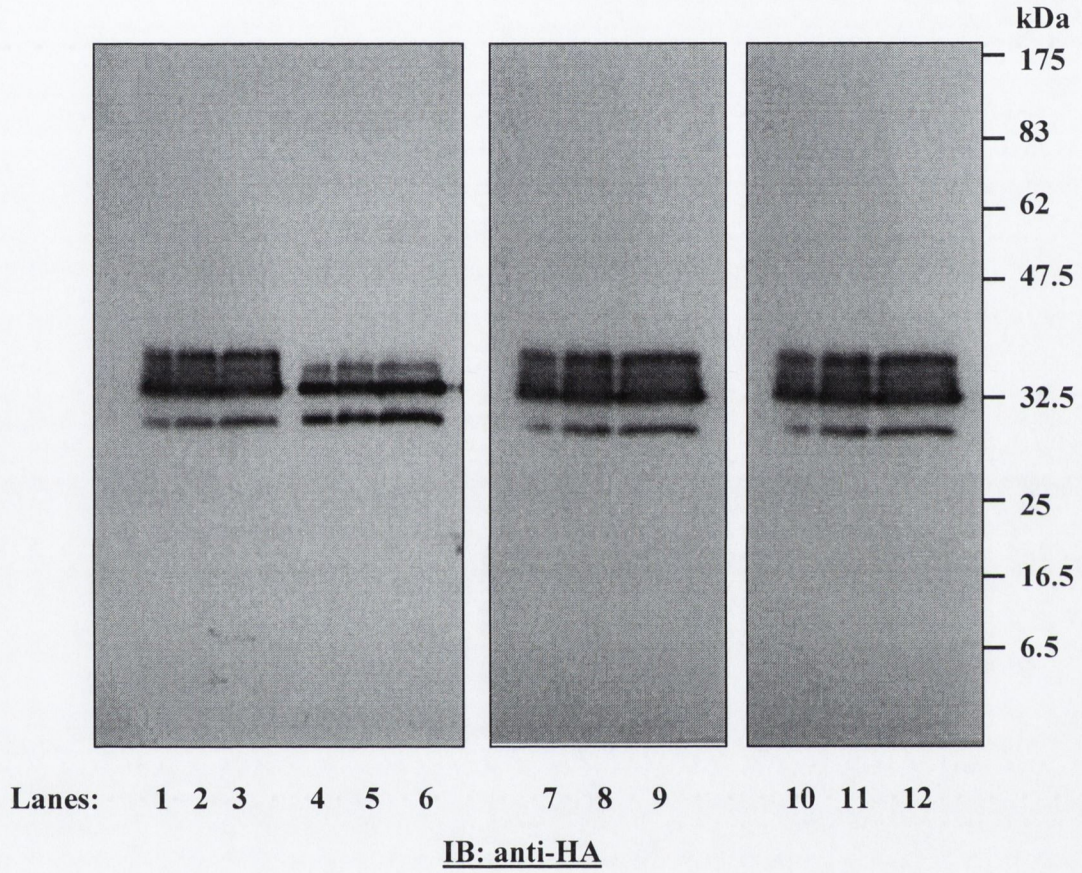

Figure 4.2.6 Analysis of the expression profile of the Mal tyrosine mutants. HEK 293 cells were transfected with 0.25 μg, 0.5 μg, and 1 μg expression plasmids encoding HA-Mal-Y159F (lanes 1-3), HA-Mal-Y187F (lanes 4-6), HA-Mal-Y195F (lanes 7-9) and HA-Mal-Y196F (lanes 10-12). Cell lysates were prepared, samples were subsequently analysed by SDS-PAGE and proteins were detected using an anti-HA antibody.

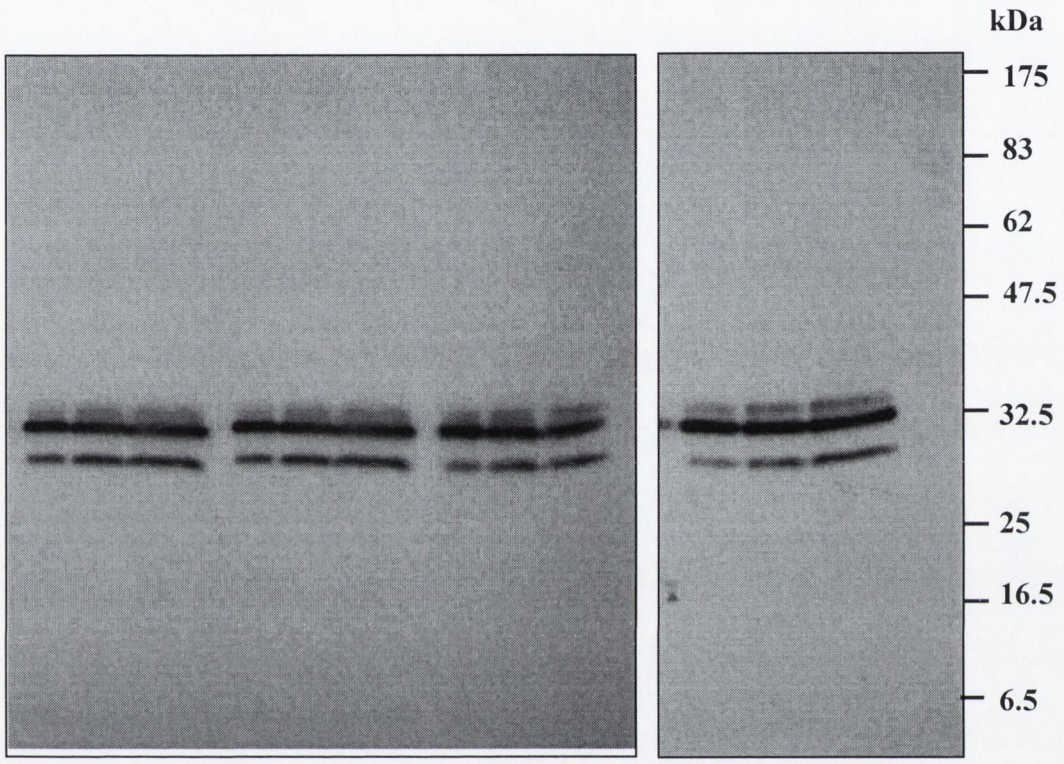

Figure 4.2.7 Analysis of the expression profile of the double and triple Mal tyrosine mutants. HEK 293 cells were transfected with 0.25 μg, 0.5 μg, and 1 μg expression plasmids encoding HA-Mal-Y86F Y106F (lanes 1-3), HA-Mal-Y86F Y106F (lanes 4-6), HA-Mal-Y106F Y187F (lanes 7-9) and HA-Mal-Y86F Y106F Y187F (lanes 10-12). Cell lysates were prepared, samples were subsequently analysed by SDS-PAGE and proteins were detected using an anti-HA antibody.

immunoprecipitated with the anti-HA antibody. Proteins were eluted with 2-D sample solution and analysed by 2D SDS-PAGE. In Figure 4.2.8, wild-type Mal migrated as 2 spots, as shown previously in Chapter 3 (Figure 3.2.3.). It was observed that whilst Mal-Y86F (Figure 4.2.9), Mal-Y106F (Figure 4.2.10), Mal-Y187F (Figure 4.2.11) and Mal-Y86F Y106F Y187F (Figure 4.2.12) still existed as two forms, there was a dramatic reduction in the quantity of the slower migrating form of Mal that exhibited the lower isoelectric point. This is consistent with the hypothesis that this form of Mal is most likely an unresolved mixture of the two slower migrating phosphorylated forms of Mal detected on a 1-D SDS-PAGE gel. Similar to 1-D SDS-PAGE analysis, the Mal mutant proteins Mal-Y159F (Figure 4.2.13), Mal-Y195F (Figure 4.2.14) and Mal-Y196F (Figure 4.2.15), all displayed the same phosphorylation profile as wild-type Mal, with the two forms existing at the same concentration level. These results further implied that the tyrosine residues located at positions 86, 106 and 187 were potential phosphorylation sites with all three tyrosine residues requiring phosphorylation for the altered mobility of Mal on SDS-PAGE.

4.2.4 The structural model of the TIR domain of Mal

Having identified Tyr-86, Tyr-106 and Tyr-187 as possible phospho-accepting Mal residues, it was of interest to analyse whether these residues were on the surface. Although the crystal structure for Mal has yet to be elucidated, a molecular model for Mal can be constructed using the crystal structures of the TIR domains from TLR1 and TLR2 (Dunne, Ejdeback et al. 2003). It was noted that both Tyr-86 and Tyr-106 appear to be surface exposed, whereas Tyr-187, just visible on the surface model, appears to be the

(a)

IP: anti-HA
IB: anti-HA

(b)

IP: anti-HA
IB: anti-HA

Figure 4.2.8 Two-dimensional gel analysis of the phosphorylation status of Mal. HEK293 cells were transiently transfected with 3 μg of a plasmid encoding (a) HA-Mal or (b) empty vector (EV). Cell lysates were prepared and HA-Mal was immunoprecipitated with an anti-HA antibody. Samples were then isoelectrophoretically focused under a pH gradient of 4 to 7. Focused proteins were then separated in the second dimension by SDS-PAGE, followed by immunoblotting with anti-HA antibody.

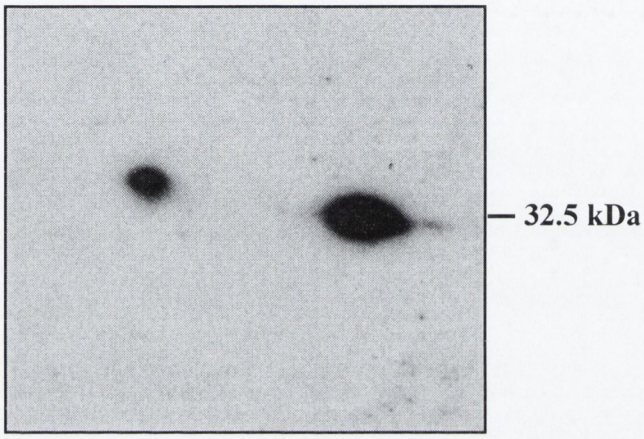

Figure 4.2.9 Two-dimensional gel analysis of the phosphorylation status of Mal-Y86F. HEK293 cells were transiently transfected with 5 μg of a plasmid encoding HA-Mal-Y86F. Cell lysates were prepared and HA-Mal-Y86F was immunoprecipitated with an anti-HA antibody. Samples were then isoelectrophoretically focused under a pH gradient of 4 to 7. Focused proteins were then separated in the second dimension by SDS-PAGE, followed by immunoblotting with anti-HA antibody.

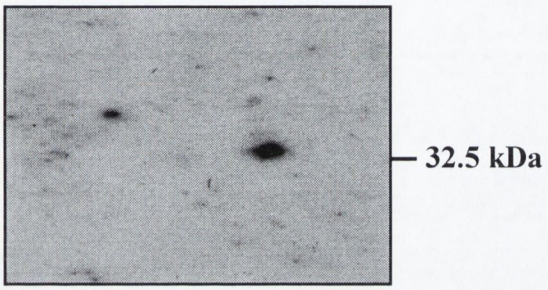

IP: anti-HA
IB: anti-HA

Figure 4.2.10 Two-dimensional gel analysis of the phosphorylation status of Mal-Y106F. HEK293 cells were transiently transfected with 5 μg of a plasmid encoding HA-Mal-Y106F. Cell lysates were prepared and HA-Mal-Y106F was immunoprecipitated with an anti-HA antibody. Samples were then isoelectrophoretically focused under a pH gradient of 4 to 7. Focused proteins were then separated in the second dimension by SDS-PAGE, followed by immunoblotting with anti-HA antibody.

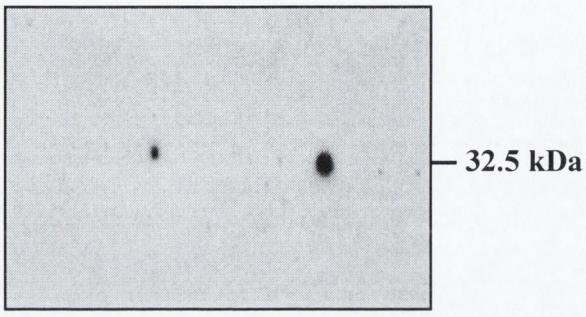

IP: anti-HA
IB: anti-HA

Figure 4.2.11 Two-dimensional gel analysis of the phosphorylation status of Mal-Y187F. HEK293 cells were transiently transfected with 5 μg of a plasmid encoding HA-Mal-Y187F. Cell lysates were prepared and HA-Mal-Y187F was immunoprecipitated with an anti-HA antibody. Samples were then isoelectrophoretically focused under a pH gradient of 4 to 7. Focused proteins were then separated in the second dimension by SDS-PAGE, followed by immunoblotting with anti-HA antibody.

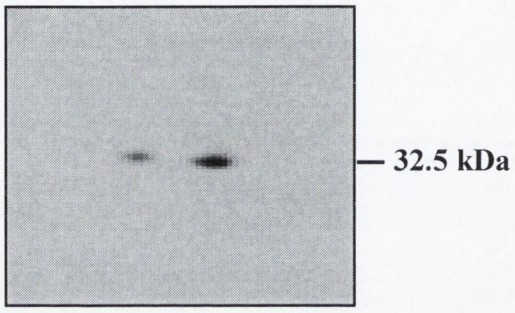

Figure 4.2.12 Two-dimensional gel analysis of the phosphorylation status of Mal-Y86F Y106F Y187F. HEK293 cells were transiently transfected with 5 μg of a plasmid encoding HA-Mal-Y86F Y106F Y187F. Cell lysates were prepared and HA-Mal-Y86F Y106F Y187F was immunoprecipitated with an anti-HA antibody. Samples were then isoelectrophoretically focused under a pH gradient of 4 to 7. Focused proteins were then separated in the second dimension by SDS-PAGE, followed by immunoblotting with anti-HA antibody. Data shown is a representative experiment from three separate experiments.

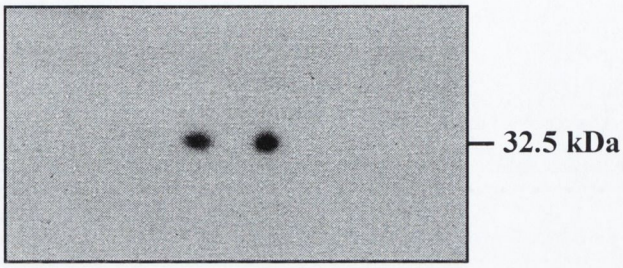

IP: anti-HA
IB: anti-HA

Figure 4.2.13 Two-dimensional gel analysis of the phosphorylation status of Mal-Y159F. HEK293 cells were transiently transfected with 5 μg of a plasmid encoding HA-Mal-. Y159F. Cell lysates were prepared and HA-Mal-Y159F was immunoprecipitated with an anti-HA antibody. Samples were then isoelectrophoretically focused under a pH gradient of 4 to 7. Focused proteins were then separated in the second dimension by SDS-PAGE, followed by immunoblotting with anti-HA antibody. Data shown is a representative experiment from three separate experiments.

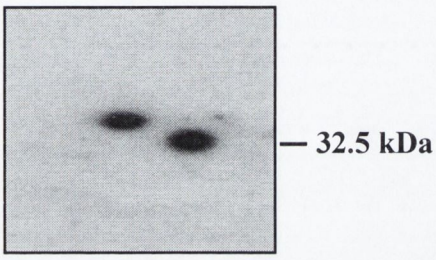

Figure 4.2.14 Two-dimensional gel analysis of the phosphorylation status of Mal-Y195F. HEK293 cells were transiently transfected with 5 μg of a plasmid encoding HA-Mal-Y195F. Cell lysates were prepared and HA-Mal-Y195F was immunoprecipitated with an anti-HA antibody. Samples were then isoelectrophoretically focused under a pH gradient of 4 to 7. Focused proteins were then separated in the second dimension by SDS-PAGE, followed by immunoblotting with anti-HA antibody. Data shown is a representative experiment from three separate experiments.

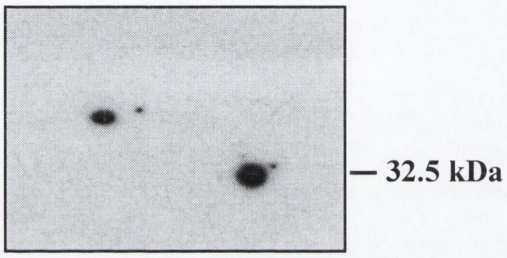

IP: anti-HA
IB: anti-HA

Figure 4.2.15 Two-dimensional gel analysis of the phosphorylation status of Mal-Y196F. HEK293 cells were transiently transfected with 5 μg of a plasmid encoding HA-Mal-Y196F. Cell lysates were prepared and HA-Mal-Y196F was immunoprecipitated with an anti-HA antibody. Samples were then isoelectrophoretically focused under a pH gradient of 4 to 7. Focused proteins were then separated in the second dimension by SDS-PAGE, followed by immunoblotting with anti-HA antibody. Data shown is a representative experiment from three separate experiments.

least accessible (Figure 4.2.16). The backbone of the TIR domain is reported to be similar to that of CheY, a bacterial chemotaxis protein (Rock, Hardiman et al. 1998). Studies have shown that CheY undergoes phosphorylation, and that this phosphorylation event triggers a conformational change, thereby regulating its association with other proteins. It is possible that phosphorylation of Mal on Tyr-86 or Tyr-106 is required to initiate a conformational change in the TIR domain of Mal, thereby exposing Tyr-187 for phosphorylation, leading to activation of downstream signals.

4.2.5 Mal is tyrosine phosphorylated

As there is evidence demonstrating the dependence of TLR signaling on tyrosine kinase activity, the tyrosine phosphorylation status of Mal was examined. Using a protein tyrosine phosphatase (PTP-1B) which specifically dephosphorylates phosphotyrosine residues, the tyrosine phosphorylation of Mal was primarily investigated. HEK 293 cells were transfected with a plasmid encoding HA-Mal, cell lysates were prepared and HA-Mal was immunoprecipitated with an anti-HA antibody. Immunoprecipitated Mal was then treated with or without Protein Tyrosine Phosphatase-1B (PTP-1B) and incubated at 37°C for 60 min. Samples were analysed by SDS-PAGE and immunoblotted with anti-HA antibody. Following phosphatase treatment the slower migrating form of Mal was eliminated, indicating that Mal is tyrosine phosphorylated (Figure 4.2.17, compare lane 2 to lane 1).

To further confirm that Mal was tyrosine phosphorylated, HEK 293 cells were transiently transfected with a plasmid encoding HA-Mal or mock transfected. Cell lysates were prepared and HA-Mal was immunoprecipitated using an anti-HA antibody. Samples

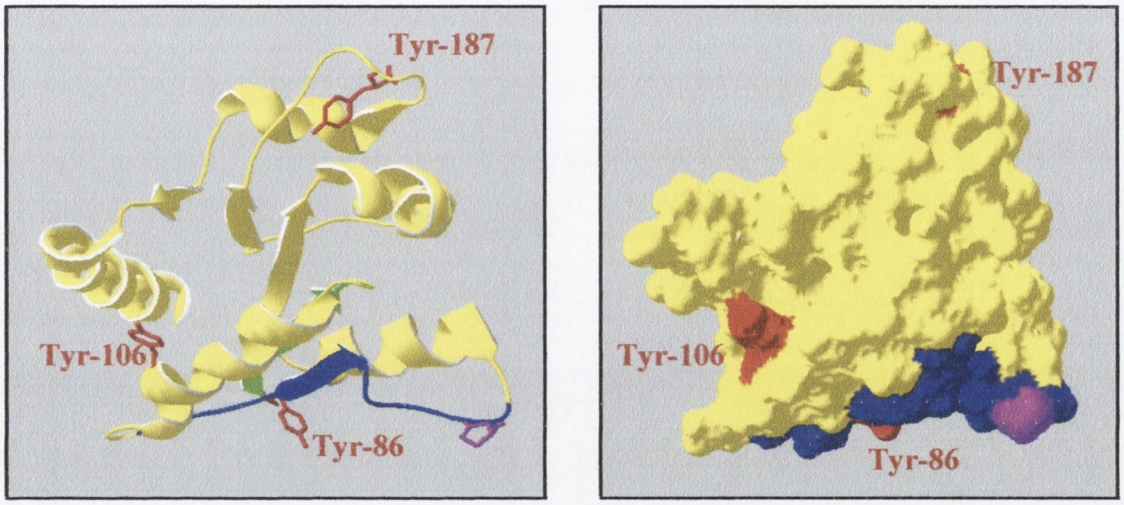

Figure 4.2.16 Structural surface analysis of the TIR domain of Mal. Structural features representing the conserved boxes of the TIR domains are shown in green (Box 1) and blue (Box 2). The side chain of the semi-conserved proline residue in the BB-loop is coloured purple. The phospho-accepting tyrosines Tyr-86, Tyr-106, and Tyr-187 are highlighted in red.

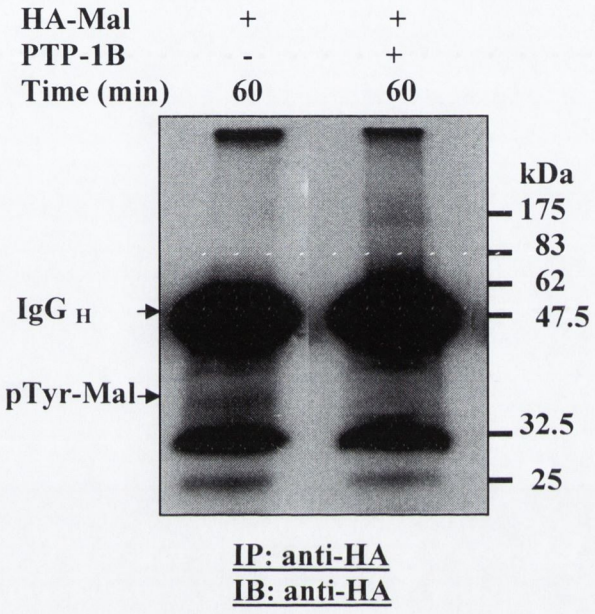

Figure 4.2.17 Mal is tyrosine phosphorylated. HEK-293 cells (1x 10^6) were transiently transfected with 5 μg of a plasmid encoding HA-Mal for 24 hours. Lysates were prepared and HA-Mal was immunoprecipitated with the HA antibody. Immunoprecipitates were washed three times and incubated at 37°C with 10U of Protein Tyrosine Phosphatase-1B (PTP-1B) (lane 2) or without PTP-1B (lane 1). Samples were analysed by 12% SDS-PAGE and immunoblotted with an anti-HA antibody. Following treatment with PTB-1B, the slowest migrating species of Mal was no longer detected (lanes 2). Data shown is a representative experiment from two separate experiments.

were then separated by SDS-PAGE and immunoblotted with an antibody that specifically recognises phosphotyrosine residues. A band corresponding to the molecular mass of the slowest migrating form of Mal was detected in the sample expressing Mal (Figure 4.2.18a, lane 2), whereas no phosphorylated tyrosine residues were detected in the mock-transfected sample (Figure 4.2.18a, lane 1). Overexpressed Mal therefore clearly undergoes tyrosine phosphorylation (Figure 4.2.18a, lane2). Samples were immunoblotted with an anti-HA antibody to confirm expression of HA-Mal (Figure 4.2.18b, lane2).

4.2.6 Endogenous Mal is tyrosine phosphorylated following stimulation with LPS.

Having determined that overexpressed Mal contained phosphorylated tyrosine residues, the tyrosine phosphorylation status of endogenous Mal was next examined. It was first necessary to identify a cell line, which naturally expresses Mal. Previous reports have determined using RT PCR analysis that Mal is expressed in a variety of cell types including mature and immature murine bone-marrow derived dendritic cells and in monocytic/macrophage cell lines (Fitzgerald, Palsson-McDermott et al. 2001). In order to assess the expression profile of endogenous Mal, a polyclonal antibody was raised against recombinant Mal as described in the Materials and Methods Section. HEK293 cells were transfected with a plasmid encoding HA-Mal (Figure 4.2.19, lanes 2 and 4) or left untransfected (Figure 4.2.19, lanes 1 and 3). Cell lysates were prepared and proteins were immunoprecipitated with an anti-HA antibody (Figure 4.2.19a, lanes 1 and 2). Samples were analysed by SDS-PAGE and immunoblotted with an anti-Mal antibody. It was confirmed that the anti-Mal antibody could detect both immunoprecipitated Mal (Figure

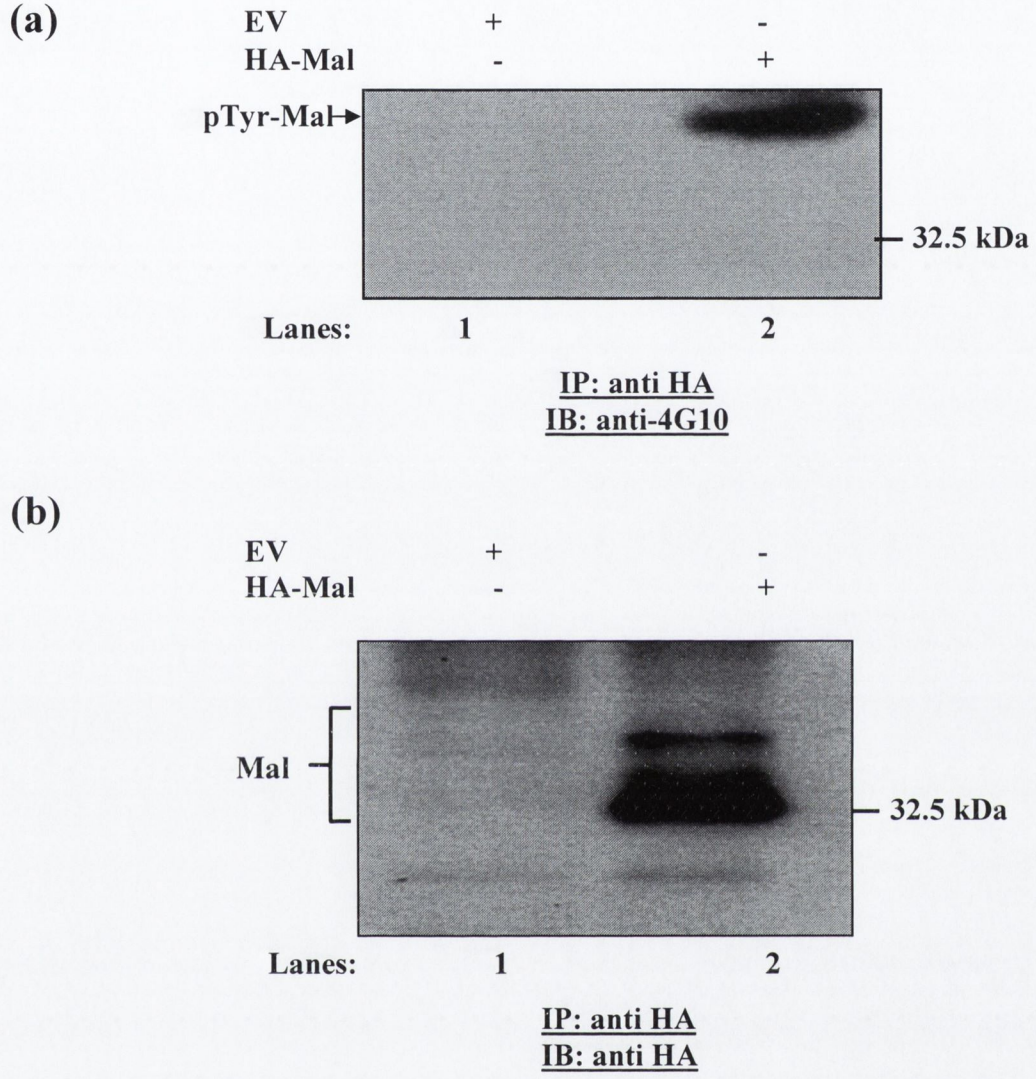

Figure 4.2.18 Mal is Tyrosine Phosphorylated. HEK-293 cells (1x 10^6) were mock-transfected (lane 1) or transfected with 5 μg of a plasmid encoding HA-Mal (lane 2). HA-Mal was immunoprecipitated from cell lysates with an anti-HA antibody. (a) Samples were analysed by 12% SDS-PAGE and immunoblotted with an antibody that recognises phospho-tyrosine residues (Anti-4G10). (b) A portion of the sample was immunoblotted with an anti-HA antibody to demonstrate that HA-Mal was present only in lane 2. Results shown are representative of three separate experiments.

Figure 4.2.19 The expression profile of endogenous Mal in (a) the HEK293 cell line and (b) the THP-1 cell line. (a) HEK293 cells were transfected with 5 μg of a plasmid encoding HA-Mal (lanes 2 and 4) or left un-transfected (lanes 1 and 3). Cell lysates were prepared and proteins were immunoprecipitated with an anti-HA antibody (lanes 1 and 2). Samples were analysed by SDS-PAGE and immunoblotted with an anti-Mal antibody. (b) Cell lysates were prepared from THP1 cells, 10 μl, 20 μl, 30 μl of cell lysates were analysed by SDS-PAGE and immunoblotted with the anti-Mal antibody. Results shown are representative of three separate experiments.

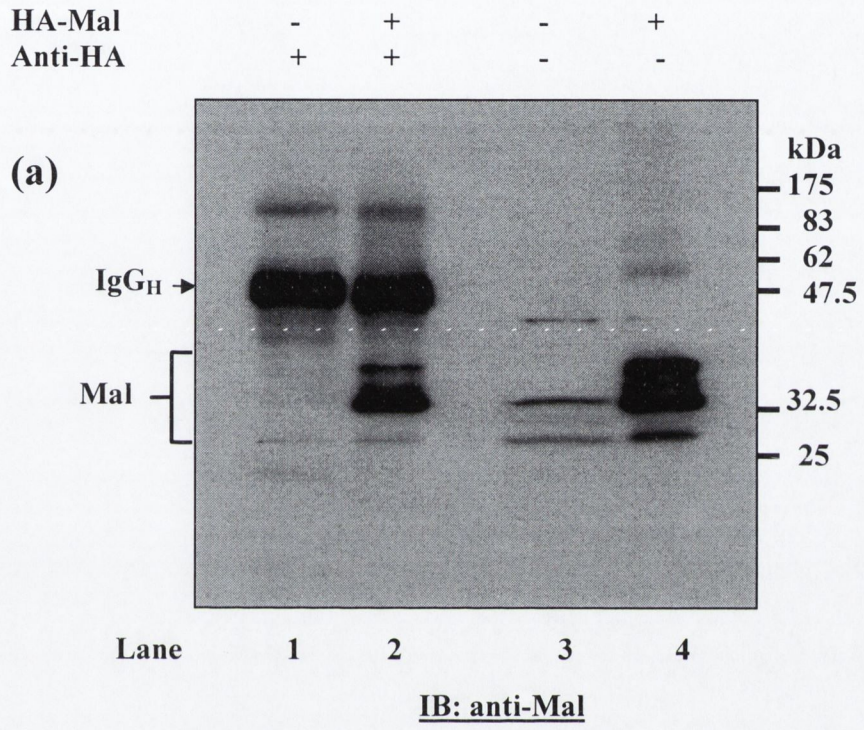
HA-Mal - + - +
Anti-HA + + - -
(a)
kDa
175
83
62
47.5
IgG$_H$
Mal
32.5
25
Lane 1 2 3 4
IB: anti-Mal

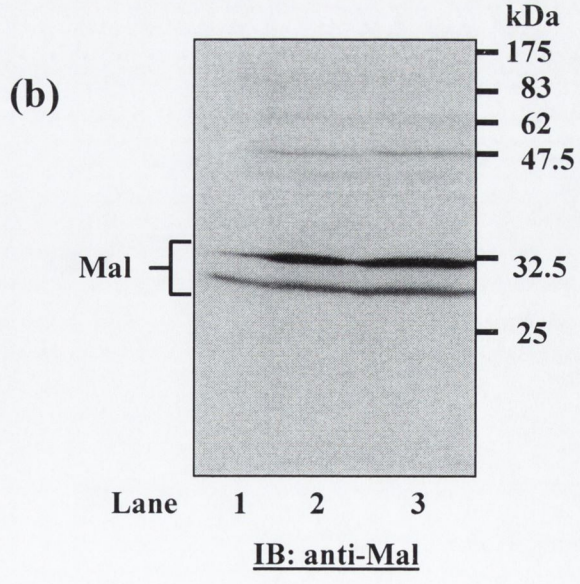
(b)
kDa
175
83
62
47.5
Mal
32.5
25
Lane 1 2 3
IB: anti-Mal

4.2.19a, lane 2) and overexpressed Mal in the cell lysate (Figure 4.2.19a, lane 4). Endogenous Mal was also detected in HEK293 cells, existing as two distinct forms (Figure 4.2.19, lane 3).

The expression profile of endogenous Mal in the human monocytic/macrophage THP-1 cell line was next assessed. Cell lysates were prepared from THP1 cells, samples were analysed by SDS-PAGE and immunoblotted with the anti-Mal antibody. Again endogenous Mal was detected as two distinct forms (Figure 4.2.19b, lanes 1-3). I next tested whether the anti-Mal antibody could immunoprecipitate endogenous Mal in HEK293 cells in order to test for phosphorylation of endogenous Mal. While the anti-Mal antibody could immunoprecipitate overexpressed Mal, it was not effective at immunoprecipitating endogenous Mal (Figure 4.2.20).

As the anti-Mal antibody could not immunoprecipitate endogenous Mal, proteins phosphorylated on tyrosine residues were immunoprecipitated from THP-1 cells with an anti-phosphotyrosine antibody and immunoblotted with an anti-Mal antibody. Cell lysates were prepared and normalised for total protein content following determination of protein concentration using the Bradford assay. To confirm that the total protein content was equal in all samples, cell lysates were immunoblotted with an anti-β-actin antibody (Figure 4.2.21d). In addition, it was verified that the THP-1 cells had responded to LPS by immunoblotting cell lysates with an anti-IκB-α antibody (Figure 4.2.21c). Blotting for endogenous Mal revealed two distinct forms (Figure 4.2.21b). No tyrosine phosphorylated Mal was detected in untreated cells (Figure 4.2.21a, lane 1). Having established that Mal was not tyrosine phosphorylated in resting cells, its phosphorylation status was investigated following LPS treatment. Treatment of cells with LPS led to

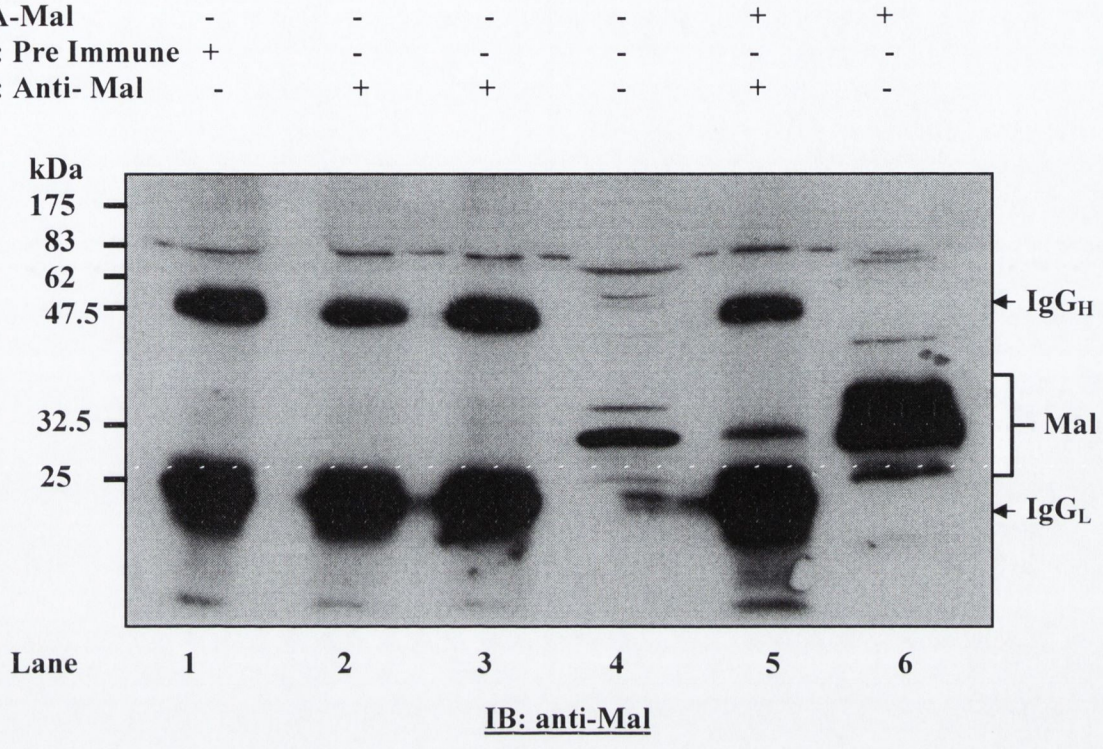

Figure 4.2.20 The anti-Mal antibody can immunoprecipitate overexpressed HA-Mal, but does not immunoprecipitate endogenous Mal. Cell lysates were prepared from un-transfected HEK293 cells (lanes 1-4) or from cells overexpressing HA-Mal (lanes 5-6) and incubated with either pre-immune anti-serum (lane 1) or with anti-Mal serum (lanes 2-3 and 6). Immunoprecipitates were washed three times with lysis buffer and analysed by SDS-PAGE. Samples were immunoblotted with an anti-Mal antibody. Cell lysates confirmed the presence of endogenous Mal (lane 4) and overexpressed HA-Mal (lane 6). Endogenous Mal could not be immunoprecipitated from HEK293 cells. Data shown is a representative experiment from ten separate experiments that were performed with various concentrations of anti-Mal antibody.

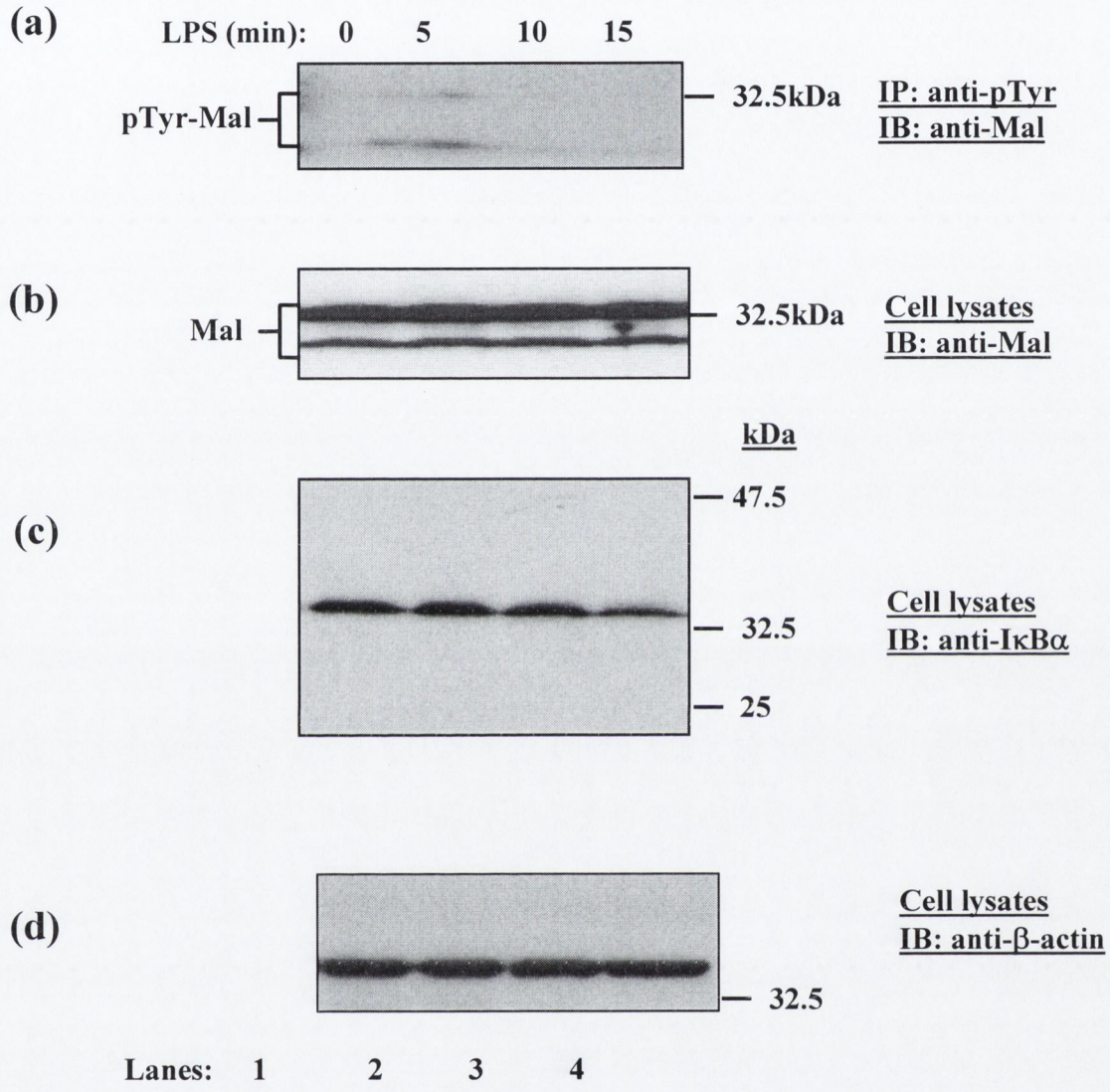

Figure 4.2.21 Tyrosine phosphorylation of endogenous Mal following LPS stimulation. THP-1 cell ($2x10^7$) were treated with 1 μg/ml of LPS for the indicated times. (a) Cell lysates were prepared and tyrosine phosphorylated proteins were immunoprecipitated with anti-phosphotyrosine agarose, followed by immunoblotting with an anti-Mal antibody. Cell lysates were also immunoblotted with (b) an anti-Mal antibody, (c) an anti-IκBα antibody and (d) an anti-β-actin antibody.

tyrosine phosphorylation of Mal, with two tyrosine phosphorylated forms of endogenous Mal proteins being detected at 5 minutes treatment time (Figure 4.2.21a, lane 2). It was noted that tyrosine phosphorylation of Mal following LPS treatment was remarkably transient with no tyrosine phosphorylation detected at later times.

4.2.7 Endogenous Mal is tyrosine phosphorylated following stimulation with MALP-2.

Given that Mal is specifically involved in TLR2 and TLR4 signalling and that it had been determined that Mal is tyrosine phosphorylated following stimulation with LPS, its phosphorylation status following activation of the TLR2 signalling pathway was next examined. THP-1 cells were treated with MALP-2, cell lysates were prepared and normalised for total protein content following determination of protein concentration using the Bradford assay. To confirm that the total protein content was equal in all samples, cell lysates were immunoblotted with an anti-β-actin antibody (Figure 4.2.22d). In addition, it was verified that the THP-1 cells had responded to MALP-2 by immunoblotting cell lysates with an anti-IκB-α antibody (Figure 4.2.22c). Blotting for endogenous Mal revealed two distinct forms (Figure 4.2.22b). Proteins phosphorylated on tyrosine residues were immunoprecipitated from THP-1 cell lysates with an anti-phosphotyrosine antibody and immunoblotted with an anti-Mal antibody. As had been previously determined, no tyrosine phosphorylated Mal was detected in untreated cells (Figure 4.2.22a, lane 1). Similar to LPS, the TLR-2 ligand MALP-2, led to tyrosine phosphorylation of Mal, the effect being evident at 10 minutes post stimulation (Figure 4.2.22a, lane 5), with two tyrosine phosphorylated forms again being detected.

Figure 4.2.22 Tyrosine phosphorylation of endogenous Mal following MALP-2 stimulation. THP-1 cell ($2x10^7$) were treated with MALP-2 (0.01nM) for the indicated times. (a) Cell lysates were prepared and tyrosine phosphorylated proteins were immunoprecipitated with anti-phosphotyrosine agarose, followed by immunoblotting with an anti-Mal antibody. Cell lysates were also immunoblotted with (b) the anti-Mal antibody, (c) the anti-IκBα antibody and (d) the anti-β-actin antibody.

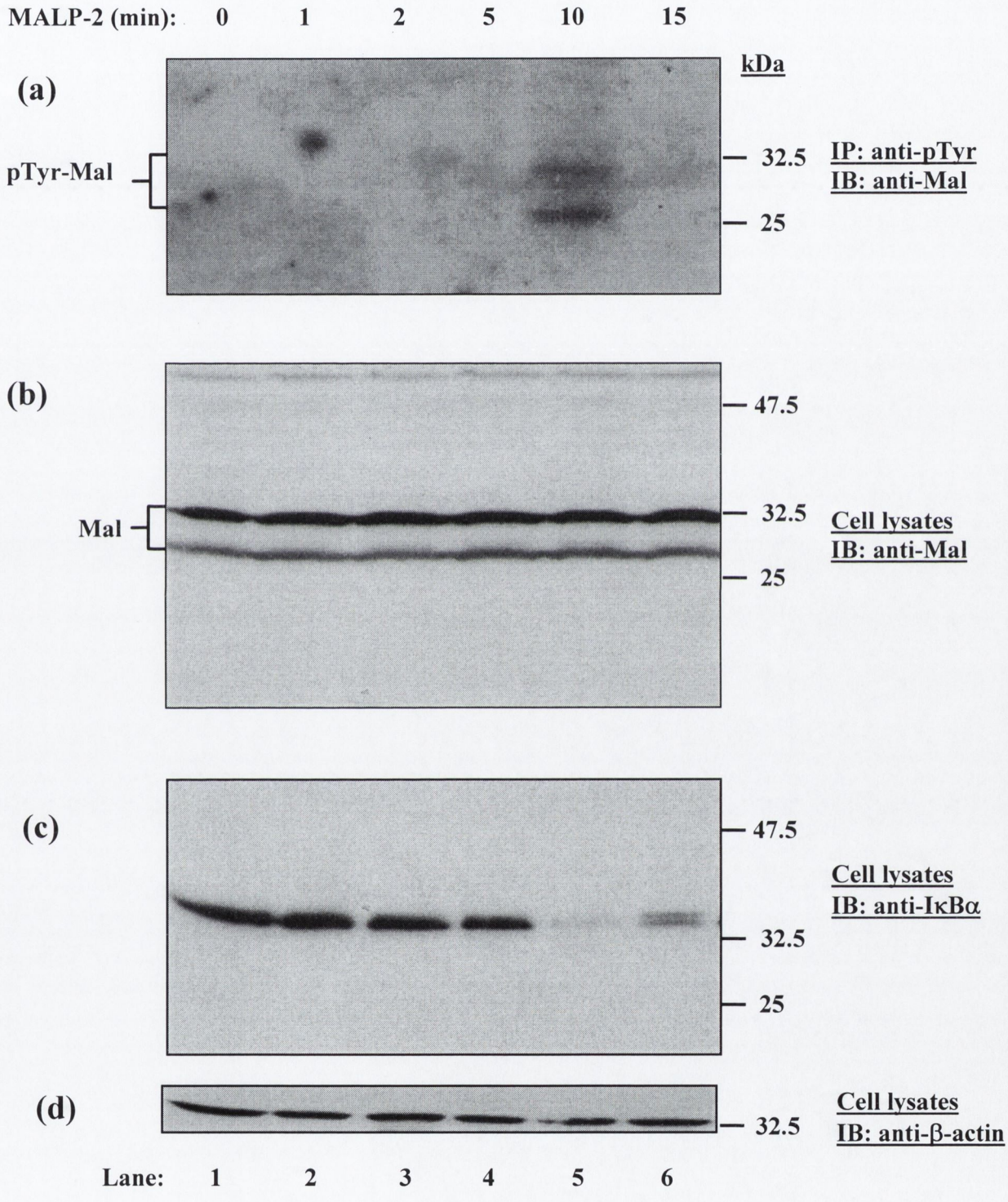
MALP-2 (min): 0 1 2 5 10 15
(a)
kDa
pTyr-Mal
32.5
25
IP: anti-pTyr
IB: anti-Mal
(b)
47.5
Mal
32.5
25
Cell lysates
IB: anti-Mal
(c)
47.5
32.5
25
Cell lysates
IB: anti-IκBα
(d)
32.5
Cell lysates
IB: anti-β-actin
Lane: 1 2 3 4 5 6

4.2.8 Tyr-86, Tyr-106 and Tyr-187 are required for Mal mediated NF-κB activation.

Previous reports have shown that overexpression of Mal activates NF-κB (Fitzgerald, Palsson-McDermott et al. 2001; Horng, Barton et al. 2001). In order to assess the requirement for the tyrosine residues in Mal to mediate NF-κB activation, Mal mutant proteins were overexpressed in HEK 293 cells in conjunction with an NF-κB-dependent luciferase reporter gene. In agreement with published results wild-type Mal strongly activated NF-κB (Figure 4.2.23) (Fitzgerald, Palsson-McDermott et al. 2001; Horng, Barton et al. 2001). In contrast, the Mal mutant proteins Mal-Y86F, Mal-Y106F and Mal-Y187F were less active, with Mal-Y86F and Mal-Y106F particularly impaired. Mal-Y159F, Mal-Y195F or Mal-Y196F activated NF-κB to a similar level as wild-type Mal (Figure 4.2.23). These results imply that it is Mal phosphorylated on Tyr-86, Tyr-106 and Tyr-187 that is the active form of Mal when overexpressed.

As we had determined that Tyr-86, Tyr-106 and Tyr-187 were important for Mal signalling, the effect of substituting all three possible phospho-accepting tyrosine residues in different combinations was investigated. As had been expected, Mal-Y86F Y106F Y187F displayed dramatically reduced NF-κB activation, similar to a mutant form of Mal in which proline 125 in Box 2 of the TIR domain is mutated to histidine (Mal-P125H) (Figure 4.2.24). In addition Mal-Y86F Y106F displayed similar NF-κB activity as the triple mutant, suggesting that the tyrosine residues at positions 86 and 106 are critical for activating NF-κB. It was noted that substitution of Tyr-187 to phenylalanine in combination with substitution of either Tyr 86 or Tyr 106 to phenylalanine reduced NF-κB activity by approximately 50% (Figure 4.2.24). Overall these results imply that

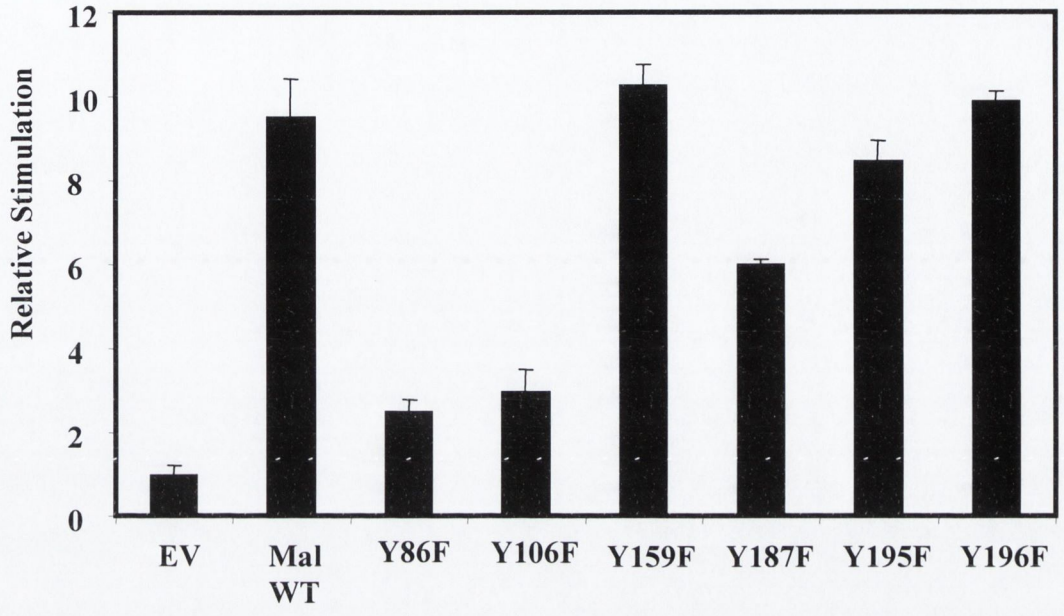

Figure 4.2.23 Mal-Y86F, Mal-Y106F and Mal-Y187F do not activate the NF-κB pathway as strongly as wild-type Mal. HEK293 cells were transfected with a 5x NF-κB reporter gene plasmid and co-transfected with plasmids encoding wild-type Mal, Mal-Y86F, Mal-Y106F, Mal-Y159F, Mal-Y187F, Mal-Y195F and Mal-Y196F, for 24 hours. Cell lysates were prepared and luciferase activity was measured. Results are normalized for *Renilla* luciferase activity and represented as fold induction relative to empty vector (EV) control. Mean relative stimulation of luciferase activity ± s.d. for a representative experiment from three separate experiments, each performed in triplicate, is shown.

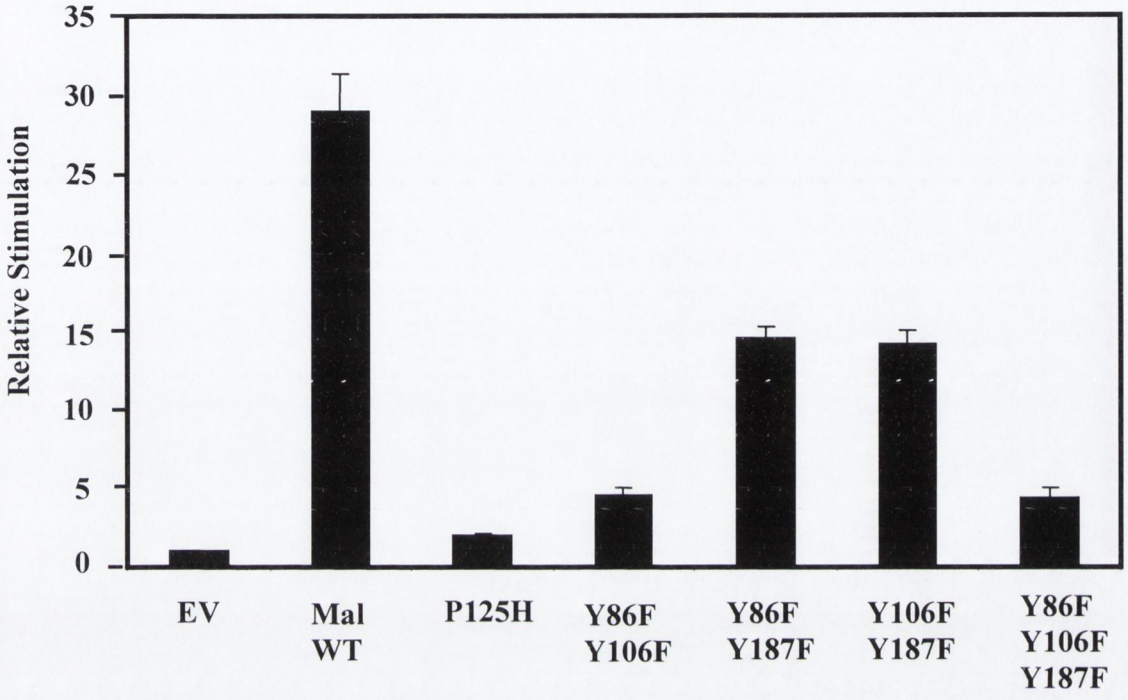

Figure 4.2.24 Multiple mutations in Mal, severely reduced Mal mediated NF-κB activation. HEK293 cells ($2x10^4$) were transiently transfected with a 5x NF-κB reporter gene plasmid and co-transfected with plasmids encoding empty vector (EV), wild-type Mal, Mal-Y86F Y106F, Mal-Y86F Y106F, Mal-Y106F Y187F, or Mal-Y86F Y106F Y187F, for 24 hours. Cell lysates were prepared and luciferase activity was measured. Results are normalized for *Renilla* luciferase activity and represented as fold induction relative to empty vector (EV) control. Results are expressed as mean ± standard deviation for a representative experiment from three separate experiments, each performed in triplicate.

tyrosine residues located at positions 159, 195 and 196 are not critical for Mal-mediated NF-κB activity, whereas Tyr-86, Tyr-106 and Tyr-187 are essential for NF-κB activity induced by Mal.

4.2.9 Involvement of specific tyrosine residues in Mal-mediated NF-κB activation

Following the discovery that specific tyrosine residues were more critical for NF-κB activation, the effect of these Mal mutants on wild-type Mal induced NF-κB activation was assessed. HEK293 cells were transiently transfected with a plasmid encoding HA-Mal and co-transfected with plasmids encoding Mal-P125H, Mal-Y86F, Mal-Y106F, Mal-Y187F and Mal-S105A. The effect of Mal on NF-κB was strongly inhibited by overexpression of Mal-P125H and Mal-Y86F, as NF-κB activation was reduced by approximately 75%. In both cases Mal-Y106F and Mal-Y187F on the other hand reduced NF-κB activation by approximately 50% (Figure 4.2.25). As an additional control the serine mutant Mal-S105A had no effect on the stimulatory effects of wild-type Mal.

4.2.10 Specific tyrosine residues can inhibit MyD88-mediated NF-κB activation

Having established that certain Mal mutant proteins inhibited wild-type Mal-induced NF-κB activation, it was of interest to determine if they would have an effect on NF-κB activation mediated by MyD88. In agreement with previous studies MyD88 strongly activated NF-κB (Figure 4.2.26) (Wesche, Henzel et al. 1997). As would be expected, co-expression of wild-type Mal with MyD88 had an additive effect on NF-κB activation induced by MyD88. In contrast, co-expression of either Mal-P125H or Mal-

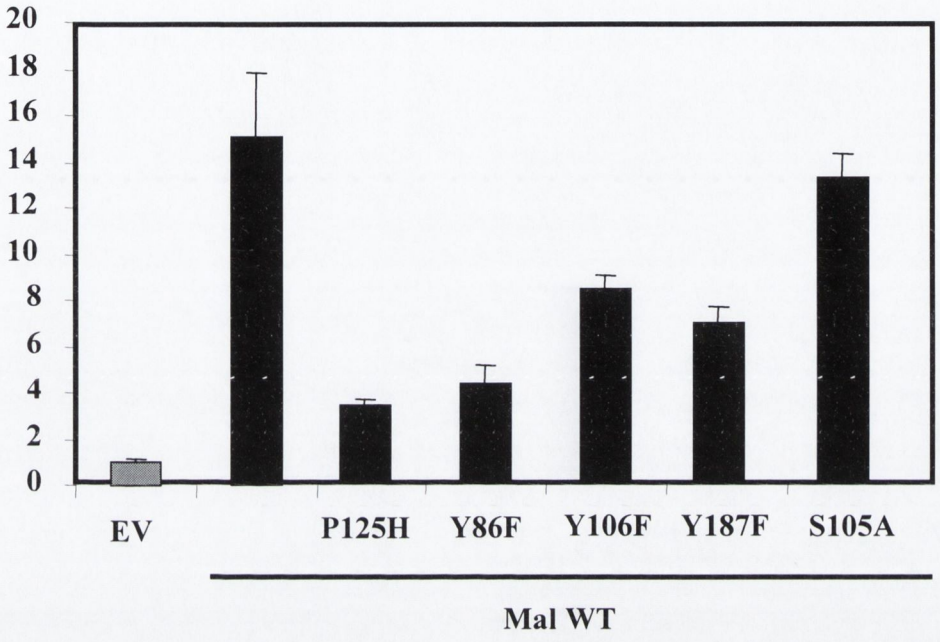

Figure 4.2.25 Wild-type Mal-mediated NF-κB activation was inhibited by Mal tyrosine mutants. HEK293 cells ($2x10^4$) were transiently transfected with a 5x NF-κB reporter gene plasmid (80ng) and thymidine kinase *Renilla* luciferase (40ng). The cells were also transfected with plasmids encoding empty vector or with plasmids encoding wild-type Mal (30ng), either by itself or with the following plasmids encoding wild-type Mal, Mal-P125H; Mal-Y86F, Mal-Y187F, or Mal-S105A, for 24 hours. Extracts were prepared and measured for luciferase activity. Results are normalized for *Renilla* luciferase activity and represented as fold induction relative to empty vector (EV) control. Results are expressed as mean ± standard deviation for a representative experiment from three separate experiments, each performed in triplicate.

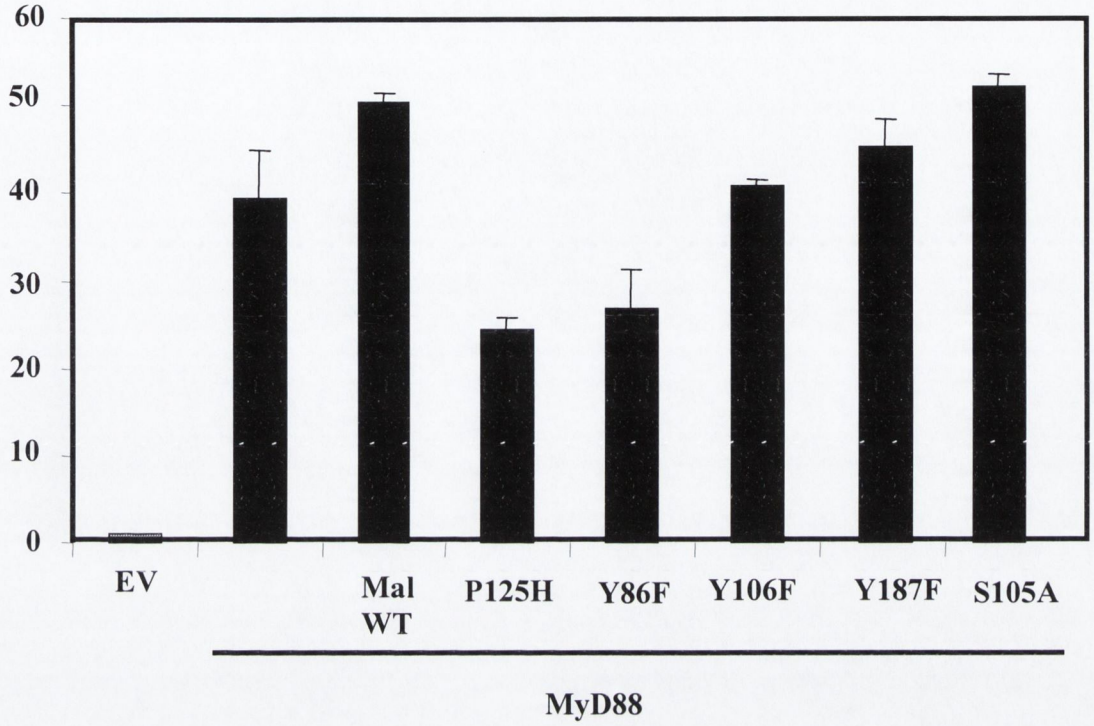

Figure 4.2.26 MyD88-mediated NF-κB activation was inhibited by Mal-P125H and Mal-Y86F. HEK293 cells ($2x10^4$) were transiently transfected with a 5x NF-κB reporter gene plasmid (80ng) and thymidine kinase *Renilla* luciferase (40ng). The cells were also transfected with plasmids encoding empty vector (EV) or with plasmids encoding MyD88 (50ng) either by itself, or with 50ng of the following plasmids encoding wild-type Mal, Mal-P125H, Mal-Y86F, Mal-Y106F, Mal-Y187F, or Mal-S105A, for 24 hours. Extracts were prepared and measured for luciferase activity. Results are normalized for *Renilla* luciferase activity and represented as fold induction relative to empty vector (EV) control. Results are expressed as mean ± standard deviation for a representative experiment from three separate experiments, each performed in triplicate.

Y86F with MyD88 reduced the ability of MyD88 to activate NF-κB by approximately 40%. Interestingly, the stimulatory effects of MyD88 were not inhibited by overexpression of either Mal-Y106F or Mal-Y187F. As an additional control the serine mutant Mal-S105A had no effect on the stimulatory effects of MyD88 (Figure 4.2.26).

4.2.11 Mal-Y86F and Mal-Y187F inhibit LPS signalling.

Given that Mal is tyrosine phosphorylated following LPS treatment, it was of interest to determine the effect that the Mal tyrosine mutants would have on NF-κB activation by LPS. HEK293 cells stably transfected with Flag-TLR-4 were transfected with a 5x NF-κB reporter gene plasmid and co-transfected with plasmids encoding Mal-P125H, Mal-Y86F, Mal-Y106F, Mal-159F, Mal-Y195F and Mal-Y196F. Cells were then left untreated or incubated with LPS for 6 hours. In agreement with previous studies, Mal-P125H strongly inhibited activation of NF-κB mediated by TLR4 (Figure 4.2.27a) (Fitzgerald, Palsson-McDermott et al. 2001; Horng, Barton et al. 2001). Interestingly, activation of NF-κB mediated by LPS was also strongly inhibited by Mal-Y86F, suggesting that this tyrosine residue is critical for efficient TLR4 signalling (Figure 4.2.27a). Mal-Y187F also blocked the LPS response albeit to a lesser degree. LPS could still stimulate NF-κB activation in cells expressing Mal-Y106F. The Mal mutant proteins Mal-Y159F, Mal-Y195F and Mal-Y196F were strongly active when overexpressed and LPS treatment had no major influence on their effect (Figure 4.2.27b). These results suggest that phosphorylation of Mal on Tyr 86 and Tyr 187 is required for Mal to signal NF-κB activation since the mutant forms of these residues inhibited the LPS response.

Figure 4.2.27 Mal-Y86F and Mal-Y187F inhibit LPS signaling. (a) HEK293 cells stably transfected with Flag-TLR-4 were transfected with a 5x NF-κB reporter gene plasmid and co-transfected with 100 ng of each plasmid encoding the following proteins: Mal-P125H, Mal-Y86F, Mal-Y106F, Mal-Y187F. Cells were then left untreated or incubated with LPS (100 ng ml-1) for 6 hours. (b) HEK293 cells stably transfected with Flag-TLR-4 were transfected with a 5x NF-κB reporter gene plasmid and co-transfected with 100 ng of each plasmid encoding the following proteins: Mal-P125H, Mal-159F, Mal-Y195F and Mal-Y196F. Cells were then left untreated or incubated with LPS (100 ng ml-1, 6 hours) 24 hours post-transfection. Mean relative stimulation of luciferase activity ± S.D. for a representative experiment from 3 separate experiments, each performed in triplicate, is shown.

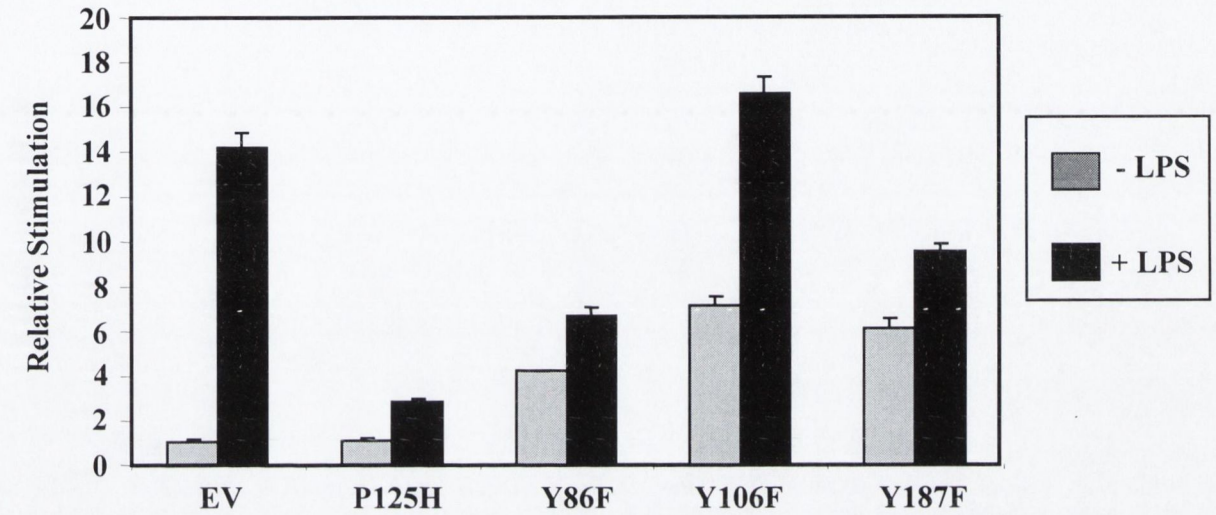
Relative Stimulation
20
18
16
14
12
10
8
6
4
2
0
EV
P125H
Y86F
Y106F
Y187F
- LPS
+ LPS

(b)

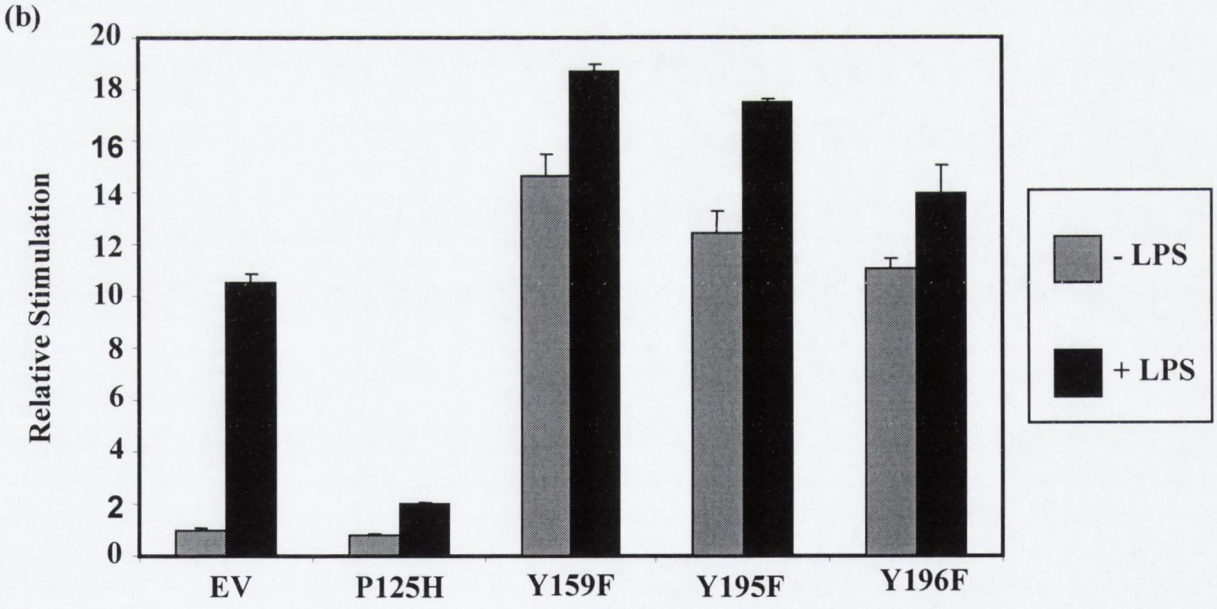
Relative Stimulation
20
18
16
14
12
10
8
6
4
2
0
EV
P125H
Y159F
Y195F
Y196F
- LPS
+ LPS

4.2.12 Interaction of Mal tyrosine mutants with wild-type Mal, MyD88 and TLR4.

Having identified Tyr-86, Tyr-106 and Tyr-187 as possible phospho-acceptors, it was of interest to investigate if mutating these tyrosine residues would interfere with their association with wild-type Mal, Mal-P125H, MyD88 and TLR4. Thus GST-Mal, GST-Mal-P125H, GST-Mal-Y106F, GST-MyD88 and GST-TLR4 fusion proteins were expressed in the BL21 strain of *Escherichia coli*. To verify that the fusion proteins were correctly prepared their ability to interact with HA-Mal was firstly confirmed. HEK293 cells were transiently transfected with a plasmid encoding HA-Mal. Cell lysates were prepared and incubated with the fusion proteins coupled to glutathione-agarose beads for 2 hours at 4°C. Samples were washed three times with lysis buffer, analysed by SDS-PAGE and immunoblotted with an anti-HA antibody. In agreement with previous findings Mal interacted with itself, Mal-P125H, MyD88 and TLR4 (Figure 4.2.28a) (Fitzgerald, Palsson-McDermott et al. 2001; Horng, Barton et al. 2001). As a control HA-Mal did not associate with the GST fusion protein. Cell lysates were immunoblotted with an anti-HA antibody to confirm expression (Figure 4.2.28, lane 6).

The ability of Mal-Y86F to interact with these fusion proteins was subsequently investigated. HEK293 cells were transiently transfected with a plasmid encoding HA-Mal-Y86F. Cell lysates were prepared and GST-pulldown assays were performed. Similar to wild-type Mal, Mal-Y86F strongly interacted with Mal and Mal-P125H (Figure 4.2.29a). A weak association with Mal-Y86F and MyD88 (Figure 4.2.29a, lane 3) was apparent and it was observed that mutation of Tyr-86 to phenylalanine severely affected the latent ability of Mal to associate with TLR4, as only a minor interaction was observed (Figure 4.2.29a, lane 4). Mal-Y86F did not interact with the GST protein

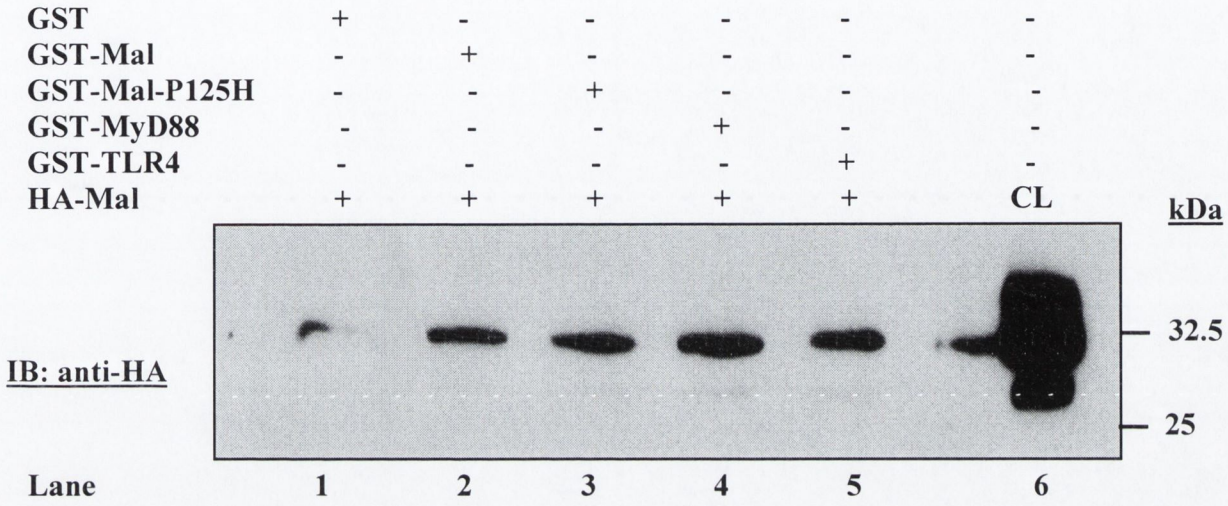

Figure 4.2.28 Wild-type Mal interacts with GST-Mal, GST-MalP125H, GST-MyD88, and GST-TLR4. (a) HEK293 cells ($1x10^6$) were transfected with 4 μg of plasmid encoding wild-type Mal. Cells were lysed and cell lysates were subsequently combined. 30 μl of cell lysate (CL) was removed and added to 5μl of SDS sample buffer (lane 6). The remaining cell lysate was incubated with equivalent amounts of purified GST (lane 1), GST-Mal (lane 2), GST-Mal-P125H (lane 3), GST-MyD88 (lane 4), and GST-TLR4 (lane 5) attached to glutathione-agarose beads for 2 hours at 4°C. The beads were isolated by centrifugation, washed three times with lysis buffer and added to 30μl of SDS sample buffer. Samples were then analysed by separation on 12% SDS-PAGE and immunoblotted with an anti-HA antibody.

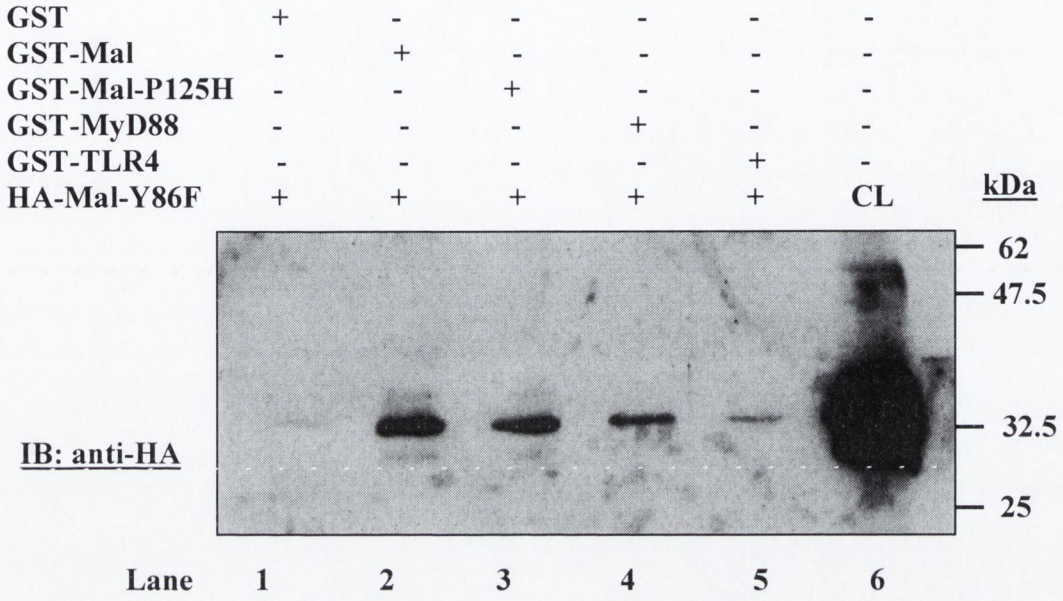

Figure 4.2.29 Mal-Y86F interacts with wild-type Mal, Mal-P125H and to a lesser extent with MyD88 and TLR4. HEK293 cells ($1x10^6$) were transfected with 4 μg of plasmid encoding HA-Mal-Y86F. Cells were lysed and cell lysates were subsequently combined. 30 μl of the cell lysate was removed and added to 5μl of SDS sample buffer (lane 6). The remaining cell lysate was incubated with equivalent amounts of purified GST (lane 1), GST-Mal (lane 2), GST-Mal-P125H (lane 3), GST-MyD88 (lane 4) and GST-TLR4 (lane 5) attached to glutathione-agarose beads for 2 hours at 4°C. The beads were isolated by centrifugation, washed three times with lysis buffer and added to 30μl of SDS sample buffer. Samples were then analysed by separation on 12% SDS-PAGE and immunoblotted with an anti-HA antibody.

confirming that each interaction is specific for the expressed fusion protein (Figure 4.2.29a, lane 1). Cell lysates were immunoblotted with an anti-HA antibody to confirm expression of HA-MalY86F (Figure 4.2.29, lane 6).

The effects of mutating Tyr-106 to phenylalanine on coupling Mal to the immediate upstream and downstream molecules in the signalling pathway was next assessed. HEK293 cells were transiently transfected with a plasmid encoding HA-Mal-Y106F. Cell lysates were prepared and GST-pulldown assays were performed. Similar interaction results for Mal-Y86F were obtained for Mal-Y106F. As can be seen in figure 4.2.30, Mal-Y106F interacted with both wild-type Mal and Mal-P125H and weakly associated with MyD88 and TLR4. No interaction was detected between Mal-Y106F and GST (Figure 4.2.30a, lane 1). Control immunoblots confirmed that Mal-Y106F was expressed at similar levels in all samples (Figure 4.2.30, lane 6).

Finally the ability of Mal-Y187F to interact with Mal, Mal-P125H, MyD88 and TLR4 was investigated. HEK293 cells were transiently transfected with a plasmid encoding HA-Mal-Y187F. Cell lysates were prepared and GST-pulldown assays were performed. It was observed that similar to Mal-Y86F and Mal-Y106F, Mal-Y187F associated with wild-type Mal, Mal-P125H, and to a lesser extent MyD88 and TLR4 (Figure 4.2.31a). No association between Mal-Y187F and GST protein was detected (Figure 4.2.31a, lanes 1), and expression of Mal-Y187F was confirmed in all the samples by immunoblotting with an anti-HA antibody (Figure 4.2.31, lane 6). These results suggest a potential mechanism for the inhibition of LPS induced NF-κB activation via Mal, as unphosphorylated Mal may sequester downstream wild-type Mal molecules from TLR4 and in this way limit its availability to participate in signalling from LPS.

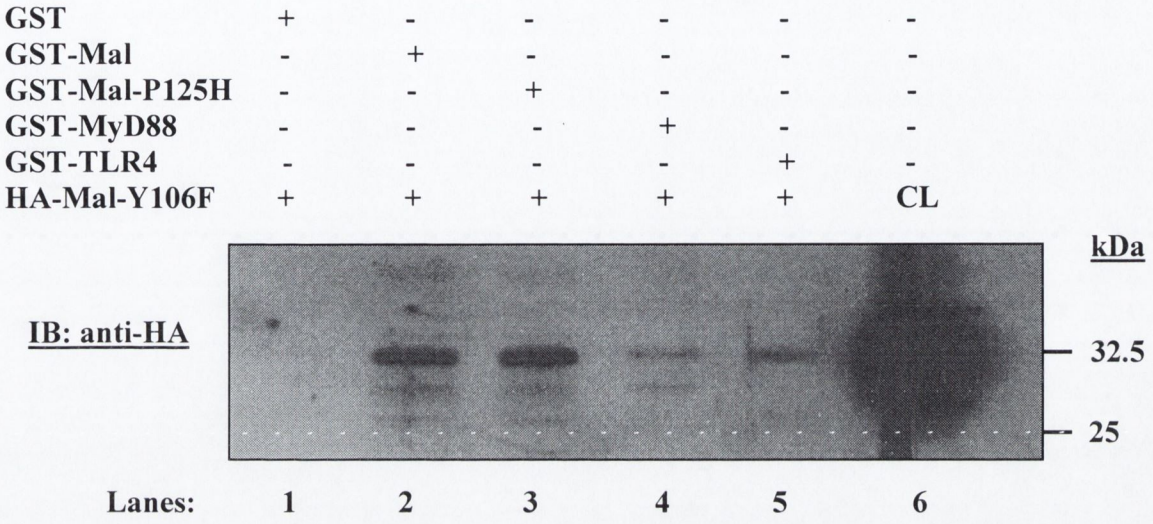

Figure 4.2.30 Mal-Y106F interacts with wild-type Mal, Mal-P125H, and to a lesser extent with MyD88 and TLR4. HEK293 cells ($1x10^6$) were transfected with 4 μg of plasmid encoding HA-Mal-(Y106F). Cells were lysed and cell lysates were subsequently combined. 25 μl of the cell lysate was removed and added to 5μl of SDS sample buffer (lane 6). The remaining cell lysate was incubated with equivalent amounts of purified GST (lane 1), GST-Mal (lane 2), GST-Mal-P125H (lane 3), GST-MyD88 (lane 4) and GST-TLR4 (lane 5) attached to glutathione-agarose beads for 2 hours at 4°C. The beads were isolated by centrifugation, washed three times with lysis buffer and added to 30μl of SDS sample buffer. Samples were then analysed by separation on 12% SDS-PAGE and immunoblotted with an anti-HA antibody.

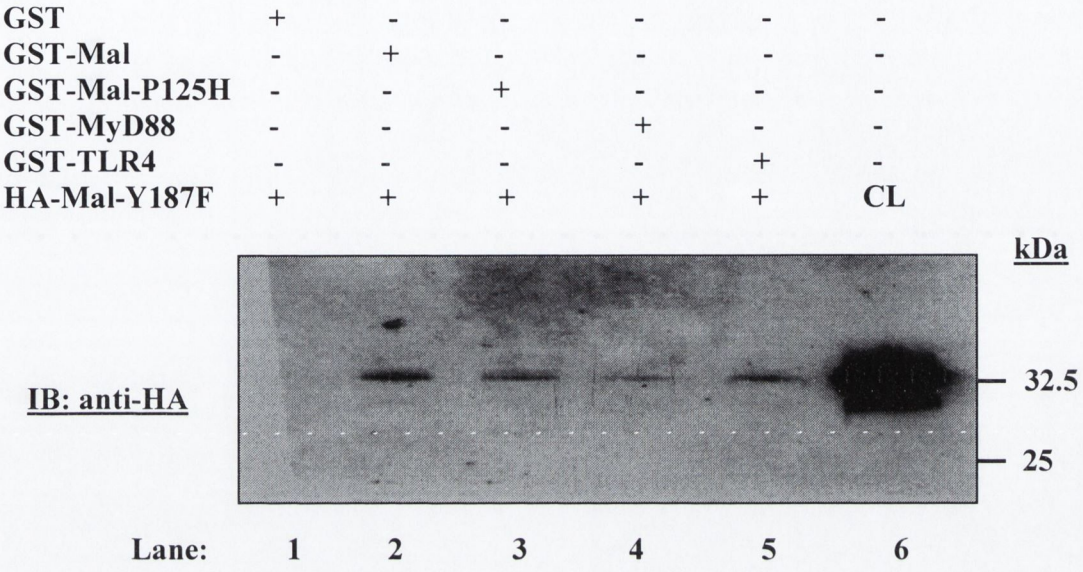

Figure 4.2.31 Mal-Y187F interacts with wild-type Mal, Mal-P125H, MyD88 and TLR4. HEK293 cells ($1x10^6$) were transfected with 4 μg of plasmid encoding HA-Mal-Y187F. Cells were lysed and cell lysates were subsequently combined.. 25 μl of the cell lysate was removed and added to 5μl of SDS sample buffer (lane 6). The remaining cell lysate was incubated with equivalent amounts of purified GST (lane 1), GST-Mal (lane 2), GST-Mal-P125H (lane 3), GST-MyD88 (lane 4) and GST-TLR4 (lane 5) attached to glutathione-agarose beads for 2 hours at 4°C. The beads were isolated by centrifugation, washed three times with lysis buffer and added to 50μl of SDS sample buffer. Samples were then analysed by separation on 12% SDS-PAGE and immunoblotted with an anti-HA antibody.

4.2.13 Recombinant Mal Y86F Y106F Y187F is phosphorylated by recombinant Btk to a lesser extent than wild type Mal.

Given that Btk was shown to phosphorylate Mal in the previous chapter and having identified Tyr-86, Tyr-106, and Tyr-187 as possible phospho-acceptors, the effects of mutating these residues on Mal phosphorylation by Btk was next investigated. In order to address this, tyrosine residues located at positions 86, 106 and 187 were conservatively mutated to phenylalanine singly or in combination using *in vitro* site directed mutagenesis on the parental DNA, pGex-Mal. The sequence of this construct was subsequently confirmed by DNA sequencing.

In vitro kinase assays were then performed and as previously observed incubation of Btk with radiolabelled ATP resulted in Btk autophosphorylation (Figure 4.2.32, lane 1). In addition as shown in chapter 3, Mal was phosphorylated by Btk, with two distinct phospho-forms appearing (Figure 4.2.32, lane 2). It was noted that Mal Y86F, Mal Y106F and Mal Y187F were still phosphorylated by Btk (Fig. 4.2.32, lanes 3-5). However, using recombinant Mal-Y86F Y106F Y187F as a substrate for Btk, Mal phosphorylation was almost completely abolished (Figure 4.2.33, lane 3). In addition, whilst phosphorylation of Mal resulted in two phospho-forms, for Mal-Y86F Y106F Y187F as a substrate, only one phospho-form was evident, consistent with these amino acids as key phospho-acceptors. Samples were also immunoblotted with an anti-Btk antibody (Figure 4.2.33b) and an anti-Mal antibody (Figure 4.2.33c) to confirm that each sample contained equal amounts of recombinant protein.

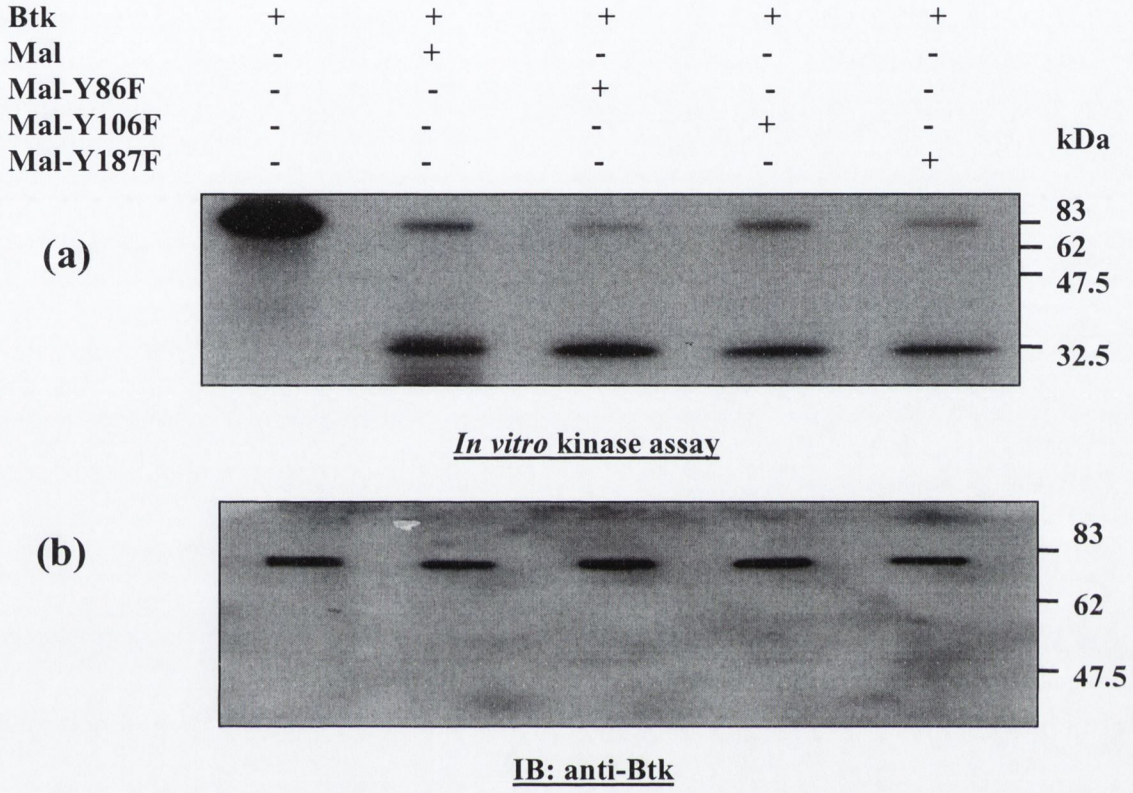

Figure 4.2.32 Recombinant Btk phosphorylates recombinant Mal. Recombinant Btk was incubated alone (lane 1), or with recombinant Mal (lane 2) or the recombinant Mal mutant proteins Mal-Y86F (lane 3), Mal-Y106F (lane 4), Mal-Y187F (lane 5). Samples were subjected to an *in vitro* kinase assay, analysed on SDS-PAGE, and visualised by autoradiography. Samples were also immunoblotted with (b) an anti-Btk antibody.

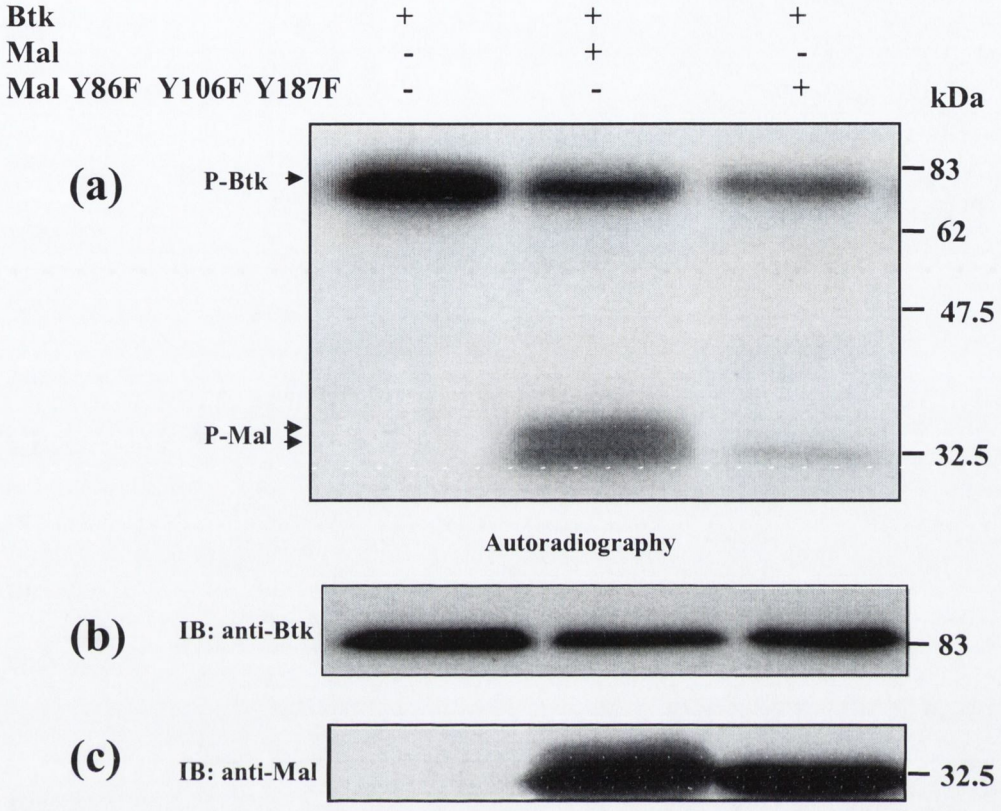

Figure 4.2.33 Recombinant Mal Y86F Y106F Y187F is phosphorylated by recombinant Btk to a lesser extent than wild type Mal.. **(a)** Recombinant Btk was incubated alone (lanes 1 and 4), or with recombinant wild-type Mal (lane 2), recombinant Mal-Y86F Y106F Y187F (lane 3) or recombinant GST-MyD88 (lane 5). Samples were subjected to an *in vitro* kinase assay, analysed on SDS-PAGE, and visualised by autoradiography. Samples were also immunoblotted with (b) an anti-Btk antibody or (c) an anti-Mal antibody.

4.2.14 Recombinant Mal is phosphorylated by endogenous Btk

As it had been determined that Mal was a substrate for recombinant Btk, the ability of endogenous Btk to phosphorylate recombinant Mal following TLR4 activation was next assessed. THP1 cells (2x 10^6) were stimulated with LPS for the indicated times. Cells were lysed and endogenous BTK was immunoprecipitated with an anti-BTK antibody. Immunoprecipitates were washed three times with lysis buffer and twice with kinase buffer. Recombinant Mal was added to each sample. Following incubation in an *in vitro* kinase assay, samples were analysed by SDS-PAGE, transferred to PVDF membrane and subjected to autoradiography. Phosphorylation of wild-type Mal by endogenous Btk was determined by incorporation of radioactive phosphate.

As figure 4.2.34 illustrates, the kinase activity of Btk was basally active prior to stimulation, but could be activated further following treatment of the cells with LPS for 60 minutes. It was observed that recombinant Mal was a substrate for endogenous Btk *in vitro* and that increased activity of Btk corresponded to an increase in the phosphorylation of recombinant Mal by Btk. Similar to previous results, phosphorylation of Mal by Btk resulted in the appearance of two phospho-forms of Mal. Samples were also immunoblotted with an anti-Mal antibody to confirm that recombinant Mal was present in the relevant samples (Figure 4.2.34b).

4.2.15 Mal Tyrosine Phosphorylation is abolished following pre-treatment with the Btk inhibitor, LFM-A13

Having established that Mal is tyrosine phosphorylated both endogenously and in overexpression studies, and that recombinant Mal is phosphorylated by endogenous Btk

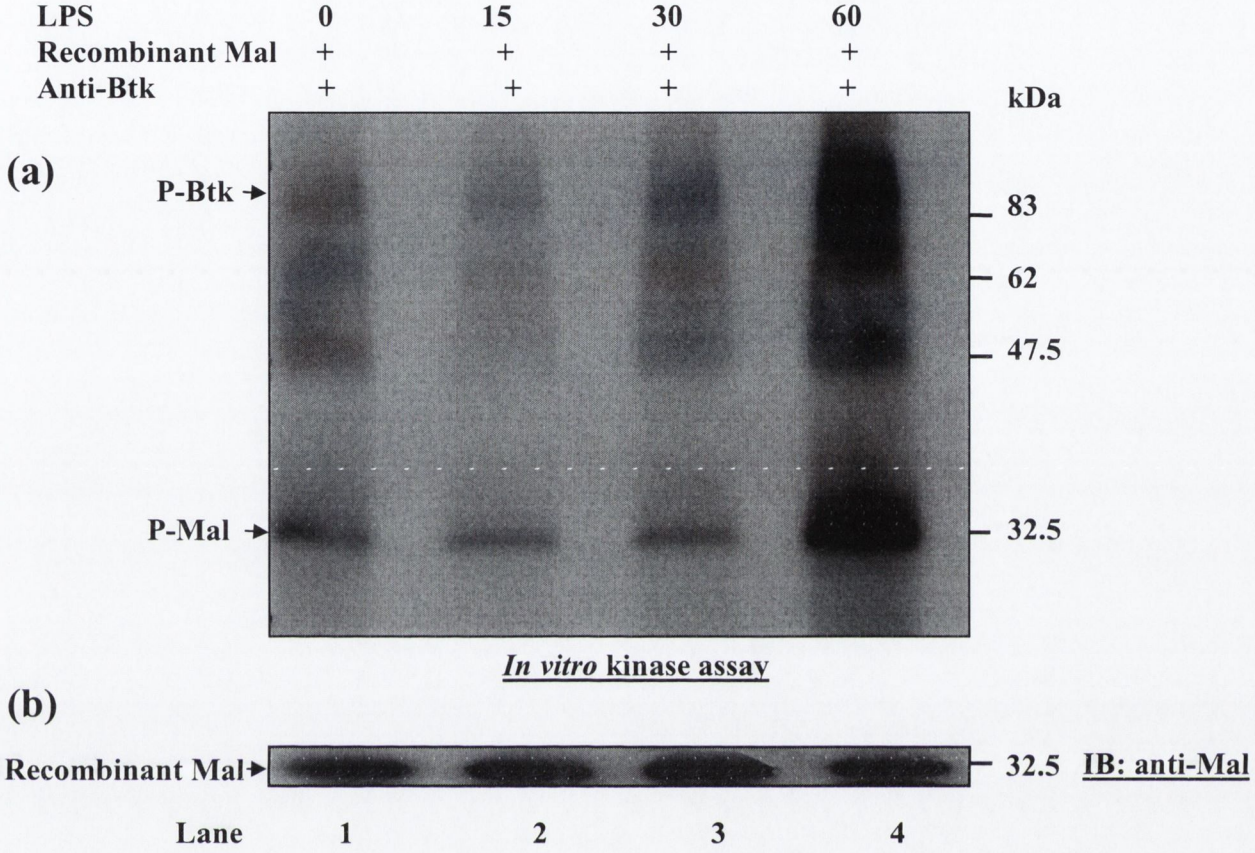

Figure 4.2.34 Recombinant Mal is phosphorylated by endogenous BTK. (a) THP1 cells (2x 10^6) were stimulated with 1μg/ml LPS for indicated times. Cells were lysed and endogenous BTK was immunoprecipitated with an anti-BTK antibody. Immunoprecipitates were washed three times with lysis buffer and twice with kinase buffer. Recombinant Mal was subsequently added to each sample. Samples were washed three times with lysis buffer and a further two times with kinase buffer and subjected to an *in vitro* kinase assay. The samples were then incubated for 30 min. at 37°C with 2μCi [γ32P] PO4. Following incubation in an *in vitro* kinase assay, samples were analysed by SDS-PAGE, transferred to PVDF membrane and subjected to autoradiography. (b) Samples were also immunoblotted with an anti-Mal antibody.

in vitro, the *in vivo* role of Btk in the tyrosine phosphorylation of Mal following stimulation with LPS or MALP-2 was next investigated. THP-1 cells were pre-treated with LFM-A13 ($C_{11}H_8Br_2N_2O_2$), a specific Btk inhibitor. Since LFM-A13 is solubilised in DMSO, THP-1 cells were also pretreated with DMSO as a control. In Figure 4.2.35a, lane 2 and Figure 4.2.36a, lane 5, LPS and MALP-2, induced transient Mal tyrosine phosphorylation as shown previously (Figure 4.2.21 and Figure 4.2.22). Pre-treatment of THP-1 cells with LFM-A13, completely abolished both LPS (Figure 4.2.35a, compare lanes 2 and 7) and MALP-2 (Figure 4.2.36a, compare lanes 5 and 11) induced tyrosine phosphorylation of Mal. Cell lysates were immunoblotted with an anti-IκBα antibody to confirm that the cells were responding to the given stimulants (Figure 4.2.35c and Figure 4.2.36c). Figure 4.2.35d and Figure 4.2.36d show the same cell lysates immunoblotted with an anti-β-actin antibody. No change is detected in the level of β-actin protein, indicating that the variation in the levels of Mal tyrosine phosphorylation or IκB-α were not due to varying amounts of protein in each sample.

4.2.16 Recombinant Mal decreases the ability of Btk to autophosphorylate *in vitro*

As mentioned above, whilst performing *in vitro* kinase assays with Btk, it was noted that the kinase activity of Btk was altered once Mal was present. To further investigate this observation increasing concentrations of Mal were incubated with a constant amount of Btk. As it had been determined that MyD88 was not phosphorylated by Btk, increasing concentrations of MyD88 were added as a control. As figure 4.2.37 illustrates, incubation of Btk with radiolabelled ATP leads to Btk autophosphorylation, but having Mal present severely limits this capacity (compare lane 1 and lane 2). It was

Figure 4.2.35 Pre-treatment of the Btk inhibitor abolished Mal tyrosine phosphorylation mediated by LPS. THP-1 cells ($2x10^7$) were pretreated with DMSO (lanes 1-4) or LFM-A13 (lanes 5-8) for 1 h prior to stimulation with LPS. (a) Cell lysates were prepared and tyrosine phosphorylated proteins were immunoprecipitated with anti-phosphotyrosine agarose, followed by immunoblotting with anti-Mal antibody. Cell lysates were also immunoblotted with (b) an anti-Mal antibody, (c) an anti-IκB-α antibody and (d) an anti-β actin antibody.

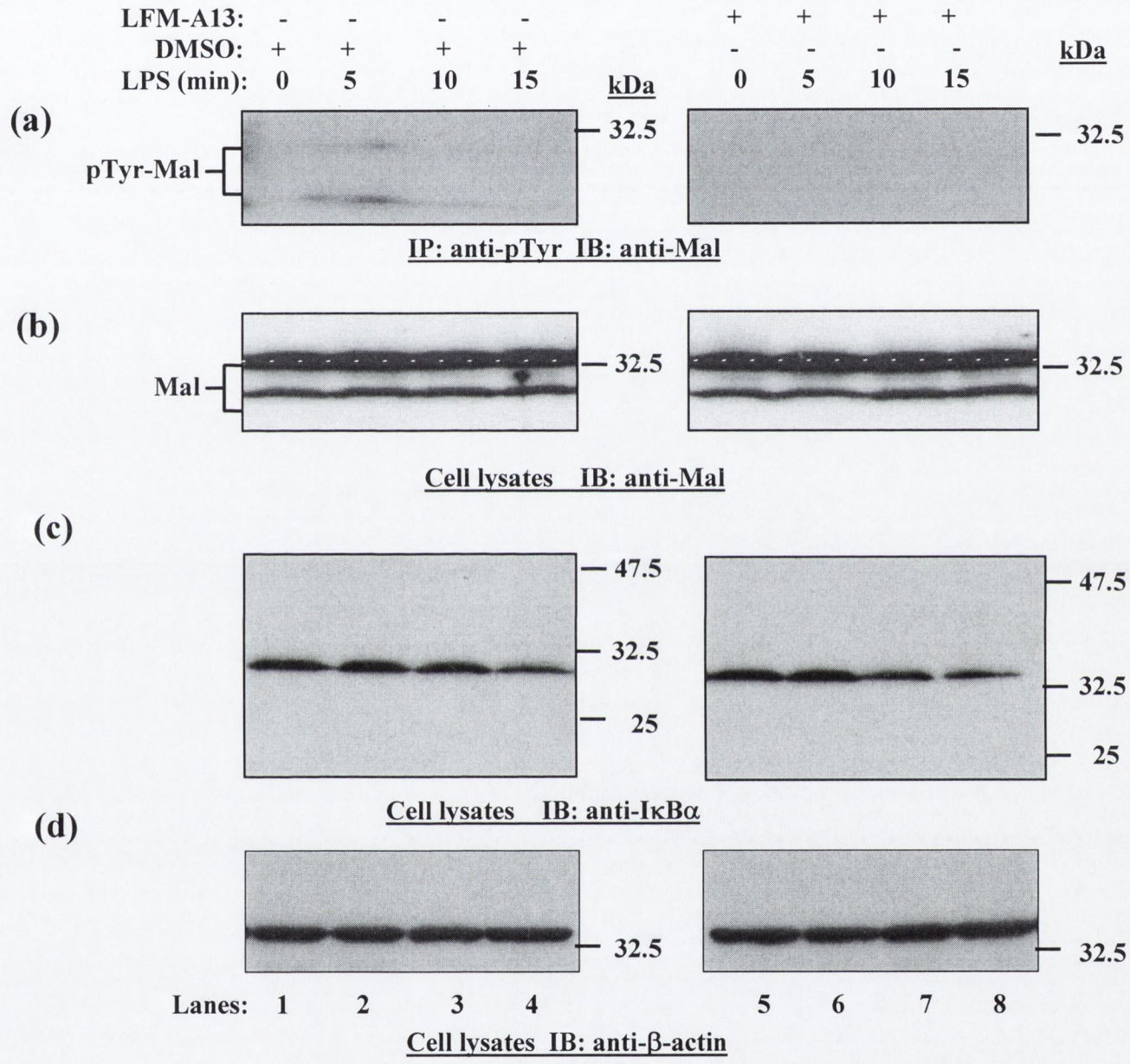
LFM-A13: - - - - + + + +
DMSO: + + + + - - - -
LPS (min): 0 5 10 15 kDa 0 5 10 15 kDa
(a)
pTyr-Mal
32.5
32.5
IP: anti-pTyr IB: anti-Mal
(b)
Mal
32.5
32.5
Cell lysates IB: anti-Mal
(c)
47.5
32.5
25
47.5
32.5
25
Cell lysates IB: anti-IκBα
(d)
32.5
32.5
Lanes: 1 2 3 4 5 6 7 8
Cell lysates IB: anti-β-actin

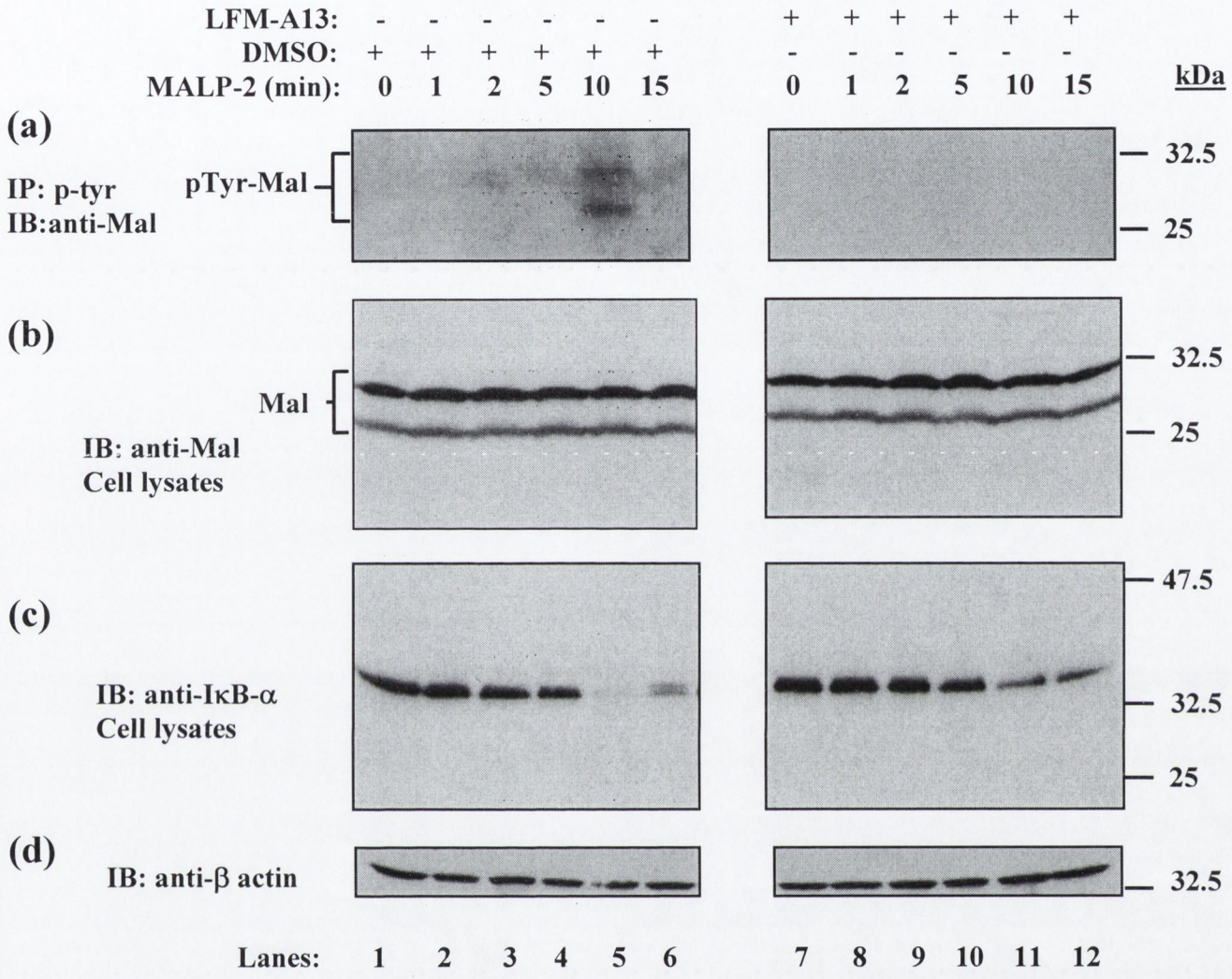

Figure 4.2.36 Pre-treatment of the Btk inhibitor abolished Mal tyrosine phosphorylation mediated by MALP-2. THP-1 cells ($2x10^7$) were pretreated with DMSO (lanes 1-6), or LFM-A13 (lanes 6-12), for 1 h prior to stimulation with MALP-2. (a) Cell lysates were prepared and tyrosine phosphorylated proteins were immunoprecipitated with anti-phosphotyrosine agarose, followed by immunoblotting with an anti-Mal antibody. Cell lysates were also immunoblotted with (b) an anti-Mal antibody, (c) an anti-IκB-α antibody and (d) an anti-β actin antibody

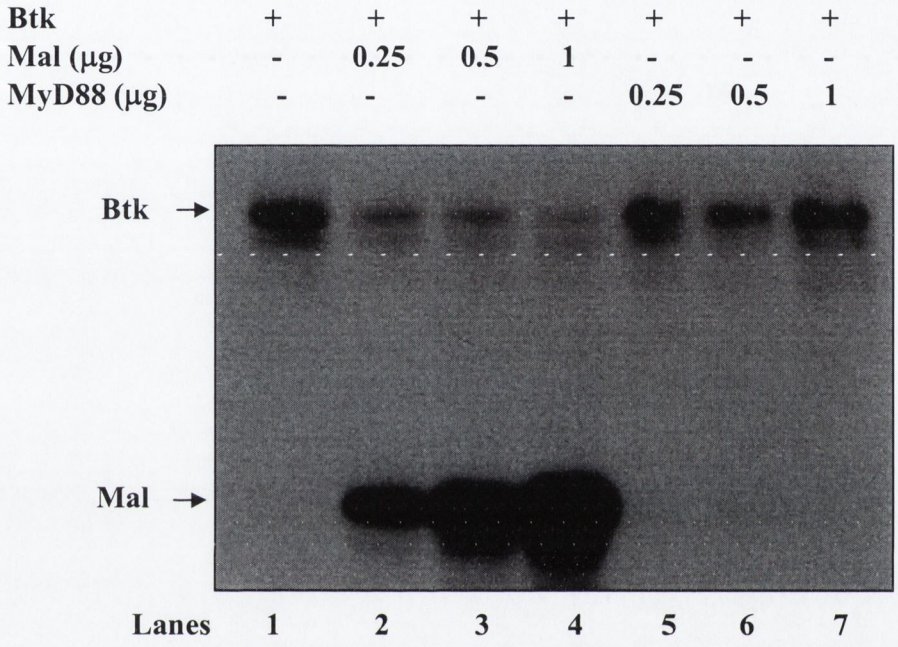

Figure 4.2.37 Recombinant Mal alters the kinase activity of Btk. Recombinant Btk was incubated with increasing concentrations of recombinant Mal (lanes2-4), or increasing concentrations of recombinant MyD88 (lanes 5-7). Samples were subjected to an *in vitro* kinase assay and phosphorylated proteins were resolved by SDS-PAGE and visualised by autoradiography

also noted that increasing the concentration of Mal dramatically reduced the kinase activity of Btk, whilst Mal phosphorylation was enhanced (Figure 4.2.37, lanes 2-4). MyD88 on the other hand did not alter the kinase activity of Btk (Figure 4.2.37, lanes 5-7).

4.3 Discussion

Prompt activation of the TLR signaling pathway has proven to be vital in the recognition of invading pathogens and in eliciting the host innate immune response. Recent studies have demonstrated that in addition to serine and threonine phosphorylation, the efficient orchestration of the TLR signaling pathway is dependent on a series of tyrosine phosphorylation events.

In the previous chapter, it was observed that Mal was a substrate for the serine/ threonine kinases IRAK1 and IRAK4 and for the tyrosine kinase, Btk. In this chapter, mutational analysis was conducted in an attempt to map the phosphorylation sites located within Mal. In order to identify phospho-accepting residues, specific serine and threonine residues were mutated conservatively to alanine. However, it was observed that all of the serine/threonine Mal mutant proteins generated behaved in a similar fashion to wild-type Mal when assayed for NF-κB activation. Moreover, they all exhibited the same mobility pattern as wild-type Mal when analysed by SDS-PAGE. As phosphorylation of Mal by IRAK1 and IRAK4 resulted in the formation of up to three phospho-proteins, this suggests that Mal is multiply phosphorylated. Therefore mutational studies cannot rule out the mutated serine or threonine residues as possible phospho-accepting residues, as they might have no effect on Mal function when mutated singly.

Mutational analysis of Mal was next conducted in order to assess the relative functional importance of the six tyrosine residues in the TIR domain of Mal. Data presented in this chapter c learly demonstrate that in Mal-Y86F, Mal-Y106F and Mal-Y187F the slowest migrating form of Mal was abolished. These results suggested that the tyrosine residues located at positions 86, 106 and 187 were potential phosphorylation

sites with all three tyrosine residues requiring phosphorylation for the altered mobility of Mal on SDS-PAGE.

Analysis of the molecular model for Mal revealed that both Tyr-86 and Tyr-106 appear to be surface exposed, whereas Tyr-187 appears to be the least accessible. It is possible therefore that phosphorylation of Mal is sequential, with phosphorylation on Tyr-86 or Tyr-106 being required to initiate a conformational change in the TIR domain of Mal, thereby exposing Tyr-187 for phosphorylation, culminating in activation of downstream signals. Indeed this may explain why Mal Y86F Y106F activates NF-κB to the same extent as Mal Y86F Y106F Y187F, as Tyr 86 and Tyr 106 are not phosphorylated, Tyr 187 may not therefore be accessible for phosphorylation by Btk. Tyrosine phosphorylation of Mal may trigger a conformational change, thereby regulating the association of Mal with other proteins. Indeed following phosphorylation a conformational change has been reported for the bacterial chemotaxis protein, CheY, which has a similar backbone to that of the TIR domain (Rock, Hardiman et al. 1998).

In the previous chapter, it had been observed that the two slower migrating forms of Mal represented phosphorylated Mal. As this had been determined using a phosphatase that dephosphorylates proteins phosphorylated on tyrosine, serine or threonine residues, a phosphatase that specifically dephosphorylates proteins phosphorylated on tyrosine residues was next employed in order to further verify that Mal contained phospho-tyrosine residues. Using PTP-1B it was established that the slowest migrating form of Mal represented tyrosine phosphorylated Mal. In addition, analysis of overexpressed Mal with an antibody that recognizes proteins phosphorylated on tyrosine residues confirmed that Mal was tyrosine phosphorylated.

Whilst it had been established that overexpressed Mal was tyrosine phosphorylated, to ensure that this was a physiologically relevant event the phosphorylation status of endogenous Mal was next examined. As has been previously stated, Mal participates solely in TLR2 and TLR4 signal transduction where it may act as a bridging adapter for MyD88 recruitment (Fitzgerald, Palsson-McDermott et al. 2001; Horng, Barton et al. 2001). Prompted by the knowledge that ligands for these receptors are known activators of tyrosine phosphorylation, the tyrosine phosphorylation of Mal was assessed following activation of the TLR2 and TLR4 signalling pathways. It was determined that both MALP-2 and LPS rapidly and transiently triggered tyrosine phosphorylation of endogenous Mal in THP-1 cells.

Given that Mal was tyrosine phosphorylated *in vivo*, the relative functional importance of the six tyrosine residues in the TIR domain of Mal was subsequently assessed. It was noted that Tyr-86, Tyr-106 and Tyr-187 were the most critical residues for maximal NF-κB activation induced by Mal. Furthermore, Mal-Y86F and Mal-Y187F acted as dominant negative inhibitors of NF-κB activation induced by LPS, whereas the other mutants of Mal did not. These results suggest that following LPS stimulation Tyr-86 and Tyr-187 are likely to undergo phosphorylation and this process is required for NF-κB activation mediated by Mal. It is likely that both require phosphorylation since mutating either resulted in an inactive dominant negative form.

It was also noted that Mal-P125H and Mal-Y86F, and to a lesser extent Mal-Y106F and Mal-Y187F acted as dominant negative inhibitors of NF-κB activation induced by wild-type Mal. These results suggest that mutating Tyr-86, Tyr-106 and Tyr-187 to phenylalanine may retain Mal in an inactive state and that phosphorylation of

these residues activates Mal. Interestingly, Mal-Y86F was the only Mal mutant that inhibited NF-κB activation mediated by MyD88, indicating that phosphorylation of Tyr-86 may be required for Mal to function as a bridging protein with MyD88.

Given that the tyrosine residues located at positions 86, 106 and 187 were required for maximal NF-κB activation induced by Mal, association studies were conducted to determine if these residues were required for downstream interactions with key proteins involved in TLR signal transduction. Previous studies have shown that Mal interacts with itself, Mal-P125H, MyD88 and TLR4. It was revealed that Mal-Y86F, Mal-Y106F and Mal-Y187F still retained the ability to interact with wild-type Mal, Mal-P125H, MyD88, and TLR4. These results suggest a potential mechanism for the inhibition of LPS induced NF-κB activation via Mal, as unphosphorylated Mal may sequester the downstream signalling molecules from TLR4 and in this way limit their availability to participate in signalling from LPS. This is consistent with the observation that mutation of Tyr-86, Tyr-106 and Tyr-187 results in reduced NF-κB activation induced by Mal.

Recent findings have shown that the tyrosine kinase Btk is activated by TLR4 and is required for LPS responses mediating NF-κB activation (Jefferies, Doyle et al. 2003). Our findings here clearly demonstrated that phosphorylation of Mal was enhanced upon increased activation of Btk following LPS stimulation. Mutational analysis of Mal suggests that Btk phosphorylates Mal on Tyr-86, Tyr-106 and Tyr-187. This observation therefore identifies that Mal is a substrate for Btk on the TLR4 pathway, with phosphorylation of Mal on Tyr-86 and Tyr-187 by Btk being required for NF-κB activation mediated by LPS.

Although Tyr-106 failed to activate NF-κB to the same extent as wild-type Mal and had a different phosphorylation profile to wild-type Mal, it had no effect on LPS signaling. All three tyrosines located at positions 86, 106 and 187 may need to undergo phosphorylation in order for Mal to exhibit retarded mobility. Given that during TLR2 and TLR4 signalling two tyrosine phosphorylated forms of Mal could be detected, it is likely that endogenous Mal is also multiply tyrosine phosphorylated. The role of Tyr-106 in Mal signaling is therefore unclear, but may be required for another Mal-mediated signal.

Recently the crystal structure of Btk has been resolved, revealing that Btk displays an extended conformation with no, or little, inter-domain interactions (Marquez 2003). This implies that unlike Src kinases, Btk does not require an assembled conformation for the regulation of its kinase activity. As Btk lacks a negative regulatory domain which is present in the Src kinases, it has led to speculation that Btk may rely on cytoplasmic proteins to regulate its kinase activity. Indeed, recent evidence has reported the identification of a new Btk-interacting protein, termed IBtk which inhibited Btk kinase activity and NF-κB activation mediated by Btk upon anti-IgM stimulation (Jefferies, Doyle et al. 2003).

Results presented in this chapter, affixes Mal to the list of Btk negative regulators, as Mal was observed to dramatically downregulate Btk kinase activity. It has been reported that in the presence of ATP, recombinant Btk can autophosphorylate Tyr-223 and Tyr-551, located within the SH3 domain and the activation loop of Btk, respectively. Mal may therefore directly inhibit Btk kinase activity by binding to its autophosphorylation sites or by blocking the formation of Btk homodimers.

Alternatively Mal may promote a conformational change in Btk, leading to inefficient autophosphorylation of Tyr-223 or Tyr-551, thereby reducing Btk kinase activity. Data presented here presents a novel role for Mal as a possible negative regulator of Btk kinase activity during TLR signal transduction.

In order to further confirm that Btk is a key tyrosine kinase for Mal phosphorylation the phosphorylation status of Mal in monocytes and splenocytes isolated from Xid mice was examined. The level of Mal however, in cells from both wild type and Xid mice was too low for detection in the endogenous phosphotyrosine immunoprecipitation assay. However the inhibitory effect of LFM-A13 and the *in vitro* evidence strongly suggest that the tyrosine kinase responsible for tyrosine phosphorylation of Mal is Btk.

The results in this chapter clearly show that Mal is a phosphoprotein that becomes tyrosine phosphorylated by Btk upon activation of the TLR2 and TLR4 signal transduction pathways. In conclusion Mal phosphorylation is required for Mal to signal, which establishes an important mechanistic step in TLR2 and TLR4 signaling.

Chapter 5

Analysis of Mal Degradation

5.1 Introduction

Activation of the TLR signalling pathway, if left unrestrained, can contribute to severe immunopathologies including Crohn's disease and septic shock. It is therefore essential that TLR signal transduction is tightly regulated in order to prevent tissue damage that arises from sustained inflammation. Multiple methods are instigated in order to control TLR signalling. Beginning at the receptor level, the first-line of negative regulation is performed by naturally produced soluble TLRs. These proteins are believed to behave as decoy receptors by preventing a direct interaction between TLRs and their bacterial ligands. To date only soluble forms of TLR2 and TLR4 have been described (Iwami, Matsuguchi et al. 2000; LeBouder, Rey-Nores et al. 2003).

Upon activation, the TLRs can be further controlled by intracellular negative regulators which are present either constitutively or are upregulated. These proteins can interfere with the formation of signalling competent TLR complexes thus limiting the TLR signalling effect, examples of which include MyD88s, ST2 and SOCS-1.

TLR activation can be further controlled by downregulation of essential components in the signalling pathway, resulting in a reduced inflammatory response. Regarding members of the TLR family, evidence has emerged indicating that Triad3A, an E3 ubiquitin-protein ligase, downregulates TLR4 and TLR9 expression through ubiquitination and degradation. Moreover, TLR2 has been shown to be basally ubiquitinated, although the exact mechanisms leading to this have yet to be determined. In addition, it has recently been discovered that expression of TGFβ mediates MyD88 degradation.

Given that TLR activation is tightly regulated throughout the signalling pathway and that members of the TLR family are degraded, this chapter investigated the regulatory role that phosphorylation of Mal might have with respect to TLR signalling, as phosphorylation is frequently used as a method to target proteins for degradation. Results determined that Mal is degraded following overexpression of SOCS-1.

5.2. Results

5.2.1 Mal is degraded following incubation in an *in vitro* kinase assay.

Having established that Mal is phosphorylated by cellular kinases in an *in vitro* kinase assay in chapter 3, it was of interest to investigate the phosphorylation status of Mal following activation of the TLR4 signalling pathway. In order to assess this THP-1 cells were stimulated with LPS, cell lysates were prepared and GST-pulldown assays were performed with GST-Mal. The samples were then subjected to *in vitro* kinase assays and analysed by SDS-PAGE, followed by autoradiography. As has been previously observed, GST-Mal becomes phosphorylated by interacting with cellular kinases (Figure 5.2.1, lane 1). Interestingly, it was noted that treatment with LPS resulted in a severe reduction of phosphorylated Mal, with the most dramatic effect being evident at 5 minutes post-stimulation (Figure 5.2.1a, lane 2).

Analysis of the Coomassie stained gel revealed that following incubation in an *in vitro* kinase assay, Mal was degraded (Figure 5.2.1b, lane 2). The reduction in phosphorylated Mal corresponded to a reduction in the amount of Mal substrate. GST-Mal was phosphorylated in resting cells, suggesting that Mal is phosphorylated by constitutively active kinases in the cell lysates. LPS stimulation is known to initiate a kinase cascade which culminates in the activation of the transcription factors, NF-κB, AP1 and IRF-3. Therefore, in this system LPS most likely activates a kinase which subsequently phosphorylates Mal. Signal-induced phosphorylation of Mal may then target it for degradation. Cell lysates were immunoblotted with an anti-IκBα antibody, to ensure that cells had responded to LPS (Figure 5.2.1c).

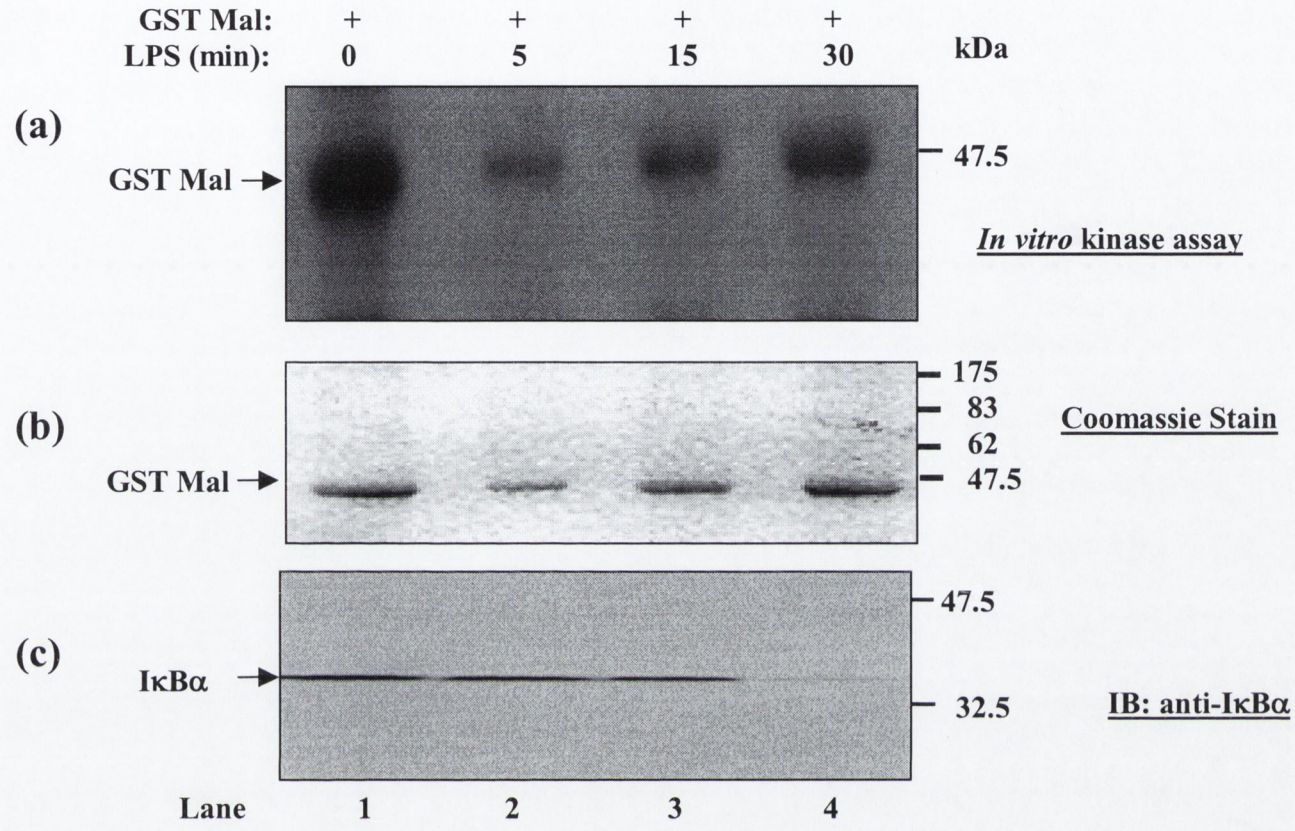

Figure 5.2.1 LPS stimulation induces Mal degradation following incubation of Mal in an *in vitro* kinase assay. (a) THP-1 cells ($1x10^6$) were stimulated with 1 μg/ml of LPS for the indicated times. Cell lysates were prepared and 5 μg of GST-Mal was incubated with each sample for 2 hours at 4°C. Samples were washed three times in lysis buffer and twice again in kinase buffer, then incubated with [γ32P]PO_4 for 30 min, at 37°C. Following incubation in an *in vitro* kinase assay, samples were analysed by SDS-PAGE, the gel was stained with Coomassie Brillant Blue (G250), then dried and subjected to autoradiography. (b) The gel stained with Coomassie Brillant Blue (G250). (c) Cell lysates immunoblotted with an anti-IκBα antibody. Data shown is a representative experiment from five separate experiments.

5.2.2 Mal interacts with SOCS-1

Given that Mal is degraded following stimulation with LPS, it was of interest to investigate the possible proteins that were involved in mediating this event. Both LPS and MALP-2 stimulation have been reported to induce expression of SOCS-1, a known negative regulator of the TLR4 signal transduction pathway (Kinjyo, Hanada et al. 2002). SOCS-1 contains an SH2 domain, which binds tyrosine phosphorylated proteins. Given that we had determined that Mal was tyrosine phosphorylated following LPS and MALP-2 stimulation, investigations were conducted in order to determine if SOCS-1 played a role in mediating these events.

Association studies were therefore carried out to establish if Mal interacted with SOCS-1. HEK293 cells were transiently transfected with plasmids encoding Myc-SOCS-1 and HA-Mal, cell lysates were prepared and proteins were immunoprecipitated with the indicated antibodies. Samples were separated by SDS-PAGE and subsequently immunoblotted with an anti-HA antibody. As illustrated in figure 5.2.2a, Mal interacts with SOCS-1 (lane 3). As a positive control, HA-Mal could be immunoprecipitated from cell lysates with an anti-HA antibody (Figure 5.2.2a, lane 4). As expected, no interaction is observed in cells expressing either HA-Mal or Myc-SOCS-1 alone (Figure 5.2.2a, lanes 1 and 2 respectively). Cell lysates were also immunoblotted with an anti-HA antibody and an anti-Myc antibody to confirm expression of both Mal and SOCS-1 in the appropriate samples (Figure 5.2.2, b and c respectively).

Figure 5.2.2 Wild-type Mal interacts with SOCS-1. (a) HEK293 cells were transiently transfected with a plasmid encoding 4 μg of either HA-Mal or Myc-SOCS-1 as indicated. Cell lysates were subjected to immunoprecipitation with the indicated antibodies. Samples were analysed by SDS-PAGE and immunoblotted with an anti-HA antibody. Cell lysates were immunoblotted with (b) an anti-HA antibody or (c) an anti-Myc antibody. Lane 2 in (b) and (c) represents samples from lanes 3 and 4 of panel (a). Data shown is a representative experiment from two separate experiments.

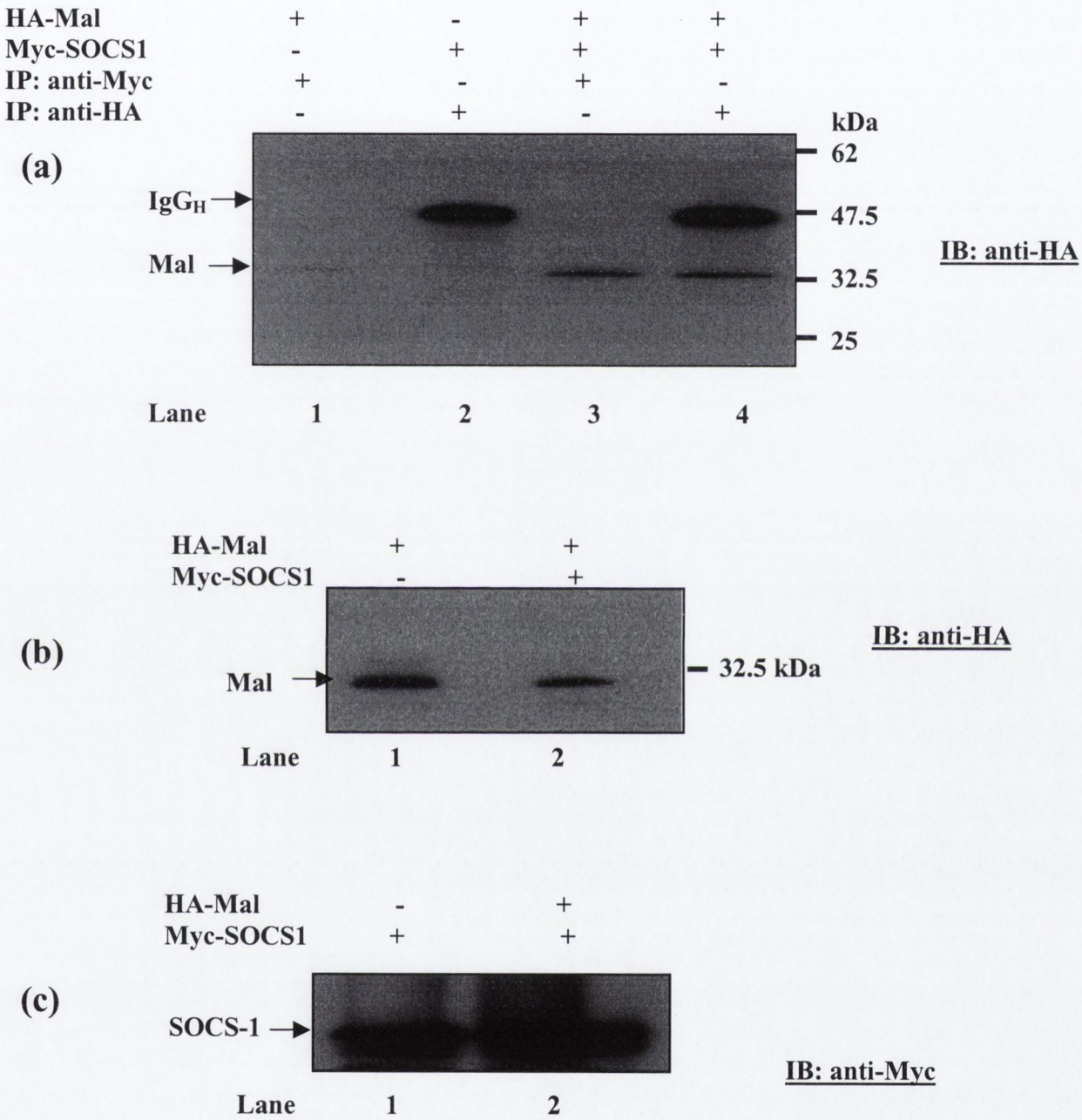
HA-Mal + - + +
Myc-SOCS1 - + + +
IP: anti-Myc + - + -
IP: anti-HA - + - +
kDa
62
47.5
32.5
25
(a)
IgG$_H$
Mal
IB: anti-HA
Lane 1 2 3 4
HA-Mal + +
Myc-SOCS1 - +
(b)
Mal
32.5 kDa
IB: anti-HA
Lane 1 2
HA-Mal - +
Myc-SOCS1 + +
(c)
SOCS-1
IB: anti-Myc
Lane 1 2

5.2.3 Mal-Y86F interacts with SOCS-1

Results illustrated in chapter 4 identified Tyr-86, Tyr-106, and Tyr-187 as possible Mal phosphorylation sites, as SOCS-1 binds to tyrosine phosphorylated proteins the effect of mutating these tyrosine residues was next assessed. HEK293 cells were transiently transfected with plasmids encoding Myc-SOCS-1 and HA-Mal-Y86F, cell lysates were prepared and proteins were immunoprecipitated with the indicated antibodies. Samples were separated by SDS-PAGE and subsequently immunoblotted with an anti-HA antibody. As can be seen in figure 5.2.3a, Mal-Y86F interacts with SOCS-1 (lane 3). As a positive control, HA-Mal could be immunoprecipitated from cell lysates with an anti-HA antibody (Figure 5.2.3a, lane 4). As expected, no interaction is observed in cells expressing either HA-Mal-Y86F or Myc-SOCS-1 alone (Figure 5.2.3a, lanes 1 and 2 respectively). Cell lysates were also immunoblotted with an anti-HA antibody and an anti-Myc antibody to confirm expression of both Mal-Y86F and SOCS-1 in the appropriate samples (Figure 5.2.3, b and c respectively).

5.2.4 Mal-Y106F interacts with SOCS-1

The ability of Mal-Y106F to interact with SOCS-1 was next assessed. HEK293 cells were transiently transfected with plasmids encoding Myc-SOCS-1 and HA-Mal-Y106F, cell lysates were prepared and proteins were immunoprecipitated with the indicated antibodies. Samples were separated by SDS-PAGE and subsequently immunoblotted with an anti-HA antibody. As can be seen in figure 5.2.4a, Mal-Y106F interacts with SOCS-1 (lane 3). As a positive control, HA-Mal-Y106F could be immunoprecipitated from cell lysates with an anti-HA antibody (Figure 5.2.4a, lane 4).

Figure 5.2.3 Mal-Y86F interacts with SOCS-1. (a) HEK293 cells were transiently transfected with a plasmid encoding 4 μg of either HA-Mal-Y86F or Myc-SOCS-1 as indicated. Cell lysates were subjected to immunoprecipitation with the indicated antibodies. Samples were analysed by SDS-PAGE and immunoblotted with an anti-HA antibody. Cell lysates were immunoblotted with (b) an anti-HA antibody or (c) an anti-Myc antibody. Lane 2 in (b) and (c) represents samples from lanes 3 and 4 of panel (a). Data shown is a representative experiment from two separate experiments.

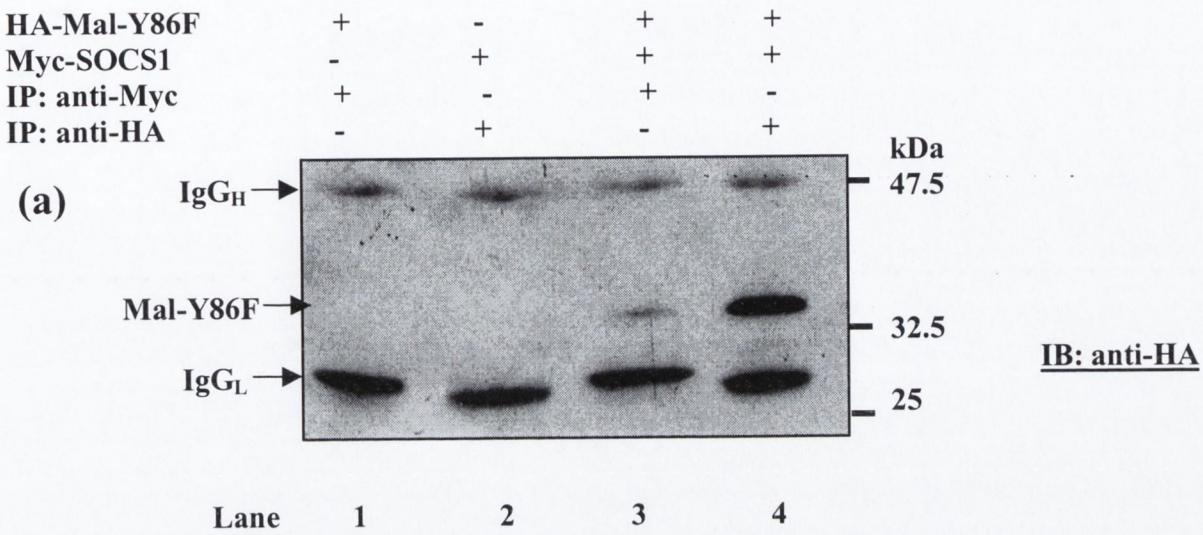
HA-Mal-Y86F + - + +
Myc-SOCS1 - + + +
IP: anti-Myc + - + -
IP: anti-HA - + - +
(a)
IgG$_H$
Mal-Y86F
IgG$_L$
kDa
47.5
32.5
25
IB: anti-HA
Lane 1 2 3 4

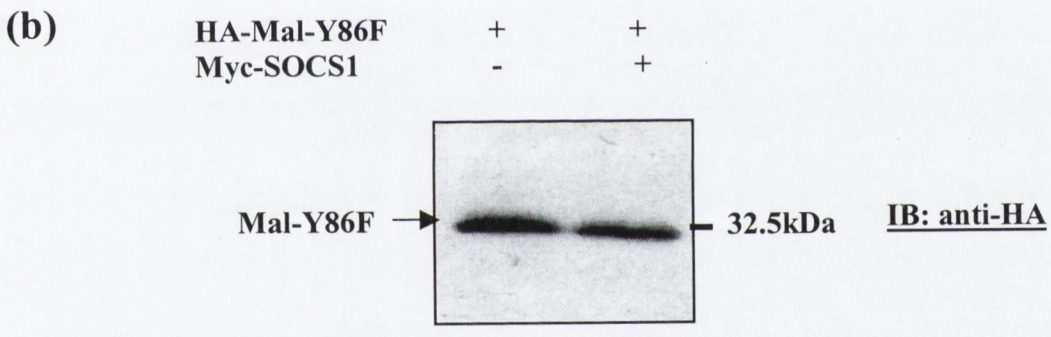
(b)
HA-Mal-Y86F + +
Myc-SOCS1 - +
Mal-Y86F
32.5kDa
IB: anti-HA
Lane 1 2

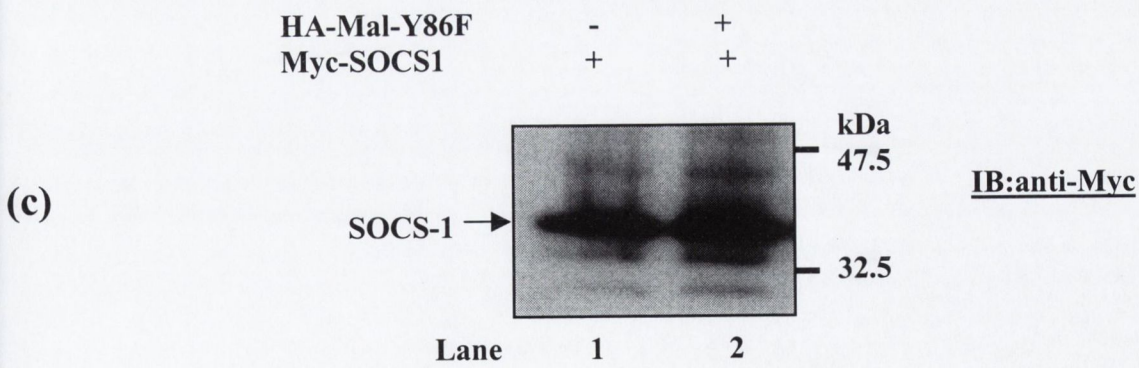
HA-Mal-Y86F - +
Myc-SOCS1 + +
(c)
SOCS-1
kDa
47.5
32.5
IB:anti-Myc
Lane 1 2

Figure 5.2.4 Mal-Y106F interacts with SOCS-1. (a) HEK293 cells were transiently transfected with a plasmid encoding 4 μg of either HA-Mal-Y106F or Myc-SOCS-1 as indicated. Cell lysates were subjected to immunoprecipitation with the indicated antibodies. Samples were analysed by SDS-PAGE and immunoblotted with an anti-HA antibody. Cell lysates were immunoblotted with (b) an anti-HA antibody or (c) an anti-Myc antibody. Lane 2 in (b) and (c) represents samples from lanes 3 and 4 of panel (a). Data shown is a representative experiment from two separate experiments.

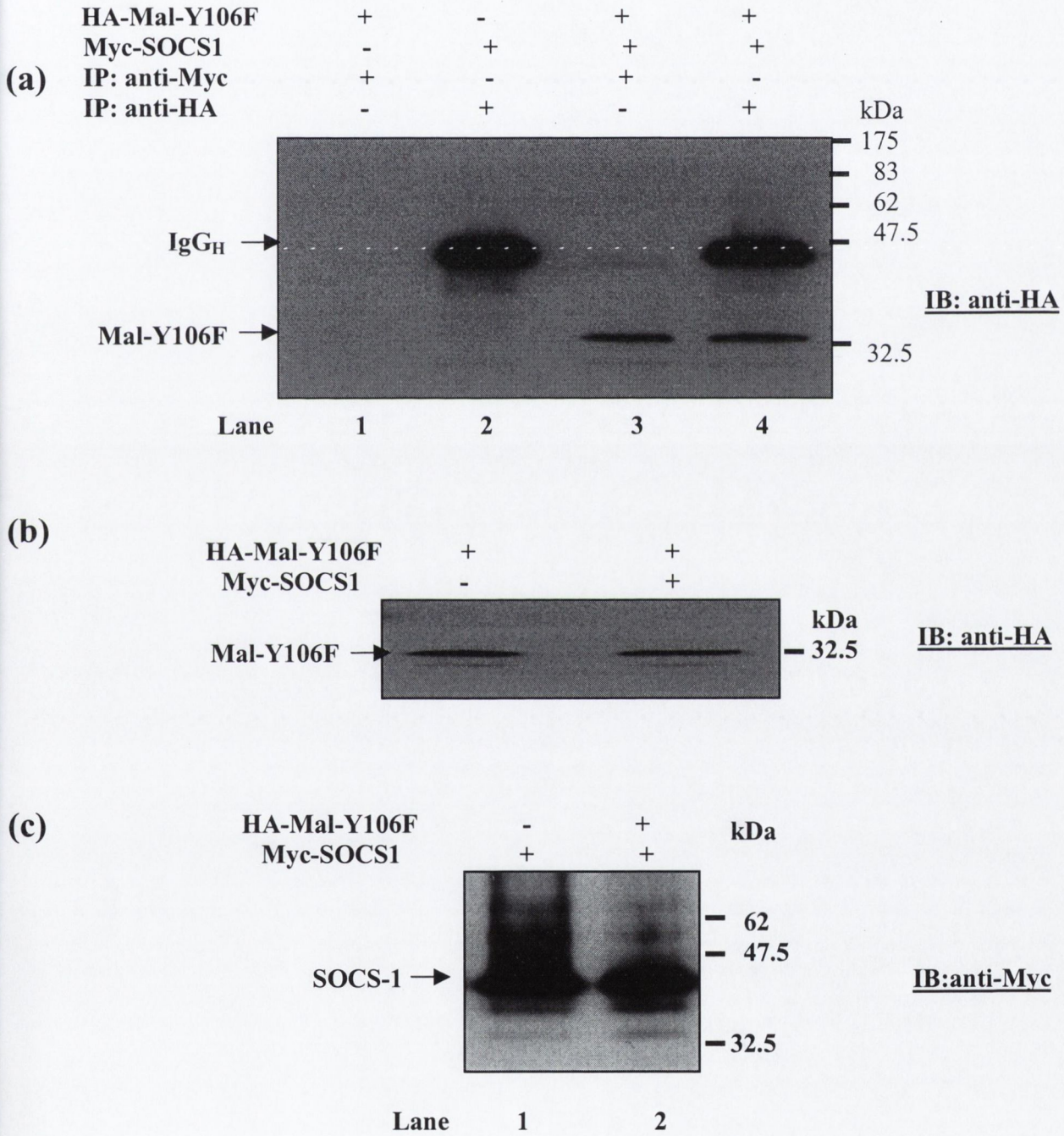
(a)
HA-Mal-Y106F + - + +
Myc-SOCS1 - + + +
IP: anti-Myc + - + -
IP: anti-HA - + - +
kDa
175
83
62
47.5
32.5
IgG$_H$
Mal-Y106F
IB: anti-HA
Lane 1 2 3 4
(b)
HA-Mal-Y106F + +
Myc-SOCS1 - +
Mal-Y106F
kDa
32.5
IB: anti-HA
(c)
HA-Mal-Y106F - +
Myc-SOCS1 + +
kDa
62
47.5
32.5
SOCS-1
IB:anti-Myc
Lane 1 2

As expected, no interaction is observed in cells expressing either HA-Mal-Y106F or Myc-SOCS-1 alone (Figure 5.2.4a, lanes 1 and 2 respectively). Cell lysates were also immunoblotted with an anti-HA antibody and an anti-Myc antibody to confirm expression of both Mal-Y106F and SOCS-1 in the appropriate samples (Figure 5.2.4, b and c respectively).

5.2.5 Mal-Y187F interacts with SOCS-1

Having observed that Mal-Y86F and Mal-Y106F still interacted with SOCS-1 it was next investigated if Mal-Y187F associated with SOCS-1. HEK293 cells were transiently transfected with plasmids encoding Myc-SOCS-1 and HA-Mal-Y187F, cell lysates were prepared and proteins were immunoprecipitated with the indicated antibodies. Samples were separated by SDS-PAGE and subsequently immunoblotted with an anti-HA antibody. As c an be seen in figure 5.2.5a, Mal-Y187F interacts with SOCS-1 (lane 3). As a positive control, HA-Mal-Y187F could be immunoprecipitated from cell lysates with an anti-HA antibody (Figure 5.2.5a, lane 4). As expected, no interaction is observed in cells expressing either HA-Mal-Y187F or Myc-SOCS-1 alone (Figure 5.2.5(a), lanes 1 and 2 respectively). Cell lysates were also immunoblotted with an anti-HA antibody and an anti-Myc antibody to confirm expression of both Mal-Y187F and SOCS-1 in the appropriate samples (Figure 5.2.5, b and c respectively).

5.2.6 Mal-Y87F Y106F Y187F interacts with SOCS-1

Given that the single tyrosine mutant Mal proteins all associated with SOCS-1, it was of interest to determine if replacement of all three tyrosine residues located at positions 86, 106 and 187 could disrupt the interaction between Mal and SOCS-1.

Figure 5.2.5 Mal-Y187F interacts with SOCS-1. (a) HEK293 cells were transiently transfected with a plasmid encoding 4 μg of either HA-Mal-Y187F or Myc-SOCS-1 as indicated. Cell lysates were subjected to immunoprecipitation with the indicated antibodies. Samples were analysed by SDS-PAGE and immunoblotted with an anti-HA antibody. Cell lysates were immunoblotted with (b) an anti-HA antibody or (c) an anti-Myc antibody. Lane 2 in (b) and (c) represents samples from lanes 3 and 4 of panel (a). Data shown is a representative experiment from two separate experiments.

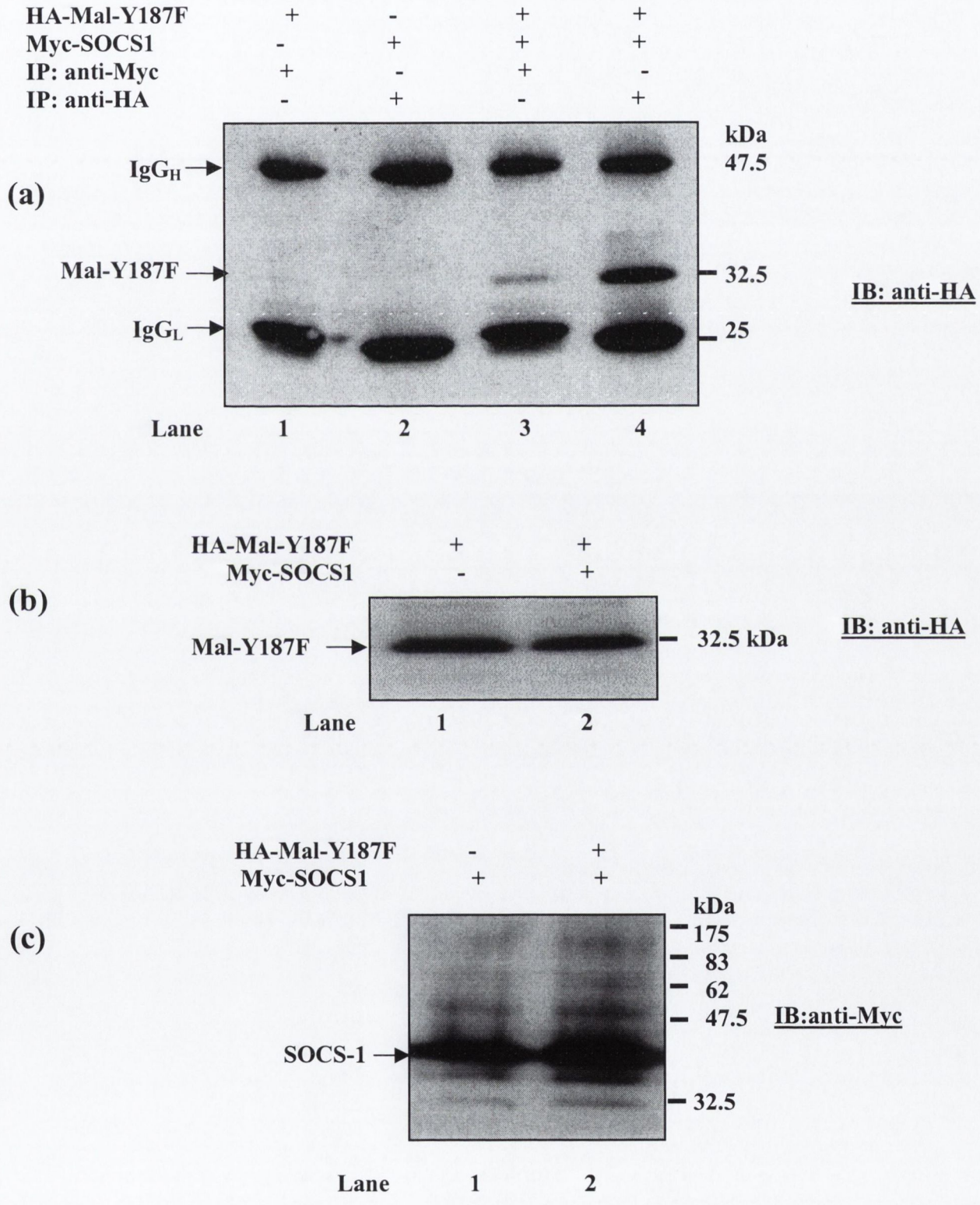
HA-Mal-Y187F + - + +
Myc-SOCS1 - + + +
IP: anti-Myc + - + -
IP: anti-HA - + - +
(a)
IgG$_H$
Mal-Y187F
IgG$_L$
kDa
47.5
32.5
25
IB: anti-HA
Lane 1 2 3 4
HA-Mal-Y187F + +
Myc-SOCS1 - +
(b)
Mal-Y187F
32.5 kDa
IB: anti-HA
Lane 1 2
HA-Mal-Y187F - +
Myc-SOCS1 + +
(c)
kDa
175
83
62
47.5
32.5
SOCS-1
IB:anti-Myc
Lane 1 2

Therefore HEK293 cells were transiently transfected with plasmids encoding Myc-SOCS-1 and HA-Mal-Y86F Y106F Y187F, cell lysates were prepared and proteins were immunoprecipitated with the indicated antibodies. Samples were separated by SDS-PAGE and subsequently immunoblotted with an anti-HA antibody. As can be seen in figure 5.2.4a, Mal-Y86F Y106F Y187F interacts with SOCS-1 (lane 3). As a positive control, HA-Mal-Y86F Y106F Y187F could be immunoprecipitated from cell lysates with an anti-HA antibody (Figure 5.2.6a, lane 4). As expected, no interaction is observed in cells expressing either HA-Mal-Y86F Y106F Y187F or Myc-SOCS-1 alone (Figure 5.2.6a, lanes 1 and 2 respectively). Cell lysates were also immunoblotted with an anti-HA antibody and an anti-Myc antibody to confirm expression of both Mal-Y106F and SOCS-1 in the appropriate samples (Figure 5.2.6, b and c respectively).

5.2.7 SOCS-1 inhibits Mal mediated NF-κB activation

As has been stated above, studies have shown that SOCS-1 markedly diminished LPS mediated NF-κB activation (Nakagawa, Naka et al. 2002). We sought to confirm this observation using a constitutively active form of TLR4, CD4-TLR4, in the NF-κB reporter gene assay. Similar to previous reports, overexpression of CD4-TLR4 in HEK293 cells activated NF-κB. Notably co-expression of CD4-TLR4 with SOCS-1 severely reduced NF-κB activation mediated by CD4-TLR4 (Figure 5.2.7). Therefore in agreement with previous studies SOCS-1 inhibited TLR4 signal transduction.

It has also been reported that SOCS-1 inhibits NF-κB activation mediated by IRAK1 and TRAF6, but has no effect on NF-κB activation induced by IKKβ (Nakagawa, Naka et al. 2002). These results indicate that SOCS-1 inhibits upstream of IKKβ. Given

Figure 5.2.6 Mal-Y86F Y106F Y187F interacts with SOCS-1. (a) (a) HEK293 cells were transiently transfected with a plasmid encoding 4 μg of either HA-Mal-Y86F Y106F Y187F or Myc-SOCS-1 as indicated. Cell lysates were subjected to immunoprecipitation with the indicated antibodies. Samples were analysed by SDS-PAGE and immunoblotted with an anti-HA antibody. Cell lysates were immunoblotted with (b) an anti-HA antibody or (c) an anti-Myc antibody. Lane 2 in (b) and (c) represents samples from lanes 3 and 4 of panel (a). Data shown is a representative experiment from two separate experiments.

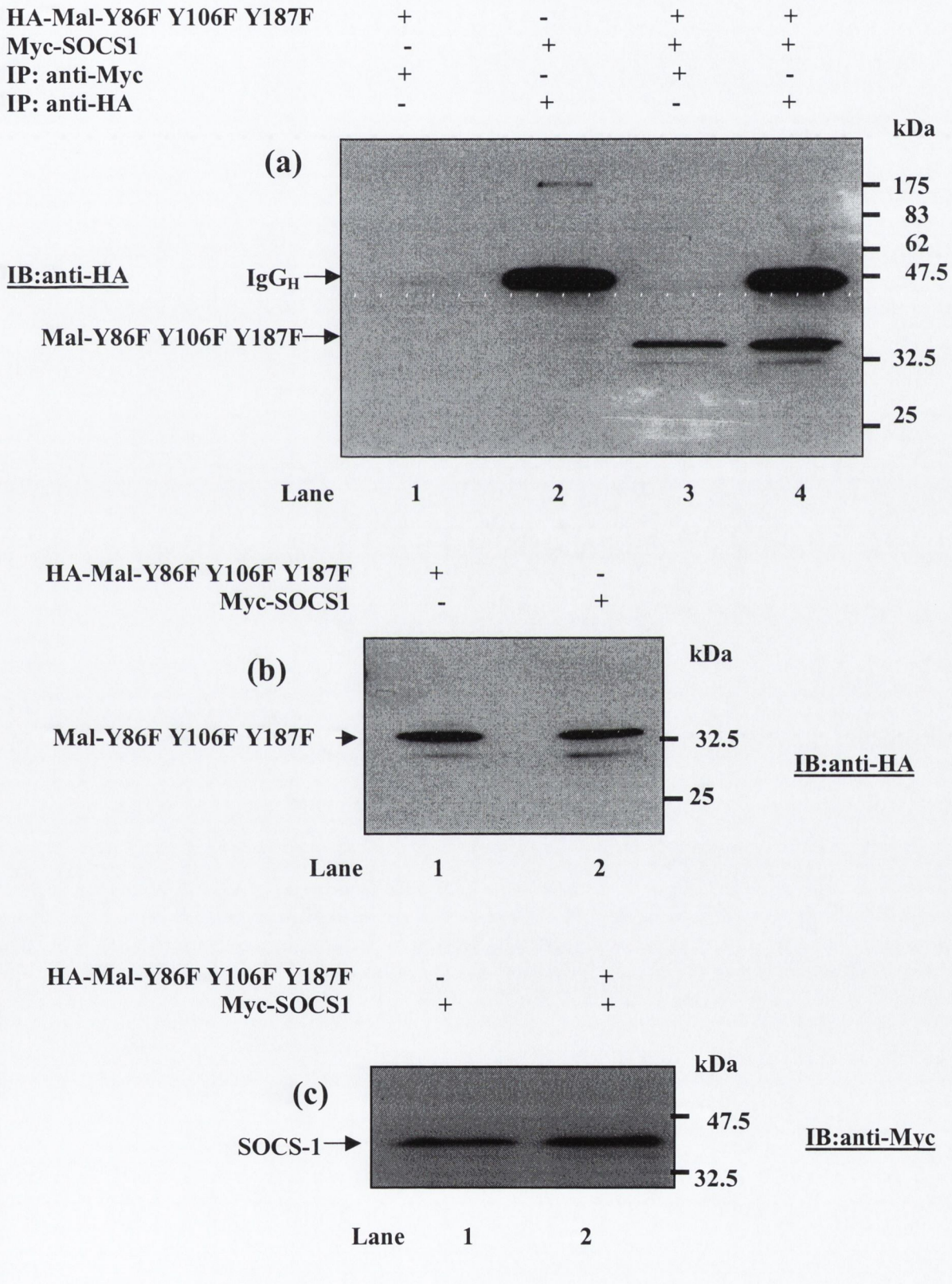
HA-Mal-Y86F Y106F Y187F + - + +
Myc-SOCS1 - + + +
IP: anti-Myc + - + -
IP: anti-HA - + - +
(a)
kDa
175
83
62
47.5
32.5
25
IB:anti-HA
IgG$_H$
Mal-Y86F Y106F Y187F
Lane 1 2 3 4
HA-Mal-Y86F Y106F Y187F + -
Myc-SOCS1 - +
(b)
kDa
Mal-Y86F Y106F Y187F
32.5
25
IB:anti-HA
Lane 1 2
HA-Mal-Y86F Y106F Y187F - +
Myc-SOCS1 + +
(c)
kDa
SOCS-1
47.5
32.5
IB:anti-Myc
Lane 1 2

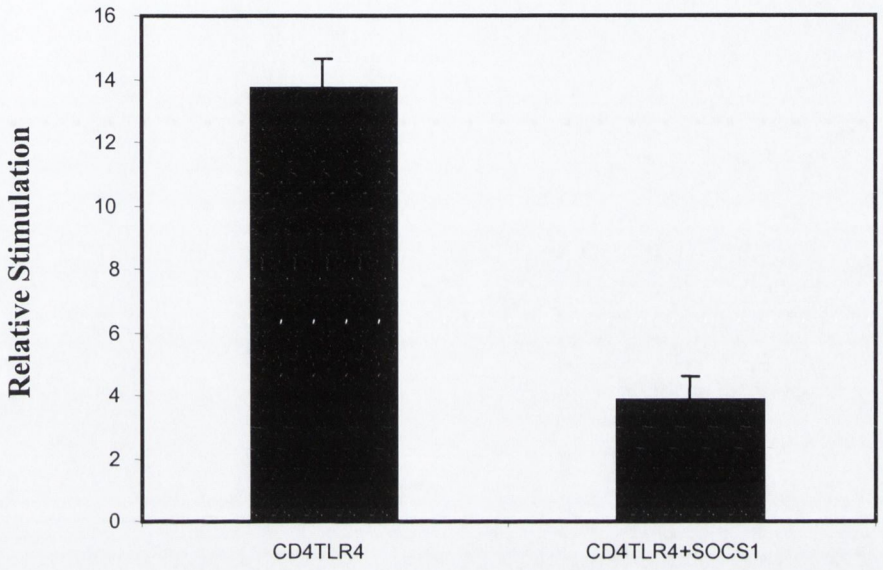

Figure 5.2.7 SOCS-1 inhibits NF-κB activation mediated by CD4-TLR4. (a) HEK293 cells were transiently transfected with a plasmid encoding CD4TLR4 alone or co-transfected with a plasmid encoding SOCS-1. Cells were harvested 24 hours after transfection, luciferase gene activity was measured and normalized on the basis of Renilla values. Data are expressed as mean relative stimulation of luciferase activity ± S.D. relative to renilla values, for a representative experiment from two separate experiments, each performed in triplicate.

that SOCS-1 interacts with Mal, the effect of SOCS-1 on Mal-mediated NF-κB activation was next assessed using an NF-κB reporter gene assay. HEK293 cells were transiently transfected with a plasmid encoding HA-Mal and co-transfected with a plasmid encoding SOCS-1. In agreement with previous reports, overexpressed SOCS-1 did not activate NF-κB, whereas Mal strongly induced NF-κB activation (Figure 5.2.8) (Nakagawa, Naka et al. 2002). Similar to IRAK1 and TRAF6, SOCS-1 severely reduced NF-κB activation mediated by Mal. As had been previously noted Mal Y86F Y106F Y187F displayed dramatically reduced NF-κB activation, compared to wild-type Mal, addition of SOCS-1 reduced NF-κB activity to the level of SOCS-1 alone.

5.2.8 SOCS-1 mediates Mal degradation

In addition to an SH2 domain, SOCS-1 contains a region termed the SOCS box, which has been reported to mediate interactions with elongins B and C, both of which are members of the E3 ubiquitin ligase complex. Studies have shown that LPS treatment induces expression of SOCS-1 in macrophages (Kinjyo, Hanada et al. 2002). Given that SOCS-1 inhibited Mal-mediated NF-κB activation, it was of interest to investigate the role of SOCS-1 with respect to Mal degradation. HEK293 cells were transfected with a constant amount of a plasmid encoding HA-Mal and co-transfected with increasing amounts of a plasmid encoding Myc-SOCS-1. Cell lysates were prepared, samples were analysed by SDS-PAGE and subsequently immunoblotted with an anti-HA antibody to detect Mal expression. As shown in figure 5.2.9a, SOCS-1 induced degradation of Mal in a dose dependent manner. Cell lysates were also immunoblotted with an anti-Myc antibody to confirm increasing expression of SOCS-1 (Figure 5.2.9b). In addition, cell

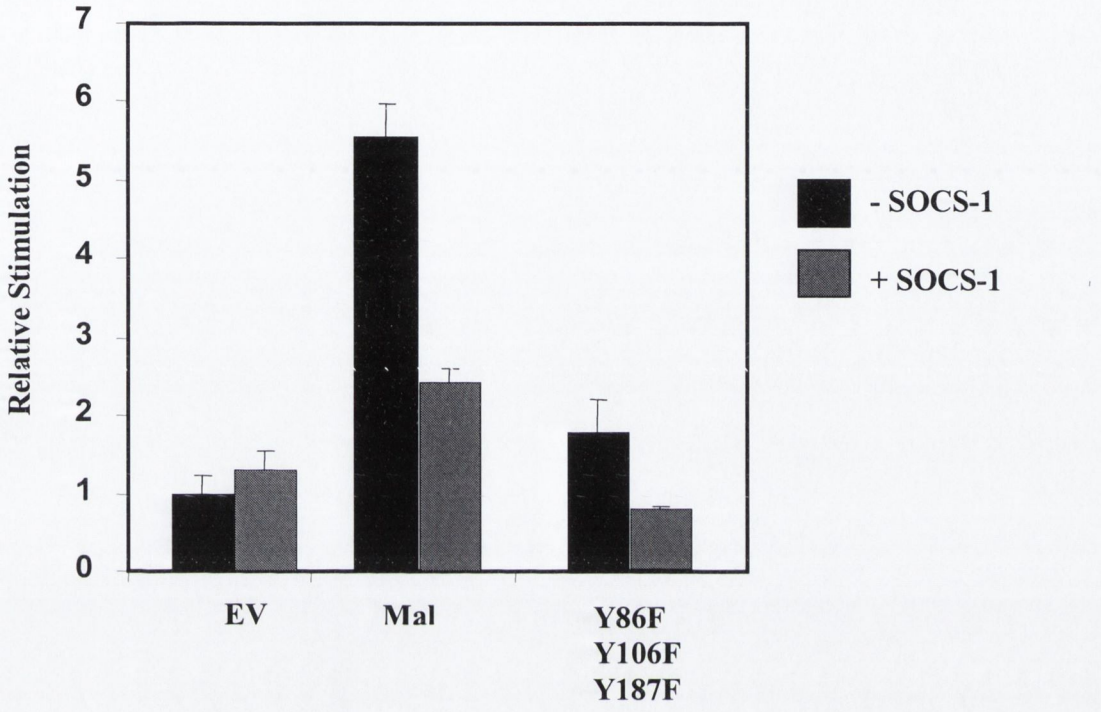

Figure 5.2.8 SOCS-1 inhibits NF-κB activation mediated by Mal. (a) HEK293 cells were transiently transfected with a plasmid encoding Mal or Mal-Y86F Y106F Y187F alone, or co-transfected with a plasmid encoding SOCS-1. Cells were harvested 24 hours after transfection, luciferase gene activity was measured and normalized on the basis of renilla values. Data are expressed as mean relative stimulation of luciferase activity ± S.D. relative to Renilla values, for a representative experiment from two separate experiments, each performed in triplicate.

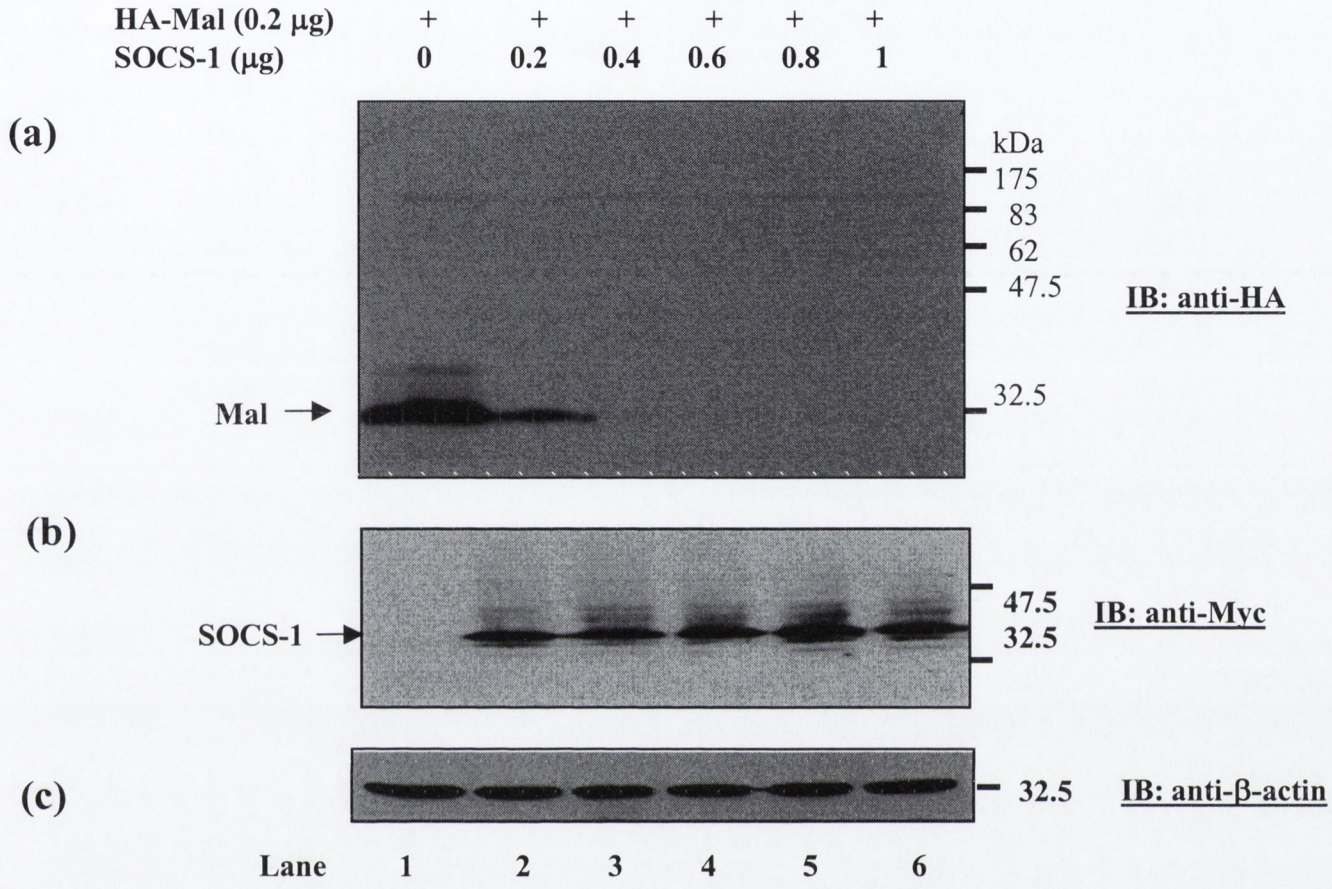

Figure 5.2.9 SOCS-1 promotes degradation of Mal in a dose-dependent manner. (a) HEK293 cells were transiently co-transfected with HA-Mal (200ng) in the absence of, or increasing concentrations of SOCS-1 (200-1000ng). Cell lysates were prepared, samples were then analysed by SDS-PAGE and immunoblotted with an anti-HA antibody. (b) Cell lysates were also analysed to confirm increasing expression of Myc-SOCS-1 by immunoblotting with an anti-Myc antibody. (c) To confirm that equal amounts of total protein were present in each samples, cell lysates were also immunoblotted with the anti-β-actin antibody. Data shown is a representative experiment from two separate experiments.

lysates were immunoblotted with an anti-β-actin antibody to verify that the total protein content was equal in all samples (Figure 5.2.9c).

5.2.9 Mal-Y86F Y106F Y187F is more resistant to SOCS-1 induced degradation than wild-type Mal

Having established that SOCS-1 degrades wild-type Mal, the effect of SOCS-1 expression on Mal-Y86F Y106F Y187F was next assessed. HEK293 cells were transfected with a constant amount of a plasmid encoding HA-Mal-Y86F Y106F Y187F and co-transfected with increasing amounts of a plasmid encoding Myc-SOCS-1. Cell lysates were prepared, samples were analysed by SDS-PAGE and subsequently immunoblotted with an anti-HA antibody to detect Mal-Y86F Y106F Y187F expression. Although SOCS-1 induced degradation of Mal-Y86F Y106F Y187F it was not as dramatic as wild-type Mal degradation, suggesting that phosphorylation of these residues may required for efficient depletion of Mal from the cells (Figure 5.2.10a). Cell lysates were also immunoblotted with an anti-Myc antibody to confirm increasing expression of SOCS-1 (Figure 5.2.10b). In addition, cell lysates were immunoblotted with an anti-β-actin antibody to verify that the total protein content was equal in all samples (Figure 5.2.10c).

5.2.10 Overexpressed SOCS-1 does not degrade MyD88

There is evidence that MyD88 undergoes tyrosine phosphorylation and degradation following stimulation with LPS. Having determined that SOCS-1 depleted Mal from HEK293 cells, it was next tested if SOCS-1 was required for MyD88 degradation. HEK293 cells were transfected with a constant amount of a plasmid

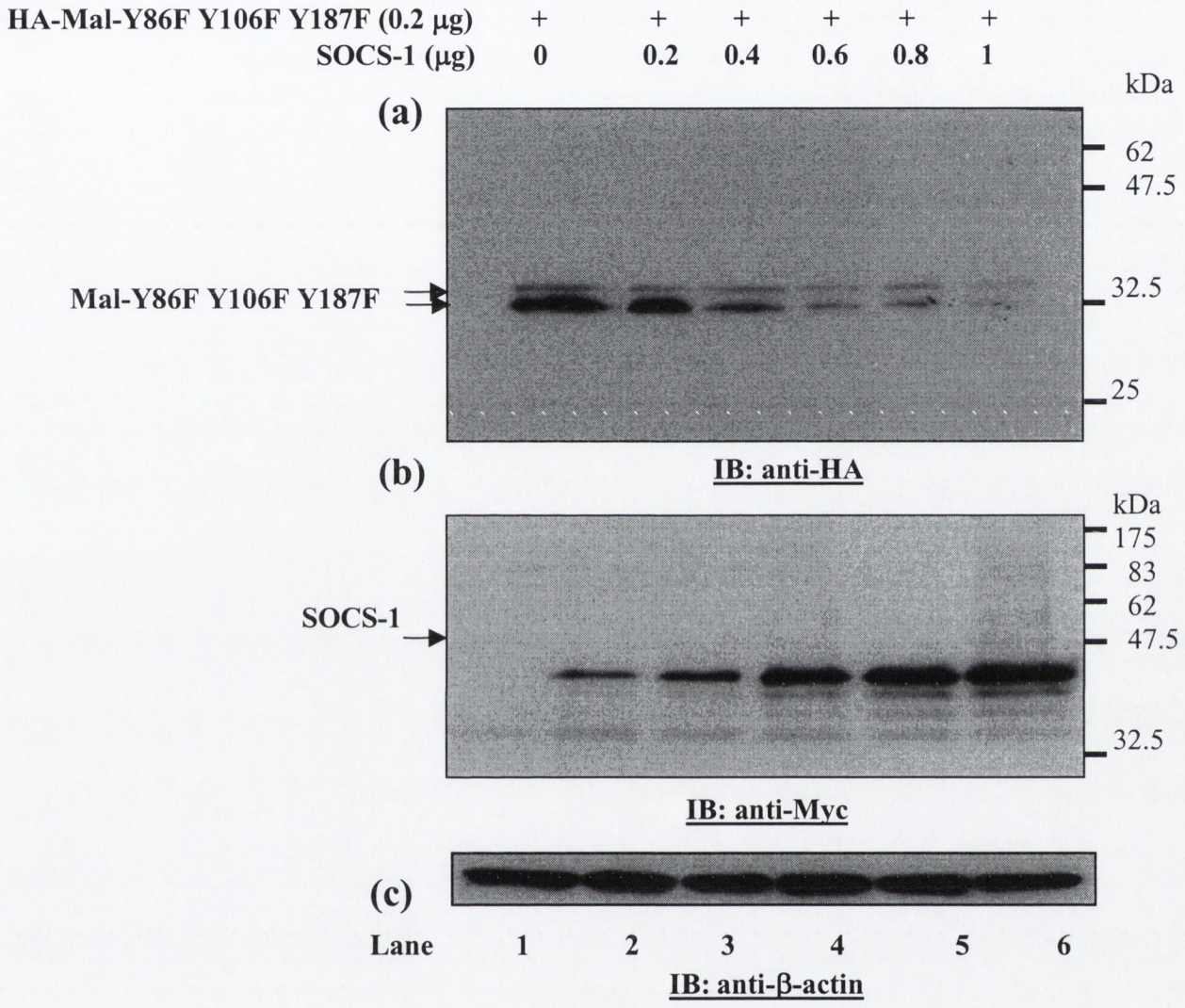

Figure 5.210 SOCS-1 promotes degradation of Mal-Y86F Y106F Y187F. (a) HEK293 cells were transiently co-transfected with HA-Mal-Y86F Y106F Y187F (200ng) in the absence of, or increasing concentrations of SOCS-1 (200-1000ng). Cell lysates were prepared, samples were then analysed by SDS-PAGE and immunoblotted with an anti-HA antibody. Cell lysates were also immunoblotted with (b) an anti-Myc antibody and (c) anti-β-actin antibody. Data shown is a representative experiment from two separate experiments.

encoding AU1-MyD88 and co-transfected with increasing amounts of a plasmid encoding Myc-SOCS-1. Cell lysates were prepared, samples were analysed by SDS-PAGE and subsequently immunoblotted with an anti-AU1 antibody to detect MyD88 expression. In contrast to Mal, SOCS-1 did not induce degradation of MyD88 (Figure 5.2.11a). Cell lysates were also immunoblotted with an anti-Myc antibody to confirm increasing expression of SOCS-1 (Figure 5.2.11b). In addition, cell lysates were immunoblotted with an anti-β-actin antibody to verify that the total protein content was equal in all samples (Figure 5.2.11c). This therefore demonstrated that SOCS-1 induced degradation was specific for Mal.

5.2.11 Mal degradation is abolished in Btk mutant cells

In chapter 4 it was determined that Mal undergoes tyrosine phosphorylation by Btk. Having established that Mal is degraded following overexpression of SOCS-1, the role of Btk in Mal degradation was next investigated. In order to assess this, splenocytes were derived from wild-type mice and Xid mice, which contain a mutated form of Btk that inactivates its kinase function. Xid and wild-type splenocytes were then stimulated with LPS for the indicated times. Cell lysates were prepared, and samples were analysed by SDS-PAGE and subsequently immunoblotted with an anti-Mal antibody (Fig. 5.2.12). It was observed that Mal degraded at 5 minutes treatment time, corresponding with the earlier findings in chapter 4 that determined that Mal was tyrosine phosphorylation at 5 minutes post LPS stimulation. However, splenocytes derived from the Xid mice failed to display Mal degradation in response to LPS-stimulation. This implies a definite role for Btk in mediating Mal degradation following stimulation with LPS.

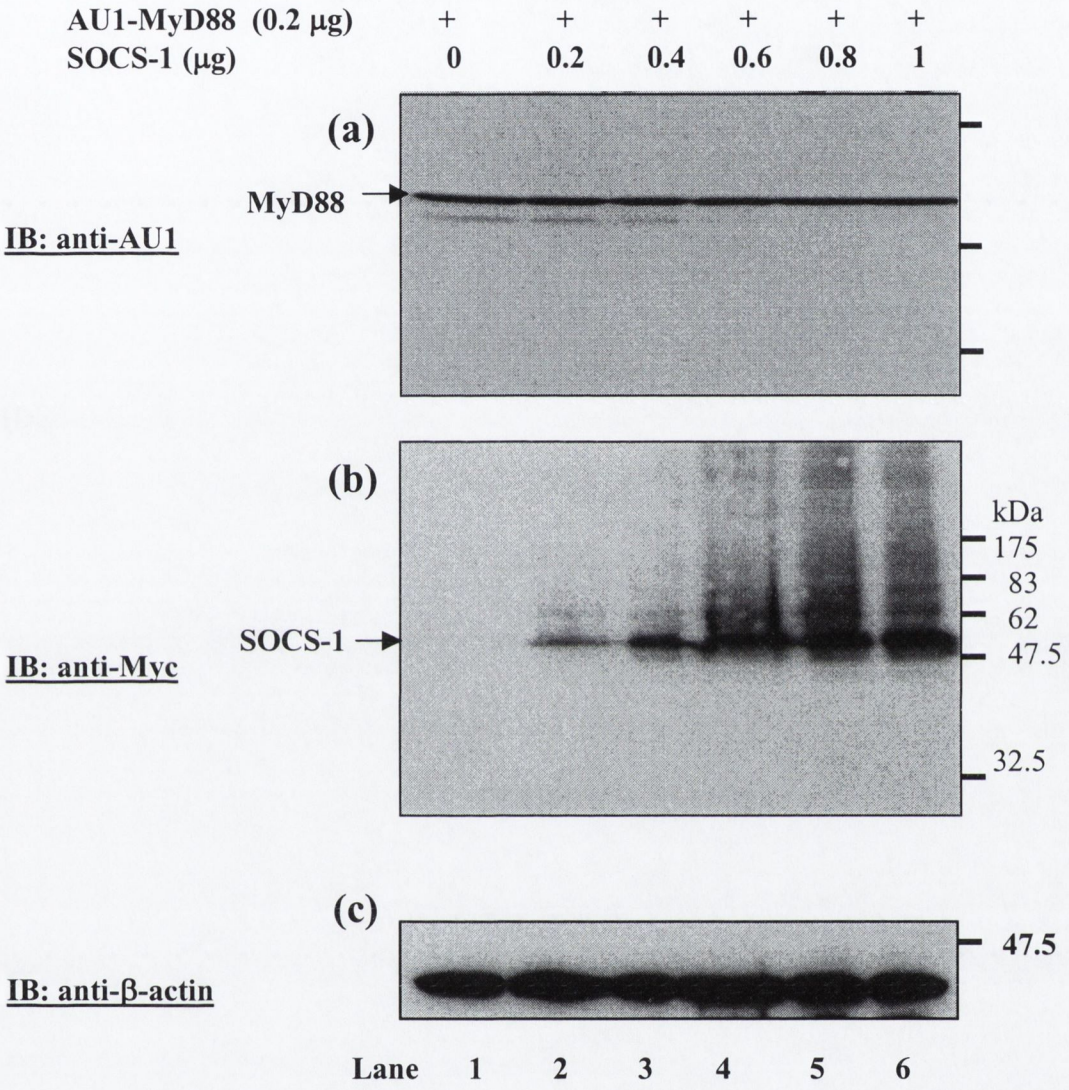

Figure 5.2.11 SOCS-1 does not promote degradation of MyD88. (a) HEK293 cells were transiently co-transfected with AU1-MyD88 (200ng) in the absence of, or increasing concentrations of SOCS-1 (200-1000ng). Cell lysates were prepared, samples were then analysed by SDS-PAGE and immunoblotted with an anti-Au1 antibody. (b) Cell lysates were also immunoblotted with (b) an anti-Myc antibody and (c) anti-β-actin antibody. Data shown is a representative experiment from two separate experiments.

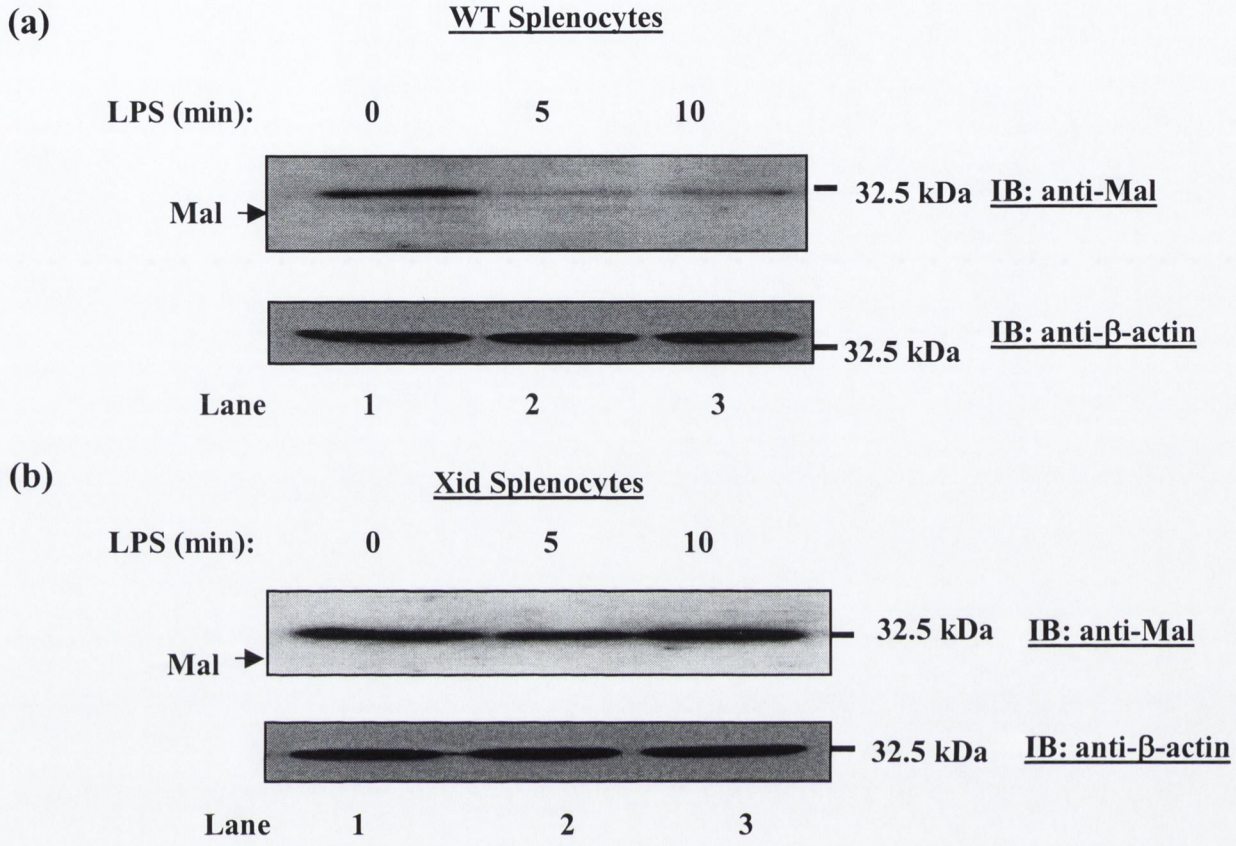

Figure 5.2.12 Mal degradation does not occur in Xid mice. Splenocytes from (a) wild-type and (b) Xid mice ($1x10^6$/ml) were stimulated with 1μg/ml of LPS for the indicated times. Cell lysates were prepared, samples were then analysed by SDS-PAGE and immunoblotted with an anti-Mal antibody (upper panel). To confirm that equal amounts of total protein were present in each sample, cell lysates were also immunoblotted with an anti-β-actin antibody (lower panel).

5.3 Discussion

It has emerged that tight regulation of signal transduction by TLRs is a prerequisite for an appropriate and efficient immune response. Overactivate the immune response and the host may incur major tissue damage, which may lead to the formation of TLR-mediated inflammatory diseases such as sepsis. Given the importance of ensuring that the inflammatory response is not over activated, intense investigations have been conducted in order to decipher the methods required to administer a suitable and controlled immune response. It has since emerged that numerous methods of control have been installed throughout the TLR signalling pathway, with members of the TLR family themselves being required to negatively regulate TLR signal transduction. With this knowledge, we sought to decipher the regulatory role of Mal with respect to TLR signal transduction control.

In this chapter, results demonstrate that Mal is degraded following LPS treatment and as there is less available substrate in the system, the amount of detectable phospho-Mal was therefore significantly reduced. This suggested that Mal interacted with cellular kinases and ubiquitin ligases residing in HEK293 cell lysates, and that these enzymes were subsequently activated during incubation in an *in vitro* kinase assay with Mal. Degradation of Mal was only evident following stimulation with LPS and was most apparent at 5 minutes post LPS stimulation, which corresponds to the time that endogenous Mal underwent tyrosine phosphorylation (Chapter 4, Figure 4.2.21). This suggests that Mal degradation may be used by the host as an additional method for limiting signalling by TLR4.

As shown in chapter 4, Mal is tyrosine phosphorylated following LPS and MALP-2 stimulation. Of the negative regulators thus far identified, SOCS-1 is the only TLR negative regulator that is known to specifically interact with tyrosine phosphorylated proteins and target them for proteasomal degradation. Studies using mice deficient in SOCS-1 have revealed that SOCS-1 acts as a negative regulator for TLR4 and TLR9 signalling. In particular, SOCS-1-deficient macrophages produced heightened levels of nitric oxide and pro-inflammatory cytokines in response to stimulation with TLR4 and TLR9 ligands. Furthermore, LPS stimulation enhanced phosphorylation of STAT1, IκB-α, p38 and JNK in SOCS-1-deficient macrophages and mice lacking SOCS-1 were found to be more sensitive to LPS shock than wild-type mice. SOCS-1 expression is also reported to be induced following stimulation with MALP-2, LPS, and CpG DNA, ligands for TLR2, TLR4 and TLR9 respectively. Moreover, studies have determined that SOCS-1 interacts with IRAK1 via its SH2 region, and that SOCS-1 inhibits NF-κB activation mediated by both IRAK1 and TRAF6.

Association studies in this chapter revealed that Mal interacted with SOCS-1. As SOCS-1 binds tyrosine phosphorylated proteins, it was thought that replacement of the Mal phospho-accepting tyrosine residues located at positions 86, 106 and 187 may prevent the Mal-SOCS-1 interaction. However, it was determined that this was not the case as SOCS-1 maintained the ability to associate with Mal-Y86F Y106F Y187F, suggesting that SOCS-1 can interact with Mal outside of Tyr-86, Tyr-106 and Tyr-187. It is therefore still not precisely clear how SOCS-1 interacts with Mal. However, as SOCS-1 has been reported to bind to IRAK1, and results in chapter 3 have shown that Mal also associates with IRAK1, it cannot be ruled out that Mal may be present in a complex with

IRAK1 and SOCS-1. Indeed, phosphorylation of Mal on Tyr 86, Tyr 106 and Tyr 187 may be required to initiate a conformational change of the Mal structure, which may lead to a transient and tightly regulated interaction between Mal and SOCS-1. This hypothesised transient interaction between Mal and SOCS-1 mediated by tyrosine phosphorylation of Mal, may subsequently result in Mal degradation by SOCS-1.

Data presented in this chapter reveals a direct role for Btk in mediating the degradation of Mal, as it was observed that this process was abolished in cells derived from Xid mice following LPS stimulation. This indicates, that tyrosine phosphorylation of Mal by Btk is most likely required to initiate degradation of Mal. In addition to SOCS-1 associating with Mal, it was determined that SOCS-1 inhibited NF-κB activation mediated by Mal. This suggests therefore that SOCS-1 negatively regulates Mal function in order to control TLR4 signalling, making Mal a target molecule for SOCS-1 regulation.

As stated above, SOCS-1 has been reported to function as an adapter protein, as it targets tyrosine phosphorylated proteins to the ubiquitin machinery, thereby resulting in proteasomal degradation of the target protein. Results presented in this chapter, determined that co-expression of SOCS-1 with Mal, resulted in Mal degradation. Mansell *et al* (submitted manuscript) have further characterised the degradation of Mal by SOCS-1. They have shown that degradation of Mal by SOCS-1 is dependent on the SH2 domain and the SOCS box, as mutant forms of these regions no longer resulted in Mal degradation. In addition, SOCS-1 was observed to mediate Mal polyubiquitination, on lysines located at positions 15 and 16. Mutation of these residues to arginines resulted in increased NF-κB activation compared to wild-type Mal as this Mal mutant was resistant

to degradation. In this chapter, it was observed that SOCS-1 did not degrade Mal-Y86F Y106F Y187F as dramatically as wild-type Mal suggesting that Mal phosphorylation is required for efficient Mal degradation. As suggested above Mal may be present in a complex with IRAK1 and SOCS-1, and phosphorylation of Mal on Tyr 86, Tyr 106 and Tyr 187 may result in a conformational change, which may move Mal in closer proximity to the SOCS-box region of SOCS-1 and the ubiquitin transferase machinery, thereby culminating in Mal degradation. Indeed this may explain why Mal-Y86F Y106F Y187F is more resistant to degradation compared to wild-type Mal. It was noted that the effect of SOCS-1 was specific to Mal, as protein expression of MyD88 was not affected by overexpression of SOCS-1, consistent with the report that SOCS-1 does not interact with MyD88.

Previous reports have shown that Mal drives p65-mediated transactivation. Further investigation by Mansell *et al*, revealed that LPS induced transient phosphorylation of p65 in wild type mouse embryonic fibroblasts (MEFs), whereas Mal-deficient MEFs displayed a complete absence of LPS-mediated p65 phosphorylation. This indicates a critical role for Mal in regulating the transcriptional activity of NF-κB. Furthermore, it was determined that p65 phosphorylation was enhanced in response to LPS in SOCS-1-deficient cells, consistent with a role for SOCS-1 as a negative regulator of Mal signalling.

Taken together results in this chapter identify Mal as a specific target of SOCS-1 immune regulation and uncover an important mechanism of regulating NF-κB signalling mediated by Mal. Indeed, it appears that SOCS-1 depletes Mal from the cells more efficiently than a mutant Mal that does contain the phospho-accepting residues Tyr-86,

Tyr-106 and Tyr187. It is tempting therefore to speculate that SOCS-1 may be required to deplete tyrosine phosphorylated Mal from the cells, thereby limiting NF-κB activation. This may explain why LPS induced tyrosine phosphorylation of endogenous Mal, noted in chapter 4, is such a transient event, as tyrosine phosphorylated Mal may be instantly degraded by SOCS-1, similar to the mechanisms of SOCS-1 negative regulation of cytokine signalling. Newly synthesised Mal that is not tyrosine phosphorylated may replenish Mal protein levels immediately. This may explain why Mal degradation is only apparent in the *in vitro* kinase assay and not in THP-1 cells. In conclusion, results presented here, define an additional method for regulating the immune response through Mal degradation mediated by SOCS-1.

Chapter 6

Final discussion and Future Perspectives

The discovery of TLRs resulted in an onslaught of intense investigation in the pursuit to decipher the precise role of these evolutionary conserved receptors. It has since emerged that prompt activation of the TLR signalling pathway is a vital process in the recognition of invading pathogens and in eliciting the host innate immune response. This investigation sought as its broad aim to further characterise the involvement of Mal in mediating the signals which are emanating from TLR2 and TLR4 following microbial invasion. In particular, this study focussed on the mechanisms of Mal phosphorylation.

The initial observation that overexpressed Mal consisted of four distinct bands following SDS-PAGE analysis suggested that Mal may be post-translationally modified. Analysis on 2-D SDS-PAGE revealed that the slower migrating forms of Mal displayed a lower isoelectric point than the predominant 32 kDa form. Reduced electrophoretic mobility of Mal, coupled with the observation that its isoelectric point is altered, implied that Mal may be phosphorylated. Indeed, CIP treatment established that the slower migrating forms of Mal represented phosphorylated Mal. The fastest migrating form has since been identified as a by-product of Mal cleavage by caspase-1 (Miggin *et al.*, submitted manuscript).

Kinases play an essential role throughout TLR signalling. They are required both for its activation and regulation. Analysis of candidate kinases that have been positioned in close proximity to Mal during signal transduction, revealed that Mal is a substrate for IRAK1, IRAK4, and Btk *in vitro*. Furthermore, it was noted that phosphorylation of Mal by IRAK1 resulted in the formation of three phospho-forms whereas both IRAK4- and Btk-mediated phosphorylation of Mal produced two phospho-forms, implying that Mal is multiply phosphorylated.

Mutational studies of Mal were unable to identify potential phospho-serine or phospho-threonine residues. A total of eleven mutant Mal proteins were generated, representing 33% of the conserved serine and threonine residues in humans and mice. However, all of the tested mutants were found to be normal when assayed for NF-κB activation and all exhibited the same mobility pattern as wild type Mal when analysed by SDS-PAGE. Nevertheless, it cannot be ruled out that these residues are in fact phosphorylated, as firstly not all phosphorylation events result in a mobility shift of a protein, as is the case of MyD88. Secondly, if these specific residues are phosphorylated they may not be required for NF-κB activation, instead their role may lie in Mal-mediated activation of ERK1/2 or JNK, or in p65-mediated transactivation induced by Mal. Thirdly, given that IRAK1 and IRAK4 create up to three Mal phospho-forms, it implies that Mal is multiply phosphorylated by these kinases, therefore it can only be stated that the mutated residues have no effect on NF-κB activation when mutated singly, as perhaps specific residues must be mutated in combination to have a significant effect on Mal signalling. A more direct route using mass spectrometry analysis must therefore be undertaken in order to explicitly identify the phospho-serine or phospho–threonine residues of Mal. Identification of the sites of phosphorylation of Mal by IRAK1 and IRAK4, will permit the generation of Mal mutants, functional studies may then be conducted in order to ascertain the importance of these phosphorylation events.

Having identified that Mal was phosphorylated by the tyrosine kinase Btk, mutational analysis determined that replacement of Tyr-86, Tyr-106 and Tyr-187 to phenylalanine residues abolished the slowest migrating form of Mal. Phosphatase treatment established that the slower migrating form of Mal represented tyrosine

phosphorylated Mal. Tyr-86, Tyr-106 and Tyr-187 were also found to be the most critical residues for maximal NF-κB activation induced by Mal. Furthermore, it was determined that both MALP-2 and LPS rapidly and transiently triggered tyrosine phosphorylation of endogenous Mal in THP-1 cells. This tyrosine phosphorylation of Mal was abolished in cells that were pre-treated with the Btk inhibitor, LFM-A13, further highlighting the fact that Btk is essential for mediating TLR induced phosphorylation of Mal. Furthermore, the findings presented in this study clearly demonstrated that phosphorylation of Mal was enhanced upon increased activation of Btk following LPS stimulation and that Tyr-86, Tyr-106 and Tyr-187 are phosphorylation sites for Btk.

In addition, it was determined that Tyr-86 and Tyr-187 are likely to undergo phosphorylation following LPS stimulation and that this process is required for NF-κB activation mediated by Mal. Although Tyr-106 failed to activate NF-κB to the same extent as wild-type Mal and had a different phosphorylation profile to wild-type Mal, it had no effect on LPS signalling. All three tyrosines located at positions 86, 106 and 187 may need to undergo phosphorylation in order for Mal to exhibit retarded mobility. Given that during TLR2 and TLR4 signalling two tyrosine phosphorylated forms of Mal could be detected, it is likely that endogenous Mal is also multiply tyrosine phosphorylated. The role of Tyr-106 in Mal signalling is therefore unclear, but may be required for another Mal-mediated signal. Future work will be required to examine this possibility.

It has also been determined that Mal interacts with the negative regulator SOCS-1, and that SOCS-1 mediates degradation of Mal. Knock-out studies have since confirmed that Mal degradation following LPS stimulation is SOCS-1 dependent. In this study, the protein levels of Mal in THP-1 cells were analysed following both LPS and MALP-2

stimulation up to 15 minutes. It has subsequently emerged that Mal degradation can be seen in these cells from 15 to 30 minutes after activation of TLR2 or TLR4 (Mansell *et al.* in press). In addition, it was shown that tyrosine phosphorylation of Mal was necessary for the SOCS-1-mediated degradation. Findings in this study determined that Mal undergoes degradation in mice at 5 minutes post-stimulation with LPS, and that in mice with a null mutation in the Btk gene, LPS-induced degradation of Mal does not occur. Taken together these results suggest that phosphorylation of Mal by Btk is likely to be required to recruit SOCS-1, which thereby results in Mal degradation.

It was however noted that SOCS-1 still associated with Mal-Y86F Y106F Y187F, it is not yet precisely clear how this interaction occurs, indeed Mal-Y86F Y106F Y187F may exist in a protein complex as opposed to interacting directly with SOCS-1. Therefore *in vitro* association studies in a cell free system must be conducted in order to determine if Mal-Y86F Y106F Y187F binds directly to SOCS-1. In addition, *in vivo* association studies analysing SOCS-1 interaction with endogenous tyrosine phosphorylated Mal following activation of the TLR2 or TLR4 signalling pathway would further confirm the requirement for tyrosine phosphorylation of Mal with respect to SOCS-1 association.

Recently other proteins in the TLR signalling family have been shown to undergo phosphorylation. It has been reported that following stimulation with their specific ligands TLR2, TLR3 and TLR4 all undergo tyrosine phosphorylation (Arbibe, Mira et al. 2000; Chen, Zuraw et al. 2003; Sarkar, Smith et al. 2003). In addition, LPS was found to induce tyrosine phosphorylation of MyD88 and it has been stated that upon overexpression, the adapters TRIF and TRAM are phosphorylated (Bin, Xu et al. 2003; Ojaniemi, Glumoff et al. 2003; Sato, Sugiyama et al. 2003). Whilst it has been

Chapter 7

References

Alexopoulou, L., A. C. Holt, et al. (2001). "Recognition of double-stranded RNA and activation of NF-kappaB by Toll-like receptor 3." Nature **413**(6857): 732-8.

Arbibe, L., J. P. Mira, et al. (2000). "Toll-like receptor 2-mediated NF-kappa B activation requires a Rac1-dependent pathway." Nat Immunol **1**(6): 533-40.

Arndt, P. G., N. Suzuki, et al. (2004). "Lipopolysaccharide-induced c-Jun NH2-terminal kinase activation in human neutrophils: role of phosphatidylinositol 3-Kinase and Syk-mediated pathways." J Biol Chem **279**(12): 10883-91.

Bin, L. H., L. G. Xu, et al. (2003). "TIRP, a novel Toll/interleukin-1 receptor (TIR) domain-containing adapter protein involved in TIR signaling." J Biol Chem **278**(27): 24526-32.

Bonnard, M., C. Mirtsos, et al. (2000). "Deficiency of T2K leads to apoptotic liver degeneration and impaired NF-kappaB-dependent gene transcription." Embo J **19**(18): 4976-85.

Born, T. L., E. Thomassen, et al. (1998). "Cloning of a novel receptor subunit, AcPL, required for interleukin-18 signaling." J Biol Chem **273**(45): 29445-50.

Bradley, L. A., A. K. Sweatman, et al. (1994). "Mutation detection in the X-linked agammaglobulinemia gene, BTK, using single strand conformation polymorphism analysis." Hum Mol Genet **3**(1): 79-83.

Brint, E. K., D. Xu, et al. (2004). "ST2 is an inhibitor of interleukin 1 receptor and Toll-like receptor 4 signaling and maintains endotoxin tolerance." Nat Immunol **5**(4): 373-9.

Burns, K., J. Clatworthy, et al. (2000). "Tollip, a new component of the IL-1RI pathway, links IRAK to the IL-1 receptor." Nat Cell Biol **2**(6): 346-51.

Burns, K., F. Martinon, et al. (1998). "MyD88, an adapter protein involved in interleukin-1 signaling." J Biol Chem **273**(20): 12203-9.

Cao, Z., W. J. Henzel, et al. (1996). "IRAK: a kinase associated with the interleukin-1 receptor." Science **271**(5252): 1128-31.

Cao, Z., J. Xiong, et al. (1996). "TRAF6 is a signal transducer for interleukin-1." Nature **383**(6599): 443-6.

Chen, L. Y., B. L. Zuraw, et al. (2003). "Involvement of protein tyrosine kinase in Toll-like receptor 4-mediated NF-kappa B activation in human peripheral blood monocytes." Am J Physiol Lung Cell Mol Physiol **284**(4): L607-13.

Chin, A. I., P. W. Dempsey, et al. (2002). "Involvement of receptor-interacting protein 2 in innate and adaptive immune responses." Nature **416**(6877): 190-4.

Chuang, T. H. and R. J. Ulevitch (2000). "Cloning and characterization of a sub-family of human toll-like receptors: hTLR7, hTLR8 and hTLR9." Eur Cytokine Netw **11**(3): 372-8.

Chuang, T. H. and R. J. Ulevitch (2004). "Triad3A, an E3 ubiquitin-protein ligase regulating Toll-like receptors." Nat Immunol **5**(5): 495-502.

Deng, L., C. Wang, et al. (2000). "Activation of the IkappaB kinase complex by TRAF6 requires a dimeric ubiquitin-conjugating enzyme complex and a unique polyubiquitin chain." Cell **103**(2): 351-61.

Diebold, S. S., T. Kaisho, et al. (2004). "Innate antiviral responses by means of TLR7-mediated recognition of single-stranded RNA." Science **303**(5663): 1529-31.

Doyle, S. L., C. A. Jefferies, et al. (2005). "Bruton's tyrosine kinase is involved in p65-mediated transactivation and phosphorylation of p65 on serine 536 during NFkappaB activation by lipopolysaccharide." J Biol Chem **280**(25): 23496-501.

Dunne, A., M. Ejdeback, et al. (2003). "Structural complementarity of Toll/interleukin-1 receptor domains in Toll-like receptors and the adaptors Mal and MyD88." J Biol Chem **278**(42): 41443-51.

Dunne, A. and L. A. O'Neill (2003). "The interleukin-1 receptor/Toll-like receptor superfamily: signal transduction during inflammation and host defense." Sci STKE **2003**(171): re3.

Dunne, A. and L. A. O'Neill (2005). "Adaptor usage and Toll-like receptor signaling specificity." FEBS Lett **579**(15): 3330-5.

Fitzgerald, K. A., E. M. Palsson-McDermott, et al. (2001). "Mal (MyD88-adapter-like) is required for Toll-like receptor-4 signal transduction." Nature **413**(6851): 78-83.

Fitzgerald, K. A., D. C. Rowe, et al. (2003). "LPS-TLR4 signaling to IRF-3/7 and NF-kappaB involves the toll adapters TRAM and TRIF." J Exp Med **198**(7): 1043-55.

Fitzgerald, K. A., S. M. McWhirter, et al. (2003). "IKKepsilon and TBK1 are essential components of the IRF3 signaling pathway." Nat Immunol **4**(5): 491-6.

Fruman, D. A., S. B. Snapper, et al. (1999). "Phosphoinositide 3-kinase knockout mice: role of p85alpha in B cell development and proliferation." Biochem Soc Trans **27**(4): 624-9.

Fry, M. J. (1994). "Structure, regulation and function of phosphoinositide 3-kinases." Biochim Biophys Acta **1226**(3): 237-68.

Fukao, T., M. Tanabe, et al. (2002). "PI3K-mediated negative feedback regulation of IL-12 production in DCs." Nat Immunol **3**(9): 875-81.

Goh, K. C., M. J. deVeer, et al. (2000). "The protein kinase PKR is required for p38 MAPK activation and the innate immune response to bacterial endotoxin." Embo J **19**(16): 4292-7.

Greene, C. and L. O'Neill (1999). "Interleukin-1 receptor-associated kinase and TRAF-6 mediate the transcriptional regulation of interleukin-2 by interleukin-1 via NFkappaB but unlike interleukin-1 are unable to stabilise interleukin-2 mRNA." Biochim Biophys Acta **1451**(1): 109-21.

Greenfeder, S. A., P. Nunes, et al. (1995). "Molecular cloning and characterization of a second subunit of the interleukin 1 receptor complex." J Biol Chem **270**(23): 13757-65.

Hashimoto, C., K. L. Hudson, et al. (1988). "The Toll gene of Drosophila, required for dorsal-ventral embryonic polarity, appears to encode a transmembrane protein." Cell **52**(2): 269-79.

Hayashi, F., K. D. Smith, et al. (2001). "The innate immune response to bacterial flagellin is mediated by Toll-like receptor 5." Nature **410**(6832): 1099-103.

Heil, F., H. Hemmi, et al. (2004). "Species-specific recognition of single-stranded RNA via toll-like receptor 7 and 8." Science **303**(5663): 1526-9.

Hemmi, H., T. Kaisho, et al. (2002). "Small anti-viral compounds activate immune cells via the TLR7 MyD88-dependent signaling pathway." Nat Immunol **3**(2): 196-200.

Hemmi, H., O. Takeuchi, et al. (2000). "A Toll-like receptor recognizes bacterial DNA." Nature **408**(6813): 740-5.

Horng, T., G. M. Barton, et al. (2002). "The adaptor molecule TIRAP provides signalling specificity for Toll-like receptors." Nature **420**(6913): 329-33.

Horng, T., G. M. Barton, et al. (2001). "TIRAP: an adapter molecule in the Toll signaling pathway." Nat Immunol **2**(9): 835-41.

Horwood, N. J., T. Mahon, et al. (2003). "Bruton's tyrosine kinase is required for lipopolysaccharide-induced tumor necrosis factor alpha production." J Exp Med **197**(12): 1603-11.

Hsu, H., J. Huang, et al. (1996). "TNF-dependent recruitment of the protein kinase RIP to the TNF receptor-1 signaling complex." Immunity **4**(4): 387-96.

Hsu, L. C., J. M. Park, et al. (2004). "The protein kinase PKR is required for macrophage apoptosis after activation of Toll-like receptor 4." Nature **428**(6980): 341-5.

Huang, J., X. Gao, et al. (1997). "Recruitment of IRAK to the interleukin 1 receptor complex requires interleukin 1 receptor accessory protein." Proc Natl Acad Sci U S A **94**(24): 12829-32.

Iwami, K. I., T. Matsuguchi, et al. (2000). "Cutting edge: naturally occurring soluble form of mouse Toll-like receptor 4 inhibits lipopolysaccharide signaling." J Immunol **165**(12): 6682-6.

Jack, R. S., X. Fan, et al. (1997). "Lipopolysaccharide-binding protein is required to combat a murine gram-negative bacterial infection." Nature **389**(6652): 742-5.

Janssens, S., K. Burns, et al. (2002). "Regulation of interleukin-1- and lipopolysaccharide-induced NF-kappaB activation by alternative splicing of MyD88." Curr Biol **12**(6): 467-71.

Jefferies, C. A., S. Doyle, et al. (2003). "Bruton's tyrosine kinase is a Toll/interleukin-1 receptor domain-binding protein that participates in nuclear factor kappaB activation by Toll-like receptor 4." J Biol Chem **278**(28): 26258-64.

Jiang, Z., J. Ninomiya-Tsuji, et al. (2002). "Interleukin-1 (IL-1) receptor-associated kinase-dependent IL-1-induced signaling complexes phosphorylate TAK1 and TAB2 at the plasma membrane and activate TAK1 in the cytosol." Mol Cell Biol **22**(20): 7158-67.

Karin, M. and Y. Ben-Neriah (2000). "Phosphorylation meets ubiquitination: the control of NF-[kappa]B activity." Annu Rev Immunol **18**: 621-63.

Kasof, G. M., J. C. Prosser, et al. (2000). "The RIP-like kinase, RIP3, induces apoptosis and NF-kappaB nuclear translocation and localizes to mitochondria." FEBS Lett **473**(3): 285-91.

Kinjyo, I., T. Hanada, et al. (2002). "SOCS1/JAB is a negative regulator of LPS-induced macrophage activation." Immunity **17**(5): 583-91.

Klemenz, R., S. Hoffmann, et al. (1989). "Serum- and oncoprotein-mediated induction of a gene with sequence similarity to the gene encoding carcinoembryonic antigen." Proc Natl Acad Sci U S A **86**(15): 5708-12.

Kollewe, C., A. C. Mackensen, et al. (2004). "Sequential autophosphorylation steps in the interleukin-1 receptor-associated kinase-1 regulate its availability as an adapter in interleukin-1 signaling." J Biol Chem **279**(7): 5227-36.

Kurosaki, T. and M. Kurosaki (1997). "Transphosphorylation of Bruton's tyrosine kinase on tyrosine 551 is critical for B cell antigen receptor function." J Biol Chem **272**(25): 15595-8.

Larsen, L. and C. Ropke (2002). "Suppressors of cytokine signalling: SOCS." Apmis **110**(12): 833-44.

LeBouder, E., J. E. Rey-Nores, et al. (2003). "Soluble forms of Toll-like receptor (TLR)2 capable of modulating TLR2 signaling are present in human plasma and breast milk." J Immunol **171**(12): 6680-9.

Leevers, S. J., B. Vanhaesebroeck, et al. (1999). "Signalling through phosphoinositide 3-kinases: the lipids take centre stage." Curr Opin Cell Biol **11**(2): 219-25.

Lemaitre, B., E. Nicolas, et al. (1996). "The dorsoventral regulatory gene cassette spatzle/Toll/cactus controls the potent antifungal response in Drosophila adults." Cell **86**(6): 973-83.

Li, S., A. Strelow, et al. (2002). "IRAK-4: a novel member of the IRAK family with the properties of an IRAK-kinase." Proc Natl Acad Sci U S A **99**(8): 5567-72.

Li, X., M. Commane, et al. (1999). "Mutant cells that do not respond to interleukin-1 (IL-1) reveal a novel role for IL-1 receptor-associated kinase." Mol Cell Biol **19**(7): 4643-52.

Liberati, N. T., K. A. Fitzgerald, et al. (2004). "Requirement for a conserved Toll/interleukin-1 resistance domain protein in the Caenorhabditis elegans immune response." Proc Natl Acad Sci U S A **101**(17): 6593-8.

Liew, F. Y., D. Xu, et al. (2005). "Negative regulation of toll-like receptor-mediated immune responses." Nat Rev Immunol **5**(6): 446-58.

Liu, W., I. Quinto, et al. (2001). "Direct inhibition of Bruton's tyrosine kinase by IBtk, a Btk-binding protein." Nat Immunol **2**(10): 939-46.

Lord, K. A., B. Hoffman-Liebermann, et al. (1990). "Nucleotide sequence and expression of a cDNA encoding MyD88, a novel myeloid differentiation primary response gene induced by IL6." Oncogene **5**(7): 1095-7.

Malinin, N. L., M. P. Boldin, et al. (1997). "MAP3K-related kinase involved in NF-kappaB induction by TNF, CD95 and IL-1." Nature **385**(6616): 540-4.

Mansell, A., E. Brint, et al. (2004). "Mal interacts with tumor necrosis factor receptor-associated factor (TRAF)-6 to mediate NF-kappaB activation by toll-like receptor (TLR)-2 and TLR4." J Biol Chem **279**(36): 37227-30.

Marquez, J. A., C. I. Smith, et al. (2003). "Conformation of full-length Bruton tyrosine kinase (Btk) from synchrotron X-ray solution scattering." Embo J **22**(18): 4616-24.

Marquez, J. A. e. a. (2003). "Confirmation of full-length Btk from synchrotron X-ray solution scattering." Embo J **22**(18): 4616-24.

Medzhitov, R., P. Preston-Hurlburt, et al. (1997). "A human homologue of the Drosophila Toll protein signals activation of adaptive immunity." Nature **388**(6640): 394-7.

Meng, F. and C. A. Lowell (1997). "Lipopolysaccharide (LPS)-induced macrophage activation and signal transduction in the absence of Src-family kinases Hck, Fgr, and Lyn." J Exp Med **185**(9): 1661-70.

Mercurio, F., H. Zhu, et al. (1997). "IKK-1 and IKK-2: cytokine-activated IkappaB kinases essential for NF-kappaB activation." Science **278**(5339): 860-6.

Meylan, E. and J. Tschopp (2005). "The RIP kinases: crucial integrators of cellular stress." Trends Biochem Sci **30**(3): 151-9.

Mink, M., B. Fogelgren, et al. (2001). "A novel human gene (SARM) at chromosome 17q11 encodes a protein with a SAM motif and structural similarity to Armadillo/beta-catenin that is conserved in mouse, Drosophila, and Caenorhabditis elegans." Genomics **74**(2): 234-44.

Mitcham, J. L., P. Parnet, et al. (1996). "T1/ST2 signaling establishes it as a member of an expanding interleukin-1 receptor family." J Biol Chem **271**(10): 5777-83.

Mukhopadhyay, S., M. Mohanty, et al. (2002). "Macrophage effector functions controlled by Bruton's tyrosine kinase are more crucial than the cytokine balance of T cell responses for microfilarial clearance." J Immunol **168**(6): 2914-21.

Muzio, M., N. Polntarutti, et al. (2000). "Toll like receptor family (TLT) and signalling pathway." Eur Cytokine Netw **11**(3): 489-90.

Naiki, Y., K. S. Michelsen, et al. (2004). "TGF-beta differentially inhibits MyD88-dependent but not TRIF-dependent LPS-induced TLR4 signaling." J Biol Chem.

Nakagawa, R., T. Naka, et al. (2002). "SOCS-1 participates in negative regulation of LPS responses." Immunity **17**(5): 677-87.

Napolitani, G., N. Bortoletto, et al. (2003). "Activation of src-family tyrosine kinases by LPS regulates cytokine production in dendritic cells by controlling AP-1 formation." Eur J Immunol **33**(10): 2832-41.

Ojaniemi, M., V. Glumoff, et al. (2003). "Phosphatidylinositol 3-kinase is involved in Toll-like receptor 4-mediated cytokine expression in mouse macrophages." Eur J Immunol **33**(3): 597-605.

O'Neill, L. A., K. A. Fitzgerald, et al. (2003). "The Toll-IL-1 receptor adaptor family grows to five members." Trends Immunol **24**(6): 286-90.

Oshiumi, H., M. Matsumoto, et al. (2003). "TICAM-1, an adaptor molecule that participates in Toll-like receptor 3-mediated interferon-beta induction." Nat Immunol **4**(2): 161-7.

Oshiumi, H., M. Sasai, et al. (2003). "TICAM-2: a bridging adapter recruiting to Toll-like receptor 4 TICAM-1 that induces interferon-beta." J Biol Chem.

Park, H., M. I. Wahl, et al. (1996). "Regulation of Btk function by a major autophosphorylation site within the SH3 domain." Immunity **4**(5): 515-25.

Parnet, P., K. E. Garka, et al. (1996). "IL-1Rrp is a novel receptor-like molecule similar to the type I interleukin-1 receptor and its homologues T1/ST2 and IL-1R AcP." J Biol Chem **271**(8): 3967-70.

Pazdernik, N. J., D. B. Donner, et al. (1999). "Mouse receptor interacting protein 3 does not contain a caspase-recruiting or a death domain but induces apoptosis and activates NF-kappaB." Mol Cell Biol **19**(10): 6500-8.

Peters, R. T. and T. Maniatis (2001). "A new family of IKK-related kinases may function as I kappa B kinase kinases." Biochim Biophys Acta **1471**(2): M57-62.

Poltorak, A., X. He, et al. (1998). "Defective LPS signaling in C3H/HeJ and C57BL/10ScCr mice: mutations in Tlr4 gene." Science **282**(5396): 2085-8.

Qureshi, S. T., L. Lariviere, et al. (1999). "Endotoxin-tolerant mice have mutations in Toll-like receptor 4 (Tlr4)." J Exp Med **189**(4): 615-25.

Rawlings, D. J. (1999). "Bruton's tyrosine kinase controls a sustained calcium signal essential for B lineage development and function." Clin Immunol **91**(3): 243-53.

Regnier, C. H., H. Y. Song, et al. (1997). "Identification and characterization of an IkappaB kinase." Cell **90**(2): 373-83.

Rock, F. L., G. Hardiman, et al. (1998). "A family of human receptors structurally related to Drosophila Toll." Proc Natl Acad Sci U S A **95**(2): 588-93.

Sarkar, S. N., H. L. Smith, et al. (2003). "Double-stranded RNA signaling by Toll-like receptor 3 requires specific tyrosine residues in its cytoplasmic domain." J Biol Chem **278**(7): 4393-6.

Sato, S., M. Sugiyama, et al. (2003). "Toll/IL-1 receptor domain-containing adaptor inducing IFN-beta (TRIF) associates with TNF receptor-associated factor 6 and TANK-binding kinase 1, and activates two distinct transcription factors, NF-kappa B and IFN-regulatory factor-3, in the Toll-like receptor signaling." J Immunol **171**(8): 4304-10.

Schumann, R. R., S. R. Leong, et al. (1990). "Structure and function of lipopolysaccharide binding protein." Science **249**(4975): 1429-31.

Sharma, S., B. R. tenOever, et al. (2003). "Triggering the interferon antiviral response through an IKK-related pathway." Science **300**(5622): 1148-51.

Shimada, T., T. Kawai, et al. (1999). "IKK-i, a novel lipopolysaccharide-inducible kinase that is related to IkappaB kinases." Int Immunol **11**(8): 1357-62.

Sims, J. E., C. J. March, et al. (1988). "cDNA expression cloning of the IL-1 receptor, a member of the immunoglobulin superfamily." Science **241**(4865): 585-9.

Starr, R., T. A. Willson, et al. (1997). "A family of cytokine-inducible inhibitors of signalling." Nature **387**(6636): 917-21.

Stefanova, I., M. L. Corcoran, et al. (1993). "Lipopolysaccharide induces activation of CD14-associated protein tyrosine kinase p53/56lyn." J Biol Chem **268**(28): 20725-8.

Stein, D. S. and L. M. Stevens (1991). "Establishment of dorsal-ventral and terminal pattern in the Drosophila embryo." Curr Opin Genet Dev **1**(2): 247-54.

Steinman, R. M. (2003). "Some interfaces of dendritic cell biology." Apmis **111**(7-8): 675-97.

Strelow, A., C. Kollewe, et al. (2003). "Characterization of Pellino2, a substrate of IRAK1 and IRAK4." FEBS Lett **547**(1-3): 157-61.

Sun, X., J. Lee, et al. (1999). "RIP3, a novel apoptosis-inducing kinase." J Biol Chem **274**(24): 16871-5.

Sun, X., J. Yin, et al. (2002). "Identification of a novel homotypic interaction motif required for the phosphorylation of receptor-interacting protein (RIP) by RIP3." J Biol Chem **277**(11): 9505-11.

Suzuki, H., Y. Terauchi, et al. (1999). "Xid-like immunodeficiency in mice with disruption of the p85alpha subunit of phosphoinositide 3-kinase." Science **283**(5400): 390-2.

Suzuki, N., S. Suzuki, et al. (2002). "Severe impairment of interleukin-1 and Toll-like receptor signalling in mice lacking IRAK-4." Nature **416**(6882): 750-6.

Suzuki, N., S. Suzuki, et al. (2003). "IL-1R-associated kinase 4 is required for lipopolysaccharide-induced activation of APC." J Immunol **171**(11): 6065-71.

Swantek, J. L., M. F. Tsen, et al. (2000). "IL-1 receptor-associated kinase modulates host responsiveness to endotoxin." J Immunol **164**(8): 4301-6.

Takeda, K. and S. Akira (2005). "Toll-like receptors in innate immunity." Int Immunol **17**(1): 1-14.

Takeda, K., O. Takeuchi, et al. (2002). "Recognition of lipopeptides by Toll-like receptors." J Endotoxin Res **8**(6): 459-63.

Takeuchi, O., K. Hoshino, et al. (1999). "Differential roles of TLR2 and TLR4 in recognition of gram-negative and gram-positive bacterial cell wall components." Immunity **11**(4): 443-51.

Takeuchi, O., T. Kawai, et al. (2001). "Discrimination of bacterial lipoproteins by Toll-like receptor 6." Int Immunol **13**(7): 933-40.

Thomas, J. A., J. L. Allen, et al. (1999). "Impaired cytokine signaling in mice lacking the IL-1 receptor-associated kinase." J Immunol **163**(2): 978-84.

Thomassen, E., B. R. Renshaw, et al. (1999). "Identification and characterization of SIGIRR, a molecule representing a novel subtype of the IL-1R superfamily." Cytokine **11**(6): 389-99.

Ting, A. T., F. X. Pimentel-Muinos, et al. (1996). "RIP mediates tumor necrosis factor receptor 1 activation of NF-kappaB but not Fas/APO-1-initiated apoptosis." Embo J **15**(22): 6189-96.

Tominaga, S. (1989). "A putative protein of a growth specific cDNA from BALB/c-3T3 cells is highly similar to the extracellular portion of mouse interleukin 1 receptor." FEBS Lett **258**(2): 301-4.

Torigoe, K., S. Ushio, et al. (1997). "Purification and characterization of the human interleukin-18 receptor." J Biol Chem **272**(41): 25737-42.

Travassos, L. H., S. E. Girardin, et al. (2004). "Toll-like receptor 2-dependent bacterial sensing does not occur via peptidoglycan recognition." EMBO Rep **5**(10): 1000-6.

Trinchieri, G. (2003). "Interleukin-12 and the regulation of innate resistance and adaptive immunity." Nat Rev Immunol **3**(2): 133-46

Uematsu, S., S. Sato, et al. (2005). "Interleukin-1 receptor-associated kinase-1 plays an essential role for Toll-like receptor (TLR)7- and TLR9-mediated interferon-{alpha} induction." J Exp Med **201**(6): 915-23.

Vogel, S. N., K. A. Fitzgerald, et al. (2003). "TLRs: differential adapter utilization by toll-like receptors mediates TLR-specific patterns of gene expression." Mol Interv **3**(8): 466-77.

Weinstein, S. L., M. R. Gold, et al. (1991). "Bacterial lipopolysaccharide stimulates protein tyrosine phosphorylation in macrophages." Proc Natl Acad Sci U S A **88**(10): 4148-52.

Werenskiold, A. K., S. Hoffmann, et al. (1989). "Induction of a mitogen-responsive gene after expression of the Ha-ras oncogene in NIH 3T3 fibroblasts." Mol Cell Biol **9**(11): 5207-14.

Wesche, H., W. J. Henzel, et al. (1997). "MyD88: an adapter that recruits IRAK to the IL-1 receptor complex." Immunity **7**(6): 837-47.

Wurfel, M. M. and S. D. Wright (1997). "Lipopolysaccharide-binding protein and soluble CD14 transfer lipopolysaccharide to phospholipid bilayers: preferential interaction with particular classes of lipid." J Immunol **158**(8): 3925-34.

Yamamoto, M., S. Sato, et al. (2003). "Role of adaptor TRIF in the MyD88-independent toll-like receptor signaling pathway." Science **301**(5633): 640-3.

Yamamoto, M., S. Sato, et al. (2002). "Essential role for TIRAP in activation of the signalling cascade shared by TLR2 and TLR4." Nature **420**(6913): 324-9.

Yamamoto, M., S. Sato, et al. (2003). "TRAM is specifically involved in the Toll-like receptor 4-mediated MyD88-independent signaling pathway." Nat Immunol **4**(11): 1144-50.

Yamamoto, M., S. Sato, et al. (2002). "Cutting edge: a novel Toll/IL-1 receptor domain-containing adapter that preferentially activates the IFN-beta promoter in the Toll-like receptor signaling." J Immunol **169**(12): 6668-72.

Yang, E. J., J. H. Yoon, et al. (2004). "Bruton's tyrosine kinase phosphorylates cAMP-responsive element-binding protein at serine 133 during neuronal differentiation in immortalized hippocampal progenitor cells." J Biol Chem **279**(3): 1827-37.

Yang, W. and S. Desiderio (1997). "BAP-135, a target for Bruton's tyrosine kinase in response to B cell receptor engagement." Proc Natl Acad Sci U S A **94**(2): 604-9.

Yu, B. and S. D. Wright (1996). "Catalytic properties of lipopolysaccharide (LPS) binding protein. Transfer of LPS to soluble CD14." J Biol Chem **271**(8): 4100-5.

Yu, P. W., B. C. Huang, et al. (1999). "Identification of RIP3, a RIP-like kinase that activates apoptosis and NFkappaB." Curr Biol **9**(10): 539-42.

Zhang, D., G. Zhang, et al. (2004). "A toll-like receptor that prevents infection by uropathogenic bacteria." Science **303**(5663): 1522-6.

Ziegler, S. F., C. B. Wilson, et al. (1988). "Augmented expression of a myeloid-specific protein tyrosine kinase gene (hck) after macrophage activation." J Exp Med **168**(5): 1801-10.

MyD88 adapter-like (Mal) is Phosphorylated by Bruton's tyrosine kinase during TLR2 and TLR4 signal transduction*

Pearl Gray, Aisling Dunne, Constantinos Brikos, Caroline A. Jefferies, Sarah L. Doyle, Luke A.J. O'Neill

From the School of Biochemistry and Immunology, Trinity College Dublin, Dublin 2, Ireland

Running Title: MyD88 adapter-like (Mal) is Phosphorylated by Bruton's Tyrosine Kinase

Address correspondence to: Luke A.J. O'Neill, School of Biochemistry and Immunology, Trinity College Dublin, Dublin 2, Ireland, Tel. 353-1-6082439; Fax. 353-1-6772400; E-mail: laoneill@tcd.ie

Members of the Toll-like receptor (TLR) family are essential players in activating the host innate immune response against infectious microorganisms. All TLRs signal through Toll/IL-1 receptor (TIR) domain-containing adapter proteins. MyD88 adapter-like (Mal) is one such adapter, which specifically is involved in TLR-2 and TLR-4 signaling. When overexpressed we have found that Mal undergoes tyrosine phosphorylation. Three possible phospho-accepting tyrosines were identified at positions 86, 106 and 187, and two mutant forms of Mal in which tyrosines 86 and 187 were mutated to phenylalanine acted as dominant negative inhibitors of NF-κB activation by LPS. Activation of THP-1 monocytic cells with the TLR4 agonist lipopolysaccharide (LPS) and the TLR2 agonist, macrophage activating lipopeptide-2 (MALP-2), induced phosphorylation of Mal on tyrosine residues. We found that the Bruton's tyrosine kinase (Btk) inhibitor LFM-A13 could block the endogenous phosphorylation of Mal on tyrosine in cells treated with MALP-2 or LPS. Furthermore Btk immunoprecipitated from THP-1 cells activated by LPS could phosphorylate Mal. Our study therefore provides the first demonstration of the key role of Mal phosphorylation on tyrosine during signaling by TLR2 and TLR4 and identifies a novel function for Btk as the kinase involved.

The primary role of the Toll-like receptor (TLR)[1] family is to recognise and signal the influx of invading pathogens, thereby activating the host innate immune response. Ten TLRs have been discovered in humans, and all have a conserved cytosolic domain termed the Toll/interleukin-1 receptor (TIR) domain, which mediates signaling by TLRs (1). Once the TLRs are activated by their respective agonists, receptor dimerization *via* the TIR domain is thought to occur. This leads to recruitment of cytosolic TIR domain-containing adapter proteins (1). Although TLRs have similar signal transduction pathways, recent evidence has emerged suggesting specificity with regard to recruitment of the adapters. The prototype TIR-containing adapter protein, MyD88, is recruited by all TLRs with the exception of the double stranded RNA (dsRNA) receptor, TLR3 (2). MyD88 adapter-like (Mal) participates solely in TLR2 and TLR4 signal transduction where it may act as a bridging adapter for MyD88 recruitment (3-6). Evidence has shown that the absence of either MyD88 or Mal results in no TNF production and delayed activation of the transcription factor NF-κB in response to the respective TLR2 and TLR4 ligands macrophage activating lipopeptide-2 (MALP-2) and lipopolysaccharide (LPS) (5-8). Similar to Mal, TIR domain-containing adapter inducing interferon (TRIF) and TRIF-related adapter molecule (TRAM) are selective adapters, with TRIF mediating TLR3 and TLR4 signaling, while TRAM is essential for TLR4 signaling alone (9-13). It has been determined that TRIF and TRAM mediate activation of another transcription factor termed interferon regulatory factor 3 (IRF3) in addition to NF-κB.

Several serine/threonine protein kinases are activated during TLR signal transduction. Mal and MyD88 recruitment leads to the subsequent recruitment and activation of IL-1 receptor-associated kinase 4 (IRAK4), which in turn activates IRAK1 (14). TNF receptor associated factor-6 (TRAF-6) is then recruited leading to activation of TGF-β-activated kinase (TAK-1) (15). TAK-1 then activates the IκB kinase (IKK)

complex leading to NF-κB activation (16). TAK-1 can also activate the upstream kinases, p38 mitogen-activated protein kinase (MAP kinase) and Jun-N-terminal kinase (JNK). TRAM and TRIF recruitment leads to the activation of the kinase receptor interacting protein (RIP)-1, which engages with the IKK complex (17). Both TRAM and TRIF can also interact with TANK-binding kinase-1 (TBK1), which phosphorylates and activates IRF-3 (18,19).

Regarding tyrosine kinase activation by TLRs, LPS has been shown to activate the tyrosine kinases Src, Hck and Lyn, although their role in LPS signaling is somewhat uncertain (20,21). Most recently we and others have shown that Bruton's tyrosine kinase (Btk), a member of the Tec family of protein tyrosine kinases, is a component of the TLR signaling pathway (22,23). In particular, it has been shown that Btk interacts with the TIR domains of TLRs 4, 6, 8 and 9 and was also found to specifically associate with MyD88, Mal and IRAK1 (22,24). LPS induces tyrosine phosphorylation of Btk and activates its kinase activity, and monocytes from patients with X-linked agammaglobulinemia, which contain mutant Btk, are unresponsive to LPS (24).

A limited number of proteins have been shown to undergo tyrosine phosphorylation during TLR signaling. To date it has been reported that MyD88, TLR2, TLR3 and TLR4 become tyrosine phosphorylated during activation (25-27). In this study, we report that Mal is tyrosine phosphorylated during TLR2 and TLR4 signaling. We demonstrate that the tyrosine residue located at position 86, 106 and 187 are likely to be phospho-accepting residues and that mutant forms of Mal in which Tyr 86 or Tyr 187 are substituted with phenylalanine act as dominant negative inhibitors of LPS signaling. Finally, we identify Btk as the responsible tyrosine kinase. Mal is therefore the first substrate for Btk in TLR signaling to be identified, its phosphorylation by Btk being an important mechanism in signaling by TLR2 and TLR4.

Materials and Methods

Biological Reagents and Cell Culture - The HEK293 cell line was cultured in DMEM medium, while the human monocytic THP 1 cell line was cultured in RPMI 1640 medium, supplemented with 10% (v/v) fetal calf serum. HEK293 cells stably expressing FLAG-tagged TLR4 were a generous gift from D. Golenbock (UMASS Medical School). Expression vectors encoding HA-Mal have been described elsewhere (28). The plasmid encoding the chimeric CD4-TLR4 was a kind gift from R. Medzhitov (Yale University School of Medicine). The NF-κB luciferase plasmid was a kind gift from R. Hofmeister (Universitaet Regensburg, Regensburg, Germany). The Btk specific inhibitor, LFM-A13, was obtained from Calbiochem (Nottingham, United Kingdom). The anti-Mal antibody (Pearl-1) was obtained from Alexis Biochemicals. All other reagents were obtained from Sigma (Poole, United Kingdom).

Immunoprecipitation and GST Pulldown Assays - HEK293 cells (1×10^6 cells) were harvested 24 h post-transfection, lysis, immunoprecipitation and GST pull-down assays were prepared as described elsewhere(22). For immunoprecipitation of phospho-Mal, cell lysates were incubated with anti-phosphotyrosine-agarose clone PT-66 overnight. After incubation, beads were washed and the tyrosine phosphorylation status of Mal was analysed by immunblotting with a Mal antibody.

Phosphatase Treatment - Immune complexes were incubated with 100U of calf intestinal alkaline phosphatase (CIP) with 30 µl of the phosphatase digestion buffer (50 mM Tris-Cl, pH 7.5, 1 mM $MgCl_2$). Samples were incubated at 37°C for 3 hours. For protein tyrosine phosphatase-1B (PTP-1B) treatment, the immune complexes were incubated with the phosphatase digestion buffer (50 mM imidazole, pH 7.5) at 37°C for 30 minutes with 10 U of PTP-1B.

In vitro Kinase Assays - Immune complexes were incubated with 30 µl of kinase buffer (20 mM Hepes, pH 7.5, 2 mM DTT, 10 mM $MgCl_2$, 50 mM NaCl, 100 µM Na_3VO_4 and 20 mM β-glycerolphosphate and protease inhibitors) containing 2 µCi [γ-^{32}P] ATP and 0.6 µM of non-radioactive ATP. Samples were then incubated at 37°C for 30 minutes. Gels were transferred onto PVDF membranes and visualised by autoradiography.

Reporter Assays - HEK293 cells (2×10^4) were transfected with 5x NF-κB luciferase reporter gene plasmid and co-transfected with expression vectors using GeneJuice (Novagen). In all cases,

40 ng/well of phRL-TK reporter gene was co-transfected to normalise data for transfection efficiency. After 24 h, reporter gene activity was measured as described elsewhere (22). Data are expressed as the mean fold induction ± SD relative to control levels, for a representative experiment from a minimum of three separate experiments, each performed in triplicate.

Two-dimensional electrophoresis of Mal - Immunoprecipitations were performed as described above and immune complexes were resuspended in 400 µl of sample solubilisation solution (8 M Urea, 50 mM DTT, 4% CHAPS, 0.2% carrier ampholytes, 0.0002% bromophenol blue). Immunoprecipitates were separated in the first dimension by isoelectric focusing performed using precast IPG strips (Immobiline™ DryStrip gels, Amersham Pharmacia Biotech), pH 4-7. Focused proteins were separated in the second dimension by SDS-PAGE.

Modelling Studies - Modelling of the TIR domain of Mal was carried out as described previously (28).

RESULTS

Mal is Tyrosine Phosphorylated - In our first analysis of Mal, we had observed in HEK293 cells transfected with a plasmid encoding Mal, that in addition to the predominant 32 kDa form, slower migrating forms of Mal could be detected following SDS-PAGE, suggesting that Mal may be covalently modified (3). As the isoelectric point of a protein is always altered once phosphorylation occurs, we examined the electrophoretic mobility of Mal by two dimensional gel analysis. As we had observed previously, one-dimensional SDS-PAGE analysis revealed three distinct bands (Fig. 1a, left panel); whilst upon two-dimensional SDS-PAGE analysis two forms of Mal were detected by immunoblotting (Fig. 1a, right panel). We observed that the slower migrating form of Mal had a lower isoelectric point than the predominant 32 kDa form, and is most likely an unresolved mixture of the two slower migrating forms detected on one-dimensional SDS-PAGE analysis. To further investigate the phosphorylation status of Mal, we treated immunoprecipitated Mal isolated from HEK293 cells overexpressing HA-Mal with calf intestinal phosphatase (CIP), which can remove phosphates from serine, threonine and tyrosine residues (29). Treatment of Mal with CIP converted the slower migrating forms into the predominant 32 kDa form (Fig. 1b, lane 2), an effect that was blocked by the addition of phosphatase inhibitors (Fig. 1b, lane 1), indicating that the slower migrating forms represent phosphorylated Mal. To confirm that Mal could incorporate phosphate we carried out an *in vitro* kinase assay. As can be seen in Fig. 1c, lane 1, GST-Mal becomes phosphorylated by interacting with kinases in the lysate. GST alone is not phosphorylated (Fig. 1c, lanes 2 and 4) and Mal does not undergo autophosphorylation (Fig. 1c, lane 3).

In order to further define the particular phospho-accepting sites in Mal we treated immunoprecipitated Mal isolated from HEK293 cells overexpressing HA-Mal with PTP-1B, a phosphatase that specifically dephosphorylates phosphotyrosine residues. The slower migrating form of Mal was eliminated following phosphatase treatment indicating that Mal is tyrosine phosphorylated (Fig. 1d, compare lane 2 to lane 1). To further confirm that Mal was tyrosine phosphorylated, immunoprecipitated Mal isolated from HEK293 cells overexpressing HA-Mal was resolved by SDS-PAGE and immunoblotted with a phosphotyrosine-specific antibody (Fig. 1e, lane 2).

Identification of Tyr-86, Tyr-106 and Tyr-187 as possible phospho-acceptors –Human Mal contains six tyrosine residues, all of which are conserved in the mouse sequence, attesting to their possible importance in the functioning of Mal (Fig. 2a). One tyrosine, Tyr-86 is a conserved residue among all TIR domain-containing proteins, and is located within Box 1, the signature sequence of the TIR domain. Tyr-106 is situated between Box 1 and Box 2, whereas the remaining four other tyrosine residues at positions 159, 187, 195 and 196 are located distally to Box 2. In order to examine the role of these tyrosine residues in Mal phosphorylation, we mutated the six tyrosine residues conservatively to phenylalanine and analysed the mobility pattern of the Mal tyrosine mutants. Interestingly, we found that the slowest migrating form of wild-type Mal was no longer evident in Mal-Y86F, Mal-Y106F or Mal-Y187F (Fig. 2b, lanes 2, 3 and 5). The mutant proteins Y159F, Y195F or Y196F retained the same electrophoretic mobility pattern as wild-type Mal

(Fig. 2b, lanes 4, 6 and 7). These results suggested that the tyrosine residues located at positions 86, 106 and 187 were potential phosphorylation sites with all three tyrosine residues requiring phosphorylation for the altered mobility of Mal on SDS-PAGE. This was also apparent from the analysis of a triple mutant of these amino acids, Mal-Y86F Y106F Y187F, which gave the same expression profile as the single mutants (Fig. 2b, lane 8).

In order to assess the requirement for the tyrosine residues in Mal mediated NF-κB activation, Mal mutant proteins were overexpressed in HEK293 cells in conjunction with an NF-κB-dependent luciferase reporter gene. In agreement with published results (3,4), wild-type Mal strongly activated NF-κB (Fig. 2c). In contrast, the Mal mutant proteins Y86F, Y106F, Y187F were less active with Mal-Y86F and Mal-Y106F particularly impaired. Analysis of the ability of the triple mutant of Mal to activate NF-κB further confirmed that Tyr-86, Tyr-106 and Tyr-187 are critical residues for NF-κB activity induced by Mal. Mal-Y159F, Mal-Y195F or Mal-Y196F activated NF-κB to a similar level as wild-type Mal (Fig. 2c). These results imply that it is Mal phosphorylated on Tyr-86, Tyr-106 and Tyr-187 that is the active form of Mal when overexpressed.

We next analysed a molecular model of the TIR domain of Mal, which we had previously constructed (28), to determine the location of Tyr-86, Tyr-106 and Tyr-187. We noted that both Tyr-86 and Tyr-106 appear to be surface exposed, whereas Tyr-187, just visible on the surface model, appears to be the least accessible (Fig. 2d). It has been reported that the backbone of the TIR domain is similar to that of CheY, a bacterial chemotaxis protein (30). Studies have shown that CheY undergoes phosphorylation, and that this phosphorylation event triggers a conformational change, thereby regulating its association with other proteins (31). It is possible that phosphorylation of Mal on Tyr-86 or Tyr-106 is required to initiate a conformational change in the TIR domain of Mal, thereby exposing Tyr-187 for phosphorylation, leading to activation of downstream signals.

We next tested whether Mal-Y86F, Mal-Y106F or Mal-Y187F could have a dominant negative effect in LPS signaling. As has been previously shown (3,4), a mutant form of Mal in which proline 125 in Box 2 of the TIR domain is mutated to histidine (P125H) strongly inhibited activation of NF-κB mediated by TLR4 (Fig. 2e). Interestingly, activation of NF-κB mediated by LPS was also strongly inhibited by Mal-Y86F, suggesting that this tyrosine residue is critical for efficient TLR4 signaling (Fig. 2e). Mal-Y187F also blocked the LPS response albeit to a lesser degree. LPS could still stimulate NF-κB activation in cells expressing Mal-Y106F. Similar to Mal-P125H, the triple mutant, Mal-Y86F Y106F Y187F, severely inhibited NF-κB activation mediated by LPS. The Mal mutant proteins Y159F, Y195F and Y196F were strongly active when overexpressed and LPS treatment had no major influence on their effect. These results suggest that phosphorylation of Mal on Tyr-86 and Tyr-187 is required for Mal to signal NF-κB activation since these mutant forms inhibited the LPS response.

Phosphorylation of Mal by Btk - We next examined the tyrosine phosphorylation status of endogenous Mal in the human monocytic THP-1 cell line which expresses TLR2 and TLR4 and therefore responds to their respective stimuli, MALP-2 and LPS. Proteins phosphorylated on tyrosine residues were immunoprecipitated from THP-1 cells with an anti-phosphotyrosine antibody and immunoblotted with an anti-Mal antibody. Blotting for endogenous Mal revealed two distinct forms (Fig. 3a and 3b, left hand side, lower panels). No tyrosine phosphorylated Mal was detected in untreated cells, (Fig. 3a, upper panel lane 1, left hand side and Fig. 3b, upper panel lane 1, left hand side). Treatment of cells with LPS led to tyrosine phosphorylation of Mal, with two tyrosine phosphorylated forms of endogenous Mal proteins being detected at 5 minutes treatment time (Fig. 3a, upper panel lane 2, left hand side). Similar to LPS, the TLR2 ligand MALP-2, led to tyrosine phosphorylation of Mal, the effect being evident at 10 minutes post stimulation (Fig. 3b, upper panel lane 5, left hand side), with two tyrosine phosphorylated forms again evident. The effect of both LPS and MALP-2 was remarkably transient with no tyrosine phosphorylation detected at later times.

To date Btk is the only tyrosine kinase known to interact with Mal (22). In this experiment, we therefore sought to determine if Btk was involved in the tyrosine phosphorylation of Mal following stimulation of THP-1 cells with LPS or MALP-2. It was noted that pre-treatment of THP-1 cells with LFM-A13, a specific Btk inhibitor completely abolished LPS induced tyrosine phosphorylation of Mal (Fig. 3a, upper panel, compare lanes 2 and 7). Similarly MALP-2 induced tyrosine phosphorylation of Mal was totally abolished following pre-treatment of THP-1 cells with LFM-A13 (Fig. 3b, upper panel, compare lanes 5 and 11).

To further confirm that Btk can phosphorylate Mal, *in vitro* kinase assays were performed. Incubation of recombinant Btk with recombinant Mal, resulted in Mal phosphorylation, with two distinct phospho-forms appearing (Fig 4a, lane 2). MyD88 was not phosphorylated by Btk under similar conditions (Fig. 4a, lane 5). Given that Tyr-86, Tyr-106 and Tyr-187 were possible phospho-acceptors, the effect of mutating these residues on Mal phosphorylation by Btk was next assessed. It was noted that phosphorylation of Mal by Btk was almost completely abolished when using recombinant Mal-Y86F Y106F Y187F as a substrate, furthermore only one phospho-form was evident (Fig 4a, lane 3). This experiment also revealed that Btk will undergo autophosphorylation as expected (Fig. 4a, lane 1 and lane 4) but having Mal present, limits this capacity, as can be seen from decreased Btk autophosphorylation (compare lanes 1 and 2). Interestingly, Mal-Y86F Y106F Y187F altered the kinase activity of Btk to a greater extent than wild type Mal (Fig. 4a, compare lanes 2 and 3). MyD88 however does not alter the kinase activity of Btk (Fig. 4a, compare lanes 4 and 5).

We next performed *in vitro* kinase assays using endogenous Btk. We found that recombinant Mal is a substrate for endogenous Btk *in vitro*. Similar to previous studies the activity of endogenous Btk was enhanced following LPS stimulation with maximal *in vitro* activity being detected at 60 minutes, as can be seen in Fig. 4b, lane 4 (23). We observed that increased activity of Btk corresponded to an increase in the phosphorylation of recombinant Mal by Btk and that phosphorylation again resulted in the appearance of two phospho-forms.

Taken together our results indicate that Mal undergoes phosphorylation on tyrosine residues by Btk during signaling, which is required for Mal to signal NF-κB activation.

DISCUSSION

Prompt activation of the TLR signaling pathway has proven to be vital in the recognition of invading pathogens and in eliciting the host innate immune response. Numerous studies have demonstrated that the efficient orchestration of the TLR signaling pathway is dependent on a series of phosphorylation events. The most receptor proximal protein kinases, which are recruited by TIR domain-containing adapters, are IRAK4 and IRAK1, RIP-1 and RIP-3, TBK-1 and Btk (1). A limited number of substrates for these kinases have been reported to date. Here we demonstrate that Mal undergoes tyrosine phosphorylation by Btk during signaling and that this phosphorylation event is required for Mal to signal NF-κB activation.

Two dimensional SDS-PAGE analysis revealed that the slower migrating form of Mal displayed a lower isoelectric point than the predominant 32 kDa form. Phosphatase treatment established that the slower migrating form of Mal represented tyrosine phosphorylated Mal. A role for tyrosine phosphorylation has previously been ascribed to the TLR2 and TLR4 signaling pathway (32,33). In this report, MALP-2 and LPS rapidly triggered tyrosine phosphorylation of endogenous Mal in THP-1 cells.

We next assessed the relative functional importance of the six tyrosine residues in the TIR domain of Mal and noted that in Mal-Y86F, Mal-Y106F and Mal-Y187F the slowest migrating form of Mal was abolished. Our findings also determined that Tyr-86, Tyr-106 and Tyr-187 were the most critical residues for maximal NF-κB activation induced by Mal. Furthermore, Mal-Y86F and Mal-Y187F acted as dominant negative inhibitors of NF-κB activation induced by LPS, whereas the other mutants of Mal did not. These results suggest that following LPS stimulation Tyr-86 and Tyr-187 are likely to undergo phosphorylation and this process is required for NF-κB activation mediated by Mal. It is likely that

both require phosphorylation since mutating either resulted in an inactive dominant negative form.

Although Tyr-106 failed to activate NF-κB to the same extent as wild-type Mal and had a different phosphorylation profile to wild-type Mal, it had no effect on LPS signaling. All three tyrosines located at positions 86, 106 and 187 may need to undergo phosphorylation in order for Mal to exhibit retarded mobility. Given that during TLR2 and TLR4 signaling two tyrosine phosphorylated forms of Mal could be detected, it is likely that endogenous Mal is also multiply tyrosine phosphorylated. The role of Tyr-106 in Mal signaling is therefore unclear, but may be required for another Mal-mediated signal. We are currently examining this possibility.

We have previously shown that Btk is activated by TLR4 and is required for LPS responses mediating NF-κB activation (22). A particular response to LPS that requires Mal is phosphorylation of the p65 subunit of NF-κB at serine 536 (Mansell A., personal communication). This response is abolished in cells from X-linked immunodeficiency (Xid) mice which contain inactive Btk (34), and is also inhibited by the Btk inhibitor LFM-A13 (22). Our findings here clearly demonstrated that phosphorylation of Mal was enhanced upon increased activation of Btk following LPS stimulation. Mutational analysis of Mal indicates that Btk phosphorylates Mal on Tyr-86, Tyr-106 and Tyr-187. This observation therefore identifies that Mal is a substrate for Btk on the TLR4 pathway, with phosphorylation of Mal on Tyr-86 and Tyr-187 by Btk being required for NF-κB activation mediated by LPS. Interestingly, we observed that Mal inhibited Btk autophosphorylation, suggesting that Mal may be required to negatively regulate the kinase activity of Btk. We attempted to confirm that Btk is a key tyrosine kinase for Mal phosphorylation by examining the phosphorylation status of Mal in monocytes and splenocytes isolated from Xid mice. The level of Mal however, in cells from both wild type and and Xid mice was too low for detection in the endogenous phosphotyrosine immunoprecipitation assay. However the inhibitory effect of LFM-A13 and the *in vitro* evidence strongly suggest that the tyrosine kinase responsible for tyrosine phosphorylation of Mal is Btk.

The tyrosine at position 86 is conserved amongst other TIR domain-containing proteins. It is therefore possible that Btk will phosphorylate the homologous tyrosine in other adapter proteins, although we found that MyD88 was not a substrate for Btk. We are currently exploring other TIR domain containing proteins, notably the other adapters.

Recently other proteins in the TLR signaling family have been shown to undergo phosphorylation. It has been reported that following stimulation with their specific ligands TLR2, TLR3 and TLR4 all undergo tyrosine phosphorylation (25-27). In addition, LPS was found to induce tyrosine phosphorylation of MyD88 and it has been stated that upon overexpression, the adapters TRIF and TRAM are phosphorylated (12,19,35). Whilst it has been established that members of the TLR superfamily undergo phosphorylation, the participating kinases have yet to be identified and to date their identity has only been speculated upon. Therefore, this report is the first to identify a kinase that directly phosphorylates a TIR domain-containing protein.

Our study has not addressed the immediate downstream consequences of tyrosine phosphorylation of Mal. Indeed similar to CheY, which is structurally similar to the TIR domain, a conformational change for signaling may occur following phosphorylation of Mal, and specific proteins might be recruited. We are currently examining these possibilities. Our results, however, clearly show that Mal is a phosphoprotein that becomes tyrosine phosphorylated by Btk upon activation of the TLR2 and TLR4 signal transduction pathways. This phosphorylation is required for Mal to signal, establishing an important mechanistic step in TLR2 and TLR4 signaling.

REFERENCES

1. Dunne, A., and O'Neill, L. A. (2005) *FEBS Lett* **579**, 3330-3335
2. Alexopoulou, L., Holt, A. C., Medzhitov, R., and Flavell, R. A. (2001) *Nature* **413**, 732-738
3. Fitzgerald, K. A., Palsson-McDermott, E. M., Bowie, A. G., Jefferies, C. A., Mansell, A. S., Brady, G., Brint, E., Dunne, A., Gray, P., Harte, M. T., McMurray, D., Smith, D. E., Sims, J. E., Bird, T. A., and O'Neill, L. A. (2001) *Nature* **413**, 78-83
4. Horng, T., Barton, G. M., and Medzhitov, R. (2001) *Nat Immunol* **2**, 835-841
5. Horng, T., Barton, G. M., Flavell, R. A., and Medzhitov, R. (2002) *Nature* **420**, 329-333
6. Yamamoto, M., Sato, S., Hemmi, H., Sanjo, H., Uematsu, S., Kaisho, T., Hoshino, K., Takeuchi, O., Kobayashi, M., Fujita, T., Takeda, K., and Akira, S. (2002) *Nature* **420**, 324-329
7. Kawai, T., Adachi, O., Ogawa, T., Takeda, K., and Akira, S. (1999) *Immunity* **11**, 115-122
8. Takeuchi, O., Kaufmann, A., Grote, K., Kawai, T., Hoshino, K., Morr, M., Muhlradt, P. F., and Akira, S. (2000) *J Immunol* **164**, 554-557
9. Yamamoto, M., Sato, S., Mori, K., Hoshino, K., Takeuchi, O., Takeda, K., and Akira, S. (2002) *J Immunol* **169**, 6668-6672
10. Oshiumi, H., Matsumoto, M., Funami, K., Akazawa, T., and Seya, T. (2003) *Nat Immunol* **4**, 161-167
11. Fitzgerald, K. A., Rowe, D. C., Barnes, B. J., Caffrey, D. R., Visintin, A., Latz, E., Monks, B., Pitha, P. M., and Golenbock, D. T. (2003) *J Exp Med* **198**, 1043-1055
12. Bin, L. H., Xu, L. G., and Shu, H. B. (2003) *J Biol Chem* **278**, 24526-24532
13. Oshiumi, H., Sasai, M., Shida, K., Fujita, T., Matsumoto, M., and Seya, T. (2003) *J Biol Chem* **278**, 49751-49762
14. Suzuki, N., Suzuki, S., Duncan, G. S., Millar, D. G., Wada, T., Mirtsos, C., Takada, H., Wakeham, A., Itie, A., Li, S., Penninger, J. M., Wesche, H., Ohashi, P. S., Mak, T. W., and Yeh, W. C. (2002) *Nature* **416**, 750-756
15. Ninomiya-Tsuji, J., Kishimoto, K., Hiyama, A., Inoue, J., Cao, Z., and Matsumoto, K. (1999) *Nature* **398**, 252-256
16. Wang, C., Deng, L., Hong, M., Akkaraju, G. R., Inoue, J., and Chen, Z. J. (2001) *Nature* **412**, 346-351
17. Meylan, E., Burns, K., Hofmann, K., Blancheteau, V., Martinon, F., Kelliher, M., and Tschopp, J. (2004) *Nat Immunol* **5**, 503-507
18. Fitzgerald, K. A., McWhirter, S. M., Faia, K. L., Rowe, D. C., Latz, E., Golenbock, D. T., Coyle, A. J., Liao, S. M., and Maniatis, T. (2003) *Nat Immunol* **4**, 491-496
19. Sato, S., Sugiyama, M., Yamamoto, M., Watanabe, Y., Kawai, T., Takeda, K., and Akira, S. (2003) *J Immunol* **171**, 4304-4310
20. Napolitani, G., Bortoletto, N., Racioppi, L., Lanzavecchia, A., and D'Oro, U. (2003) *Eur J Immunol* **33**, 2832-2841
21. Beaty, C. D., Franklin, T. L., Uehara, Y., and Wilson, C. B. (1994) *Eur J Immunol* **24**, 1278-1284
22. Jefferies, C. A., Doyle, S., Brunner, C., Dunne, A., Brint, E., Wietek, C., Walch, E., Wirth, T., and O'Neill, L. A. (2003) *J Biol Chem* **278**, 26258-26264

23. Mukhopadhyay, S., Mohanty, M., Mangla, A., George, A., Bal, V., Rath, S., and Ravindran, B. (2002) *J Immunol* **168**, 2914-2921
24. Horwood, N. J., Mahon, T., McDaid, J. P., Campbell, J., Mano, H., Brennan, F. M., Webster, D., and Foxwell, B. M. (2003) *J Exp Med* **197**, 1603-1611
25. Chen, L. Y., Zuraw, B. L., Zhao, M., Liu, F. T., Huang, S., and Pan, Z. K. (2003) *Am J Physiol Lung Cell Mol Physiol* **284**, L607-613
26. Sarkar, S. N., Smith, H. L., Rowe, T. M., and Sen, G. C. (2003) *J Biol Chem* **278**, 4393-4396
27. Arbibe, L., Mira, J. P., Teusch, N., Kline, L., Guha, M., Mackman, N., Godowski, P. J., Ulevitch, R. J., and Knaus, U. G. (2000) *Nat Immunol* **1**, 533-540
28. Dunne, A., Ejdeback, M., Ludidi, P. L., O'Neill, L. A., and Gay, N. J. (2003) *J Biol Chem* **278**, 41443-41451
29. Ben-Yehoyada, M., Ben-Dor, I., and Shaul, Y. (2003) *J Biol Chem* **278**, 34475-34482
30. Rock, F. L., Hardiman, G., Timans, J. C., Kastelein, R. A., and Bazan, J. F. (1998) *Proc Natl Acad Sci U S A* **95**, 588-593
31. Drake, S. K., Bourret, R. B., Luck, L. A., Simon, M. I., and Falke, J. J. (1993) *J Biol Chem* **268**, 13081-13088
32. Hazeki, K., Masuda, N., Funami, K., Sukenobu, N., Matsumoto, M., Akira, S., Takeda, K., Seya, T., and Hazeki, O. (2003) *Eur J Immunol* **33**, 740-747
33. Geng, Y., Gulbins, E., Altman, A., and Lotz, M. (1994) *Proc Natl Acad Sci U S A* **91**, 8602-8606
34. Rawlings, D. J., Saffran, D. C., Tsukada, S., Largaespada, D. A., Grimaldi, J. C., Cohen, L., Mohr, R. N., Bazan, J. F., Howard, M., Copeland, N. G., and et al. (1993) *Science* **261**, 358-361
35. Ojaniemi, M., Glumoff, V., Harju, K., Liljeroos, M., Vuori, K., and Hallman, M. (2003) *Eur J Immunol* **33**, 597-605

FOOTNOTES

*We thank M. Ejdebäck for constructing the molecular model of the TIR domain of Mal. This work was supported by Science Foundation Ireland.

[1]The abbreviations used are: Btk, Bruton's tyrosine kinase; HEK, Human Embryonic Kidney, LPS, lipopolysaccharide; MALP-2, Macrophage stimulating lipopeptide-2; Mal, MyD88 Adapter-Like; TLR, Toll like-receptor; TIR, Toll/interleukin-1 receptor.

FIGURE LEGENDS

Fig. 1. Mal is a phosphoprotein. **(a)** Left panel: HEK293 cells were transiently transfected with a plasmid encoding HA-Mal (lane 2) or empty vector, EV, (lane 1). Cell lysates were prepared and samples were immunoblotted with an anti-HA antibody. Right panel: two-dimensional gel analysis of the phosphorylation status of Mal. HEK293 cells were transiently transfected with a plasmid encoding HA-Mal. Cell lysates were prepared and Mal was immunoprecipitated with an anti-HA antibody. The sample was then analysed by two-dimensional SDS-PAGE, followed by immunoblotting with an anti-HA antibody. The sample was electrofocused at a pH gradient of 4 (left) to 7 (right). **(b)** Phosphatase

treatment results in the disappearance of the slower migrating forms of Mal. HEK293 cells were transiently transfected with a plasmid encoding HA-Mal. Cell lysates were prepared and Mal was immunoprecipitated with an anti-HA antibody. Immunoprecipitates were incubated at 37°C for 3 hrs with 100 U of CIP, in the presence (lane 1) or absence of CIP inhibitors (lane 2). Samples were then analysed by SDS-PAGE and immunoblotted with an anti-HA antibody. **(c)** GST-Mal is phosphorylated, but does not undergo autophosphorylation when subjected to an *in vitro* kinase assay. GST-Mal (lane 1) and GST (lane 2) were incubated with cell lysates from the HEK293 cell line, or with lysis buffer alone (lanes 3 and 4) for 2 hours at 4°C. Samples were subjected to an *in vitro* kinase assay, separated by SDS-PAGE, and visualised by autoradiography (upper panel). Samples were also stained with Coomassie Stain (lower panel) **(d)** Mal is tyrosine phosphorylated. HA-Mal was immunoprecipitated from HEK293 cells as described in (b). Immunoprecipitates were incubated with (lane 2) or without (lane 1) 10U of PTP-1B. Samples were analysed by SDS-PAGE and immunoblotted with an anti-HA antibody. **(e)** HEK293 cells ($1x10^6$) were mock-transfected (lane 1) or transiently transfected with a plasmid encoding HA-Mal (lane 2). HA-Mal was immunoprecipitated with an anti-HA antibody and samples were immunoblotted with an antibody that recognises phospho-tyrosine residues (clone 4G10, Upstate). Results shown are representative of at least three separate experiments.

Fig. 2 **(a)** Alignment of human Mal (hMal) and murine Mal (mMal). Two regions, Box 1 and Box 2, which are conserved among all TIR domain-containing proteins, are indicated. The tyrosine residues conserved in both hMal and mMal are underlined and numbered according to their location in hMal. **(b)** SDS-PAGE reveals that replacement of Tyr 86, 106 or 187 to Phe, alters the phosphorylation profile of wild-type Mal. HEK293 cells were transiently transfected with plasmids encoding wild-type (WT) Mal (lane 1), Mal-Y86F (lane 2), Mal-Y106F (lane 3), Mal-Y159F (lane 4), Mal-Y187F (lane 5), Mal-Y195F (lane 6), Mal-Y196F (lane 7) and Mal-Y86F Y106F Y187F (lane 8), for 24h. Lysates were resolved by SDS-PAGE and immunoblotted with an anti-HA antibody. **(c)** Mal-Y86F, Mal-Y106F and Mal-Y187F do not activate the NF-κB pathway as strongly as wild-type Mal. HEK293 cells were transiently transfected with a 5x NF-κB reporter gene plasmid and co-transfected with plasmids encoding wild-type Mal, Mal-Y86F, Mal-Y106F, Mal-Y159F, Mal-Y187F, Mal-Y195F, Mal-Y196F and Mal-Y86F Y106F Y187F, for 24h. Luciferase activity is expressed as fold induction relative to mock-transfected cells (EV). Mean relative stimulation of luciferase activity ± s.d. for a representative experiment from three separate experiments, each performed in triplicate, is shown. **(d)** Structural surface analysis of the TIR domain of Mal. Structural features representing the conserved boxes of the TIR domains are shown in green (Box 1) and blue (Box 2). The side chain of the semi-conserved proline residue in the BB-loop is coloured purple. The phospho-accepting tyrosines Tyr-86, Tyr-106, and Tyr-187 are highlighted in red. **(e)** Mal-Y86F and Mal-Y187F inhibit LPS signaling. HEK293 cells stably transfected with Flag-TLR4 were transfected with a 5x NF-κB reporter gene plasmid and co-transfected with plasmids encoding Mal-P125H, Mal-Y86F, Mal-Y106F, Mal-159F, Mal-Y195F, Mal-Y196F and Mal Y86F Y106F Y187F. Cells were then left untreated or incubated with LPS (100 ng ml-1) for 6 hours. Mean relative stimulation of luciferase activity ± s.d. for a representative experiment from 3 separate experiments, each performed in triplicate, is shown.

Fig. 3. Endogenous Mal is phosphorylated by Btk. THP-1 cells ($2x10^7$) were pretreated with DMSO (left hand side) or LFM-A13 (right hand side) for 1 h prior to stimulation with either **(a)** LPS or **(b)** MALP-2. Cell lysates were prepared and tyrosine phosphorylated proteins were immunoprecipitated with anti-phosphotyrosine agarose, followed by immunoblotting with an anti-Mal antibody. Cell lysates were also immunoblotted with the anti-Mal antibody (lower panel).

Fig. 4. Mal is a substrate for Btk. **(a)** Recombinant Btk was incubated alone (lanes 1 and 4), or with recombinant wild-type Mal (lane 2), recombinant Mal-Y86F Y106F Y187F (lane 3) or recombinant GST-MyD88 (lane 5). Samples were subjected to an *in vitro* kinase assay, analysed on SDS-PAGE, and

visualised by autoradiography. Samples were also immunoblotted with either an anti-Btk antibody (middle panel), an anti-Mal antibody (left hand side, lower panel) or with an anti-MyD88 antibody (right hand side, lower panel) **(b)** THP1 cells were treated with LPS (1 μg/ml) as indicated, cell lysates were prepared and immunoprecipitations were performed using an anti-Btk antibody. Recombinant Mal was added to each sample. *In vitro* kinase assays were performed, samples were then analysed by SDS-PAGE and visualised by autoradiography (upper panel). Samples were also immunoblotted with an anti-Mal antibody (lower panel).

Figure 1

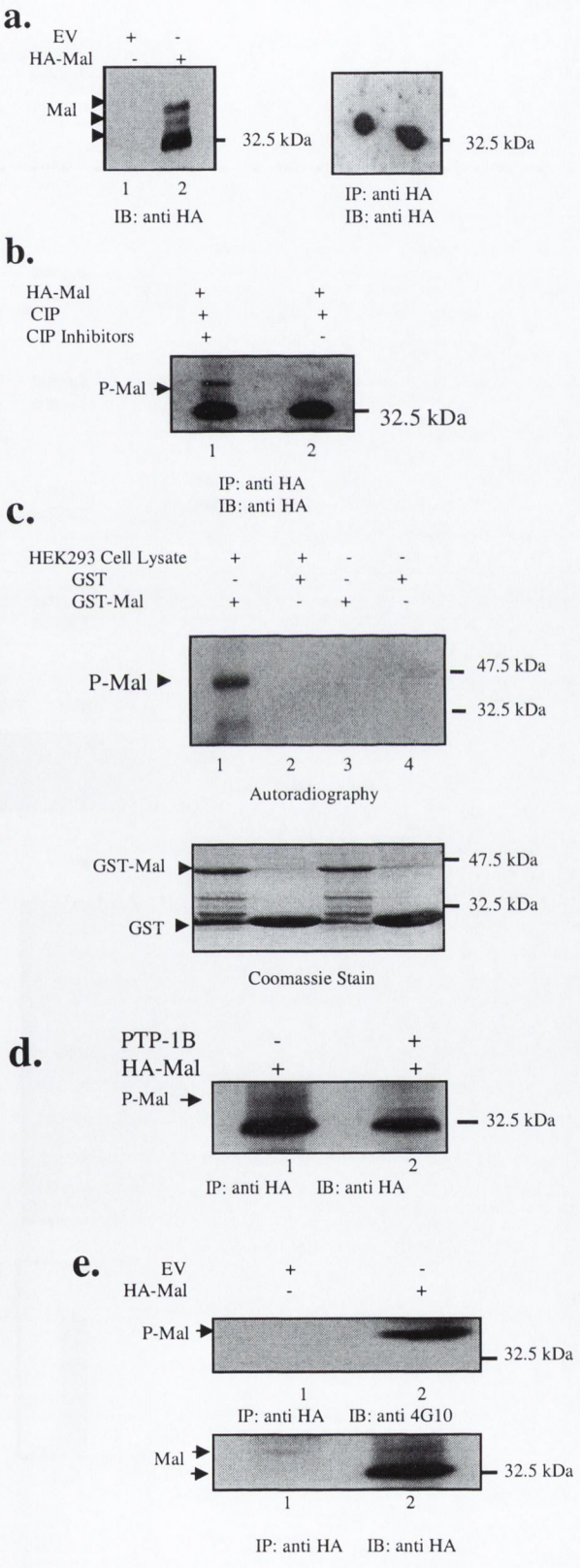
a.
EV + -
HA-Mal - +
Mal
32.5 kDa
32.5 kDa
1 2
IB: anti HA
IP: anti HA
IB: anti HA
b.
HA-Mal + +
CIP + +
CIP Inhibitors + -
P-Mal
32.5 kDa
1 2
IP: anti HA
IB: anti HA
c.
HEK293 Cell Lysate + + - -
GST - + - +
GST-Mal + - + -
P-Mal
47.5 kDa
32.5 kDa
1 2 3 4
Autoradiography
GST-Mal
GST
47.5 kDa
32.5 kDa
Coomassie Stain
d.
PTP-1B - +
HA-Mal + +
P-Mal
32.5 kDa
1 2
IP: anti HA IB: anti HA
e.
EV + -
HA-Mal - +
P-Mal
32.5 kDa
1 2
IP: anti HA IB: anti 4G10
Mal
32.5 kDa
1 2
IP: anti HA IB: anti HA

Figure 2

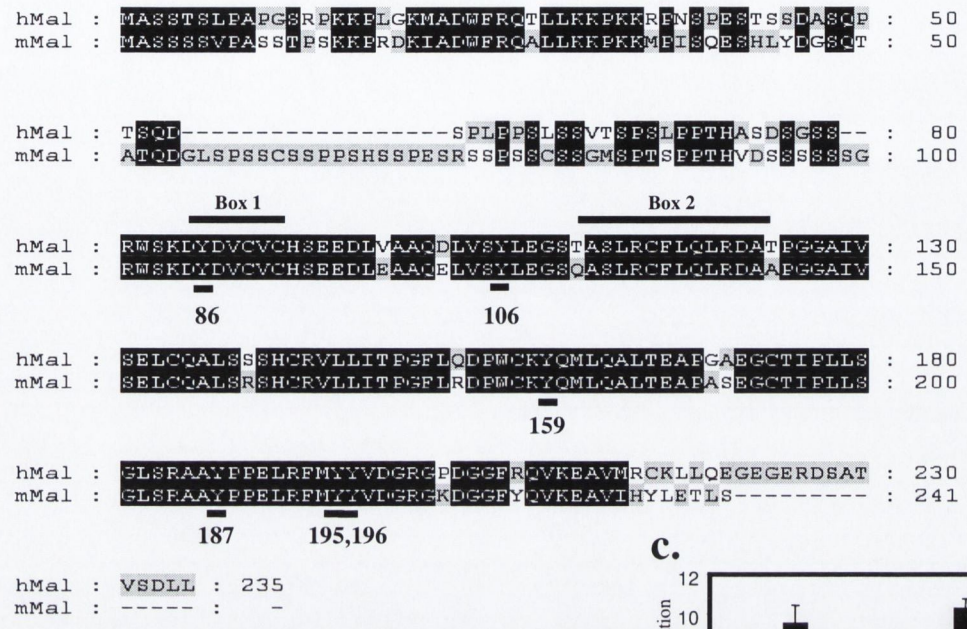
a.
hMal : MASSTSLPAPGSRPKKPLGKMADWFRQTLLKKPKKRPNSPESTSSDASQP : 50
mMal : MASSSSVPASSTPSKKPRDKIADWFRQALLKKPKKMPISQESHLYDGSQT : 50
hMal : TSQL----------SPLPPSLSSVTSPSLPPTHASDSGSS-- : 80
mMal : ATQLGLSPSSCSSPPSHSSPESRSSPSSCSSGMSPTSPPTHVDSSSSSSG : 100
Box 1
Box 2
hMal : RWSKDYDVCVCHSEEDLVAAQDLVSYLEGSTASLRCFLQLRDATPGGAIV : 130
mMal : RWSKDYDVCVCHSEEDLEAAQELVSYLEGSQASLRCFLQLRDAAPGGAIV : 150
86
106
hMal : SELCQALSSSHCRVLLITPGFLQDPWCKYQMLQALTEAPGAEGCTIPLLS : 180
mMal : SELCQALSRSHCRVLLITPGFLRDPWCKYQMLQALTEAPASEGCTIPLLS : 200
159
hMal : GLSRAAYPPELRFMYYVDGRGPDGGFRQVKEAVMRCKLLQEGEGERDSAT : 230
mMal : GLSRAAYPPELRFMYYVDGRGKDGGFYQVKEAVIHYLETLS--------- : 241
187
195,196
hMal : VSDLL : 235
mMal : ----- : -

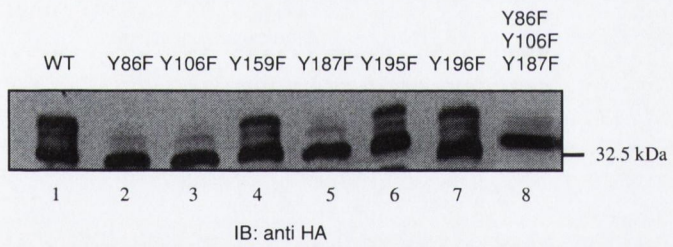
b.
WT
Y86F
Y106F
Y159F
Y187F
Y195F
Y196F
Y86F Y106F Y187F
32.5 kDa
1 2 3 4 5 6 7 8
IB: anti HA

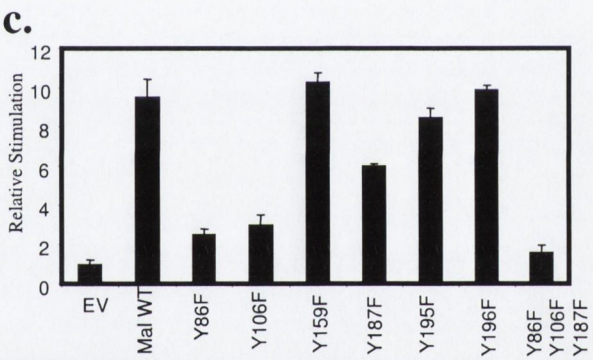
c.
Relative Stimulation
0 2 4 6 8 10 12
EV
Mal WT
Y86F
Y106F
Y159F
Y187F
Y195F
Y196F
Y86F Y106F Y187F

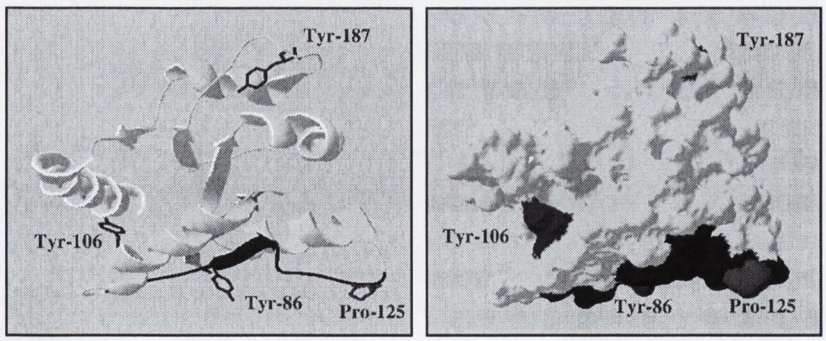
d.
Tyr-187
Tyr-106
Tyr-86
Pro-125
Tyr-187
Tyr-106
Tyr-86
Pro-125

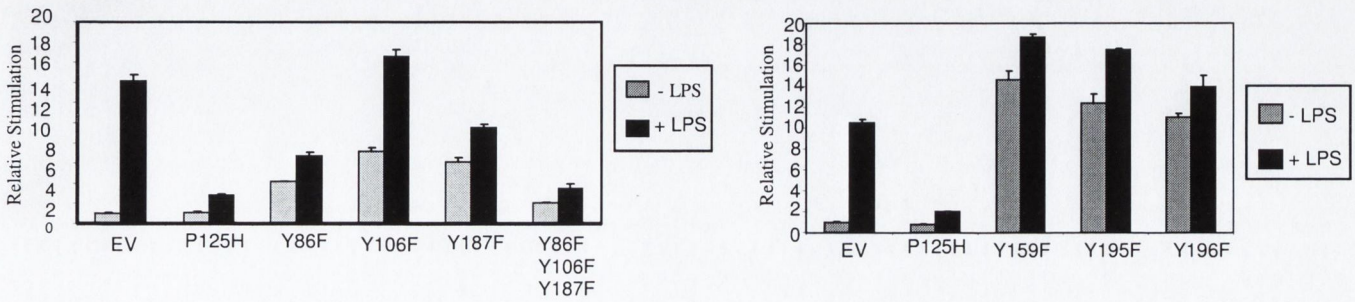
e.
Relative Stimulation
0 2 4 6 8 10 12 14 16 18 20
EV
P125H
Y86F
Y106F
Y187F
Y86F Y106F Y187F
- LPS
+ LPS
Relative Stimulation
0 2 4 6 8 10 12 14 16 18 20
EV
P125H
Y159F
Y195F
Y196F
- LPS
+ LPS

Figure 3

a.

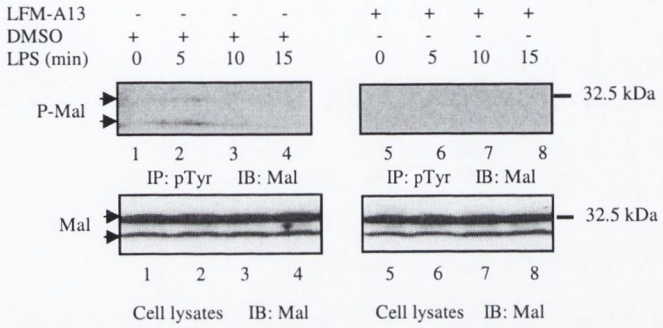
LFM-A13 - - - - + + + +
DMSO + + + + - - - -
LPS (min) 0 5 10 15 0 5 10 15
P-Mal
32.5 kDa
1 2 3 4 5 6 7 8
IP: pTyr IB: Mal IP: pTyr IB: Mal
Mal
32.5 kDa
1 2 3 4 5 6 7 8
Cell lysates IB: Mal Cell lysates IB: Mal

b.

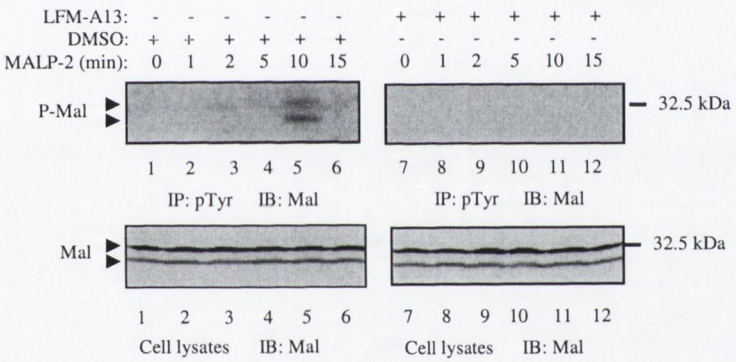
LFM-A13: - - - - - - + + + + + +
DMSO: + + + + + + - - - - - -
MALP-2 (min): 0 1 2 5 10 15 0 1 2 5 10 15
P-Mal
32.5 kDa
1 2 3 4 5 6 7 8 9 10 11 12
IP: pTyr IB: Mal IP: pTyr IB: Mal
Mal
32.5 kDa
1 2 3 4 5 6 7 8 9 10 11 12
Cell lysates IB: Mal Cell lysates IB: Mal

Figure 4

a.

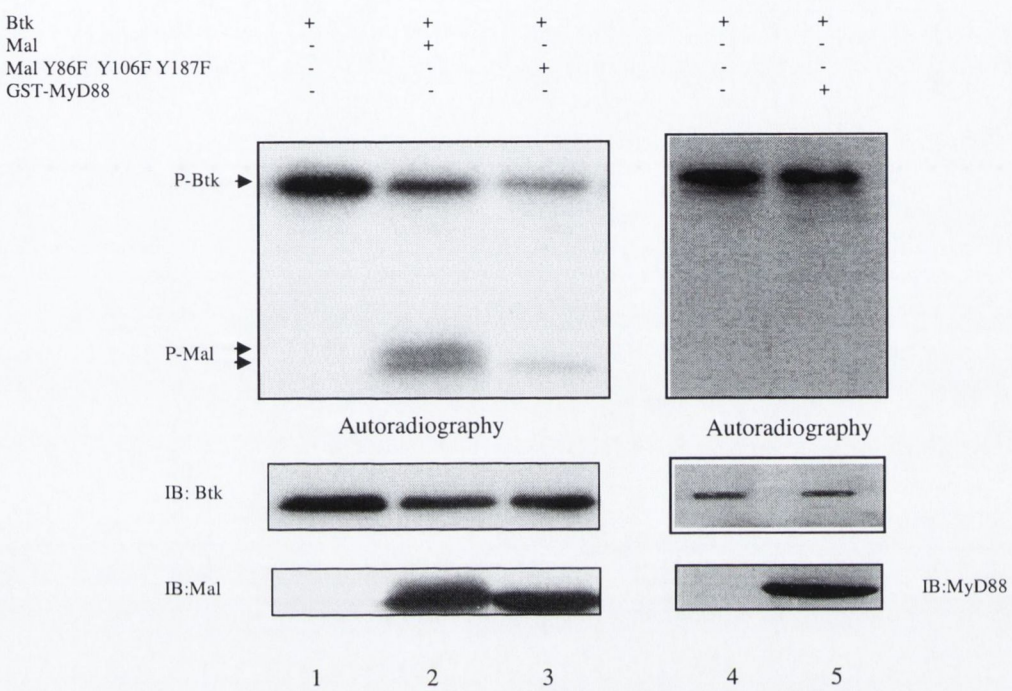
Btk + + + + +
Mal - + - - -
Mal Y86F Y106F Y187F - - + - -
GST-MyD88 - - - - +
P-Btk
P-Mal
Autoradiography
Autoradiography
IB: Btk
IB:Mal
IB:MyD88
1 2 3 4 5

b.

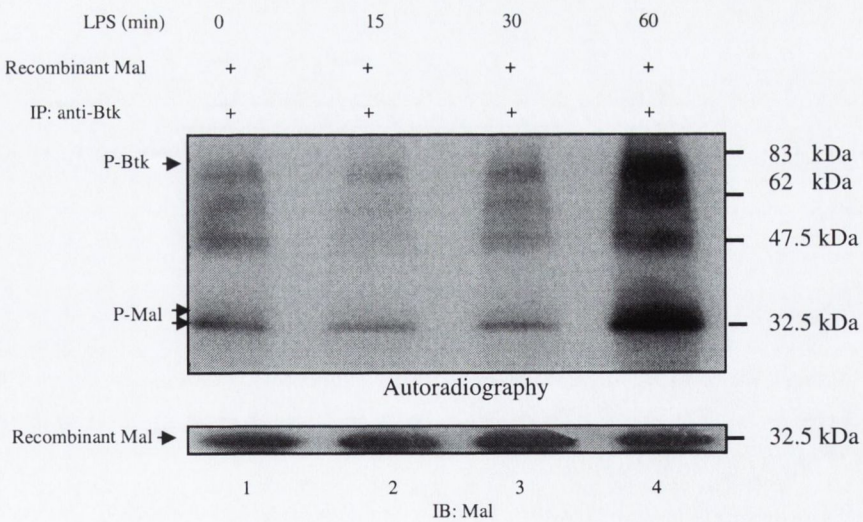
LPS (min) 0 15 30 60
Recombinant Mal + + + +
IP: anti-Btk + + + +
P-Btk
P-Mal
83 kDa
62 kDa
47.5 kDa
32.5 kDa
Autoradiography
Recombinant Mal
32.5 kDa
1 2 3 4
IB: Mal

nature immunology

Suppressor of cytokine signaling 1 negatively regulates Toll-like receptor signaling by mediating Mal degradation

Ashley Mansell[1], Rosealee Smith[1], Sarah L Doyle[2], Pearl Gray[2], Jennifer E Fenner[1], Peter J Crack[1], Sandra E Nicholson[3], Douglas J Hilton[3], Luke A J O'Neill[2,4] & Paul J Hertzog[1,4]

Toll-like receptor (TLR) signals that initiate innate immune responses to pathogens must be tightly regulated to prevent excessive inflammatory damage to the host. The adaptor protein Mal is specifically involved in signaling via TLR2 and TLR4. We demonstrate here that after TLR2 and TLR4 stimulation Mal becomes phosphorylated by Bruton's tyrosine kinase (Btk) and then interacts with SOCS-1, which results in Mal polyubiquitination and subsequent degradation. Removal of SOCS-1 regulation potentiates Mal-dependent p65 phosphorylation and transactivation of NF-κB, leading to amplified inflammatory responses. These data identify a target of SOCS-1 that regulates TLR signaling via a mechanism distinct from an autocrine cytokine response. The transient activation of Mal and subsequent SOCS-1–mediated degradation is a rapid and selective means of limiting primary innate immune response.

Redacted

Redacted

Redacted

Redacted

Redacted

Redacted

Redacted